

Synthesis and immobilisation of biologically active substances

Dissertation

Zur Erlangung des Doktorgrades der Naturwissenschaften

(Dr. rer. nat.)

der naturwissenschaftlichen Fakultät IV

– Chemie und Pharmazie –

der Universität Regensburg

vorgelegt von

Thomas Walenzyk

aus Rüsselsheim

2005



Synthesis and immobilisation of biologically active substances

Dissertation

Zur Erlangung des Doktorgrades der Naturwissenschaften

(Dr. rer. nat.)

der naturwissenschaftlichen Fakultät IV

– Chemie und Pharmazie –

der Universität Regensburg



vorgelegt von

Thomas Walenzyk

aus Rüsselsheim

2005

The experimental part of this work was carried out between October 2001 and November 2004 at the Institute for Organic Chemistry at the University of Regensburg, under the supervision of *Prof. Dr. B. König*.

The PhD thesis was submitted on: 16.02.2005

The colloquium took place on: 24.03.2005

Board of Examiners:	Prof. Dr. G. Schmeer	(Chairman)
	Prof. Dr. B. König	(1st Referee)
	Prof. Dr. W. Kunz	(2nd Referee)
	Prof. Dr. A. Göpferich	(3rd Referee)

Acknowledgements

I would like to express my sincere gratitude to Prof. Dr. B. König, for his continued guidance, advice and encouragement throughout this work.

I would also like to thank Merck KGaA in Darmstadt for financing my research, especially Dr. H. Buchholz who allowed me to conduct my research in his laboratory. I also thank all my coworkers in the department Pigments R&D Cosmetics, for assisting me in my efforts.

Thanks are extended to the analytical departments of Merck KGaA for the prompt and accurate measurement of my numerous, often difficult samples. Special thanks to Mr. H. Opfermann (SEM images), Ms. J. Donath and Ms. N. Blatt (UV samples), Dr. F. Pfluecker and Ms. G. Witte (photostability tests), Mr. T. Stein (ICP-OES), Dr. H. Ackermann (DPPH tests) and Dr. B. Schubach (MALDI-MS). Thanks are also extended to the analytical departments of the Faculty of Chemistry and Pharmacy at the University of Regensburg. Special thanks to Dr. T. Burgemeister, Mr. F. Kastner, Ms. N. Pustet, Ms. A. Schramm and Ms. G. Stühler (NMR), Dr. K. K. Mayer, Mr. J. Kiermaier and Herrn W. Söllner (MS), Mr. G. Wandinger, Ms. S. Stempfhuber and Mr. H. Schüller (elemental analysis) and Dr. M. Zabel (X-ray crystallography).

My special thanks go to:

All colleagues, past and present, both at Merck KGaA and at the University of Regensburg, for making the working environment positive, constructive, as well as relaxed. Dr. C. Carola for giving me advice, guidance and always an open ear for discussions. Dr. T. Mujica for making sure that the day was always lively and never ordinary. Thanks for the long discussions and many great laughs. Mr. M. Kruppa for being my partner in crime. The willingness to help and give advice was only outdone by the many great experiences we had outside of the laboratory. Mr. R. Roskopf for always having an answer to any problem or task I threw at him. Thanks for your persistence and thoroughness, and always with a smile. Mr. M. Subat for the good cooperation on one of the projects. For the long and interesting discussions and showing me there are always two ways to tackle a problem.

My family & Daniela

Table of Contents

1. MOLECULAR RECOGNITION OF AZAMACROCYCLES.....	1
1.1 INTRODUCTION.....	1
1.1.1 General Properties of metal complexes of azamacrocycles.....	1
1.1.2 Scope.....	2
1.2 STRUCTURES OF 1,4,7,10-TETRAAZA-CYCLODODECANE ([12]ANEN ₄ OR CYCLEN) COMPLEXES IN SOLID STATE	4
1.2.1 Co(III) complexes	4
1.2.2 Cu(II) complexes.....	6
1.2.3 Ni(II) complexes.....	6
1.2.4 Zn(II) complexes	8
1.3 STRUCTURES OF 1,4,7,10-TETRAAZA-CYCLODODECANE ([12]ANEN ₄ OR CYCLEN) COMPLEXES IN SOLID STATE (TABULATED)	12
1.4 MOLECULAR RECOGNITION OF 1,4,7,10-TETRAAZA-CYCLODODECANE ([12]ANEN ₄ OR CYCLEN) COMPLEXES IN SOLUTION.....	18
1.4.1 Co(III) complexes	18
1.4.2 Cd(II) complexes.....	18
1.4.3 Zn(II) complexes	19
1.5 IMMOBILISED 1,4,7,10-TETRAAZA-CYCLODODECANE ([12]ANEN ₄ OR CYCLEN) COMPLEXES	25
1.5.1 Zn(II) complexes	25
1.6 STRUCTURES OF 1,4,8,11-TETRAAZA-CYCLOTETRADECANE ([14]ANEN ₄ OR CYCLAM) COMPLEXES IN SOLID STATE	28
1.6.1 Zn(II) complexes	28
1.6.2 Ni(II) complexes.....	29
1.7 STRUCTURES OF 1,4,8,11-TETRAAZA-CYCLOTETRADECANE ([14]ANEN ₄ OR CYCLAM) COMPLEXES IN SOLID STATE (TABULATED).....	31
1.8 MOLECULAR RECOGNITION OF 1,4,8,11-TETRAAZA-CYCLOTETRADECANE ([14]ANEN ₄ OR CYCLAM) COMPLEXES IN SOLUTION.....	37
1.8.1 Zn(II) complexes	37
1.8.2 Ni(II) complexes.....	39
1.8.3 Hg(II) complexes.....	40
1.9 IMMOBILISED 1,4,8,11-TETRAAZA-CYCLOTETRADECANE ([14]ANEN ₄ OR CYCLAM) COMPLEXES..	41
1.9.1 Ni(II) complexes.....	41
1.10 STRUCTURES OF 1,5,9-TRIAZA-CYCLODODECANE ([12]ANEN ₃) COMPLEXES IN SOLID STATE	42
1.10.1 Zn(II) complexes	42
1.11 MOLECULAR RECOGNITION OF 1,5,9-TRIAZA-CYCLODODECANE ([12]ANEN ₃) COMPLEXES IN SOLUTION	42
1.11.1 Zn(II) complexes	42
1.12 IMMOBILISED 1,5,9-TRIAZA-CYCLODODECANE ([12]ANEN ₃) COMPLEXES	43
1.13 STRUCTURES OF 1,4,7-TRIAZONANE ([9]ANEN ₃ OR TACN) COMPLEXES IN SOLID STATE.....	43

1.13.1	<i>Cu(II) complexes</i>	43
1.14	STRUCTURES OF 1,4,7-TRIAZONANE ([9]ANEN ₃ OR TACN) COMPLEXES IN SOLID STATE (TABULATED)	44
1.15	MOLECULAR RECOGNITION OF 1,4,7-TRIAZONANE ([9]ANEN ₃ OR TACN) COMPLEXES IN SOLUTION	49
1.15.1	<i>Cu(II) complexes</i>	49
1.16	IMMOBILISED 1,4,7-TRIAZONANE ([9]ANEN ₃ OR TACN) COMPLEXES	49
1.16.1	<i>Cu(II) complexes</i>	49
1.17	CONCLUSION	51
1.18	REFERENCES	52
2.	IMMOBILISED ZN (II) CYCLEN COMPLEXES AS CATALYTIC REAGENTS FOR PHOSPHODIESTER HYDROLYSIS	63
2.1	INTRODUCTION	64
2.1.1	<i>Metalloenzymes</i>	64
2.1.2	<i>Models</i>	65
2.1.3	<i>Synzymes - Synthetic polymers with enzyme like activities</i>	67
2.2	RESULTS AND DISCUSSION	68
2.2.1	<i>Synthesis of mono-Zn(II)Cyc polymer</i>	68
2.2.2	<i>Kinetic measurements for the phosphodiester cleavage reaction with mono-Zn(II)Cyc complexes bound to a solid support</i>	71
2.2.2.1	Calculation of the molar extinction coefficient for <i>para</i> -nitrophenolate	71
2.2.2.2	Non-catalysed hydrolysis of bis-(4-nitrophenyl)phosphate (BNPP)	74
2.2.2.3	Hydrolysis of BNPP with immobilised mononuclear Zn(II)Cyc complexes (batch reaction)	75
2.2.2.4	Hydrolysis of BNPP with immobilised mononuclear Zn(II)Cyc complexes (PBR Reactor)	78
2.2.3	<i>Synthesis of bis-Zn(II)Cyc Polymer</i>	80
2.2.4	<i>Kinetic measurements for the phosphodiester cleavage reaction with bis-Zn(II)Cyc complexes bound to a solid support</i>	82
2.3	CONCLUSION	83
2.4	EXPERIMENTAL	84
2.4.1	<i>General</i>	84
2.4.1.1	Spectroscopy	84
2.4.1.2	Analysis	85
2.4.1.3	Synthesis	85
2.4.2	<i>Synthesis of New Compounds</i>	85
2.5	REFERENCES	93
3.	SYNTHESIS OF MONO-DISPERSED SPHERICAL SILICA PARTICLES CONTAINING COVALENTLY BONDED CHROMOPHORES	97
3.1	INTRODUCTION	98
3.1.1	<i>Background</i>	98
3.1.2	<i>Bioaccumulation and degradation of UV filters in humans</i>	98
3.1.3	<i>Non-penetrating inorganic UV filters</i>	99

3.1.4	<i>New advances in non-penetrating UV filters</i>	100
3.2	RESULTS AND DISCUSSION	101
3.2.1	<i>Synthesis of Microspheres</i>	101
3.2.2	<i>Choice of UV filter</i>	101
3.2.3	<i>Synthesis of monomer</i>	102
3.2.4	<i>Microspheres containing a chromophore (MSI)</i>	104
3.2.5	<i>Microspheres with chromophores on the surface (MSS)</i>	107
3.2.6	<i>Microspheres containing chromophores in the core and on the surface (MSIG)</i>	110
3.2.7	<i>Photostability</i>	111
3.3	CONCLUSION	113
3.4	EXPERIMENTAL	114
3.4.1	<i>General</i>	114
3.4.1.1	<i>Spectroscopy</i>	114
3.4.1.2	<i>Analysis</i>	114
3.4.1.3	<i>Synthesis</i>	115
3.4.2	<i>Synthesis of New Compounds</i>	116
3.5	REFERENCES.....	134
4.	CHROMONE DERIVATIVES WHICH BIND TO HUMAN HAIR.....	139
4.1	INTRODUCTION.....	140
4.1.1	<i>Chromones</i>	140
4.1.2	<i>Biological Activity of Flavonoids</i>	140
4.1.3	<i>Structure Activity Relationships</i>	141
4.1.4	<i>Reactive Oxygen Species</i>	141
4.1.5	<i>Multifunctional Chromones</i>	141
4.2	RESULTS AND DISCUSSION.....	142
4.2.1	<i>Background</i>	142
4.2.2	<i>Synthesis of Chromone Derivatives with Hair Substantivity</i>	142
4.2.3	<i>Synthesis of substituted chromone derivatives</i>	143
4.2.4	<i>Hair Substantivity</i>	145
4.2.4.1	<i>SEM Images of treated and untreated hair</i>	148
4.2.5	<i>Antioxidant activities</i>	149
4.2.6	<i>Cyclic Voltammetry</i>	150
4.2.7	<i>UV absorption of substituted chromones</i>	151
4.3	CONCLUSION	152
4.4	EXPERIMENTAL	153
4.4.1	<i>General</i>	153
4.4.1.1	<i>Spectroscopy</i>	153
4.4.1.2	<i>Analysis</i>	154
4.4.1.3	<i>Synthesis</i>	155
4.4.1.4	<i>Hair Substantivity</i>	155
4.4.1.5	<i>X-ray Crystallography</i>	156

4.4.2	<i>Synthesis of New Compounds</i>	160
4.5	REFERENCES.....	181
5.	APPENDIX	185

1. Molecular Recognition of Azamacrocycles¹

1.1 Introduction

The field of coordination chemistry of polyazamacrocycles has undergone immense growth since the publication of seminal articles by Curtis ^[1] and Thompson and Curtin ^[2] in the early 1960s. Especially two cyclic tetraamines have played a key role in this field, namely 1,4,7,10-tetraaza-cyclododecane ([12]aneN₄ or cyclen) and 1,4,8,11-tetraaza-cyclotetradecane ([14]aneN₄ or cyclam).

1.1.1 General Properties of metal complexes of azamacrocycles

The fit between the size of the metal ion and the cavity provided by the macrocycle is crucial for the design of metal complexes. On complexation with transition metals, the stereo-electronic requirements must also be taken into account.^[3,4] As the cavity of the 12-membered cyclen is smaller than that of 14-membered cyclam, the macrocycle tends to fold around metal ions with octahedral coordination geometry adopting a *cis* conformation.^[4-6]

In general, tetraazamacrocycles exhibit high basicity in the first two protonation steps and rather low basicity in the last two steps. The critical protonation constants ($\log K^{\text{H}}_{\text{i}}$) for cyclen and cyclam and stability constants ($\log K_{\text{M}_m\text{H}_h\text{L}_l}$) of their complexes with several metal ions are reported in Table 1.

¹ The results of this chapter are in preparation for submission:

Kruppa, M.; Walenzyk, T.; Koenig, B. *Chem. Rev.*

Table 1: Protonation constants ($\log K^H_i$) for cyclen and cyclam and stability constants ($\log K_{M_mH_hL_l}$) of their complexes with selected metal ions. T = 25 °C.

Ion	Equilibrium quotient	Cyclam	Cyclen
H^+	$[HL]/[L] \times [H]$	11.58, ^a 11.3 ^b	10.97 ^h
	$[H_2L]/[HL] \times [H]$	10.62, ^a 10.23 ^b	9.87 ^h
	$[H_3L]/[H_2L] \times [H]$	1.61, ^a 1.43 ^b	1.6 ⁱ
	$[H_4L]/[H_3L] \times [H]$	2.42, ^a 2.27 ^b	0.8 ⁱ
	$[H_4L]/[L] \times [H]^4$	26.23, ^a 25.23 ^b	23.24 ^{h,i}
Ni^{2+}	$[ML]/[M] \times [L]$	22.2, ^c 20.1 ^d	16.4 ^j
	$[MHL]/[ML] \times [H]$	2.3 ^d	
Cu^{2+}	$[ML]/[M] \times [L]$	26.5, ^b 27.2 ^e	23.29, ^b 24.8 ^e
Zn^{2+}	$[ML]/[M] \times [L]$	15.0, ^e 15.5 ^f	16.2 ^f
	$[ML]/[MLOH] \times [H]$	3.99 ^g	5.74 ^g
Cd^{2+}	$[ML]/[M] \times [L]$	11.23 ^b	14.3 ^f
Pb^{2+}	$[ML]/[M] \times [L]$	10.83 ^b	15.9 ^f
Co^{2+}	$[ML]/[M] \times [L]$	12.7 ⁱ	
Hg^{2+}	$[ML]/[M] \times [L]$	23.0 ^k	25.5 ^k

^a I = 0.5 mol dm⁻³ KNO₃ [7], ^b I = 0.1 mol dm⁻³ NaNO₃ [8], ^c I = 0.1 mol dm⁻³ NaOH [9], ^d I = 0.5 mol dm⁻³ NaCl [10], ^e I = 0.2 mol dm⁻³ KNO₃ [11,12], ^f I = 0.2 mol dm⁻³ NaClO₄ [13], ^g I = 0.2 mol dm⁻³ KNO₃ [14], ^h I = 0.5 mol dm⁻³ KNO₃ [15], ⁱ I = 0.2 mol dm⁻³ NaClO₄ [16], ^j I = 0.1 mol dm⁻³ NaNO₃ [17], ^k I = 0.2 mol dm⁻³ KNO₃ [18]

1.1.2 Scope

In this review the role of metal complexes of 1,4,7-triazonane ([9]aneN₃), 1,5,9-triaza-cyclododecane ([12]aneN₃), 1,4,7,10-tetraaza-cyclododecane (cyclen or [12]aneN₄) and 1,4,8,11-tetraaza-cyclotetradecane (cyclam or [14]aneN₄) as molecular binding sites is discussed (Figure 1). Many metal complexes of azamacrocycles have in addition to the azamacrocyclic ligand additional reversibly coordinated ligands. Their binding and exchange can be used in molecular recognition, if reversible and rapid. In the following review we discuss the current literature (up to early 2005) available for such binding situations. Reported X-ray structure analyses of [9]aneN₃ cyclen and cyclam metal

complexes which coordinate additional ligands and the literature on solution studies involving reversible coordination to [9]aneN₃, [12]aneN₃, cyclen and cyclam complexes are summarised and discussed.

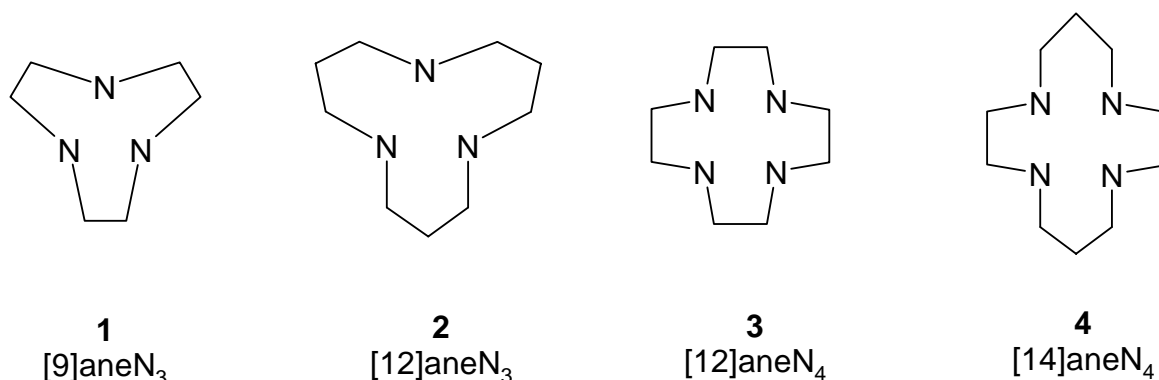


Figure 1: The parent structures [9]aneN₃, [12]aneN₃, [12]aneN₄ and [14]aneN₄.

In order to be considered, the parent structure needed to complex a metal, thereby coordinating to all nitrogens (3 in the case of [9]aneN₃ and [12]aneN₃ and 4 in the case of [12]aneN₄ and [14]aneN₄) in the azamacrocycle. Alkyl, phenyl and aryl substitution at any position (carbon or nitrogen substitution) was allowed provided such substitution did not affect the geometry of the parent structure nor introduce additional ligands which coordinate to the metal and thus induce a change in the coordination geometry.

Such metal complexes needed to undergo an intermolecular coordination with another molecule. Only metal coordination with O, N and S atoms was examined. Metal complexes which only coordinated to halogens, sulfates, perchlorates, cyanides, isothiocyanides, azides, nitrates, nitrites, carbonates and solvent molecules (DMF, DMSO, H₂O) were excluded. In general the guest molecule should be an organic entity which can coordinate to the host, ideally under physiological conditions.

1.2 Structures of 1,4,7,10-tetraaza-cyclododecane ([12]aneN₄ or cyclen) complexes in solid state

1.2.1 Co(III) complexes

[Co(cyclen)-(X)Y]ⁿ⁺ species exhibit exclusive *cis* stereochemistry, but exist as various isomeric forms depending on the orientation (*syn* or *anti*) of the *sec*-NH protons at the two equatorial sites.^[19] The X-ray structure analysis of [Co(cyclen)(O₂C₂O₂)]⁺ (Figure 2) shows the oxalate coordinated with a *cis* stereochemistry with the Co(III) atom adopting a distorted octahedral geometry which is typical for Co(III) cyclen complexes.^[20-23] Similar complexes such as [Co(cyclen)-(O₂CCH₂CO₂)]⁺,^[19] show the same geometry.

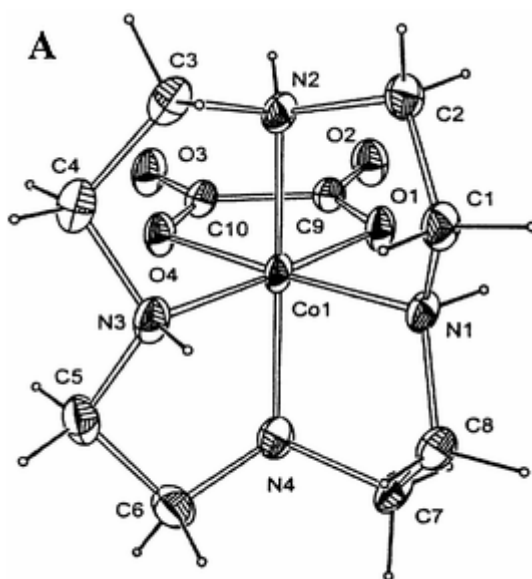


Figure 2: Structure of *syn,anti*-[Co(cyclen)(O₂C₂O₂)]⁺ in the crystal. Thermal ellipsoids are drawn at the 50 % probability level.

On coordination with a monodentate ligand such as a phosphite anion, Co(III) cyclen maintains its octahedral geometry by also coordinating a water molecule (Figure 3).^[24]

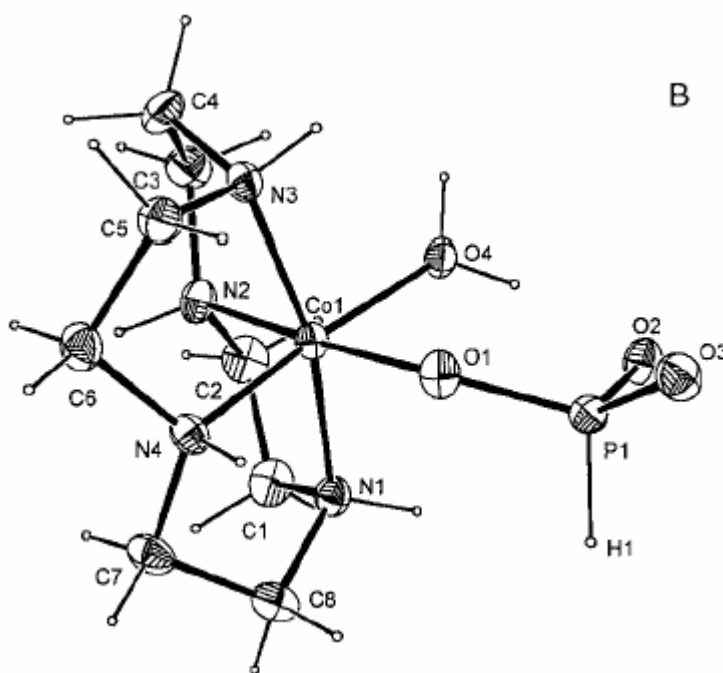


Figure 3: Structure of $\text{syn}(\text{OP}(\text{H})(\text{O})_2), \text{anti}(\text{OH}_2)-[\text{Co}(\text{cyclen})(\text{OH}_2)\{\text{OP}(\text{H})(\text{O})_2\}]^+$ in the solid state. Thermal ellipsoids are drawn at the 50 % probability level.

Co(III) complexes of cyclen also coordinate diamines, such as ethylenediamine, 2-(aminomethyl)pyridine, (*R*)-1,2-propanediamine, (*R,R*)-1,2,-diaminocyclohexane, trimethylenediamine or 2-methyl-1,3-diaminopropane.^[25,26]

In addition the coordination of amino acids such as alanine to Co(III) complexes has been reported.^[20,27] Figure 4 shows the *cis* octahedral geometry, with the macrocycle coordinated in a folded manner which leaves space available for the coordination of two other monodentate ligands or a bidentate one.

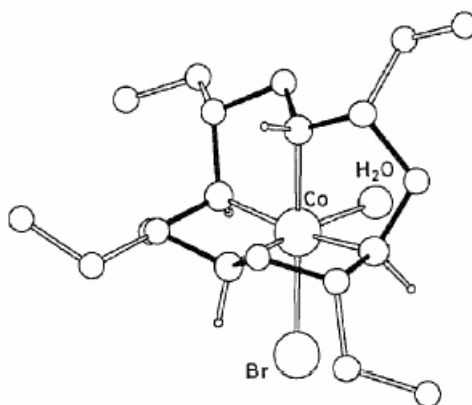


Figure 4: The structure of the Co(III) complex of (2*R*,5*R*,8*R*,11*R*)-2,5,8,11-tetraethyl-1,4,7,10-tetra-azacyclododecane.

Figure 5 shows the X-ray structure of the Co(III) complex of (2*R*,5*R*,8*R*,11*R*)-2,5,8,11-tetraethyl-1,4,7,10-tetra-azacyclododecane bound to (*S*)-alanine. The stereochemistry of the amino acid is maintained upon coordination to Co(III) ion.^[28]

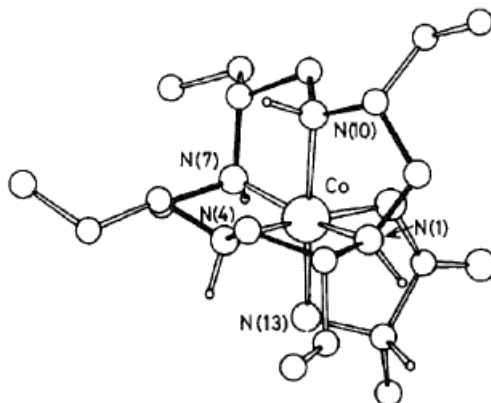


Figure 5: The crystal structure of the Co(III) complex of (2*R*,5*R*,8*R*,11*R*)-2,5,8,11-tetraethyl-1,4,7,10-tetra-azacyclododecane bound to (*S*)-alanine.

1.2.2 Cu(II) complexes

Several structures of Cu(II) complexes of cyclen have been reported.^[29,30] X-ray analyses show that copper is coordinated in a square planar geometry with the four nitrogens of cyclen.^[31] However no solid state structures of complexes with additional ligands coordinated to copper have been reported.

1.2.3 Ni(II) complexes

Nickel(II) cyclen complexes have an octahedral coordination sphere by binding two water molecules in a *cis* orientation that only slowly exchange with other ligands.^[32,33] Figure 6 shows the structure of the $[\text{Ni}(\text{cyclen})(\text{H}_2\text{O})_2]^{2+}$ cation in the solid state.^[34]

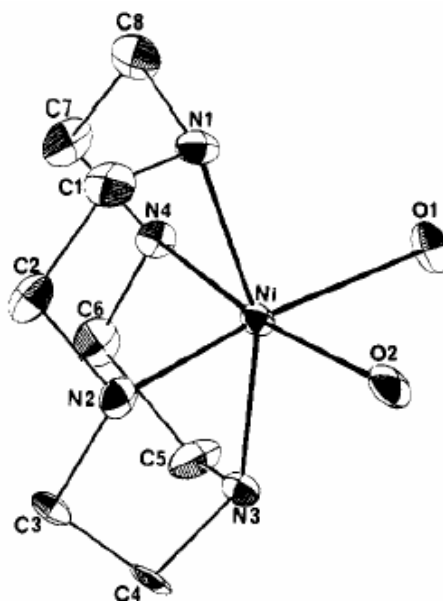


Figure 6: Structure of the $[\text{Ni}(\text{cyclen})(\text{H}_2\text{O})_2]^{2+}$ cation in the solid state. Hydrogen atoms are omitted for clarity. Probability ellipsoids are 30 %.

An N-methylated Ni(II) cyclen derivative leads to the $[\text{Ni}_2(\text{Me}_2\text{-cyclen})_2\text{ox}]^{2+}$ binuclear cation (where ox = oxalate anion).^[34] The oxalate dianion acts a tetradentate bridging ligand between two Ni(II) cyclen complexes.

The Ni(II) cyclen complex was also found to coordinate imidazole. The X-ray structure analysis shows the Ni(II) ion in a distorted octahedral coordination geometry consisting of four nitrogen atoms from cyclen as ligands, one nitrogen atom from the imidazole and one oxygen atom from one of the perchlorate ions.^[35] The same distorted octahedral geometry is also illustrated in the following example where a Ni(II) cyclen complex binds an acetate anion (Figure 7).^[36]

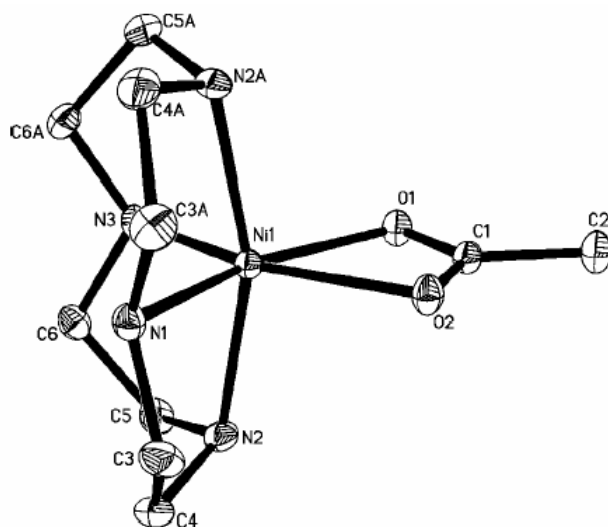


Figure 7: Structure of $[\text{Ni}(\text{cyclen})(\eta^2\text{-CH}_3\text{CO}_2)]^+$ cation in the solid state. Hydrogen atoms are omitted for clarity. Probability ellipsoids are 30%.

Ni(II) cyclen complexes coordinate phenanthroline (phen) (Figure 8) ^[37] and 7,7,8,8-tetracyanoquinodimethane (TCNQ) ^[30] as additional ligands giving distorted octahedral coordination geometry consisting of four nitrogen atoms from cyclen and two nitrogens atoms from the heteroaromatic ligand.

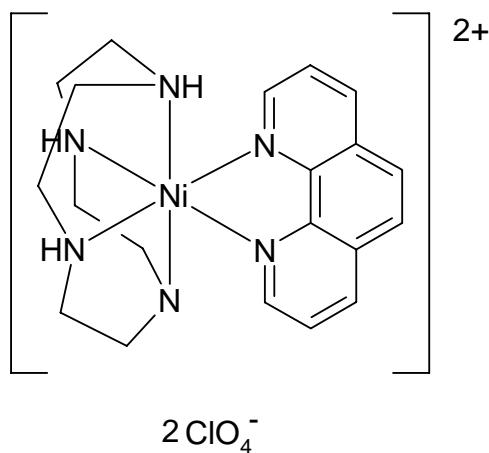


Figure 8: Molecular structure of $[\text{Ni}(\text{cyclen})(\text{phen})](\text{ClO}_4)_2$.

1.2.4 Zn(II) complexes

Zn(II) cyclen complexes interact with uridine (U) and thymidine (T) nucleotides by specific Zn^{2+} -imide N^- coordination (Figure 9).^[38] Additional stabilisation of this structure

by hydrogen bonds between amine N-H of the cyclen ligand and the carbonyl groups of the heterocycle have been proposed, but solid evidence is missing.

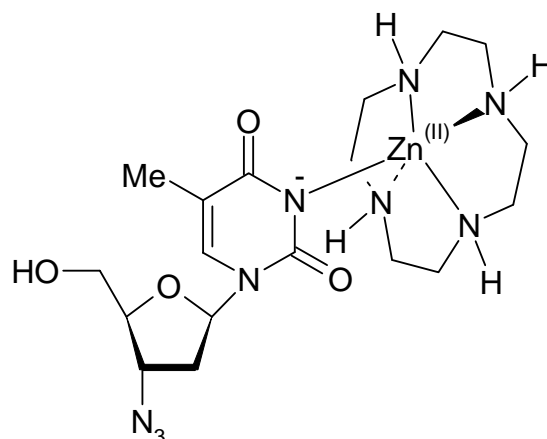


Figure 9: Zn(II) cyclen complexes selectively coordinate the imide group in nucleosides, such as 3'-azido-3'-deoxythymidine (AZT).

The X-ray structure analysis of $[\text{Zn}(\text{cyclen})(\text{AZT})](\text{H}_2\text{O})_2(\text{ClO}_4)$ reveals a distorted square pyramidal N_5 -coordination geometry for the Zn(II) ion (Figure 10).^[38]

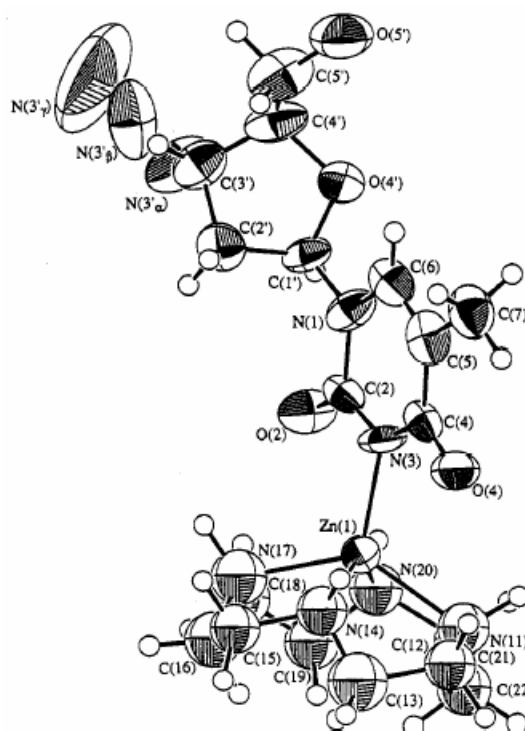


Figure 10: Structure of $[\text{Zn}(\text{cyclen})(\text{AZT})](\text{H}_2\text{O})_2(\text{ClO}_4)$ (AZT = 3'-azido-3'-deoxythymidine) in the crystal. A perchlorate anion and two water molecules are omitted for clarity. Probability ellipsoids are 50%.

This distorted square pyramidal geometry is also present when Zn(II) cyclen coordinates to the important metabolite creatinine (Figure 11).^[39]

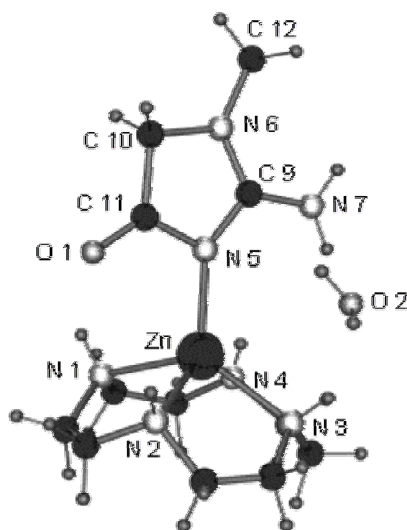


Figure 11: Structure of $[\text{Zn}(\text{cyclen})(\text{creatinine})](\text{ClO}_4)_2$. Two perchlorate anions are omitted for clarity.

Zn(II) cyclen complexes coordinated with phosphate anions as additional ligands have been described and characterised by X-ray analysis. (Figure 12).^[40] The *para*-nitro phenyl ester of phosphate (NPP^{2-}) forms a complex with three Zn(II) cyclen complexes. The three oxygen atoms of the phosphate anion act as the fifth ligand for the Zn(II) ions coordinated by the cyclen ligand.

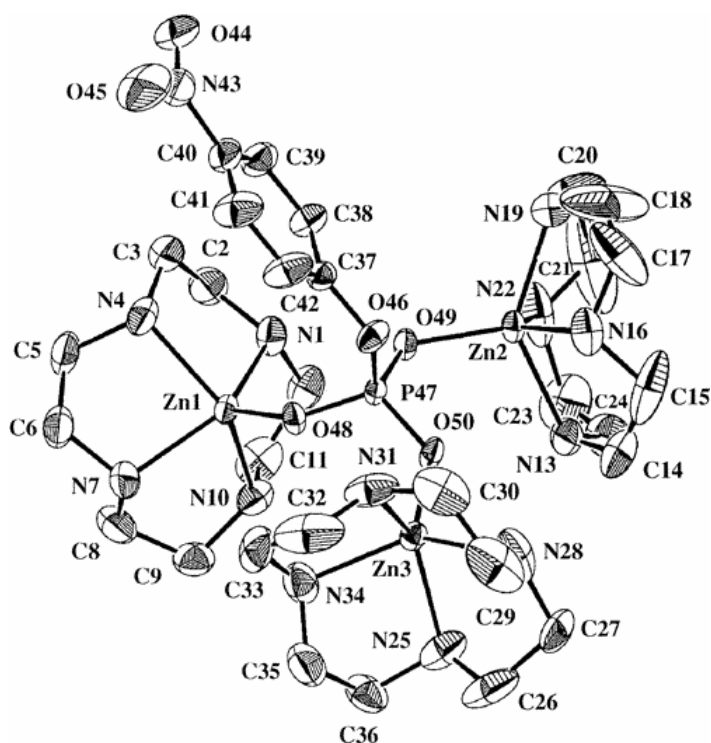


Figure 12: Structure of $\text{Zn}(\text{cyclen})_3\text{-NPP}^{2-}$ in the solid state. All hydrogen atoms, perchlorate anions and water molecules are omitted for clarity. Probability ellipsoids are 30%.

An imidazolate anion can act as a bridging ligand for two $\text{Zn}(\text{II})$ cyclen complexes. The X-ray structure analysis (Figure 13) shows the two $\text{Zn}(\text{II})$ ions with distorted square pyramidal coordination geometry composed of four nitrogen atoms from cyclen ligand and one nitrogen atom from the bridging imidazolate ion.^[35]

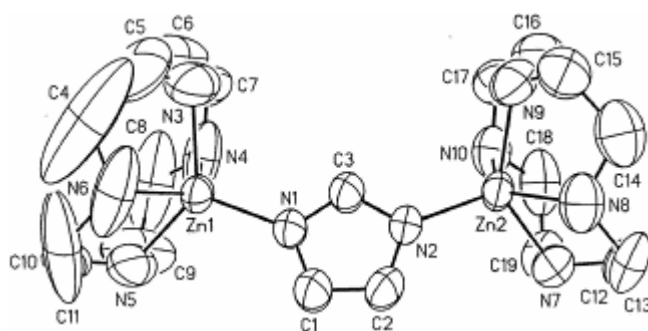


Figure 13: Structure of $[\text{Zn}(\text{cyclen})]_2\text{-im}$ (im = imidazolate) in the solid state.

Structures of bis- $\text{Zn}(\text{II})$ cyclen complexes coordinate barbitol (Figure 14)^[41] as well as thymidine and uridine nucleosides, such as thymidine 5'-monophosphate (5'-dTMP).^[42] The aggregates have a 2:2 stoichiometry and consist of a macrocyclic arrangement.

Tris-Zn(II) cyclen variations have also been reported to coordinate organic phosphate dianions.^[40]

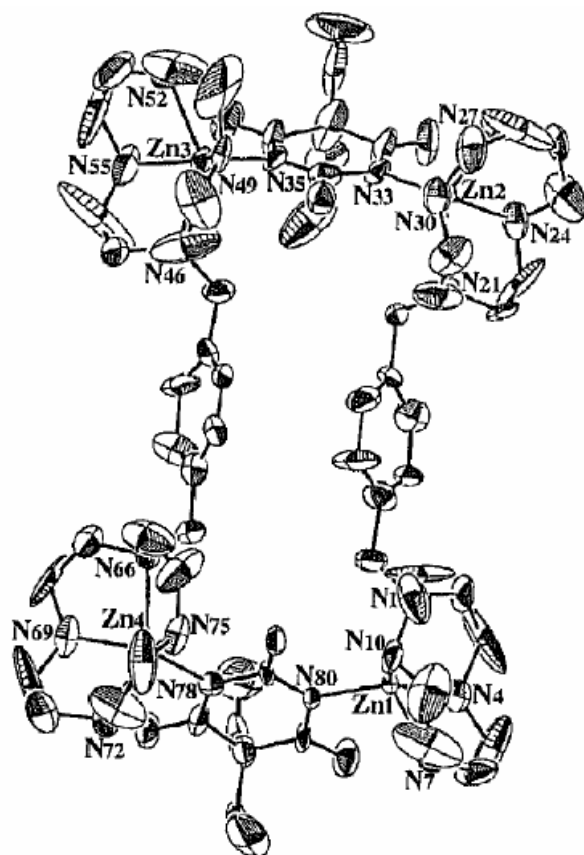
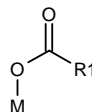
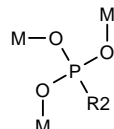
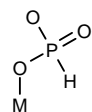
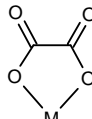
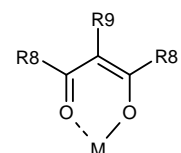
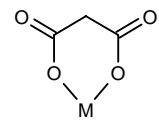


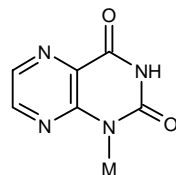
Figure 14: Structure of bis-[Zn(cyclen)]-bar²⁻ (bar = barbitate) as a 2:2 complex in the crystal. All hydrogen atoms, perchlorate anions and water molecules are omitted for clarity. Probability ellipsoids are 30%.

1.3 Structures of 1,4,7,10-tetraaza-cyclododecane ([12]aneN₄ or cyclen) complexes in solid state (Tabulated)

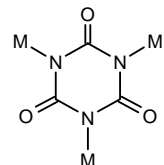
Table 2 summarises all X-ray structures registered at the Cambridge Crystallographic Database according to the selection criteria previously mentioned.

Table 2: Structurally characterised metal complexes of 1,4,7,10-tetraaza-cyclododecane with additional ligand coordinated to the metal ion in the solid state.

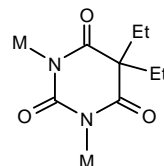
Structure of the additional ligand	Metal ions				
	Zn ²⁺	Ni ²⁺	Co ³⁺	Rh ³⁺	Ru ²⁺
	⁽¹⁾ See ref. [43]				
	⁽²⁾ See ref. [40,44]				
			⁽³⁾ See ref. [24]		
			⁽⁴⁾ See ref. [19]		
		⁽⁵⁾ See ref. [45]	⁽⁶⁾ See ref. [46]		
			⁽⁷⁾ See ref. [19]		



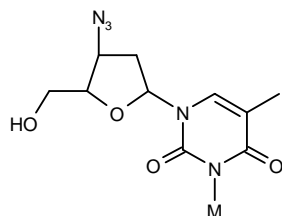
⁽⁸⁾ See ref.
[47]



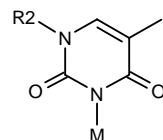
⁽⁹⁾ See ref.
[48]



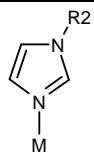
⁽¹⁰⁾ See ref.
[49]



⁽¹¹⁾ See ref.
[38]

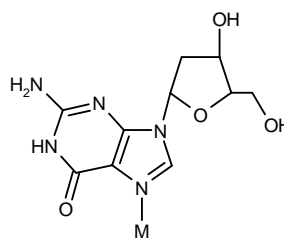


⁽¹²⁾ See ref.
[50,51]

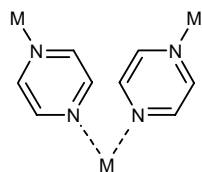


(13) See ref.
[35]

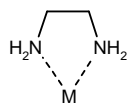
(14) See ref.
[35]



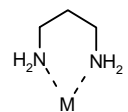
(15) See ref.
[50]



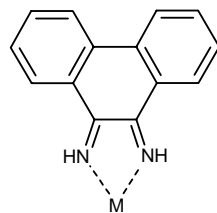
(16) See ref.
[52]



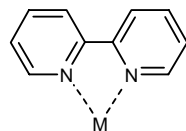
(17) See ref.
[26]



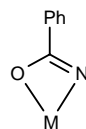
(18) See ref.
[26]



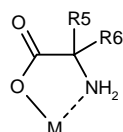
⁽¹⁹⁾ See ref.
[53]



⁽²⁰⁾ See ref.
[37,54]

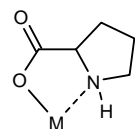


⁽²¹⁾ See ref.
[21]

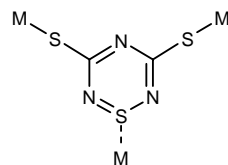


⁽²²⁾ See ref.
[55]

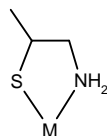
⁽²³⁾ See ref.
[20,56-65]



⁽²⁴⁾ See ref.
[66]



⁽²⁵⁾ See ref.
[67]



⁽²⁶⁾ See ref.

[68]

⁽¹⁾ Substitution - n-aryl; R1 = aryl; ⁽²⁾ a) Substitution - none; R2 = *p*-nitrophenolate; ⁽²⁾ b) Substitution - n-alkyl; R2 = O; ⁽³⁾ Substitution - none; ⁽⁴⁾ Substitution - none; ⁽⁵⁾ Substitution - n-alkyl (cage); R8 = CH₃, R9 = H; ⁽⁶⁾ a) Substitution - none; R8 = CH₃, R9 = H; ⁽⁶⁾ b) Substitution - none; R8 = CH₃, R9 = Br; ⁽⁷⁾ Substitution - none; ⁽⁸⁾ Substitution - none; ⁽⁹⁾ Substitution - none; ⁽¹⁰⁾ Substitution - none; ⁽¹¹⁾ Substitution - none; ⁽¹²⁾ Substitution - n-aryl; R2 = CH₃; ⁽¹³⁾ Substitution - none; R2 = Metal; ⁽¹⁴⁾ Substitution - none; R2 = H; ⁽¹⁵⁾ Substitution - n-aryl; ⁽¹⁶⁾ Substitution - none; ⁽¹⁷⁾ Substitution - none; ⁽¹⁸⁾ Substitution - none; ⁽¹⁹⁾ Substitution - none; ⁽²⁰⁾ Substitution - none; ⁽²¹⁾ Substitution - n-alkyl; ⁽²²⁾ Substitution - n-alkyl; R5 = H, R6 = CH₃ (alanine); ⁽²³⁾ a) Substitution - c-alkyl; R5 = H, R6 = CH₃ (alanine); ⁽²³⁾ b) Substitution - c-alkyl; R5 = COOH, R6 = CH₃; ⁽²³⁾ c) Substitution - c-alkyl; R5 = H, R6 = CH₂OH (serine); ⁽²³⁾ d) Substitution - c-alkyl; R5 = CH₃, R6 = CH₂OH (methylserine); ⁽²³⁾ e) Substitution - c-alkyl; R5 = H, R6 = H (glycine); ⁽²³⁾ f) Substitution - c-alkyl; R5 = H, R6 = -CH₂CH₂-S-CH₃; ⁽²³⁾ g) Substitution - c-alkyl; R5 = H, R6 = CH(OH)CH₃ (threonine); ⁽²³⁾ h) Substitution - c-alkyl; R5 = CH₃, R6 = CH₂PhOH (methyltyrosine); ⁽²⁴⁾ Substitution - none; ⁽²⁵⁾ Substitution - none; ⁽²⁶⁾ Substitution - none

1.4 Molecular recognition of 1,4,7,10-tetraaza-cyclododecane ([12]aneN₄ or cyclen) complexes in solution

1.4.1 Co(III) complexes

The optically active Co(III) complex of (2*R*,5*R*,8*R*,11*R*)-2,5,8,11-tetraethyl-1,4,7,10-tetraazacyclododecane was found to react with several neutral amino acids at pH 8 to form the corresponding amino acidato complexes.^[56] The stereochemistry of the amino acid was retained on complexation with the macrocycle.

1.4.2 Cd(II) complexes

The Cd(II) complex of cyclen containing 7-amino-4-trifluoromethylcoumarin, **5** was designed as a fluorescent reporter.^[69] Particular phosphate and citrate anions are bound by the metal complex, thus displacing the aromatic amino group of the coumarin and causing a change of the excitation spectrum (Figure 15).

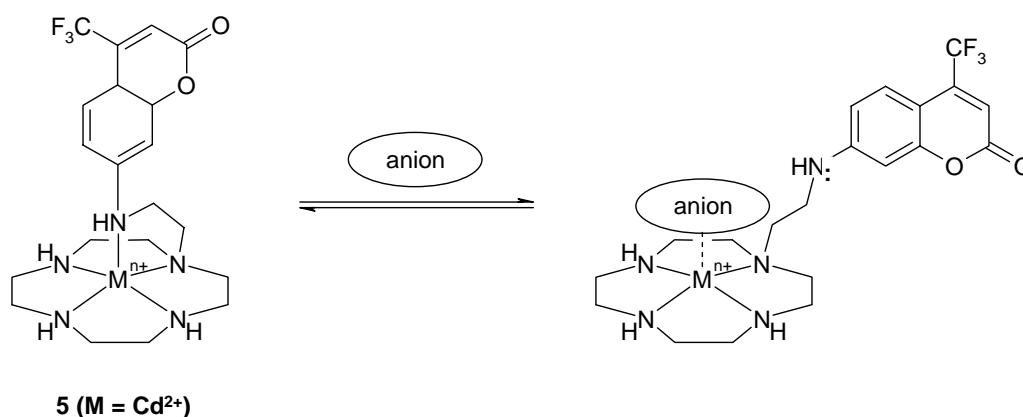


Figure 15: Sensoric principle of phosphate ion sensing with **5**.

The metal complex detects pyrophosphate and citrate with high selectivity, whilst no response was shown for fluoride or perchlorate. Organic anions such as adenosine triphosphate (ATP) and adenosine diphosphate (ADP) also gave strong signals whilst cyclo-adenosine monophosphate (cAMP) showed little response (Table 3). The sensing mechanism was shown to be reversible.

Table 3: Apparent dissociation constants (K_d) of sensor **5** for anions in 100 mM HEPES Buffer (pH 7.4).

Anion	K_d (M)
Pyrophosphate	7.5×10^{-5}
Citrate	9.0×10^{-5}
Phosphate	1.5×10^{-2}
ATP	1.4×10^{-5}
ADP	2.6×10^{-5}
GMP	4.8×10^{-5}
AMP	4.4×10^{-4}
UMP	1.7×10^{-3}
UMP	1.7×10^{-3}
cAMP	a

a K_d is too large to be calculated.

1.4.3 Zn(II) complexes

The prevalence of Zn(II) ions in biological systems has led to a large number of Zn(II) complexes as models for such systems. A comprehensive review on the molecular interactions of Zn(II) cyclen and its derivatives was recently published.^[70] On complexation with cyclen, the acidity of the Zn(II) ion is reinforced, which results in a lowering of the pK_a value of the Zn(II)-bound water from 9.0 to 7.9 at 25 °C.^[38] Zn(II) cyclen forms 1:1 complexes with deprotonated sulfonamides at neutral pH, despite the weak acidity of sulfonamides with pK_a values of 7-10 (Figure 16).^[71,72]

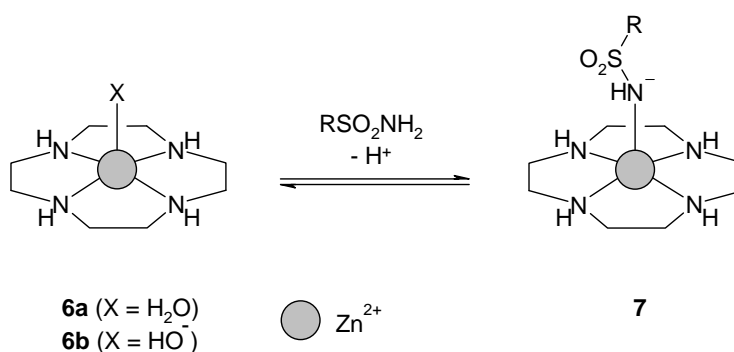


Figure 16: Reversible coordination of sulphonamide anions to Zn(II) cyclen

Following a similar principle, Zn(II) cyclen complexes have been applied to the molecular recognition of nucleobases, thymine (dT) and uracil (U), which possess similarly weak acidic (pK_a around 10) protons at their ‘imide’ groups.^[73] The centrosymmetric linear

arrangement of the three-point functional groups in **8** comprises the acidic Zn(II) acting to yield the ‘imide’ anion to form a stable Zn(II)-N(3)⁻ bond and the two hydrogens attached to cyclen nitrogens to form two complementary hydrogen bonds with each of the ‘imide’ carbonyls. This specific Zn²⁺-imide N⁻ coordination allows the reversible coordination of flavin derivatives, which are important cofactors of flavoproteins^[74-76] and photolyases.^[77] These electronic and structural fittings also permit formation of extremely strong 1:1 complexes of **8** with dT, AZT, U, Ff (5-fluorouracil) and riboflavin (Figure 17). Zn(II) cyclen complexes appended with polyaromatic rings were shown to selectively bind to T- or U-rich sequences in double stranded DNA (or RNA) to denature them.^[50,78] It does not interact with the other DNA nucleosides (i.e. dG, dA and dC) making the reversible coordination selective.

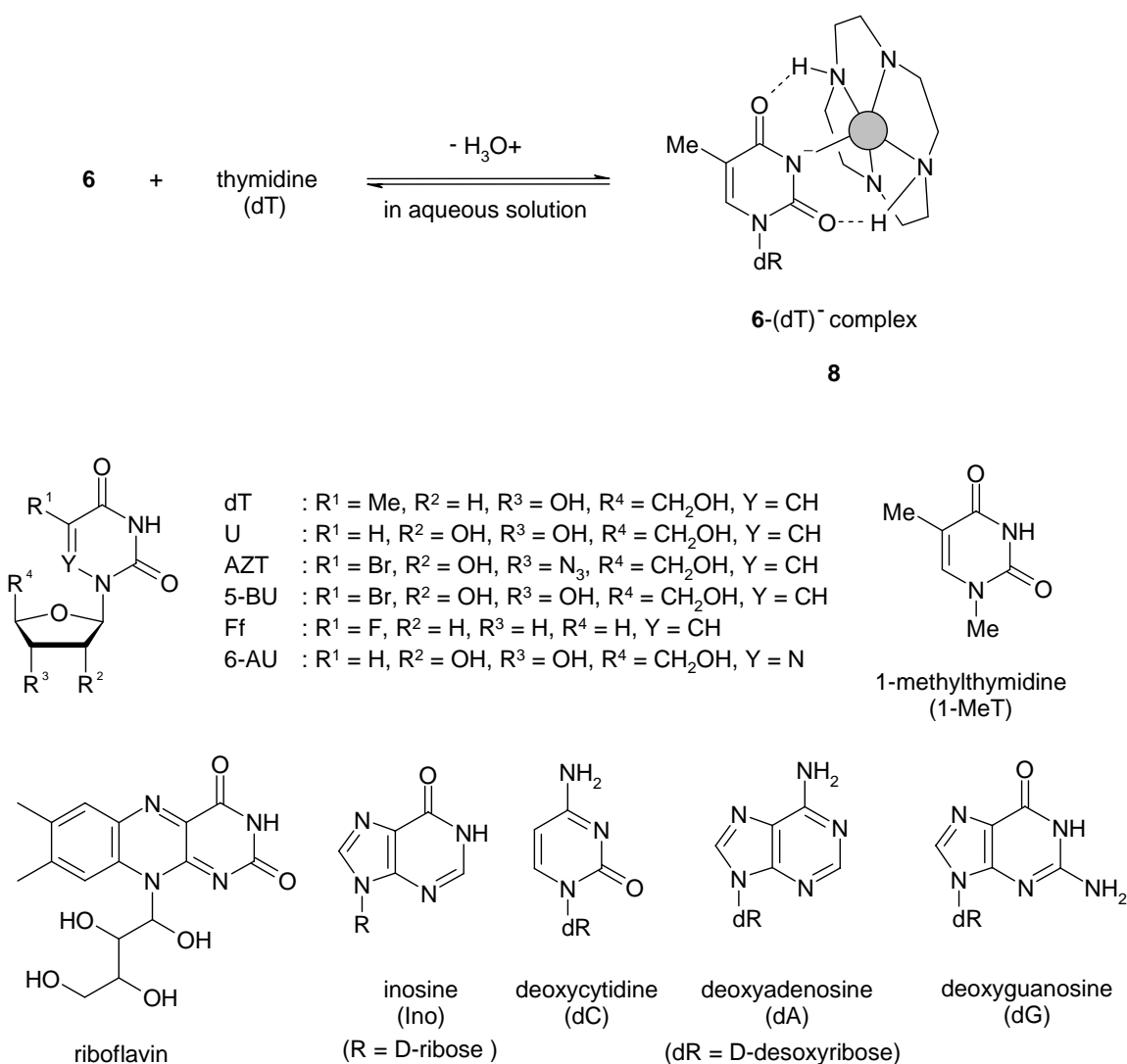


Figure 17: Zn(II) cyclen complex coordination to molecules bearing slightly acidic imide groups.

Zn(II) cyclen complexes reversibly coordinate phosphate dianions such as HPO_4^{2-} , phenyl phosphate (PP^{2-}) and 4-nitrophenyl phosphate (NPP^{2-}) as monodentate ligands to yield 1:1 complexes **9** in solution (Figure 18).^[79] The observed binding affinities in neutral aqueous solution are in the millimolar range.

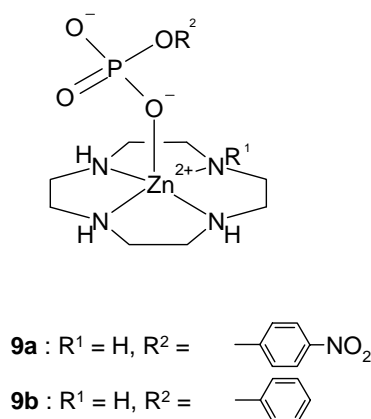


Figure 18: Zn(II) cyclen coordinating monodentate phosphate dianions.

The dianions of phosphate monoesters, RPO_3^{2-} are potential bidentate donors and bridge two Zn(II) ions (Figure 19). A bis-Zn(II) cyclen complex linked with a *meta*-xylene spacer forms a stable complex with NPP^{2-} with $\log K_s$ of 4.0 in aqueous solution ($I = 0.1 \text{ NaClO}_4$ at 25°C).^[41]

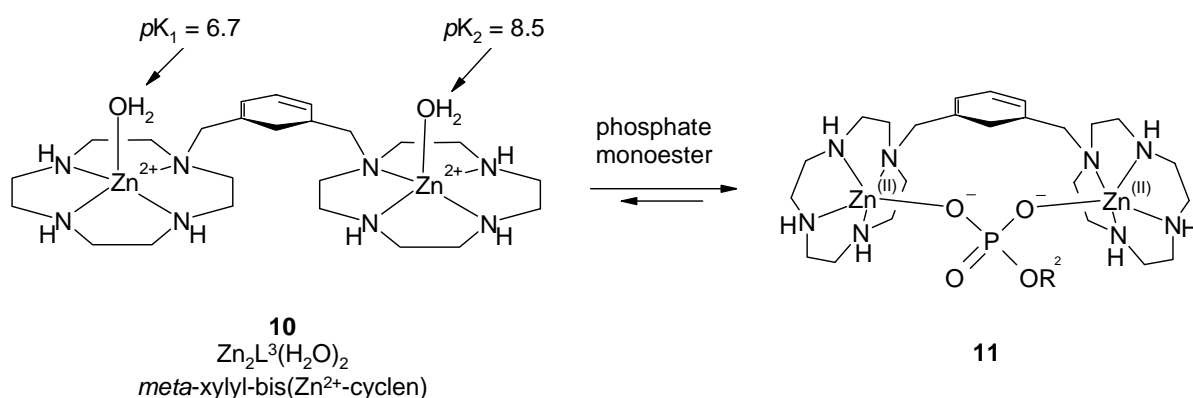
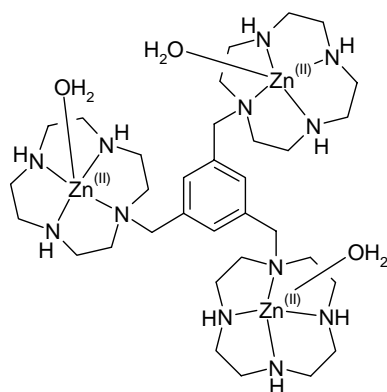


Figure 19: Bis-Zn(II) cyclen complexes bind phosphate monoesters in a bidentate fashion.



12
 $\text{Zn}_3\text{L}^5(\text{H}_2\text{O})_3$
 tris(Zn^{2+} -cyclen)

Figure 20: The C_3 -symmetric tris-Zn(II) cyclen complex **12**.

A yet higher binding constant could be achieved for tris-Zn(II) cyclen complexes (Figure 20).^[40] Table 4 summarises the phosphate affinity constants of Zn(II) cyclen, bis-Zn(II) cyclen and tris-Zn(II) cyclen.

Table 4: Phosphate (phosphonate) affinity constants ($\log K_s$)² of Zn(II) cyclen **9**, *m*-bis(Zn(II) cyclen) **10** and tris(Zn(II) cyclen) **12**, for NPP^- , PP^{2-} , phenyl phosphonate (PhP^{2-}), and α -D-glucose 1-phosphate ($\alpha\text{-Glu-P}^{2-}$) at 25 °C and $I = 0.10$ (NaNO_3).^[80]

Phosphate (phosphonate)	$(\text{p}K_2')^b$	$\text{Log } K_s^a$		
		9	10	12
NPP^{2-}	(5.2)	3.1	4.0	5.8
PP^{2-}	(5.9)	3.5	4.6	6.6
$\alpha\text{-Glu-P}^{2-}$	(6.1)	-	-	7.0
PhP^{2-}	(7.0)	-	-	7.9

^a $K_s = [\text{ZnL}^1\text{-RPO}_3^{2-} \text{ complex}] / [\text{ZnL}^1][\text{RPO}_3^{2-}]$ (M^{-1}) for **9**, $[\text{Zn}_2\text{L}^3\text{-RPO}_3^{2-} \text{ complex}] / [\text{Zn}_2\text{L}^3][\text{RPO}_3^{2-}]$ (M^{-1}) for **10**, or $[\text{Zn}_3\text{L}^5\text{-RPO}_3^{2-} \text{ complex}] / [\text{Zn}_3\text{L}^5][\text{RPO}_3^{2-}]$ (M^{-1}) for **12**.

^b $K_2' = -\log ([\text{RPO}_3^{2-}]a_{\text{H}} + [\text{RPO}_3\text{H}^-])$ obtained by pH titration at 25 °C with $I = 0.10$ (NaNO_3).

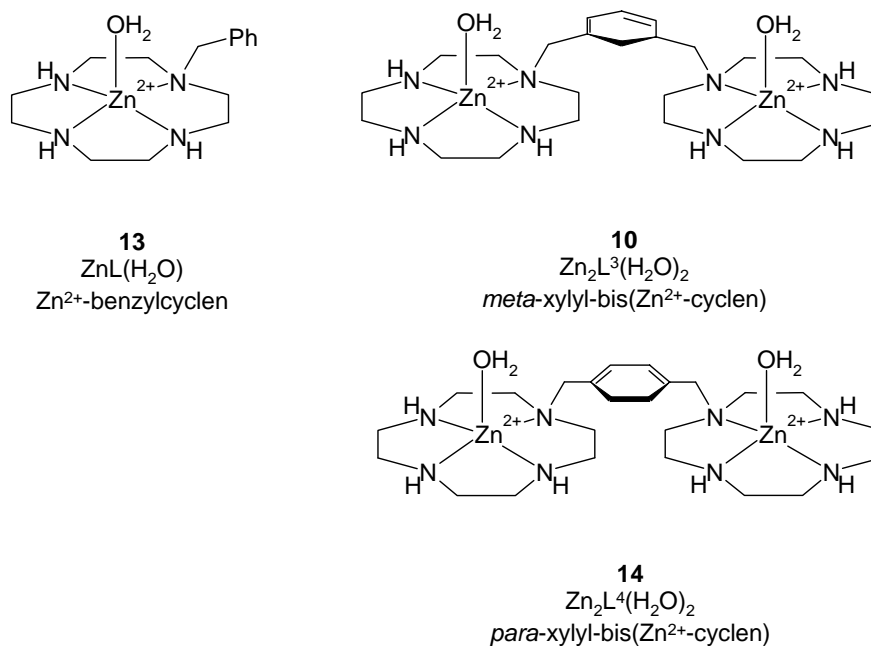


Figure 21: Zn(II) benzylcyclen, *m*-xylyl-bis-[Zn(II) cyclen] and *p*-xylyl-bis-[Zn(II) cyclen].

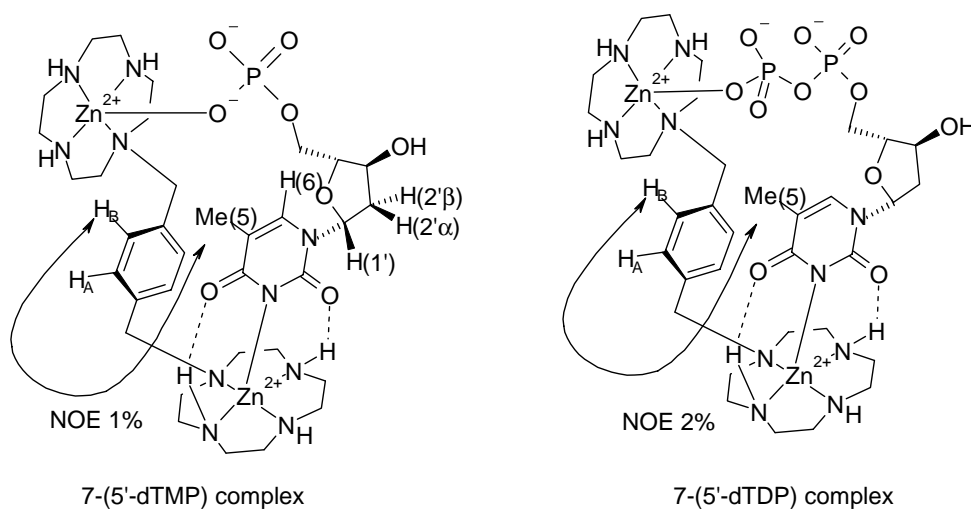


Figure 22: The binding of *p*-bis-[Zn(II) cyclen] to 5'-dTMP and 5'-dTDP respectively, showing the NOE interactions.

The bis-[Zn(II) cyclen] complexes **10** and **14** (Figure 21 and 22) can bind imide-containing nucleotides. Table 5 compares the apparent complexation constants of **13**, **10** and **14**.^[80]

Table 5: Apparent complexation constants ($\log K_{\text{app}}$) for imide-containing nucleotides with Zn(II) cyclen complexes at pH 7.6 and 25 °C.

	13	10	14
dT	3.2 ^a (5.7) ^d	3.2, 3.2 ^b	
	3.4 ^c	(10:dT = 1:2)	
c-dTMP	3.3 ^c	3.5, 3.5 ^b	
		(10:c-dTMP = 1:2)	
5'-CMP	3.3 ^a (3.7) ^d	3.2 ^a (4.3) ^d	
	3.3 ^b	3.4 ^b	
3'-dTMP		5.2 ^a (8.6) ^d	5.9 ^a (8.9) ^d
		5.3 ^b	5.8 ^{b,e}
		5.4 ^{c,f}	5.8 ^{c,f}
5'-dTMP	3.4, 3.4 ^b	5.5 ^a (9.3) ^d	6.4 ^a (9.6) ^d
	(27:5'-dTMP = 2:1)	5.5 ^b	> 6 ^{b,e}
		5.7 ^{c,f}	> 6 ^{c,f}
2'-UMP		5.7 ^b	
3'-UMP		4.8 ^a (7.8) ^d	5.5 ^a (8.5) ^d
		5.2 ^{c,f}	5.7 ^{c,f}
5'-UMP		5.4 ^a (8.3) ^d	6.2 ^a (8.8) ^d
		5.5 ^{c,f}	> 6 ^b
			> 6 ^{c,f}
5'-dTDP		5.6 ^b	> 6 ^b
		5.5 ^{c,f}	> 6 ^{c,f}
5'-dTTP		5.0 ^b	5.6 ^b
5'-AZTMP		5.5 ^b	> 6 ^{b,e}
		5.7 ^{c,f}	> 6 ^{c,f}
5'-AZTDP		5.3 ^b	5.9 ^b
		5.5 ^c	> 6 ^{c,f}

^a Determined by potentiometric pH titration.

^b Determined by isothermal titration calorimetry (50 mM HEPES buffer).

^c Determined by UV titration in 50 mM HEPES buffer with $I = 0.1$ (NaNO₃).

^d For the intrinsic complexation constants K_s , see reference.

^e Titrations were carried out at [5'-dTMP] = 0.2 mM and 0.1 mM and the average values were listed.

^f Titrations were carried out at [nucleotide] = 0.1 mM and 50 μ M and the average values were listed.

The search for small molecules that interact with RNA is currently attracting great interest for drug discovery in AIDS therapeutics.^[81] The transcription of HIV-1 genome is facilitated by a HIV-1 regulatory protein Tat which activates the synthesis of full-length HIV-1 mRNA by its binding to a TAR (*trans*-activation responsive) element RNA.^[82] The TAR element comprising the first 59 nucleotides of the HIV-1 primary transcript adopts a hairpin structure with a uracil (U)-rich bulge (UUU or UCU), which is the Tat binding site. Linear tris-[Zn(II) cyclen] complexes inhibit HIV-1 TAR RNA-Tat peptide binding due to its strong binding to the UUU bulge.^[81,83] Figure 23 shows the coordination of dT⁻pdT⁻pdT⁻ with a linear tris-[Zn(II) cyclen] complex.

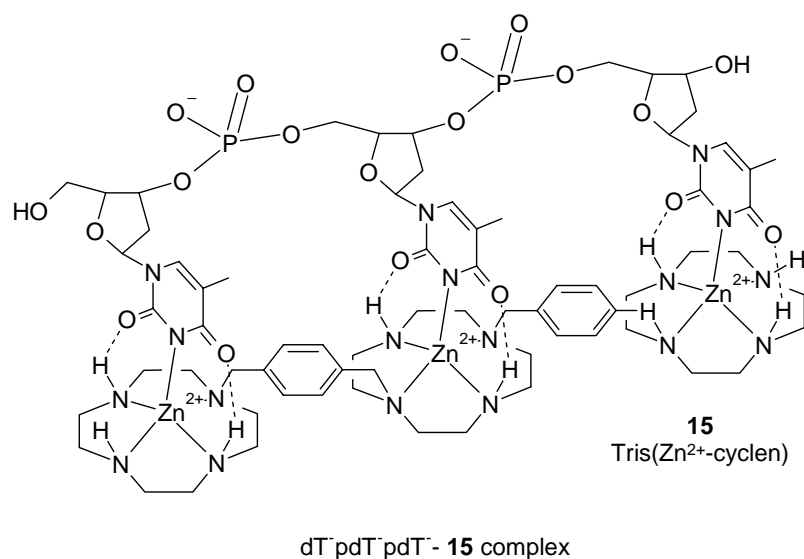


Figure 23: The binding of tris-[Zn(cyclen)] to dT⁻pdT⁻pdT⁻.

1.5 Immobilised 1,4,7,10-tetraaza-cyclododecane ([12]aneN₄ or cyclen) complexes

1.5.1 Zn(II) complexes

Zn(II) cyclen complexes have been bound to polymers and used to extract riboflavin from aqueous solutions. The reversible recognition of Zn(II) cyclen complexes to flavin imide moieties allowed the quantitative and selective extraction (and release from the polymer) of Vitamin B2 (riboflavin) from a mixture of compounds at physiological pH (Figure 24).^[84]

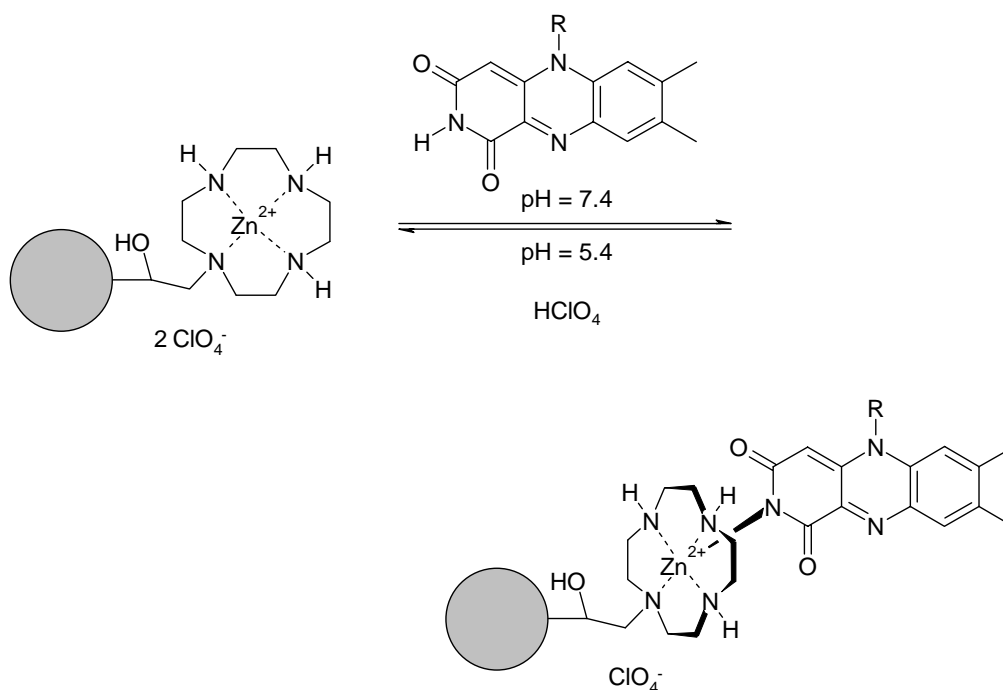


Figure 24: Binding equilibrium of Zn(II) cyclen polymer with riboflavin (R = ribityl) or its tetraacetate [R = CH₂CH(OAc)CH(OAc)CH(OAc)CH₂OAc].

A molecular imprinted polymer (MIP) from polymerisable Zn(II) cyclen complexes and ethylene glycol dimethyl acrylate has been prepared.^[39] Creatinine, **8** was used as the template molecule which was reversibly coordinated to the zinc atom (Figure 25). The imprinted polymer reverses the binding selectivity of Zn(II) cyclen for creatinine and thymine from 1:34 in homogenous solution to 3.5:1 in the MIP.

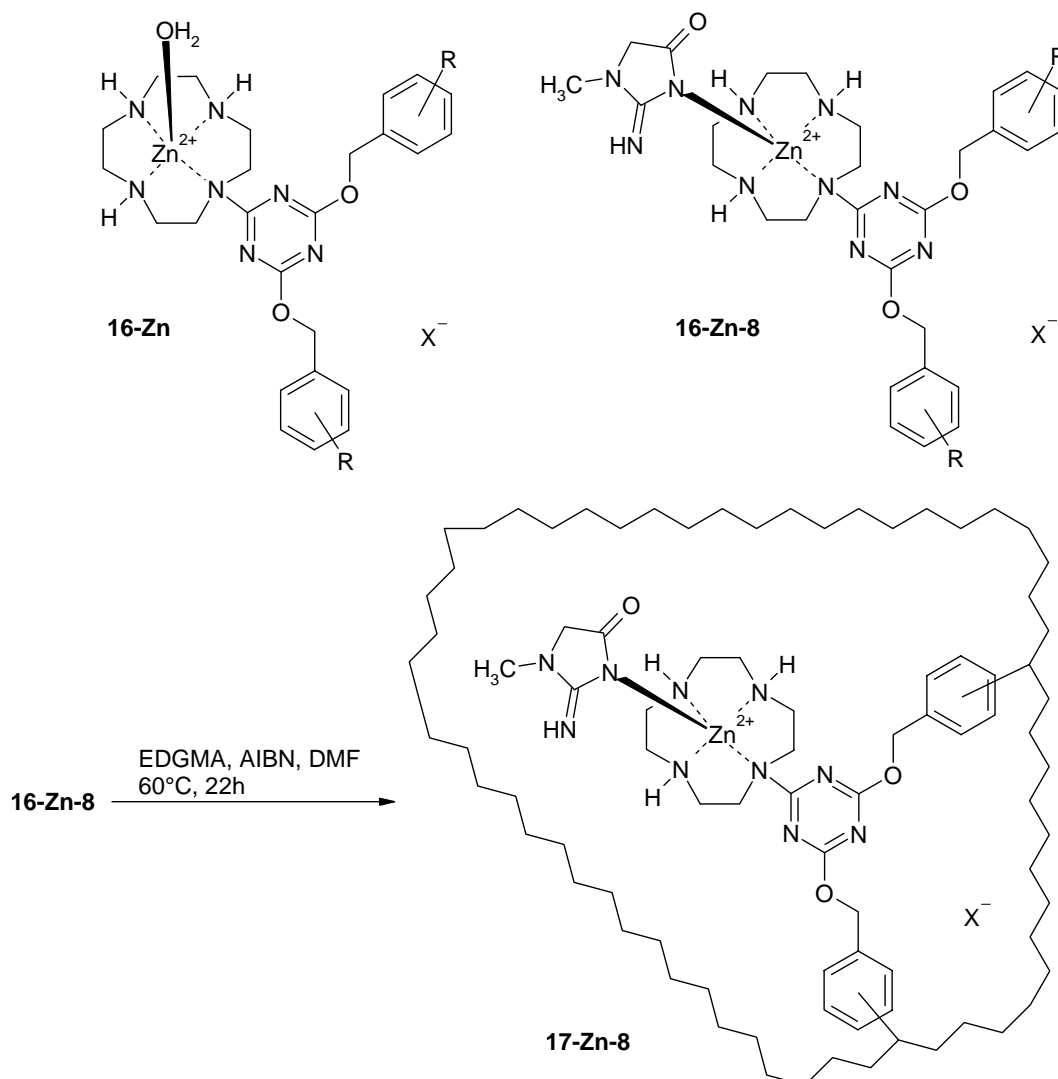


Figure 25: Preparation of a stoichiometric template Zn(II) cyclen-creatinine monomer salt and copolymerisation of **16-Zn-8** with ethylene glycol dimethyl acrylate (EDGMA).

A similar MIP polymer was prepared for the selective recognition and separation of phosphates.^[85] Here again a polymerisable Zn(II) cyclen complex (ZnL^2) was copolymerised with ethylene glycol dimethyl acrylate. The polymer interacts selectively with phosphomonoester dianions such as deoxyadenosine 5'-monophosphate (5'-dAMP) and 4-nitrophenyl phosphate (4-NPP) over deoxyadenosine (dA) and adenosine 3',5'-cyclic-monophosphate (3',5'-cAMP). The apparent complexation constants for the 1:1 complex of ZnL^2 on the MIP and 5'-dAMP and 4-NPP, $\log K_{\text{app}}(\text{ZnL-S}^{2-})$ (S^{2-} = phosphomonoester dianion), at pH 7.0 and 25°C were determined as 4.1.

1.6 Structures of 1,4,8,11-tetraaza-cyclotetradecane ([14]aneN₄ or cyclam) complexes in solid state

1.6.1 Zn(II) complexes

Zn(II) cyclam complexes can coordinate carboxylates as additional ligand. The X-ray structure of a Zn₂-xylyl-bicyclam with an acetate anion is shown (Figure 26).^[86] Both cyclam units adopt the *cis*-V configuration (according to the nomenclature of Bosnich^[87]) with chelation by acetate on one cyclam face and twofold H-bonding on the other.

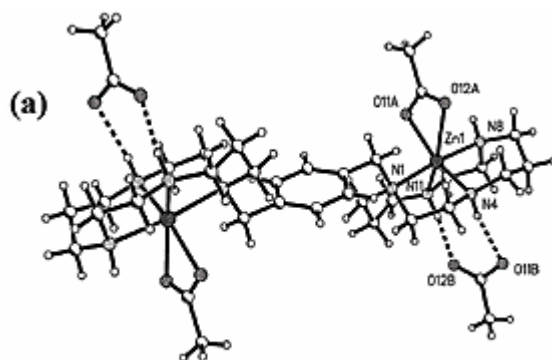


Figure 26: X-ray crystal structure of [Zn₂-xylyl-bicyclam(OAc)₂](OAc)₂·2CH₃OH. CH₃OH is not shown for clarity.

The Zn(II) complex of 1,4,8,11-tetraazacyclotridecane-5-one can coordinate glycine by glycine amine-Zn(II) coordination.^[88] The X-ray structure (Figure 27) shows a distorted square pyramidal geometry. The Zn atom has an irregular five-coordinate geometry, with the donors being three nitrogen atoms and one oxygen atom from the azamacrocycle and one coordinated chloride.

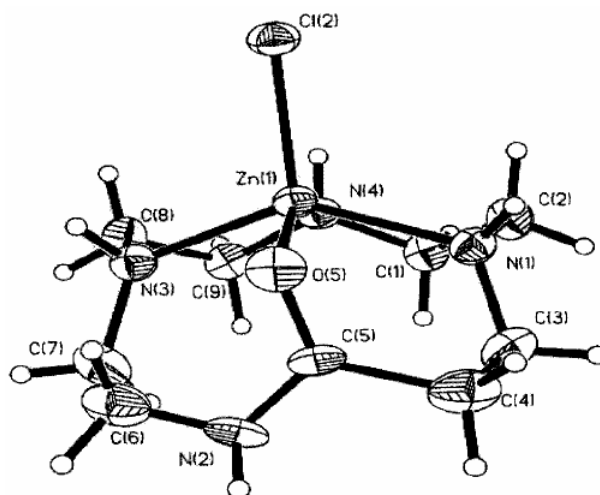


Figure 27: Structure of Zn(II) complex of 1,4,8,11-tetraazacyclotridecane-5-one in the solid state.

1.6.2 Ni(II) complexes

Cyclam forms thermodynamically and kinetically more stable complexes with copper and nickel, where the cyclic amine is arranged in a strain-free conformation with the metal atom located in the plane defined by the four nitrogen atoms of the cyclam.^[4-6] There is some evidence that Ni(II) cyclam can bind benzoates and that the metal free cyclams preorganise the ligands. The X-ray structure (Figure 28) of Ni(*O*-benzoato)₂(cyclam) quite closely parallels that of nickel free (4-*t*-butylbenzoato)₂(cyclamH₂). The X-ray structure of the Ni(II) cyclam distinctly shows that a Ni-O bond is formed in the case of Ni(*O*-benzoato)₂(cyclam).

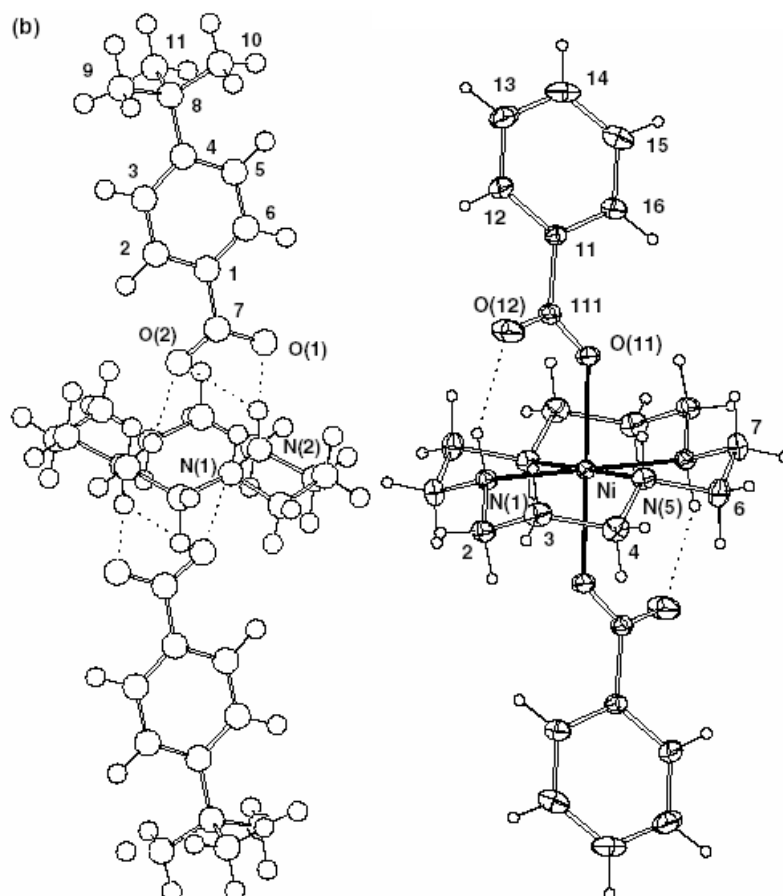


Figure 28: Structure of $(4\text{-}t\text{-butylbenzoato})_2(\text{cyclamH}_2)$ and $\text{Ni}(\text{O-benzoato})_2(\text{cyclam})$ respectively, in the solid state.

Similar geometries were found for the corresponding Cu(II) complexes. However in the case of copper, the two carboxylate anions remain hydrogen bound to the (coordinated) cyclam ligand, and do not take part in the metal's inner coordination sphere and no Cu-O bond is formed.^[89]

The Ni(II) complex of 1,4,7,10-tetraazacyclododecane-2,9-dione coordinates the dipeptide glycine-glycine.^[90] The X-ray structure (Figure 29) shows an octahedral coordination geometry. The Ni atom has a regular six-coordinate geometry, with the donors being four nitrogen atoms and two oxygen atoms from two macrocyclic ligands.

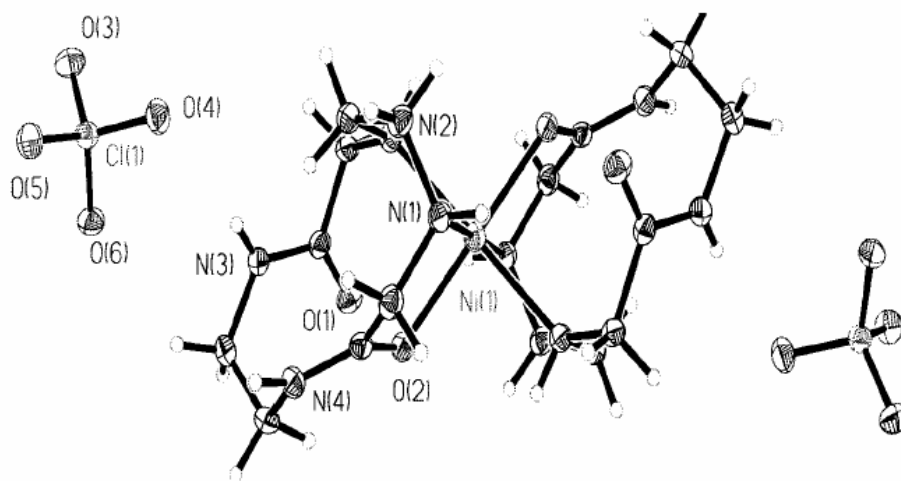
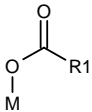
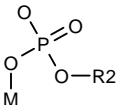
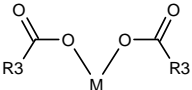
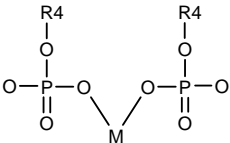
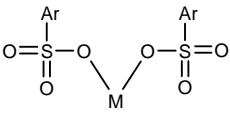
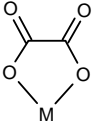


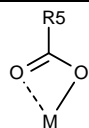
Figure 29: Structure of Ni(II) complex of 1,4,7,10-tetraazacyclododecane-2,9-dione) in the crystal.

1.7 Structures of 1,4,8,11-tetraaza-cyclotetradecane ([14]aneN₄ or cyclam) complexes in solid state (tabulated)

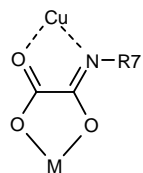
Table 6 summarises all X-ray structures registered at the Cambridge Crystallographic Database according to the selection criteria previously mentioned.

Table 6: Structurally characterised metal complexes of 1,4,8,11-tetraaza-cyclotetradecane with additional ligand coordinated to the metal ion in the solid state.

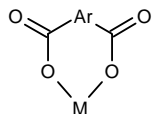
Structure of the additional ligand	Metal ions									
	Ga ³⁺	Zn ²⁺	Cd ²⁺	Cu ²⁺	Ni ²⁺	Co ³⁺	Fe ²⁺	Ru ²⁺	Mn ³⁺	Cr ³⁺
					⁽¹⁾ See ref. [91]					
	⁽²⁾ See ref. [92,93]			⁽³⁾ See ref. [92,93]		⁽⁴⁾ See ref. [94]				
		⁽⁵⁾ See ref. [95,96]		⁽⁶⁾ See ref. [91,97]	⁽⁷⁾ See ref. [89,98-103]				⁽⁸⁾ See ref. [104]	
					⁽⁹⁾ See ref. [105]					
			⁽¹⁰⁾ See ref. [106]	⁽¹¹⁾ See ref. [107]	⁽¹²⁾ See ref. [108]					
					⁽¹³⁾ See ref. [109]				⁽¹⁴⁾ See ref. [110]	



⁽¹⁵⁾ See ref. ⁽¹⁶⁾ See ref.
[111-113] [114]

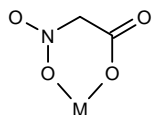


⁽¹⁷⁾ See ref.
[115]

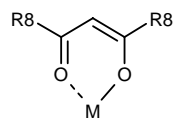


⁽¹⁸⁾ See ref. ⁽¹⁹⁾ See ref.
[116] [117-119]

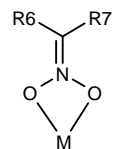
⁽²⁰⁾ See ref.
[120]



⁽²¹⁾ See ref.
[121]



⁽²²⁾ See ref. ⁽²³⁾ See ref.
[45,122,123] [125]

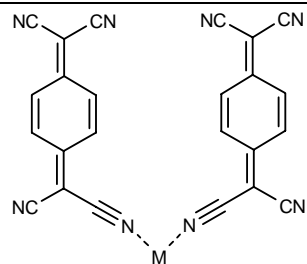


⁽²⁴⁾ See ref.
[126]

⁽²⁵⁾ See ref.
[126,127]

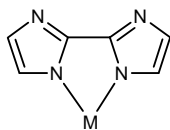


⁽²⁶⁾ See ref. ⁽²⁷⁾ See ref.
[128] [129]

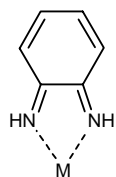


⁽²⁸⁾ See ref.
[130]

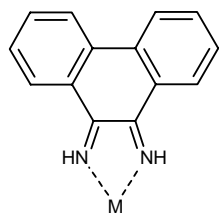
⁽²⁹⁾ See ref.
[131]



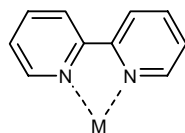
⁽³⁰⁾ See ref.
[132]



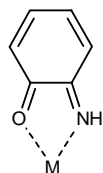
⁽³¹⁾ See ref.
[133]



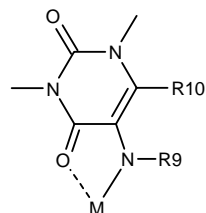
⁽³²⁾ See ref.
[133]



⁽³³⁾ See ref.
[134]



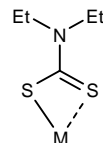
⁽³⁴⁾ See ref.
[135]



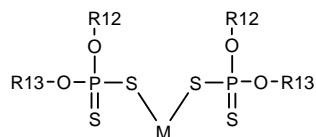
⁽³⁵⁾ See ref.
[136,137]



⁽³⁶⁾ See ref.
[138-140]



⁽³⁷⁾ See ref.
[141]



⁽³⁸⁾ See ref. ⁽³⁹⁾ See ref.
[142] [142]

⁽¹⁾ Substitution - n-alkyl; R1 = CH₃; ⁽²⁾ Substitution - none; R2 = Ga³⁺; ⁽³⁾ Substitution - none; R2 = Ga³⁺; ⁽⁴⁾ Substitution - c-alkyl; R3 = Al³⁺; ⁽⁵⁾ a) Substitution - none; R3 = Ar; ⁽⁵⁾ b) Substitution - none; R3 = OMe; ⁽⁶⁾ a) Substitution - none; R3 = Ar; ⁽⁶⁾ b) Substitution - none; R3 = OMe; ⁽⁷⁾ a) Substitution - none; R3 = Ar; ⁽⁷⁾ b) Substitution - none; R3 = cyclohexane; ⁽⁸⁾ Substitution - none; R3 = pyridine; ⁽⁹⁾ Substitution - none; R4 = H; ⁽¹⁰⁾ Substitution - none; ⁽¹¹⁾ Substitution - none; ⁽¹²⁾ Substitution - none; ⁽¹³⁾ Substitution - c-

alkyl; ⁽¹⁴⁾ Substitution - none; ⁽¹⁵⁾ a) Substitution - c-alkyl; R3 = aryl; ⁽¹⁵⁾ b) Substitution - c-alkyl; R3 = pyridine; ⁽¹⁶⁾ Substitution - c-alkyl; R3 = aryl; ⁽¹⁷⁾ Substitution - c-alkyl; R7 = alkyl or aryl; ⁽¹⁸⁾ Substitution - c-alkyl; ⁽¹⁹⁾ a) Substitution - none; ⁽¹⁹⁾ b) Substitution - c-alkyl; ⁽²⁰⁾ Substitution - c-alkyl; ⁽²¹⁾ Substitution - c-alkyl; ⁽²²⁾ a) Substitution - n-alkyl (caged); R8 = CH₃; ⁽²²⁾ b) Substitution - c-phenyl; R8 = CH₃; ⁽²³⁾ Substitution - none; R8 = CH₃; ⁽²⁴⁾ Substitution - n-alkyl; R6 = R7 = CH₃; ⁽²⁵⁾ a) Substitution - c-alkyl; R6 = R7 = H; ⁽²⁵⁾ b) Substitution - n-alkyl; R6 = H, R7 = CH₃; ⁽²⁵⁾ c) Substitution - c-alkyl; R6 = R7 = CH₂CH₃; ⁽²⁶⁾ Substitution - none; R1 = quinonedi-imine; ⁽²⁷⁾ Substitution - n-alkyl; R1 = 2-cyanoethene-1,2-dithiolate; ⁽²⁸⁾ Substitution - none; ⁽²⁹⁾ Substitution - none; ⁽³⁰⁾ Substitution - none; ⁽³¹⁾ Substitution - none; ⁽³²⁾ Substitution - none; ⁽³³⁾ Substitution - none; ⁽³⁴⁾ Substitution - none; ⁽³⁵⁾ Substitution - c-alkyl; R9 = O, R10 = NH-alkyl; ⁽³⁶⁾ a) Substitution - c-alkyl; R11 = Ar; ⁽³⁶⁾ b) Substitution - c-alkyl; R11 = -SCH₂COO⁻; ⁽³⁶⁾ c) Substitution - c-alkyl; R11 = -CH₂CH₂COO⁻; ⁽³⁷⁾ Substitution - c-alkyl; ⁽³⁸⁾ Substitution - c-alkyl; R12 = R13 = CH₂CH₂-Ph; 39) Substitution - c-alkyl; R12 = R13 = CH₂CH₂-Ph

1.8 Molecular recognition of 1,4,8,11-tetraaza-cyclotetradecane ([14]aneN₄ or cyclam) complexes in solution

1.8.1 Zn(II) complexes

The bicyclam **18** (Figure 30) is a very potent anti-HIV agent.^[143] Entry of T-lymphotropic HIV-1 and HIV-2 strains is blocked by specific binding to the CXCR4 coreceptor.^[144] Since the level of free Zn(II) in plasma is ca. 1 nM and cyclam and its alkylated derivatives strongly bind Zn(II), it is reasonable to expect that the active compound *in vivo* is the Zn(II) complex.^[86]

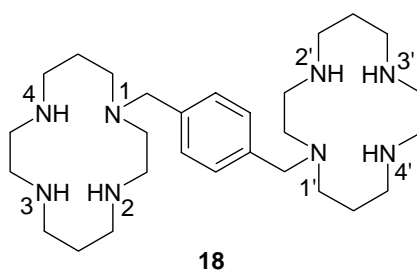


Figure 30: Molecular structure of xylyl-bis-cyclam, 1,1'-[1,4-phenylenebis(methylene)]-bis(1,4,8,11-tetraazacyclotetradecane) **18**. The octa-HCl salt of the compound is registered as the anti-HIV drug AMD3100.

The interaction of the Zn(II) complex of xylyl-bis-cyclam, which is 10 times more active than **18** in its interaction with the CXCR4 receptor,^[145] with acetate was studied. In solution, acetate binds^[146] to the Zn(II) bis-cyclam complex with a binding constant of $\log K = 2.75 \pm 0.15$, assuming the formation of 1:1 complexes of acetate with Zn(II) cyclam units and that the two Zn(II) cyclam units are independent.^[86]

Both in solution and in the solid state the complex adopts a *cis*-V configuration (according to the nomenclature of Bosnich^[87]) via chelation and second coordination sphere double H-bonding.^[86] It was shown that only Zn(II) cyclams could bind acetates. Pd(II) cyclams do not coordinate acetates, as the acetate does not induce configurational changes of Pd(II) cyclam nor Pd(II)₂-xylyl-bis-cyclam, and Pd(II) cyclams cannot readily adopt a *cis*-V configuration.^[86,145]

Although Co(III) cyclams are known to bind strongly to carboxylates, and are capable of undergoing isomerisations from *cis* to *trans* configurations,^[147] Co(III)₂-xylyl-bis-cyclam

has a very low activity towards CXCR4.^[145] This is most likely attributable to the kinetic inertness of Co(III) cyclams.^[148]

The Zn(II) complex of 1,4,8,11-tetraazacyclotridecane-5-one was found to be extremely efficient in the recognition of glycine in aqueous solution (Figure 31).^[88]

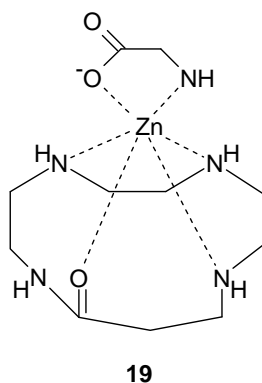


Figure 31: Zn(II) complex of 1,4,8,11-tetraazacyclotridecane-5-one can bind glycine.

The carboxylate group is capable of forming a coordinative bond to the Zn(II) ion, while the H-atom of the amide on the macrocycle may also favour aggregate formation. Table 7 shows the stability constants for the Zn(II) 1,4,8,11-tetraazacyclotridecane-5-one glycine complex **19**.

Table 7: Stability constants for the Zn(II) 1,4,8,11-tetraazacyclotridecane-5-one (L) glycine complex **19** ($\mu = 0.10$ M KCl, 25 °C).

Stoichiometry				Quotient K	log K
(L)	Zn	Glycine	H		
1	1	0	0	$[LZn] / [L][Zn]$	9.33
1	1	0	1	$[LZnH] / [LZn][H]$	6.44
1	1	0	2	$[LZnH_2] / [LZn][H]^2$	6.65
1	1	1	0	$[LZnGly^-] / [LZn][Gly^-]$	12.25
1	1	1	1	$[LZnGlyH] / [LZnH][Gly]$	2.58
1	1	1	-1	$[LZnGlyOH] / [LZnOH][Gly]$	1.00
1	1	1	-2	$[LZnGlyOH_2] / [LZnOH_2][Gly]$	0.88

1.8.2 Ni(II) complexes

The Ni(II) complex of 1,4,7,10-tetraazacyclododecane-2,9-dione was found to be efficient in the recognition of the dipeptide glycine-glycine in aqueous solution (Figure 32).^[90]

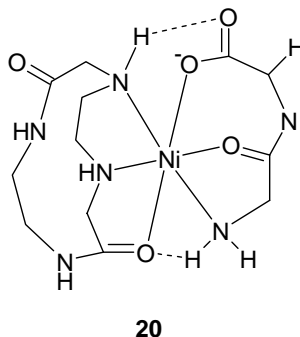


Figure 32: Ni(II) complex of 1,4,7,10-tetraazacyclododecane-2,9-dione can coordinate the dipeptide glycine-glycine.

Table 8: Stability constants for the Ni(II) 1,4,7,10-tetraazacyclododecane-2,9-dione (L) glycine-glycine (G) complex **20** ($\mu = 0.10$ M KCl, 25 °C).

Stoichiometry				Quotient K	$\log K$
(L)	Ni	G	H		
1	1	0	0	$[\text{LNi}] / [\text{L}][\text{Ni}]$	15.51
1	1	0	1	$[\text{LHNi}] / [\text{LNi}][\text{H}]$	4.50
1	1	0	2	$[\text{LH}_2\text{Ni}] / [\text{LHNi}][\text{H}]$	4.11
1	1	0	-1	$[\text{LNiOH}] / [\text{LNi}][\text{H}]$	6.31
1	1	0	-2	$[\text{LNiOH}_2] / [\text{LNiOH}][\text{OH}]$	-9.64
1	1	1	0	$[\text{LNiG}] / [\text{LNi}][\text{G}]$	19.20
1	1	1	-1	$[\text{LNiGOH}] / [\text{LNiG}][\text{OH}]$	10.07
1	1	1	-2	$[\text{LNiGOH}_2] / [\text{LNiGOH}][\text{OH}_2]$	0.29

The formation of a stable ternary complex, L-Ni(II)-Gly-Gly⁻ leads to a very high binding constant of $\log K = 19.20$ (Table 8). The strong recognition may also be partially attributed to the formation of an H-bond between the macrocycle and the dipeptide.

1.8.3 Hg(II) complexes

Mallik et al. have shown that the Hg(II)-xylyl-biscyclam **21** (Figure 33) could bind imidazole in DMSO (binding constants $\gg 100 \text{ M}^{-1}$).^[149,150]

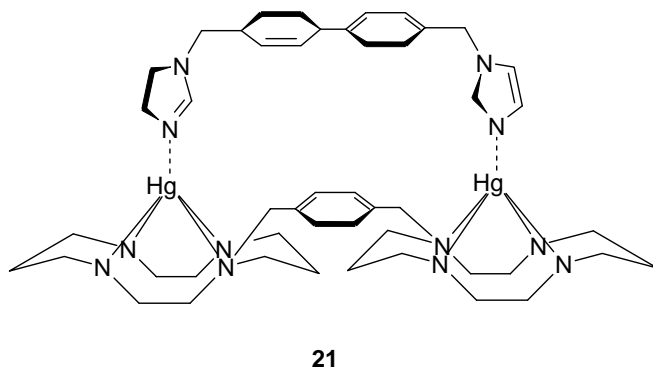


Figure 33: The Hg(II)-xylyl-bis-cyclam **21** bound to two imidazole units.

An improvement in imidazole binding was shown with the tris-cyclam ligand **22** which when complexed with Hg^{2+} recognised a model histidine peptide **23** with a $K > 10^5 \text{ M}^{-1}$ in DMSO solution (Figure 34).^[151]

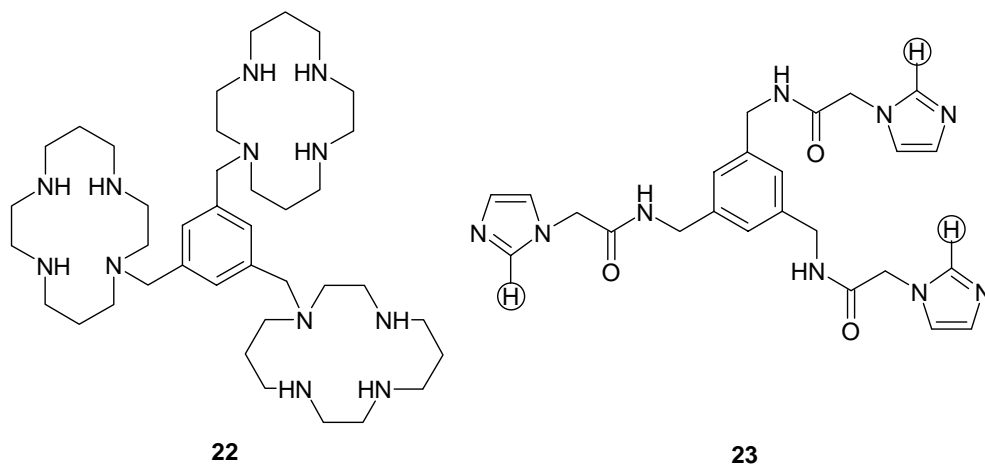


Figure 34: A tris-cyclam **22** when complexed with Hg(II) recognises the model tris-histidine peptide **23**, which is complementary in geometry.

1.9 Immobilised 1,4,8,11-tetraaza-cyclotetradecane ([14]aneN₄ or cyclam) complexes

1.9.1 Ni(II) complexes

A linear polymer containing Ni(II) cyclam and 2,2'-bipyridyl-5,5'-dicarboxylate (bpydc²⁻) was synthesised (Figure 35). The polymer binds guests in the order of ethanol \approx phenol (formation constant, $K_f = 42 \text{ M}^{-1}$) $>$ pyridine ($K_f = 13 \text{ M}^{-1}$) $>$ benzene ($K_f = 3 \text{ M}^{-1}$) in isooctane solution.^[152]

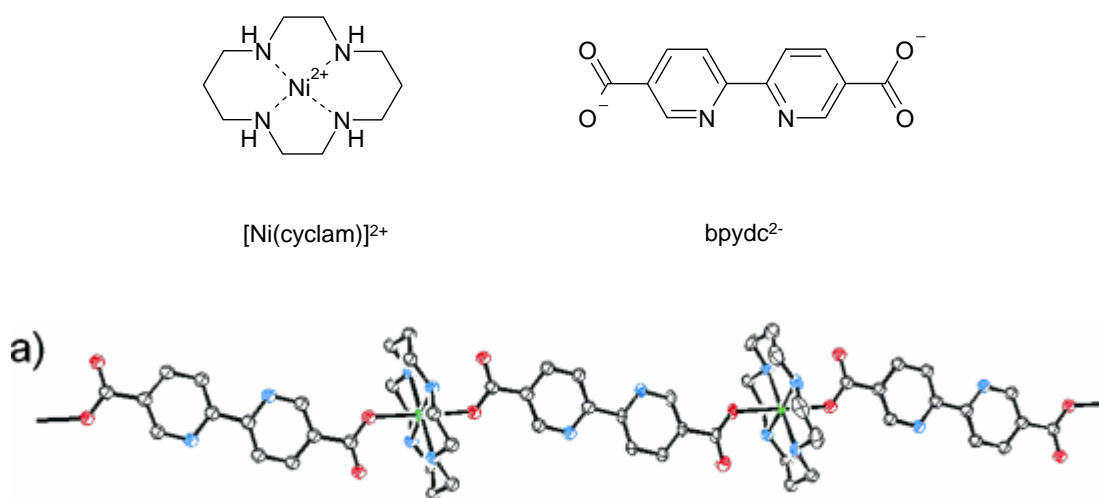


Figure 35: Structure of the linear polymer containing Ni(II) cyclam and bpydc²⁻.

1.10 Structures of 1,5,9-triaza-cyclododecane ([12]aneN₃) complexes in solid state

1.10.1 Zn(II) complexes

Although the coordination of Zn(II) [12]aneN₃ to acetazolamide and sulfonamides has been reported in solution,^[14,71] no X-ray structures were found for their coordination in the solid state. The X-ray structure of Zn(II) [12]aneN₃ shows a zinc atom with slightly distorted tetrahedral coordination environment, with a bound water molecule (Figure 36).

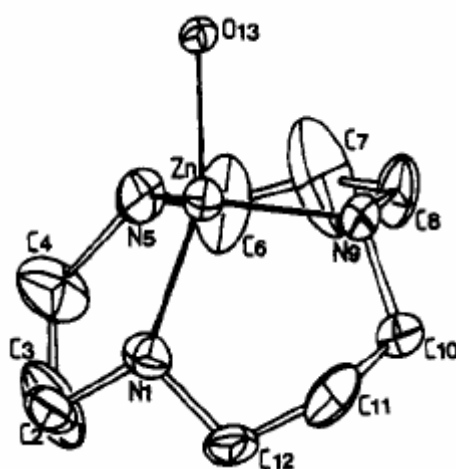


Figure 36: Structure of Zn(II) [12]aneN₃ in the crystal. Perchlorate anions and hydrogen atoms are omitted for clarity. Probability ellipsoids are 30%.

1.11 Molecular recognition of 1,5,9-triaza-cyclododecane ([12]aneN₃) complexes in solution

1.11.1 Zn(II) complexes

The Zn(II) complex of the 12-membered triamine, [12]aneN₃ forms 1:1 complexes with acetazolamide and sulfonamides.^[14,71] The intermolecular affinities of aromatic sulfonamides to Zn(II) [12]aneN₃ (ZnL) are summarised in the Table 9.

Table 9: Comparison of critical affinity constants, K_i (M^{-1}) and K [Zn(II) [12]aneN₃-I] (M^{-1}).^[71]

	$\log K_i$	$\log K[\text{Zn(II) [12]aneN}_3\text{-I}]$
acetazolamide	3.6	4.9
4-nitrobenzenesulfonamide	2.6	4.8
<i>p</i> -toluenesulfonamide	2.4	5.7

Determined by inhibition kinetics at pH 8.4 (50 mM TAPS buffer), $I = 0.10$ and 25 °C.

Due to the poor solubility of the sulfonamides, the potentiometric pH titration method could not be used to determine the binding constants. The binding constants were measured by a kinetic inhibition method of the Zn(II) [12]aneN₃ promoted 4-nitrophenyl acetate hydrolysis, which is analogous to the procedure used to determine sulphonamide binding to carbonic anhydrase (CA).^[153] The apparent binding constants are consistent with previous biochemical data reported for CA models which makes such Zn(II) [12]aneN₃ complexes good models for CA.

1.12 Immobilised 1,5,9-triaza-cyclododecane ([12]aneN₃) complexes

No reports on immobilised [12]aneN₃ complexes have appeared in the literature so far.

1.13 Structures of 1,4,7-triazonane ([9]aneN₃ or TACN) complexes in solid state

1.13.1 Cu(II) complexes

The smallest azamacrocycles which forms metal complexes is [9]aneN₃. Its Cu(II) complex binds to the amino acid histidine, forming a square pyramidal Cu(II) coordination geometry.^[154] The X-ray structure analysis confirms that the distorted square-pyramidal Cu(II) coordination sphere is comprised of three nitrogen donors from the [9]aneN₃ plus one carboxylate atom and the primary nitrogen from L-histidine (Figure 37).

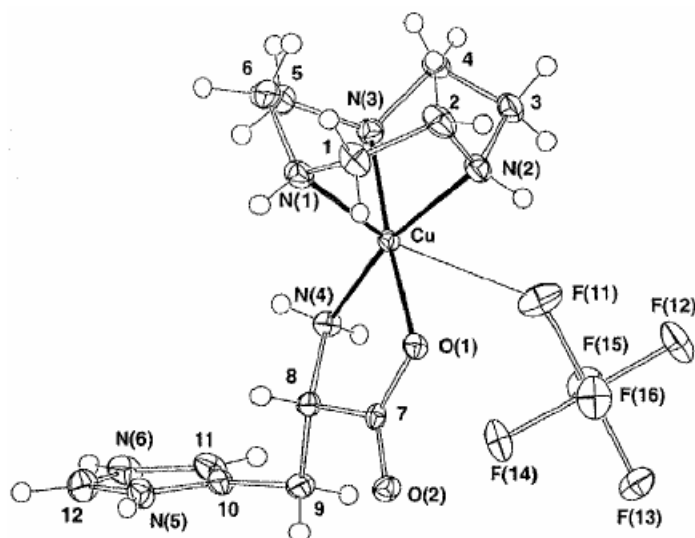


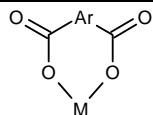
Figure 37: The structure of $[\text{Cu}(\text{TACN})(\text{histidine})]^{2+}(\text{PF}_6)^-$ in the solid state.

1.14 Structures of 1,4,7-triazonane ([9]aneN₃ or TACN) complexes in solid state (Tabulated)

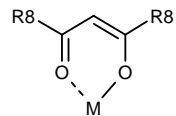
Table 10 summarises all X-ray structures registered at the Cambridge Crystallographic Database according to the selection criteria previously mentioned.

Table 10: Structurally characterised metal complexes of 1,4,7-triazonane with additional ligand coordinated to the metal ion in the solid state.

Structure of the additional ligand	Zn ²⁺	Cu ²⁺	Ni ²⁺	Co ³⁺	Rh ³⁺	Fe ³⁺	Fe ²⁺	Ru ²⁺	Mn ³⁺	Cr ³⁺	V ³⁺	Zr ⁴⁺
			(1) See ref. [155-157]									
			(2) See ref. [158]									
			(3) See ref. [155,159]									
			(4) See ref. [160]									
			(6) See ref. [161,162]									
			(7) See ref. [163]									
			(8) See ref. [164,165]									
						(9) See ref. [166,167]				(10) See ref. [168]		



⁽¹¹⁾ See ref.
[156]



⁽¹²⁾ See ref.
[169]

⁽¹³⁾ See ref.
[170]

⁽¹⁴⁾ See ref.
[170]

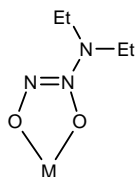
⁽¹⁵⁾ See ref.
[171]

⁽¹⁶⁾ See ref.
[172]

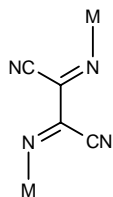
⁽¹⁷⁾ See ref.
[169,173,174]

⁽¹⁸⁾ See ref.
[175,176]

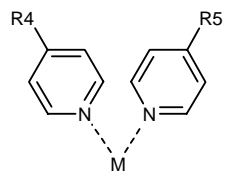
⁽¹⁹⁾ See ref.
[177]



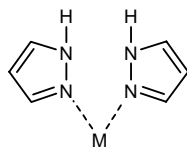
⁽²⁰⁾ See ref.
[178]



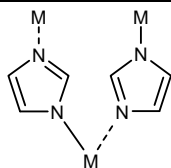
⁽²¹⁾ See ref.
[179]



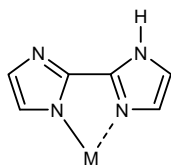
⁽²²⁾ See ref.
[180]



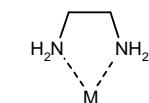
⁽²³⁾ See ref.
[181]



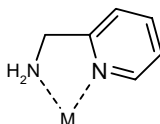
⁽²⁴⁾ See ref.
[182,183]



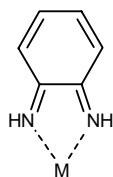
⁽²⁵⁾ See ref.
[184,185]



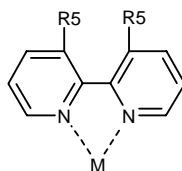
⁽²⁶⁾ See ref.
[186]



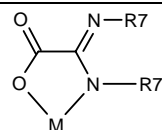
⁽²⁷⁾ See ref.
[186]



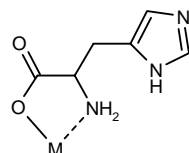
⁽²⁸⁾ See ref.
[187]



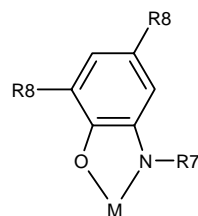
⁽²⁹⁾ See ref.
[188,189]



⁽³⁰⁾ See ref.
[190,191]



⁽³¹⁾ See ref.
[154]



⁽³²⁾ See ref.
[192]

⁽¹⁾ a) Substitution - none; R1 = aryl; ⁽¹⁾ b) Substitution - n-alkyl; R1 = aryl; ⁽²⁾ Substitution - n-alkyl; R4 = Ph; ⁽³⁾ a) Substitution - n-alkyl; R2 = aryl; ⁽³⁾ b) Substitution - none; R2 = aryl; ⁽⁴⁾ Substitution - n-alkyl; R4 = CH₂Ph; ⁽⁵⁾ Substitution - n-alkyl; R4 = Ph; ⁽⁶⁾ Substitution - none; ⁽⁷⁾ Substitution - none; ⁽⁸⁾ a) Substitution - n-CH₂Ph; ⁽⁸⁾ b) Substitution - n-alkyl; ⁽⁹⁾ Substitution - n-alkyl; ⁽¹⁰⁾ Substitution - n-alkyl; ⁽¹¹⁾ Substitution - n-alkyl; ⁽¹²⁾ Substitution - n-alkyl; R8 = CH₃; ⁽¹³⁾ Substitution - n-alkyl; R8 = Ph; ⁽¹⁴⁾ Substitution - n-alkyl; R8 = Ph; ⁽¹⁵⁾ Substitution - n-alkyl; R8 = CH₃; ⁽¹⁶⁾ Substitution - n-alkyl; R8 = CH₃; ⁽¹⁷⁾ Substitution - n-alkyl; R8 = CH₃; ⁽¹⁸⁾ Substitution - n-alkyl; R8 = CH₃; ⁽¹⁹⁾ Substitution - none; R8 = CH₃; ⁽²⁰⁾ Substitution - n-alkyl; ⁽²¹⁾ Substitution - n-alkyl; ⁽²²⁾ Substitution - none; R5 = pyridine; ⁽²³⁾ Substitution - n-alkyl; ⁽²⁴⁾ a) Substitution - none; ⁽²⁴⁾ b) Substitution - n-alkyl; ⁽²⁵⁾ Substitution - none; ⁽²⁶⁾ Substitution - none; ⁽²⁷⁾ Substitution - none; ⁽²⁸⁾ Substitution - n-alkyl; ⁽²⁹⁾ a) Substitution - n-alkyl; R5 = CH₃; ⁽²⁹⁾ b) Substitution - n-alkyl; R5 = O-alkyl; ⁽³⁰⁾ a) Substitution - n-alkyl; R7 = H; ⁽³⁰⁾ b) Substitution - none; R7 = CH₃; ⁽³¹⁾ Substitution - none; ⁽³²⁾ Substitution - n-alkyl; R7 = Ph, R8 = *tert*-butyl

1.15 Molecular recognition of 1,4,7-triazonane ([9]aneN₃ or TACN) complexes in solution

1.15.1 Cu(II) complexes

TACN strongly chelates Cu(II) ($\log K = 15.5$ at 25 °C).^[193] Above pH 8 one of the two equatorial coordination sites available on the copper atom is occupied by an hydroxide ion.^[194] Above pH 9 glucose readily displaces water and hydroxide to form a ternary TACN-Cu(II)-glucose complex, which results in the net release of protons (Figure 38). The measurement of this proton release by pH titration gives apparent binding constants of 35 M^{-1} at pH 10.25 to 1200 M^{-1} at pH 11.5 for the complexation of Cu(II) TACN with glucose.^[195] The Cu(II) TACN complex **24** exhibits considerable selectivity depending on the diol. At alkaline pH it can bind *cis*-diols 1,4-anhydroerythritol and glucose, while *trans*-diol sugar analogue and 1,4-anhydro-L-threitol cannot be coordinated.

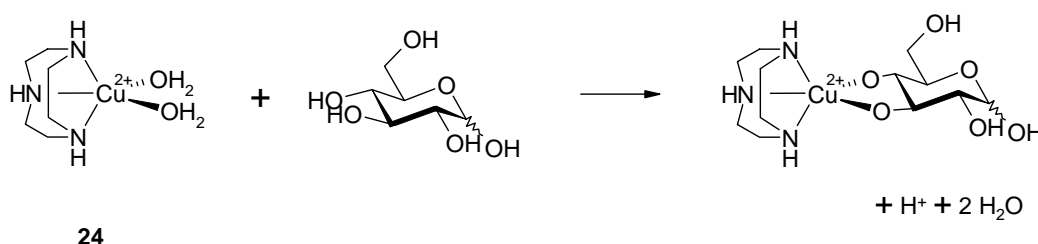


Figure 38: The Cu(II) TACN complex coordinates glucose at alkaline pH.

1.16 Immobilised 1,4,7-triazonane ([9]aneN₃ or TACN) complexes

1.16.1 Cu(II) complexes

A polymerisable Cu(II) TACN glucopyranoside complex **25** has been copolymerised with a cross linking monomer to form a porous polymer.^[195] After washing to remove the template, a polymer which rebinds glucose and thereby releasing protons into the surrounding solution was created (Figure 39). The change in pH provides a convenient measure of glucose concentration over a clinically relevant range (0-25 mM) (Figure 40).

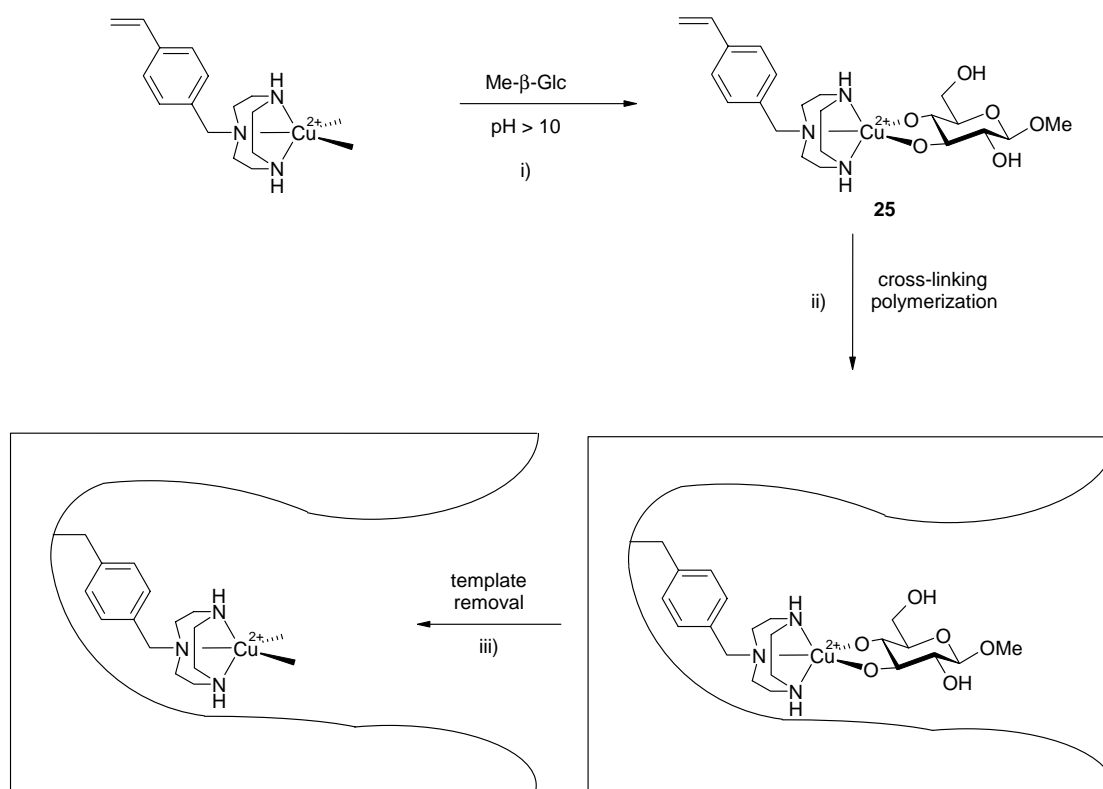


Figure 39: Preparation of a glucose sensing Cu(II) TACN containing polymer.

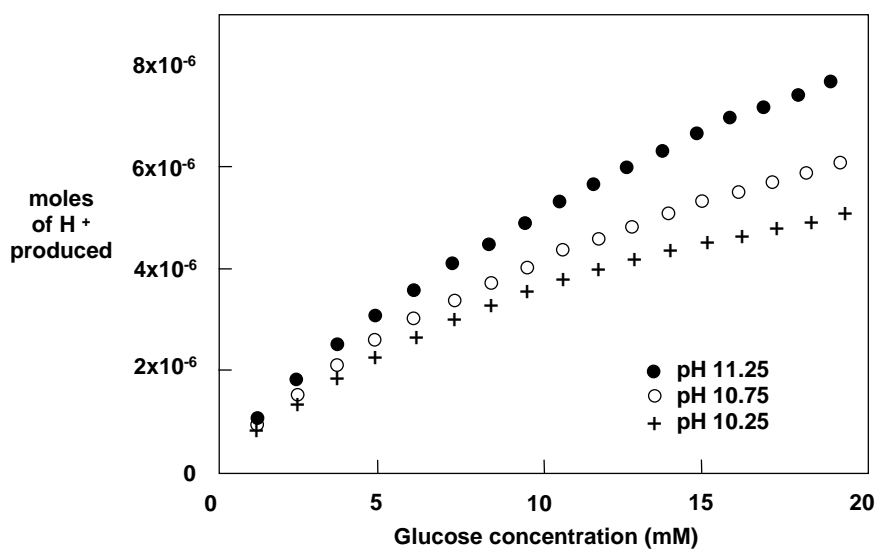


Figure 40: Titration of methyl-β-D-glucopyranoside-imprinted polymer (0.034 mmol Cu(II)) with D-glucose in 0.15 M NaCl, 25 °C at pH 10.25, 10.75 and 11.25 at constant pH.

The high ratio of cross-linker in the polymer generates a microporous polymer which allows the small glucose molecules to bind, but hinders larger molecules such as glycosylated proteins which may otherwise also bind to the metal complex. The polymers

ability to sense glucose is not impeded by the many potential competing species present in a complex biological sample such as porcine plasma (adjusted to pH 11.25).^[196]

1.17 Conclusion

A variety of transition metal complexes of [9]aneN₃, [12]aneN₄ and [14]aneN₄ reversibly coordinate additional donor molecules in the solid state, in solution or immobilised on polymer support. In many cases this coordination of an additional ligand is selective for a particular functional group. In solution binding affinities in the milli or micromolar range are observed, even at physiological conditions. This allows the selective molecular recognition of target molecules with high binding strength in biological media, a process which is difficult to achieve using synthetic receptors based on hydrogen bonding. Therefore many transition metal complexes of azamacrocyclic ligands are ideally suited as molecular binding sites for analytes, and many applications in diagnostics, bioanalytics, biotechnology or material sciences may be envisaged.

1.18 References

- [1] Curtis, N. F. *J. Chem. Soc.* **1960**, 4409
- [2] Tompson, M. C.; Busch, D. H. *J. Am. Chem. Soc.* **1964**, 86, 3561
- [3] Izatt, R. M.; Pawlak, K.; Bradshaw, J. S.; Bruening, R. L. *Chem. Rev.* **1995**, 95, 2529
- [4] Bianchi, A.; Micheloni, M.; Paoletti, P. *Chem. Rev.* **1991**, 110, 17
- [5] Boeyens, J. C. A.; Dobson, S. M. in *Stereochemical and Stereophysical Behaviour of Macrocycles*, ed. Bernal, I.; Elsevier, Amsterdam, Vol. 2, **1987**, 1-102
- [6] Curtis, N. F.; in *Coordination Chemistry of Macrocyclic Compounds*, ed. Melson, G. A.; Plenum Press, **1979**, 219-344
- [7] Micheloni, M.; Sabatini, A.; Paoletti, P. *J. Chem. Soc., Perkin Trans. 2* **1978**, 828
- [8] Thöm, V. J.; Hosken, G. D.; Hancock, R. D. *Inorg. Chem.* **1985**, 24, 3378
- [9] Hinz, F. P.; Margerum, D. W. *Inorg. Chem.* **1974**, 13, 2941
- [10] Evers, A. Hancock, R. D. *Inorg. Chim. Acta* **1989**, 160, 245
- [11] Kodama, M.; Kimura, E. *J. Chem. Soc., Dalton Trans.* **1977**, 1473
- [12] Kodama, M.; Kimura, E. *J. Chem. Soc., Dalton Trans.* **1978**, 1081
- [13] Kodama, M.; Kimura, E. *J. Chem. Soc., Dalton Trans.* **1977**, 2269
- [14] Kimura, E.; Shiota, T.; Moike, T.; Shiro, M.; Kodama, M. *J. Am. Chem. Soc.* **1990**, 112, 5805
- [15] Leugger, A. P.; Hertli, L.; Kaden, T. A. *Helv. Chim. Acta* **1978**, 61, 2296
- [16] Kodama, M.; Kimura, E. *J. Chem. Soc., Dalton Trans.* **1980**, 327
- [17] Thöm, V. J., Hancock, R. D. *J. Chem. Soc., Dalton Trans.* **1985**, 1877
- [18] Kodama, M.; Kimura, E. *J. Chem. Soc., Dalton Trans.* **1976**, 2335
- [19] Clarkson, A. J.; Blackman, A. G.; Clark, C. R. *J. Chem. Soc. Dalton Trans.* **2001**, 758
- [20] Buckingham, D. A.; Clark, C. R.; Rogers, A. J. *Aust. J. Chem.* **1998**, 51, 461
- [21] Kim, J. H.; Britten, J.; Chin, J. *J. Am. Chem. Soc.* **1993**, 115, 3618
- [22] Iitaka, Y.; Shina, M.; Kimura, E. *Inorg. Chem.* **1974**, 13, 2886
- [23] Loehlin, J. H.; Fleischer, E. B. *Acta Crystallogr., Sect. B* **1976**, 32, 3063
- [24] Carrington, S. J.; Buckingham, D. A.; Simpson, J.; Blackman, A. G.; Clark, C. R. *J. Chem. Soc. Dalton Trans.* **1999**, 3809
- [25] Nonoyama, M.; Kurimoto, T. *Polyhedron* **1985**, 4, 471

-
- [26] Clarkson, A. J.; Buckingham, D. A.; Rogers, A. J.; Blackman, A. G.; Clark, C. R. *Inorg. Chem.* **2000**, *39*, 4769
- [27] Buckingham, D. A.; Clark, C. R.; Rogers, A. J. *J. Am. Chem. Soc.* **1997**, *119*, 4050
- [28] Ajioka, M.; Yano, S.; Matsuda, K.; Yoshikawa, S. *J. Am. Chem. Soc.* **1981**, *103*, 2459
- [29] Styka, M. C.; Smierciak, R. C.; Blinn, E. L.; DeSimone, R. S.; Passariello, J. V. *Inorg. Chem.* **1978**, *17*, 82
- [30] Ballester, L.; Gutiérrez, A.; Perpiñán, M. F.; Sánchez, A. E.; Azcondo, M. T.; González, M. J. *Inorg. Chim. Acta* **2004**, *357*, 1054
- [31] Clay, R. M.; Murray-Rust, P. Murray-Rust, J. *Acta Crystallogr., Sect. B.* **1979**, *35*, 1894
- [32] Smierciak, R. C.; Passariello, J.; Blinn, E. L. *Inorg. Chem.* **1977**, *16*, 2646
- [33] Plassman, W. H.; Swisher, R. G.; Blinn, E. L. *Inorg. Chem.* **1980**, *19*, 1101
- [34] Bencini, A.; Bianchi, A.; Garcia-España, E.; Jeannin, Y.; Julve, M.; Marcelino, V.; Philoche-Levisalles, M. *Inorg. Chem.* **1990**, *29*, 963
- [35] Pariya, C.; Chi, T.-Y.; Mishra, T. K.; Chung, C.S. *Inorg. Chem. Comm.* **2002**, *5*, 119
- [36] Li, J.; Ren, Y.-W.; Zhang, J.-H.; Yang, P. *J. Chem. Cryst.* **2004**, *34*, 409
- [37] Lin, Y.-C.; Lu, T.-H.; Liao, F.-L.; Chung, C.-S. *Anal. Sci.* **2003**, *19*, 967
- [38] Shionoya, M.; Kimura, E.; Shiro, M. *J. Am. Chem. Soc.* **1993**, *115*, 6730
- [39] Subat, M.; Borovik, A. S.; Koenig, B. *J. Am. Chem. Soc.* **2004**, *126*, 3185
- [40] Kimura, E.; Aoki, S.; Koike, T.; Shiro, M. *J. Am. Chem. Soc.* **1997**, *119*, 3068
- [41] Fujioka, H.; Koike, T.; Yamada, N.; Kimura, E. *Heterocycles* **1996**, *42*, 775
- [42] Aoki, S.; Kimura, E. *J. Am. Chem. Soc.* **2000**, *122*, 4542
- [43] Kimura, E.; Ikeda, T.; Shionoya, M.; Shiro, M. *Angew. Chem., Int. Ed.* **1995**, *34*, 663
- [44] Koike, T.; Kajitani, S.; Nakamura, I.; Kimura, E.; Shiro, M. *J. Am. Chem. Soc.* **1995**, *117*, 1210
- [45] Hubin, T. J.; Alcock, N. W.; Clase, H. J.; Busch, D. H. *Supramol. Chem.* **2001**, *13*, 261
- [46] Matsumoto, N.; Hirano, A.; Hara, T.; Ohyoshi, A. *J. Chem. Soc., Dalton Trans.* **1983**, 2405
- [47] Han, M.S.; Kim, D.H. *Supramol. Chem.* **2003**, *15*, 59
- [48] Aoki, S.; Shiro, M.; Koike, T.; Kimura, E. *J. Am. Chem. Soc.* **2000**, *122*, 576

-
- [49] Koike, T.; Takashige, M.; Kimura, E.; Fujioka, H.; Shiro, M. *Chem. Eur. J.* **1996**, *2*, 617
- [50] Shionoya, M.; Ikeda, T.; Kimura, E.; Shiro, M. *J. Am. Chem. Soc.* **1994**, *116*, 3848
- [51] Kimura, E.; Katsube, N.; Koike, T.; Shiro, M.; Aoki, S. *Supramol. Chem.* **2002**, *14*, 95
- [52] Lau, V. C.; Berben, L. A.; Long, J. R. *J. Am. Chem. Soc.* **2002**, *124*, 9042
- [53] Krotz, A. H.; Kuo, L. Y.; Barton, J. K. *Inorg. Chem.* **1993**, *32*, 5963
- [54] Lu, T.-H.; Panneerselvam, K.; Chen, L.-H.; Lin, Y.-J.; Liao, F.-L.; Chung, C.-S. *Anal. Sci.* **2001**, *17*, 571
- [55] Buckingham, D. A.; Clark, C. R.; Rogers, A. J.; Simpson, J. *Inorg. Chem.* **1995**, *34*, 3646
- [56] Tsuboyama, S.; Sakurai, T.; Tsuboyama, K. *J. Chem. Soc., Dalton Trans.* **1987**, *4*, 721
- [57] Tsuboyama, S.; Shiga, Y.; Takasyo, Y.; Chijimatsu, T.; Kobayashi, K.; Tsuboyama, K.; Sakurai, T. *J. Chem. Soc., Dalton Trans.* **1992**, 1783
- [58] Tsuboyama, S.; Takishima, T.; Sakurai, T.; Tsuboyama, K. *Nippon Kagaku Kaishi (Jap.) (J. Chem. Soc. Jpn.)* **1987**, 313
- [59] Tsuboyama, S.; Tsuboyama, K.; Sakurai, T. *Acta Crystallogr., Sect.C: Cryst. Struct. Commun.* **1989**, *45*, 669
- [60] Tsuboyama, S.; Tsuboyama, K.; Sakurai, T. *Acta Crystallogr., Sect.C: Cryst. Struct. Commun.* **1990**, *46*, 727
- [61] Tsuboyama, S.; Miki, S.; Chijimatsu, T.; Tsuboyama, K.; Sakurai, T. *J. Chem. Soc., Dalton Trans.* **1989**, 2359
- [62] Kobayashi, K.; Tsuboyama, S.; Tsuboyama, K.; Ito, T. *Anal. Sci.* **1996**, *12*, 821
- [63] Kobayashi, K.; Tsuboyama, S.; Tabata, N.; Tsuboyama, K.; Sakurai, T. *Anal. Sci.* **1996**, *12*, 531
- [64] Tsuboyama, S.; Kobayashi, K.; Tsuboyama, K.; Sakurai, T. *Anal. Sci.* **1995**, *11*, 707
- [65] Kobayashi, K.; Takahashi, H.; Nishio, M.; Umezawa, Y.; Tsuboyama, K.; Tsuboyama, S. *Anal. Sci.* **2000**, *16*, 1103
- [66] Tsuboyama, S.; Matsudo, M.; Tsuboyama, K.; Sakurai, T. *Acta Crystallogr., Sect.C: Cryst. Struct. Commun.* **1989**, *45*, 872
- [67] Aoki, S.; Shiro, M.; Kimura, E. *Chem.-Eur. J.* **2002**, *8*, 929

-
- [68] Kojima, M.; Nakabayashi, K.; Ohba, S.; Okumoto, S.; Saito, Y.; Fujita, J. *Bull. Chem. Soc. Jpn.* **1986**, *59*, 277
- [69] Mizukami, S.; Nagano, T.; Urano, Y.; Odani, A.; Kikuchi, K. *J. Am. Chem. Soc.* **2002**, *124*, 3920
- [70] Aoki, S.; Kimura, E. *Chem. Rev.* **2004**, *104*, 769
- [71] Koike, T.; Kimura, E.; Nakamura, I.; Hashimoto, Y.; Shiro, M. *J. Am. Chem. Soc.* **1992**, *114*, 7338
- [72] Koike, T.; Watanabe, T.; Aoki, S.; Kimura, E.; Shiro, M. *J. Am. Chem. Soc.* **1996**, *118*, 12696; Kimura, E.; Aoki, S.; Kikuta, M.; Koike, T. *Proc. Natl. Acad. Sci. U.S.A.* **2003**, *100*, 3731; Aoki, S.; Kaido, S.; Fujioka, H.; Kimura, E. *Inorg. Chem.* **2003**, *42*, 1023; Koike, T.; Abe, T.; Takahashi, M.; Ohtani, K.; Kimura, E.; Shiro, M. *J. Chem. Soc., Dalton Trans.* **2002**, 1764; Kimura, E.; Koike, T. *Chem. Soc. Rev.* **1998**, *27*, 179; Kimura, E. *S. Afr. J. Chem.* **1997**, *50*, 240; Kimura, E.; Aoki, S. *BioMetals* **2001**, *14*, 191
- [73] Kimura, E.; Koike, T. *J. Chem. Soc., Chem. Commun.* **1998**, 1495
- [74] Koenig, B.; Pelka, M.; Zieg, H.; Ritter, T.; Bouas-Laurent, H.; Bonneau, R.; Desvergne, J.-P. *J. Am. Chem. Soc.* **1999**, *121*, 1681
- [75] Koenig, B.; Pelka, M.; Reichenbach-Klinke, R.; Schelter, J.; Daub, J. *Eur. J. Org. Chem.* **2001**, 2297
- [76] Reichenbach-Klinke, R.; Kruppa, M.; Koenig, B. *J. Am. Chem. Soc.* **2002**, *124*, 12999
- [77] Wiest, O.; Harrison, C. B.; Saettel, N. J.; Cibulka, R.; Sax, M.; Koenig, B. *J. Org. Chem.* **2004**, *69*, 8183
- [78] Kimura, E.; Ikeda, T.; Aoki, S.; Shionoya, M. *J. Biol. Inorg. Chem.* **1998**, *3*, 259; Kikuta, E.; Murata, M.; Katsube, N.; Koike, T.; Kimura, E. *J. Am. Chem. Soc.* **1999**, *121*, 5426; Kikuta, E.; Katsube, N.; Kimura, E. *J. Biol. Inorg. Chem.* **1999**, *4*, 431; Kimura, E.; Koike, T.; Kimura, E. *J. Inorg. Biochem.* **2000**, *79*, 253; Kikuta, E.; Matsubara, R.; Katsube, N.; Koike, T.; Kimura, E. *J. Inorg. Biochem.* **2000**, *82*, 239; Kimura, E.; Kikuta, E. *J. Biol. Inorg. Chem.* **2000**, *5*, 139; Kimura, E.; Kitamura, H.; Ohtani, K.; Koike, T. *J. Am. Chem. Soc.* **2000**, *122*, 4668; Kikuta, E.; Aoki, S.; Kimura, E. *J. Biol. Inorg. Chem.* **2002**, *7*, 473
- [79] Koike, T.; Kimura, E. *J. Am. Chem. Soc.* **1991**, *113*, 8935
- [80] Aoki, S.; Kimura, E. *Rev. Mol. Biotechnol.* **2002**, *90*, 129
- [81] Kikuta, E.; Aoki, S.; Kimura, E. *J. Am. Chem. Soc.* **2001**, *123*, 7911

-
- [82] Jones, K. A.; Peterlin, B. M. *Annu. Rev. Biochem.* **1994**, *63*, 717
- [83] Kimura, E.; Kikuchi, M.; Kitamura, H.; Koike, T. *Chem. Eur. J.* **1999**, *5*, 3113
- [84] Koenig, B.; Gallmeier, H.-C.; Reichenbach-Klinke, R. *Chem Commun.* **2001**, 2390
- [85] Aoki, S.; Jikiba, A.; Takeda, K.; Kimura, E. *J. Phys. Org. Chem.* **2004**, *17*, 489
- [86] Liang, X.; Parkinson, J. A.; Weishaupl, M.; Gould, R. O.; Paisey, S. J.; Park, H.; Hunter, T. M.; Blindauer, C. A.; Parsons, S.; Sadler, P. J. *J. Am. Chem. Soc.* **2002**, *124*, 9105
- [87] Bosnich, B.; Poon, C. K.; Tobe, M. L. *Inorg. Chem.* **1965**, *4*, 1102
- [88] Gao, J.; Martell, A. E.; Reibenspies, J. H. *Helv. Chim. Acta* **2003**, *86*, 196
- [89] Lindoy, L. F.; Mahinay, M. S.; Skelton, B. W.; White, A. H. *J. Coord. Chem.* **2003**, *56*, 1203
- [90] Gao, J.; Reibenspies, J. H.; Sun Y.; Martell, A. E. *Helv. Chim. Acta* **2003**, *86*, 563
- [91] Kato, M.; Ito, T. *Bull. Chem. Soc. Jpn.* **1986**, *59*, 285
- [92] Wragg, D. S.; Hix, G. B.; Morris, R.E. *J. Am. Chem. Soc.* **1998**, *120*, 682287
- [93] Morris, R. E. *J. Mater. Chem.* **2001**, *11*, 513
- [94] Wheatley, P. S.; Love, C. J.; Morrison, J. J.; Shannon, I. J.; Morris, R. E. *J. Mater. Chem.* **2000**, *12*, 477
- [95] Liang, Xiangyang; Weishaupl, M.; Parkinson, J. A.; Parsons, S.; McGregor, P. A.; Sadler, P. J. *Chem. Eur. J.* **2003**, *9*, 4709
- [96] Kato, M.; Ito, T. *Inorg. Chem.* **1985**, *24*, 509
- [97] Kim, J. C.; Jo, H.; Lough, A. J.; Cho, J.; Lee, U.; Pyun, S. Y. *Inorg. Chem. Commun.* **2003**, *6*, 474
- [98] Glidewell, C.; Ferguson, G.; Gregson, R. M.; Lough, A. J. *Acta Crystallogr., Sect. C: Cryst. Struct. Commun.* **2000**, *56*, 174
- [99] Suh, M. P.; Min, K. S.; Ko, J. W.; Choi, H. J. *Eur. J. Inorg. Chem.* **2003**, 1373
- [100] Suh, M. P.; Choi, H. J.; So, S. M.; Kim, B. M. *Inorg. Chem.* **2003**, *42*, 676
- [101] Zakaria, C. M.; Ferguson, G.; Lough, A. J.; Glidewell, C. *Acta Crystallogr., Sect. B: Struct. Sci.* **2002**, *58*, 78
- [102] Zakaria, C. M.; Ferguson, G.; Lough, A. J.; Glidewell, C. *Acta Crystallogr., Sect. C: Cryst. Struct. Commun.* **2001**, *57*, 683
- [103] Choi, K.-Y.; Ryu, H.; Lim, Y.-M.; Sung, N.-D.; Shin, U.-S.; Suh, M. *Inorg. Chem. Commun.* **2003**, *6*, 412
- [104] Shaikh, N.; Panja, A.; Banerjee, P.; Kubiak, M.; Ciunik, Z.; Puchalska, M.; Legendziewicz, J.; Vojtisek, P. *Inorg. Chim. Acta* **2004**, *357*, 25

-
- [105] Namouchi-Cherni, S.; Driss, A.; Jouini, T. *Acta Crystallogr., Sect. C: Cryst. Struct. Commun.* **1999**, *55*, 345
- [106] Chen, C.-H.; Cai, J.; Liao, C.-Z.; Feng, X.-L.; Chen, X.-M.; Ng, S. W.; *Inorg. Chem.* **2002**, *41*, 4967
- [107] Cai, J.; Chen, C.-H.; Liao, C.-Z.; Yao, J.-H.; Hu, X.-P.; Chen, X.-M. *J. Chem. Soc., Dalton Trans.* **2001**, 1137
- [108] Cai, J.-W.; Chen, C.-H.; Zhou, J.-S.; *Wuji Huaxue Xuebao (Chin.) (Chin. J. Inorg. Chem.)* **2003**, *19*, 81
- [109] Tang, J.-K.; Gao, E.-Q.; Zhang, L.; Liao, D.-Z.; Jiang, Z.-H.; Yan, S.-P. *J. Coord. Chem.* **2002**, *55*, 527
- [110] Choi, J.-H.; Suzuki, T.; Kaizaki, S. *Private Communication to Cambridge Database* **2002**
- [111] Gao, E.-Q.; Zhao, Q.-H.; Tang, J.-K.; Liao, D.-Z.; Jiang, Z.-H.; Yan, S.-P. *J. Coord. Chem.* **2002**, *55*, 205
- [112] Basiuk, E. V.; Basiuk, V. A.; Hernandez-Ortega, S.; Martinez-Garcia, M.; Saniger-Blesa, J.-M. *Acta Crystallogr., Sect. C: Cryst. Struct. Commun.* **2001**, *57*, 553
- [113] Basiuk, E.V.; Basiuk, V. V.; Gomez-Lara, J.; Toscano, R. A. *J. Inclusion Phenom. Macrocyclic Chem.* **2000**, *38*, 45
- [114] Toby, B. H.; Hughey, J. L.; Fawcett, T. G.; Potenza, J. A.; Schugar, H. J. *Acta Crystallogr., Sect. B: Struct. Crystallogr. Cryst. Chem.* **1981**, *37*, 1737
- [115] Gao, E.-Q.; Tang, J.-K.; Liao, D.-Z.; Jiang, Z.-H.; Yan, S.-P.; Wang, G.-L. *Inorg. Chem.* **2001**, *40*, 3134
- [116] Benelli, C.; Dei, A.; Gatteschi, D.; Pardi, L. *Inorg. Chem.* **1988**, *27*, 2831; Lemma, K.; Ellern, A.; Bakac, A. *Inorg. Chem.* **2003**, *42*, 3662
- [117] Caneschi, A.; Dei, A.; Gatteschi, D.; Tangoulis, V. *Inorg. Chem.* **2002**, *41*, 3508
- [118] Caneschi, A.; Dei, A.; de Biani, F. F.; Gutlich, P.; Ksenofontov, V.; Levchenko, G.; Hofer, A.; Renz, F. *Chem. Eur. J.* **2001**, *7*, 3926
- [119] Cador, O.; Dei, A.; Sangregorio, C. *Chem. Commun.* **2004**, 652
- [120] Escuer, A.; Vicente, R.; Salah El Fallah, M.; Solans, X.; Font-Bardia, M. *Inorg. Chim. Acta* **1998**, *278*, 43
- [121] Ito, H.; Ito, T. *Bull. Chem. Soc. Jpn.* **1985**, *58*, 2133
- [122] Cook, D. F.; Curtis, N. F.; Gladkikh, O. P.; Weatherburn, D. C. *Inorg. Chim. Acta* **2003**, *355*, 15;
- [123] Curtis, N. F.; Swann, D. A.; Waters, T. N. *J. Chem. Soc., Dalton Trans.* **1973**, 1408

-
- [124] Cook, D. F.; Curtis, N. F.; Rickard, C. E. F.; Waters, J. M.; Weatherburn, D. C. *Inorg. Chim. Acta* **2003**, 355, 1
- [125] Simon, E.; Haridon, P.L.; Pichon, R.; L'Her, M. *Inorg. Chim. Acta* **1998**, 282, 173
- [126] Ito, H.; Ito, T. *Chem. Lett.* **1985**, 1251
- [127] Ito, H.; Ito, T. *Bull. Chem. Soc. Jpn.* **1985**, 58, 1755
- [128] Oshio, H. *Inorg. Chem.* **1993**, 32, 4123
- [129] Nowicka, B.; Schmauch, G.; Chihara, T.; Heinemann, F.W.; Hagiwara, M.; Wakatsuki, Y.; Kisch, H. *Bull. Chem. Soc. Jpn.* **2002**, 75, 2169
- [130] Ballester, L.; Gil, A. M.; Gutierrez, A.; Perpignan, M. F.; Azcondo, M. T.; Sanchez, A. E.; Amador, U.; Campo, J.; Palacio, F. *Inorg. Chem.* **1997**, 36, 5291
- [131] Ballester, L.; Gutierrez, A.; Perpignan, M. F.; Amador, U.; Azcondo, M. T.; Sanchez, A. E.; Bellitto, C. *Inorg. Chem.* **1997**, 36, 6390
- [132] Tadokoro, M.; Sato, K.; Shiomi, D.; Takui, T.; Itoh, K. *Mol. Cryst. Liq. Cryst. Sci. Technol., Sect. A* **1997**, 306, 49
- [133] Chan, H.-L.; Liu, H.-Q.; Tzeng, B.-C.; You, Y.-S.; Peng, S.-M.; Yang, M.; Che, C.-M. *Inorg. Chem.* **2002**, 41, 3161
- [134] Sakai, K.; Yamada, Y.; Tsubomura, T. *Inorg. Chem.* **1996**, 35, 3163
- [135] Vasconcellos, L. C. G.; Oliveira, C. P.; Castellano, E. E.; Ellena, J.; Moreira, I. S. *Polyhedron* **2001**, 20, 493
- [136] Colacio, E.; Dominguez-Vera, J. M.; Escuer, A.; Kivekas, R.; Romerosa, A. *Inorg. Chem.* **1994**, 33, 3914
- [137] Colacio, E.; Dominguez-Vera, J. M.; Escuer, A.; Kivekas, R.; Klinga, M.; Moreno, J.-M.; Romerosa, A. *J. Chem. Soc., Dalton Trans.* **1997**, 1685
- [138] Hughey, J. L.; Fawcett, T. G.; Rudich, S. M.; Lalancette, R. A.; Potenza, J. A.; Schugar, H. J. *J. Am. Chem. Soc.* **1979**, 101, 2617
- [139] John, E.; Bharadwaj, P. K.; Krogh-Jespersen, K.; Potenza, J. A.; Schugar, H. J. *J. Am. Chem. Soc.* **1986**, 108, 5015
- [140] John, E.; Bharadwaj, P. K.; Potenza, J.A.; Schugar, H.J. *Inorg. Chem.* **1986**, 25, 3065
- [141] Vicente, R.; Escuer, A.; Ribas, J.; Dei, A.; Solans, X.; Calvet, T. *Polyhedron* **1990**, 9, 1729
- [142] Xie, B.; Li, K.-B.; Zou, L.-K.; Mao, Z.-H.; Hong, Z. *Jiegou Huaxue (Chin.) (Chinese J. Struct. Chem.)* **2004**, 23, 324

-
- [143] De Clercq, E.; Yamamoto, N.; Pauwels, R.; Baba, M.; Schols, D.; Nakashima, H.; Balzarini, J.; Debyser, Z.; Murrer, B. A.; Schwartz, D.; Thornton, D.; Bridger, G.; Fricker, S.; Henson, G.; Abrams, M.; Picker, D. *Proc. Natl. Acad. Sci. U.S.A.* **1992**, *89*, 5286
- [144] De Clercq, E. *Mol. Pharmacol.* **2000**, *57*, 833
- [145] Esté, J. A.; Cabrera, C.; De Clercq, E.; Struyf, S.; Van Damme, J.; Bridger, G.; Skerlj, R. T.; Abrams, M. J.; Henson, G.; Gutierrez, A.; Clotet, B.; Schols, D. *Mol. Pharmacol.* **1999**, *55*, 67
- [146] Gerlach, L. O.; Skerlj, R. T.; Bridger, G. J.; Schwartz, T. W. *J. Biol. Chem.* **2001**, *276*, 14153
- [147] Hung, Y.; Martin, L. Y.; Jackels, S. C.; Tait, A. M.; Busch, D. H. *J. Am. Chem. Soc.* **1977**, *99*, 4029; Hung, Y.; Busch, D. H. *J. Am. Chem. Soc.* **1977**, *99*, 4977
- [148] Cooksey, C. J.; Tobe, M. L. *Inorg. Chem.* **1978**, *17*, 1558
- [149] Mallik, S.; Johnson, R. D.; Arnold, F. H. *J. Am. Chem. Soc.* **1994**, *116*, 8902
- [150] Mallik, S.; Johnson, R. D.; Arnold, F. H. *J. Am. Chem. Soc.* **1993**, *115*, 2518
- [151] Sun, S.; Saltmarsh, J.; Mallik, S.; Thomasson, K. *Chem. Commun.* **1998**, 519
- [152] Lee, E. Y.; Suh, M. P. *Angew. Chem. Int. Ed.* **2004**, *43*, 2798
- [153] Pocker, Y.; Stone, J. T. *Biochemistry* **1967**, *6*, 668
- [154] Graham, B.; Hearn, M. T. W.; Spiccia, L.; Skelton, B. W.; White, A. H. *Aust. J. Chem.* **2003**, *56*, 1259
- [155] Wang, Q.-L.; Xie, C.-Z.; Liao, D.-Z.; Yan, S.-P.; Jiang, Z.-H.; Cheng, P. *Transition Met. Chem.* **2003**, *28*, 16
- [156] Chaudhuri, P.; Oder, K.; Wieghardt, K.; Gehring, S.; Haase, W.; Nuber, B.; Weiss, J. *J. Am. Chem. Soc.* **1988**, *110*, 3657
- [157] Burger, K.-S.; Chaudhuri, P.; Wieghardt, K.; Nuber, B. *Chem. Eur. J.* **1995**, *1*, 583
- [158] Fry, F. H.; Jensen, P.; Kepert, C. M.; Spiccia, L. *Inorg. Chem.* **2003**, *42*, 5637
- [159] Chaudhuri, P.; Stockheim, C.; Wieghardt, K.; Deck, W.; Gregorzik, R.; Vahrenkamp, H.; Nuber, B.; Weiss, J. *Inorg. Chem.* **1992**, *31*, 1451
- [160] Gross, F.; Muller-Hartmann, A.; Vahrenkamp, H. *Eur. J. Inorg. Chem.* **2000**, 2363
- [161] Zhang, L.; Yan, H.-L.; Yan, S.-P.; Jiang, Z.-H.; Liao, D.-Z.; Wang, G.-L. *Pol. J. Chem.* **1999**, *73*, 391
- [162] Zhang, L.; Bu, W.-M.; Yan, S.-P.; Jiang, Z.-H.; Liao, D.-Z.; Wang, G.-L. *Polyhedron* **2000**, *19*, 1105

-
- [163] Bencini, A.; Bianchi, A.; Paoli, P.; Garcia-Espana, E.; Julve, M.; Marcelino, V. J. *Chem. Soc., Dalton Trans.* **1990**, 2213
- [164] Berreau, L. M.; Mahapatra, S.; Halfen, J. A.; Houser, R. P.; Young Junior, V. G.; Tolman, W. B. *Angew. Chem., Int. Ed.* **1999**, 38, 207
- [165] Gallert, S.; Weyhermuller, T.; Wieghardt, K.; Chaudhuri, P. *Inorg. Chim. Acta* **1998**, 274, 111
- [166] Justel, T.; Muller, M.; Weyhermuller, T.; Kressl, C.; Bill, E.; Hildebrandt, P.; Lengen, M.; Grodzicki, M.; Trautwein, A. X.; Nuber, B.; Wieghardt, K. *Chem. Eur. J.* **1999**, 5, 793
- [167] Jo, D.-H.; Que Junior, L. *Angew. Chem., Int. Ed.* **2000**, 39, 4284
- [168] Shiren, K.; Tanaka, K. *Inorg. Chem.* **2002**, 41, 5912
- [169] Bossek, U.; Haselhorst, G.; Ross, S.; Wieghardt, K.; Nuber, B. *J. Chem. Soc., Dalton Trans.* **1994**, 2041
- [170] Muller, M.; Weyhermuller, T.; Bill, E.; Wieghardt, K. *J. Biol. Inorg. Chem. (JBIC)* **1998**, 3, 96
- [171] Schneider, R.; Weyhermuller, T.; Wieghardt, K.; Nuber, B. *Inorg. Chem.* **1993**, 32, 4925
- [172] Wieghardt, K.; Pohl, K.; Bossek, U. *Z. Naturforsch., B: Chem. Sci.* **1988**, 43, 1184
- [173] Bossek, U.; Wieghardt, K.; Nuber, B.; Weiss, J. *Angew. Chem., Int. Ed.* **1990**, 29, 1055
- [174] Niemann, A.; Bossek, U.; Haselhorst, G.; Wieghardt, K.; Nuber, B. *Inorg. Chem.* **1996**, 35, 906
- [175] Knopp, P.; Wieghardt, K.; Nuber, B.; Weiss, J.; Sheldrick, W. S. *Inorg. Chem.* **1990**, 29, 363
- [176] Knopp, P.; Wieghardt, K.; Nuber, B.; Weiss, J. *Z. Naturforsch., B: Chem. Sci.* **1991**, 46, 1077
- [177] Jeske, P.; Wieghardt, K.; Nuber, B.; Weiss, J. *Inorg. Chim. Acta* **1992**, 193, 9
- [178] Schneider, J. L.; Young Junior, V. G.; Tolman, W. B. *Inorg. Chem.* **1996**, 35, 5410
- [179] Shores, M. P.; Long, J. R. *J. Am. Chem. Soc.* **2002**, 124, 3512
- [180] Xu, J.-Y.; Gu, W.; Bian, H.-D.; Bian, F.; Yan, S.-P.; Cheng, P.; Liao, D.-Z.; Jiang, Z.-H.; Shen, P.-W. *Inorg. Chem. Commun.* **2003**, 6, 513
- [181] Sudfeld, M.; Sheldrick, W. S. *Z. Anorg. Allg. Chem.* **2002**, 628, 1366
- [182] Chaudhuri, P.; Karpenstein, I.; Winter, M.; Lengen, M.; Butzlaff, C.; Bill, E.; Trautwein, A. X.; Florke, U.; Haupt, H.-J. *Inorg. Chem.* **1993**, 32, 888

-
- [183] Chaudhuri, P.; Karpenstein, I.; Winter, M.; Butzlaff, C.; Bill, E.; Trautwein, A. X.; Florke, U.; Haupt, H. H. *Chem. Commun.* **1992**, 321
- [184] Tadokoro, M.; Toyoda, J.; Isobe, K.; Itoh, T.; Miyazaki, A.; Enoki, T.; Nakasuji, K. *Chem. Lett.* **1995**, 613
- [185] Tadokoro, M.; Isobe, K.; Miyazaki, A.; Enoki, T.; Nakasuji, K. *Mol. Cryst. Liq. Cryst. Sci. Technol., Sect. A* **1996**, 278, 199
- [186] Derwahl, A.; Dickie, A. J.; House, D. A.; Jackson, W. G.; Schaffner, S.; Svensson, J.; Turnbull, M. M.; Zehnder, M. *Inorg. Chim. Acta* **1997**, 257, 179
- [187] Justel, T.; Bendix, J.; Metzler-Nolte, N.; Weyhermuller, T.; Nuber, B.; Wieghardt, K. *Inorg. Chem.* **1998**, 37, 35
- [188] Cheng, W.-C.; Yu, W.-Y.; Zhu, J.; Cheung, K.-K.; Peng, S.-M.; Poon, C.-K.; Che, C.-M. *Inorg. Chim. Acta* **1996**, 242, 105
- [189] Yu, W.-Y.; Fung, W.-H.; Zhu, J.-L.; Cheung, K.-K.; Ho, K.-K.; Che, C.-M. *J. Chin. Chem. Soc.(Taipei)* **1999**, 46, 341
- [190] Florke, U.; Haupt, H.-J.; Karpenstein, I.; Chaudhuri, P. *Acta Crystallogr., Sect. C: Cryst. Struct. Commun.* **1993**, 49, 1625
- [191] Giesbrecht, G. R.; Shafir, A.; Arnold, J. *Chem. Commun.* **2000**, 2135
- [192] Chaudhuri, P.; Verani, C. N.; Bill, E.; Bothe, E.; Weyhermuller, T.; Weighardt, K. *J. Am. Chem. Soc.* **2001**, 123, 2213
- [193] Yang, R.; Zompa, L. J. *Inorg. Chem.* **1976**, 14, 1499
- [194] Martell, A. E.; Motekaitis, R. J. Determination and use of stability constants, 2nd Ed., VCH Publishers Inc. **1992**
- [195] Chen, C.-T.; Chen, G.; Guan, Z.; Lee, D.; Arnold, F. H. *Polymer Reprints* **1996**, 37, 216
- [196] Chen, G.; Sundaresan, V.; Arnold, F. H. *Polym. Mat. Sci. Eng.* **1997**, 76, 378

2. Immobilised Zn (II) cyclen complexes as catalytic reagents for phosphodiester hydrolysis²

Abstract:

Many hydrolases found in nature have Zn(II) ions at their active site. Artificial hydrolases as alternatives for non-enzymatic hydrolysis were prepared by attaching Zn(II) cyclen complexes with an alcohol pendant to a polymeric support. These modified polymers showed a 10^4 fold enhanced intrinsic reactivity for the hydrolysis of phosphodiester over the non-catalysed reaction in solution.

² The results of this chapter have been published:

Walencyk, T.; Koenig, B. *Chim. Inorg. Acta* **2005**, 358, 2269

2.1 Introduction

2.1.1 Metalloenzymes

Phosphate esters exist ubiquitously in nature ^[1] in the form of nucleoside phosphates (nucleotides) as components of RNA (or DNA), sugar nucleotides for glycosylation of oligosaccharides or proteins, activated form of proteins responding to extracellular signals, and chemical mediators playing central roles in intracellular signals.^[2] Most nucleases contain in their active site metal ions, typically Zn(II), Ca(II), Mg(II) and Fe(II), which can play fundamental catalytic roles.^[3] Phosphodiester linkages of DNA are very stable to hydrolysis, with a half-life for spontaneous hydrolysis estimated at 10^{11} years at pH 7 and 25 °C.^[4]

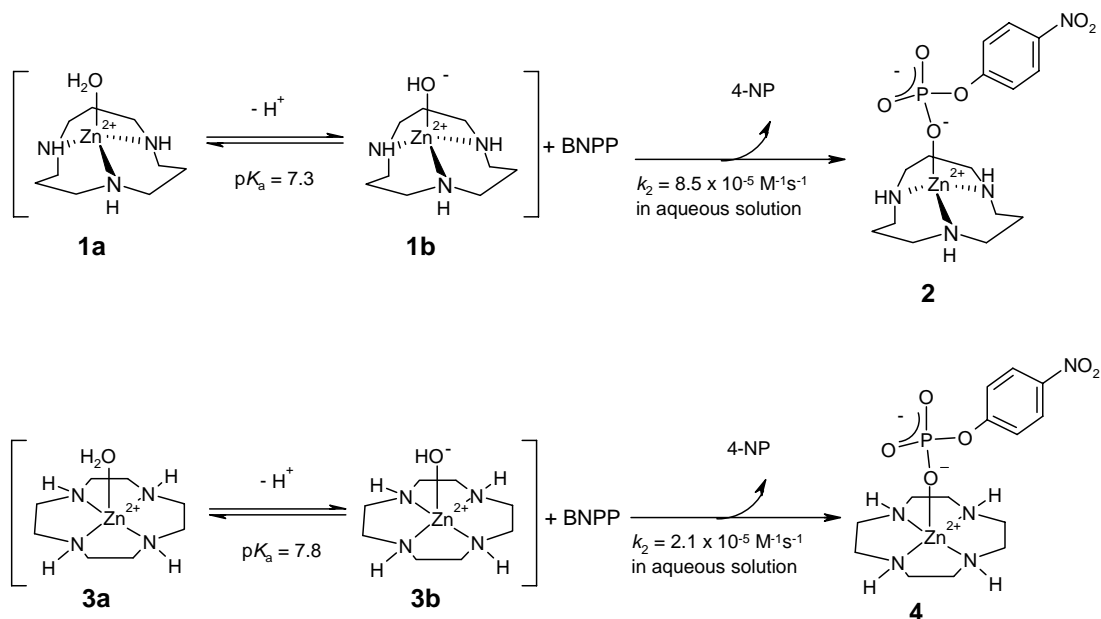
Zn(II) is used by hydrolases over other metals due to its specific properties. Zn(II) does not have any redox activity (no generation of radical sites), is a strong Lewis acid and binds strongly to oxyanions. Zinc has intermediate polarisability (hard-soft character) and flexible coordination geometry (coordination number between four and six), which is essential for hydrolytic processes involving expansion of the coordination sphere.^[5]

Typical hydrolases which have Zn(II) at their active centre include carboxypeptidase (CPD), thermolysin, β -lactamase, phosphomonoesterase [such as alkaline phosphatase (AP)], phosphodiesterase, phosphotriesterase, matrix metalloproteinase (MMP) and carbonic anhydrase (CA).^[1,5,6,7,8,9] There are three primary types of zinc binding sites: structural, catalytic and cocatalytic. In catalytic sites zinc forms complexes, which are tetrahedral or trigonal-bipyramidal, with water and four or five amino acid residues, with His, Glu, Asp and Cys being the most common.^[9] The coordinated water may be polarised and activated by the Zn(II) alone, or together with a base of an active-site amino acid at neutral pH. This generates OH⁻ ions and displacement of water or expansion of the coordination spheres results in Lewis acid catalysis by the catalytic zinc atom.^[8,9,10,11,12,13] This is generally done by strong ligands or inhibitors such as iodide, sulphonamide, alcohol, thiol, phosphates or phenol.^[6]

2.1.2 Models

In order to gain a better understanding of the chemistry of the Zn(II) ion in zinc hydrolases, simple models have been designed, generally featuring tridentate or tetradentate ligands with free binding sites.^[11,12,14,15,16]

Scheme 1. Acceleration of phosphate ester hydrolysis by azamacrocycles.

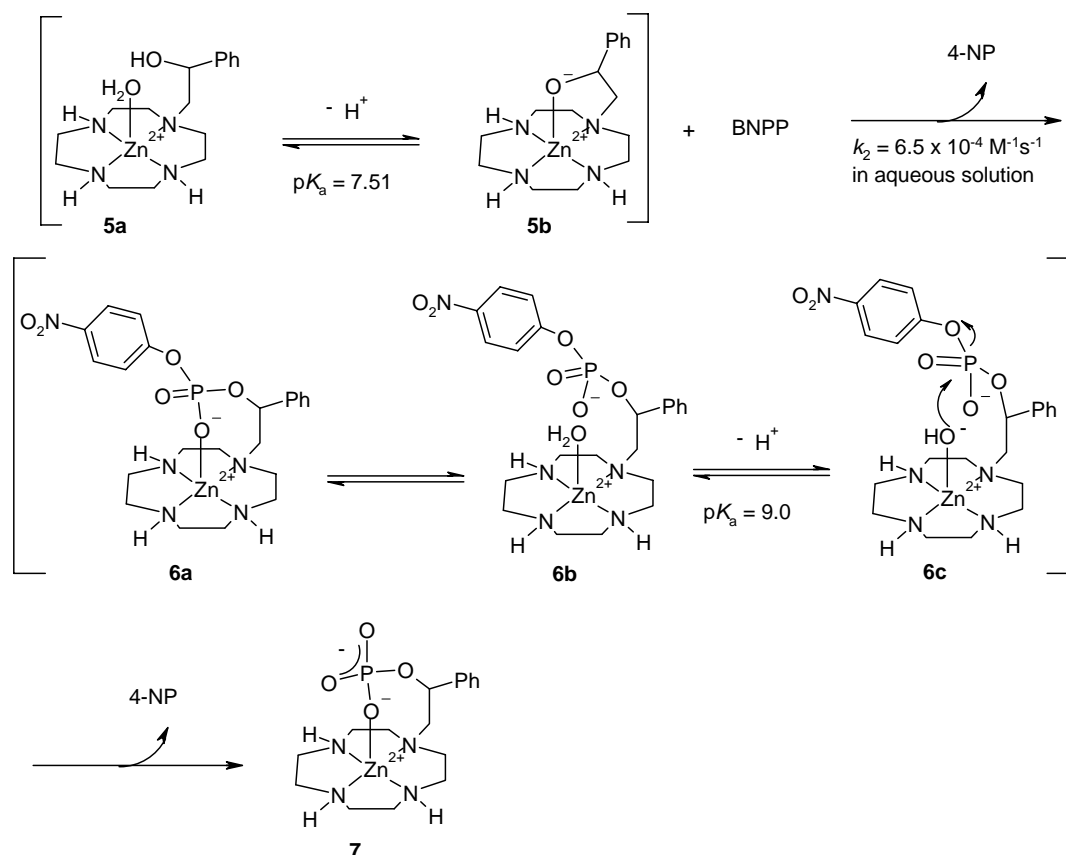


The macrocyclic complex **1b** was found to mimic the pH dependant CO_2 hydration and HCO_3^- dehydration of CA, suggesting that the $\text{Zn(II)-OH}^-/\text{Zn(II)-OH}_2$ equilibrium at the active centre controlled the catalysis.^[17,18,19,20] The acceleration of hydrolysis of phosphate esters by metal complexes has in particular lead to a large number of simple artificial nucleases.^[11,15,16,21] The 12-membered macrocyclic tetraamine, 1,4,7,10-tetracyclododecane (cyclen or Cyc) **3** was also shown to be a useful biomimetic model for CA^[17,20,22] and AP.^[19] Kimura and co-workers found that **1** and **3** (with **1b** and **3b** being the active species) hydrolysed bis(4-nitrophenyl) phosphate (BNPP) with second order rate constants of $8.5 \times 10^{-5} \text{ M}^{-1} \text{ s}^{-1}$ and $2.1 \times 10^{-5} \text{ M}^{-1} \text{ s}^{-1}$ respectively, at 35°C .^[23]

A Zn(II)Cyc complex with an alcohol-pendant **5** mimicked the Zn(II) activated serine of AP and gave a second-order rate constant for the 4-nitrophenolate release reaction from BNPP of $6.5 \times 10^{-4} \text{ M}^{-1} \text{ s}^{-1}$ in aqueous solution at 35°C .^[23] In the proposed mechanism the alcohol group is deprotonated by the proximate Zn(II) to an alkoxide (**5b**). This alkoxide is 125 times a better nucleophile to the phosphate substrate than the Zn(II) -bound hydroxide

of **3**, and attacks BNPP to give a phosphoryl intermediate **6**. This intermediate is susceptible to further hydrolysis by the intramolecular Zn(II)-bound hydroxide to give **7**. The studies of Kimura showed that phosphomonoesters are not substrates for mononuclear Zn(II) phosphatase models, but rather inhibitors as shown by the isolation of the stable complexes **2**, **4** and **7**.^[6]

Scheme 2. Proposed hydrolytic mechanism of Zn(II)Cyc with an alcohol-pendant.



Since dianions of phosphate monoesters are potentially bidentate donors, RPO_3^{2-} may bridge two Zn(II) ions.^[24] A number of various bis-Zn(II)Cyc^[25] and tris-Zn(II)Cyc^[26] complexes were synthesised in an attempt to improve the binding affinity to phosphate monoesters. It was found that tris-Zn(II)Cyc complexes bind NPP^{2-} 300 times better than bis-Zn(II)Cyc and 60 times better than Zn(II)Cyc.^[24]

2.1.3 Synzymes - Synthetic polymers with enzyme like activities

In enzyme-substrate complexes, polar interactions such as hydrogen bonding and dipole-dipole interactions as well as electrostatic interactions between the enzyme and substrate contribute significantly to the stabilisation of the transition states.^[27] These polar interactions are enhanced in the hydrophobic microenvironment provided by the enzyme. Construction and control of such an environment of a catalyst-substrate complex is not easy with a small molecular framework.^[28] The easiest way to obtain a hydrophobic environment in water is to attach the catalytic centre to a synthetic polymer.^[29] Metal complexes as active sites for polymeric artificial enzymes have been constructed and their enhanced intrinsic reactivity for the hydrolysis of peptide or phosphodiester bonds shown.^[30,31,32] The most common technique employed so far for creating such active sites has been molecular imprinting.^[33] The disadvantage of molecular imprinted polymers (MIPs) is that a large number of the catalytic sites are embedded within the polymeric body and substrates have limited access to these cavities.^[31,34]

Cu(II)Cyc complexes which were attached to poly(chloromethylstyrene-*co*-divinylbenzene) (PCD) beads were found to enhance the proteolytic activity up to 10^4 times when compared to Cu(II)Cyc complex.^[31] The Co(III)Cyc complex is one of the most effective synthetic catalysts for the hydrolysis of supercoiled DNA.^[35] Suh and co-workers attached the Co(III)Cyc complex to PCD derivatives and showed that the reactivity of the resulting polymer is enhanced 200 times toward super coiled DNA^[36] and 150 times toward linear DNA^[32] when compared to the Co(III)Cyc complex. To further increase the catalytic activity of artificial active sites, Suh increased the catalytic group density by synthesising polymers with dinuclear and tetranuclear sites containing Cu(II)Cyc.^[37]

By attaching a preassembled catalytic module to a synthetic polymer, all sites are on the surface and thus have access to the substrate (unlike in MIPs) and it is easier to interpret the catalytic outcome on a molecular basis as the structure is already known. The catalytic module chosen was Zn(II)Cyc with an alcohol pendant, due to the strong binding of Zn(II) to Cyc,^[38] the hydrolytic abilities of such complexes^[24] and their known mechanisms.^[6]

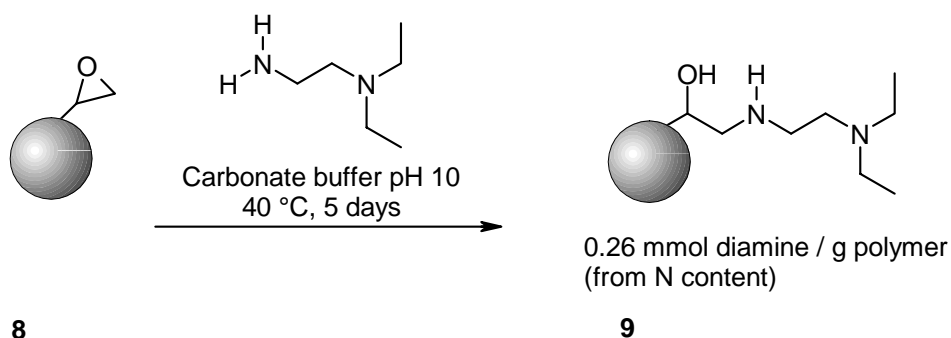
2.2 Results and discussion

2.2.1 Synthesis of mono-Zn(II)Cyc polymer

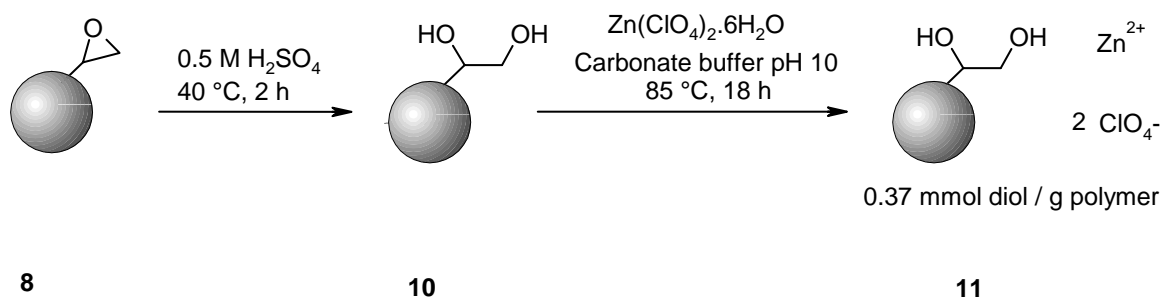
The solid support chosen for the synthesis was a 40-90 μm Fractogel Epoxy bead **8**.^[39] The presence of the epoxide groups on the surface allowed for an efficient way to incorporate an alcohol pendant into the catalytic module. The epoxide ring opening can form two regiomers, however only one is shown in the structures for simplicity.

In order to determine the maximum amount of epoxide groups available on the surface for nucleophilic attack, diethylaminoethylamine was coupled to the polymer. Standard conditions^[40] gave polymer **9**, with an amine loading of 0.26 mmol g^{-1} , which was taken to be the maximum loading for the polymer.

Scheme 3. Determination of maximum loading of the epoxide polymer.



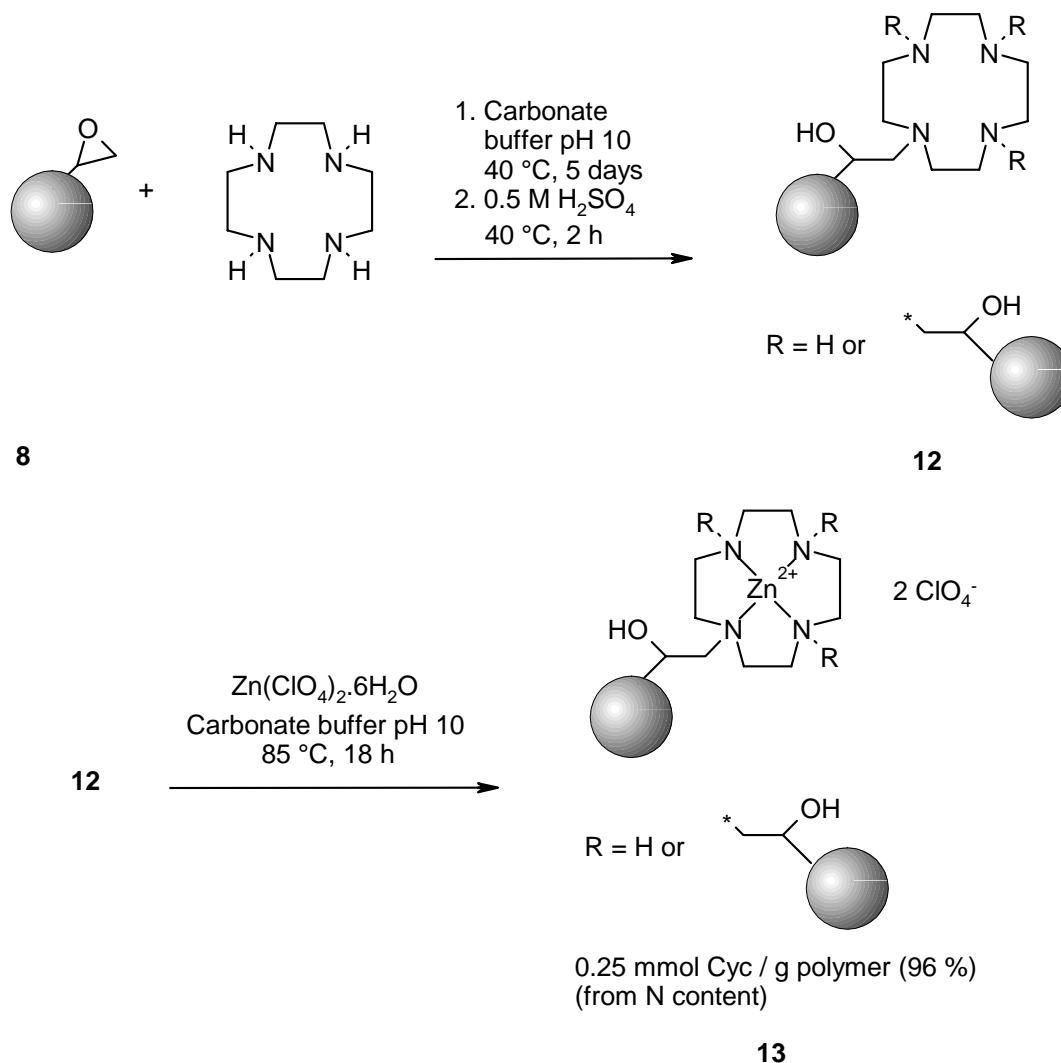
A blank polymer was also generated in order to quantify the hydrolytic effect of the polymer itself. The epoxide polymer **8**, with $0.394 \text{ mmol epoxide/g polymer}$, was heated with dilute H_2SO_4 to generate the diol **10**. This diol was then complexed with zinc perchlorate to yield polymer **11**. The corresponding diol loading of polymer **11** was calculated to be 0.37 mmol/g .

Scheme 4. Synthesis of the Zn(II) diol polymer **11**.

To generate a Zn(II)Cyc with an alcohol pendant (analogous to **5**) on a solid support, 1,4,7,10-tetraazacyclododecane (Cyc) was coupled to the epoxide polymer under standard conditions. After deactivation of the remaining epoxide groups with dilute H_2SO_4 , the corresponding Zn(II) complex **13** was generated by reacting the polymer with aqueous zinc(II) perchlorate hexahydrate solution at pH 10. The Zn(II)Cyc loading of the polymer can be calculated from the N content via elemental analysis, giving a value of 0.25 mmol Cyc / g polymer. This corresponds to a yield of 96 % when the loading of polymer **9** is taken to be the maximum loading. A Zn content of 8.9 % in the polymer was determined by ICP-OES analysis. This large value suggests that in addition to quantitative zinc complexation of the Cyc, amphoteric Zn(OH)_2 formation occurred. The precipitation of polymeric zinc hydroxide above neutral pH is known in the development of zinc-based hydrolytic agents.^[41,42,43]

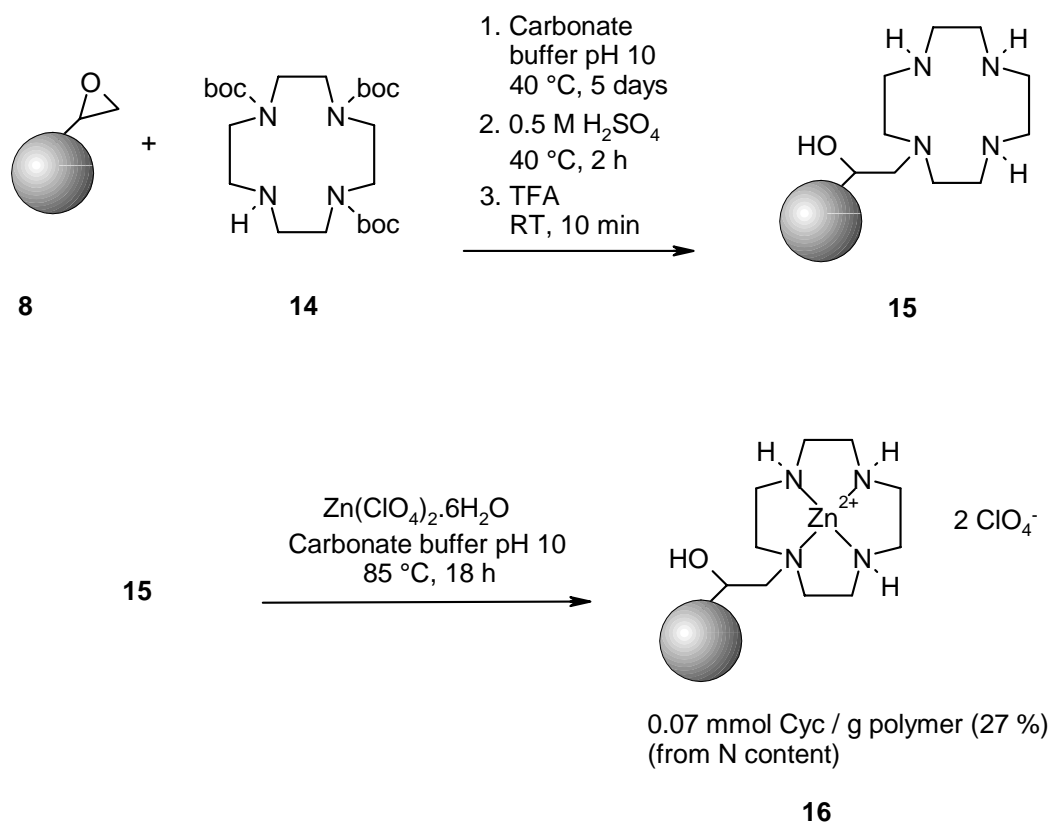
Although the Zn(II)Cyc loading is very high, it is not certain if the Cyc modules are present as schematically drawn. The Cyc has 4 possible amines which could attack an epoxide thus causing cross-linked structures.

Scheme 5. Synthesis of a polymer bearing a Zn(II)Cyc complex with an alcohol pendant **11**.



Another polymer was generated using 1,4,7,-tris-*tert*-butoxycarbonyl-1,4,7,10-tetraazacyclododecane **14**^[44] instead of Cyc. After deactivation of the remaining epoxide groups with dilute H₂SO₄, the boc-protecting groups were removed quantitatively with TFA. Generation of the corresponding Zn(II) complex **16** occurred by reacting the polymer with aqueous zinc(II) perchlorate hexahydrate solution at pH 10. The loading of the polymer was determined to be 0.07 mmol Cyc / g polymer (27 % when compared to polymer **9**) which is much lower than the loading of polymer **13**. Possible reasons for the lower loading could include steric hindrance through the protecting groups and decreased reactivity of the free amine. The strategy has however the great advantage that only one of the amines of the Cyc can react with the epoxide, thereby only allowing the generation of the desired hydrolytic module.

Scheme 6. Synthesis of a polymer bearing a Zn(II)Cyc complex with an alcohol pendant **16**.

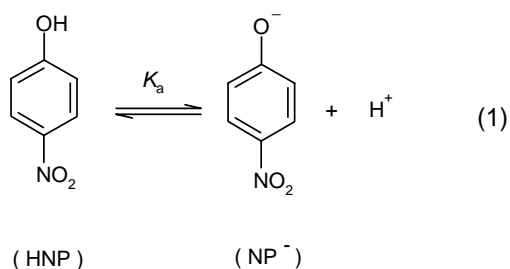


2.2.2 Kinetic measurements for the phosphodiester cleavage reaction with mono-Zn(II)Cyc complexes bound to a solid support

2.2.2.1 Calculation of the molar extinction coefficient for *para*-nitrophenolate

The hydrolysis of bis-*p*-nitrophenylphosphate (BNPP) releases *p*-nitrophenolate as a product which can be detected spectroscopically. Due to the protonation equilibrium of the nitrophenolate ion, its molar extinction coefficient depends on the pH and the used buffer system. The molar extinction coefficient of *p*-nitrophenolate was determined experimentally for the pH range 7 to 9 in the buffer system Tris/HCl (20 - 80 mM).

For the protonation equilibrium and the corresponding equilibrium constant (K_a) applies:



$$K_a = \frac{[\text{NP}^-][\text{H}^+]}{[\text{HNP}]} \quad (2)$$

According to the *Lambert-Beer* Law the absorption in dilute solutions is:

$$\text{Abs} = \epsilon_{\text{obs}} d [\text{HNP}]^{\text{total}} = \epsilon_{\text{NP}} d [\text{NP}^-] \quad (3)$$

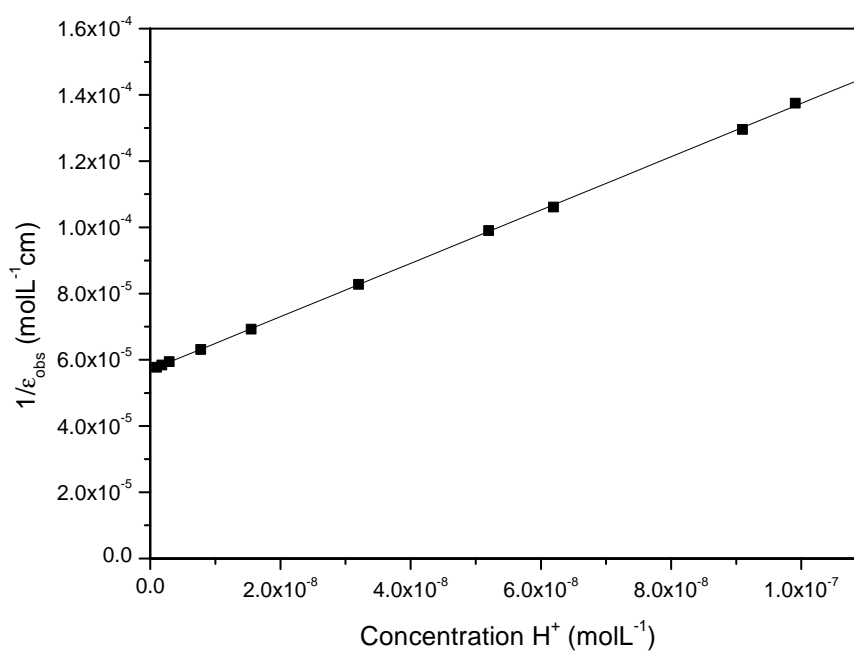
ϵ_{obs} is the measured extinction coefficient of HNP, ϵ_{NP} the extinction coefficient of the *p*-nitrophenolate ion and d the thickness of the cell. Equations (2) and (3) give Equation (4) which correlates the molar extinction coefficient with the pH value.

$$\epsilon_{\text{obs}} = \frac{\epsilon_{\text{NP}} K_a}{K_a + [\text{H}^+]} \quad (4)$$

By plotting $1/\epsilon_{\text{obs}}$ against $[\text{H}^+]$ the molar extinction coefficient for the *p*-nitrophenolate can be determined for various pH values and various buffer systems. In the pH range of 7 to 9 for the buffer system Tris/HCl the respective ϵ_{obs} values were obtained with a regression coefficient of $R^2 > 0.999$ using a dilution series ($c = 1 \times 10^{-4}$ to $5 \times 10^{-7} \text{ molL}^{-1}$ *p*-nitrophenol). The ϵ_{obs} values for 408 nm are summarised in Table 1.

Table 1. ϵ_{obs} values for *p*-nitrophenolate at 408 nm (25 °C, 50 mM Tris/HCl).

pH Value ^[a]	ϵ_{obs} for 408 nm
	[mol ⁻¹ cm ⁻¹]
7.01	7274
7.04	7717
7.21	9421
7.28	10097
7.50	12082
7.81	14436
8.11	15835
8.53	16824
8.75	17123
9.01	17310

^[a] $\Delta \text{pH} = \pm 0.005$ **Figure 1.** Calculation of ϵ_{obs} for *p*-nitrophenolate at 408 nm (25 °C, 50 mM Tris/HCl).

The $[\text{H}^+]$ concentration was plotted against the $1/\epsilon_{\text{obs}}$, with a linear regression of $R^2 > 0.9999$ (See Figure 1). With the help of the reciprocal of Equation (4), and the gradient and y-intercept from Figure 1, the equilibrium constant ($\text{p}K_{\text{a}} = 7.14 \pm 0.01$) and

molar extinction coefficient ($\epsilon_{\text{NP}, 408\text{nm}} = 17565 \text{ mol}^{-1}\text{cm}^{-1}$) could be calculated respectively. This calculated equilibrium constant agrees sufficiently well with the literature values.^[45]

Variations in the buffer concentration (Tris/HCl 20 and 80 mM) or in the ionic strength show no significant changes in the molar extinction coefficient. Changes in the region of $\Delta\epsilon_{\text{NP}} \approx \pm 70 \text{ mol}^{-1}\text{cm}^{-1}$ were detected.

2.2.2.2 Non-catalysed hydrolysis of bis-(4-nitrophenyl)phosphate (BNPP)

In addition to the metal catalysed hydrolysis of BNPP, the nucleophilic attack of OH^- from the used solvent mixtures is a parallel reaction which contributes (although only to a small extent) to the overall hydrolysis and must also be considered (base hydrolysis). The base hydrolysis is a bimolecular reaction which can be expressed as the general Equation (5):

$$v = k_{x+y} [\text{OH}^-]^x [\text{BNPP}]^y \quad (5)$$

Under the used reaction conditions, the rate of reaction of the base hydrolysis v_{base} is directly proportional to the concentration of the ester and the hydroxide ions. Here the reaction rate of the base hydrolysis follows 2nd order kinetics, with 1st order for each of the reactants. At constant pH, Equation (5) gives Equation (6) which can be simplified to Equation (7).

$$v_{\text{base}} = \frac{d(\text{Abs})}{d(t) \epsilon_{\text{obs}}} = k_{\text{obs}} [\text{BNPP}] = k_{\text{OH}} [\text{OH}^-] [\text{BNPP}] \quad (6)$$

$$k_{\text{obs}} = k_{\text{OH}} [\text{OH}^-] \quad (7)$$

The hydrolysis reaction is monitored spectroscopically, following the increase in absorptivity at 408 nm due to released *p*-nitrophenolate. The processing of the corresponding Absorption vs Time curves can be carried out using two different methods, whereby both generate pseudo-first-order kinetics due to the presence of an excess reactant. The ‘initial slope’ method is used for reactions with small turnovers (< 5 %).^[46] With this method the rate of reaction is calculated from the gradient of the absorption vs time curves which is plotted against concentration of the varying reactant, giving a k_{obs} (s^{-1}) value. For reactions with larger turnovers, the ‘log-plot’ method is used which allows for a linearisation of the absorption vs time curve.^[46] With this method the k_{obs} value is the gradient from a plot of $\ln(\text{Abs}^*/\epsilon)$ vs time (for more detailed information to Abs^* see

literature). Both methodologies give within the range of the experimental error the same k_{obs} values for the base hydrolysis of BNPP.

2.2.2.3 Hydrolysis of BNPP with immobilised mononuclear Zn(II)Cyc complexes (batch reaction)

The rate of reaction (v_{obs}) for a metal catalysed hydrolysis of BNPP is comprised of two terms, namely the base hydrolysis (v_{base}) and the metal catalysed hydrolysis (v_{cat}).

$$v_{\text{obs}} = v_{\text{cat}} + v_{\text{base}} \quad (8)$$

The phosphodiester cleavage reaction (i.e. *p*-nitrophenolate release reaction) rates of bis-(4-nitrophenyl) phosphate (BNPP) in the presence of immobilised metal catalyst were measured by following the time-dependant release of 4-nitrophenolate (at 408 nm) in buffered solutions at 25 °C. The kinetic data were collected under the conditions of [Zn-L] (concentration of the Zn(II)Cyc complex when the polymer is assumed to be dissolved) \gg [BNPP]₀ (the initially added concentration of BNPP). As [Zn-L] is constant pseudo-first-order kinetics can be assumed.

$$v_{\text{cat}} = k_{\text{cat}} [\text{Zn-L}]^{\text{total}} [\text{BNPP}] \quad (9)$$

By monitoring a sample containing no immobilised metal catalyst parallel to each reaction, the rate of reaction for the base hydrolysis could be determined. Substituting Equations (6) and (9) into Equation (8) gives Equation (10).

$$v_{\text{obs}} = (k_{\text{OH}} [\text{OH}^-] + k_{\text{cat}} [\text{Zn-L}]^{\text{total}}) [\text{BNPP}] \quad (10)$$

$$[\text{Zn-L}]^{\text{total}} = [\text{Zn-L-OH}^-] + [\text{Zn-L-OH}_2] \quad (11)$$

By subtracting v_{base} from the observed metal catalysed reaction rate (v_{obs}), v_{cat} and k_{cat} can be determined according to Equation (10).

The various immobilised catalysts were added to BNPP in buffered solutions at varying pH and allowed to shake in the dark at 25 °C for 24 hours. Polymer **11**, a polymer containing no Zn(II)Cyc complex was taken as a reference. Polymer **13** has Cyc on the surface (free Cyc strategy), where all four nitrogen atoms of the cyclen were free to react with the epoxide groups on the surface. In polymer **16** only one nitrogen atom could react thus generating solely a cyclen moiety analogous to **5**.

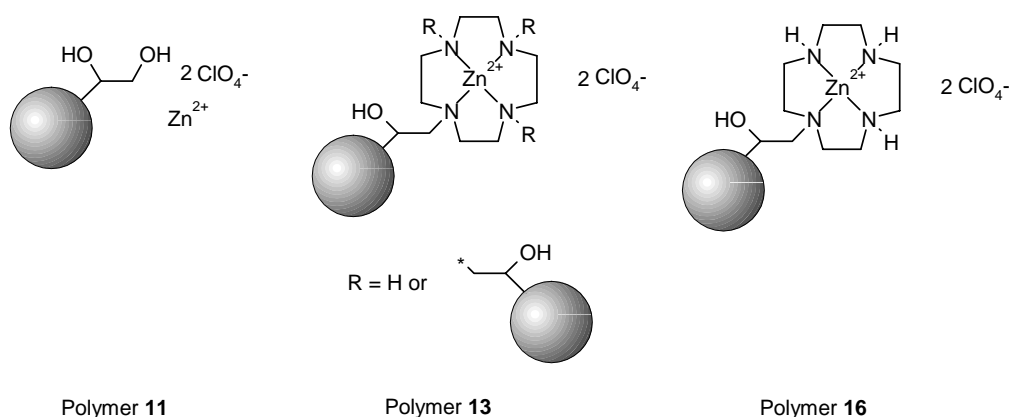


Figure 2. Proposed structure of polymer **11**, **13** and **16**.

The k_{cat} values for polymers **13** and **16** are shown in Table 2. The k_{cat} values for polymer **13** are approximately half than those of polymer **16**. This can be attributed to the fact that polymer **13** has catalytic sites cross-linked on the surface and thus not all can contribute effectively to the hydrolysis. Polymer **16**, with a catalytic module analogous to **5**, showed the highest k_{cat} values at pH 9.00, where 97 % of the catalytic site was present as Zn-L-OH⁻ (see Equation (11)).^[47] From this value a k_{BNPP} value of $3.8 \times 10^{-3} \text{ M}^{-1}\text{s}^{-1}$ at 25 °C was calculated. Kimura reported a k_{BNPP} value of $6.5 \times 10^{-4} \text{ M}^{-1}\text{s}^{-1}$ at 35 °C for **5b**.^[23]

Table 2. The k_{cat} values ($\text{M}^{-1}\text{s}^{-1}$) for the hydrolysis of BNPP by polymer **13**, polymer **16** at 25 °C.

	pH 7.00	pH 8.00	pH 9.00
Polymer 13	$(5.2 \pm 0.5) \times 10^{-4}$	$(8.6 \pm 0.9) \times 10^{-4}$	$(1.2 \pm 0.1) \times 10^{-3}$
Polymer 16	$(8.9 \pm 0.9) \times 10^{-4}$	$(1.9 \pm 0.2) \times 10^{-3}$	$(3.7 \pm 0.4) \times 10^{-3}$

Table 3 summarises the intrinsic rate of reaction enhancements for **5** and the polymer-catalysed hydrolysis of BNPP. The uncatalysed hydrolysis reaction of BNPP is taken as a reference and is assigned a value of 1.

Table 3. Rate of reaction enhancements for the hydrolysis of BNPP by polymer **11**, **5**, polymer **13** and polymer **16** and at 25 °C (Base hydrolysis has a rate enhancement of 1).

	pH 7.00	pH 8.00	pH 9.00
Polymer 11	23	5	1
5 ^[48]	186	56	9
Polymer 13	1169	195	34
Polymer 16	2001	430	98

All three polymers showed decreasing rate enhancements with increasing pH. For polymer **11**, where no catalytic module was present to enhance the rate of hydrolysis, the intrinsic reaction rate enhancement was most likely due to the polymer surface. The hydroxide concentration in the system at pH 9.00 is high and thus the polymer surface has little influence accelerating the hydrolysis (supported by a reaction rate enhancement factor of 1 at pH 9.00). At pH 7.00 however the hydroxide concentration on the surface of the polymer has an influence on the base hydrolysis as the concentration of hydroxide ions in solution is much lower. Similar observations are noted for polymer **13** and polymer **16**, however here the enhancements effect is much larger as the catalytic site plays the central role.

By comparing the rate enhancement of polymer **13** and **16** and taking polymer **11** as a reference, the rate enhancement effects of the polymer and its surface are removed. Table 4 shows that the rate enhancement of both polymers is much more stable to changes in pH.

Table 4. Rate of reaction enhancements for the hydrolysis of BNPP by polymer **13** and polymer **16** at 25 °C (polymer **11** has a rate enhancement of 1).

	pH 7.00	pH 8.00	pH 9.00
Polymer 13	51	37	26
Polymer 16	87	82	77

2.2.2.4 Hydrolysis of BNPP with immobilised mononuclear Zn(II)Cyc complexes (PBR Reactor)

The advantages of immobilised hydrolytic agents are most marked in continuous flow reactors. In these reactors the average residence time of the substrate molecules within the reactor is far shorter than that of the immobilised catalyst. This results in a far greater productivity from a fixed amount of catalyst than is achieved in batch processes. In a packed bed reactor (PBR) the substrate flows through the reactor as a plug. Ideally all of the substrate flows at the same velocity, in a parallel fashion with no back-mixing. In a PBR the conditions for pseudo-first-order kinetics, namely C_0 (concentration of the Zn(II)Cyc complex when the polymer is assumed to be dissolved) $\gg S_0$ (the initial concentration of BNPP) are met.

The volume of substrate (Vol_s) which has contact with the catalyst is an important parameter as it effectively determines the concentration of the system where reaction is taking place. The volume at any one time can be determined by comparing the mass of a packed reactor containing pre-swelled catalyst with a packed reactor containing pre-swelled catalyst with the minimum amount of solvent needed to completely wet it. The calculated volume varies according to the characteristics (swelling ability, hydrophilicity, etc) of the polymer.

The flow rate (F) of the reactor can be determined by measuring the time taken for each fraction to pass through the reactor.

$$F = \frac{Vol_{frac}}{t_{frac}} \quad (12)$$

As each fraction consists of numerous plugs (each with a volume of Vol_s) passing through the reactor, the average contact time (CT) of one plug can be calculated from Equation (13). Combining Equations (10) and (13) gives Equation (14), from which k_{cat} can be calculated.

$$CT = \frac{Vol_s}{F} \quad (13)$$

$$v_{obs} = \frac{d(Abs)}{CT \epsilon_{obs}} = (k_{OH} [OH^-] + k_{cat} [Zn-L]^{total}) [BNPP] \quad (14)$$

A PBR with polymer **11** containing Zn(II) ions but no Cyc complex (3.7×10^{-4} mol/g diol on the surface, with a contact volume of 0.15 ml) was eluted with BNPP (8.75×10^{-4} M in Tris/HCl buffer, pH 9.00). Once a steady state was achieved, a pseudo-first-order rate constant (k_{cat}) of $(4.5 \pm 1.6) \times 10^{-6} \text{ LMol}^{-1}\text{s}^{-1}$ was calculated from Equation (14), with the catalytic site taken as the diols generated from the epoxide opening. Polymer **11** showed an average rate enhancement of 51 ± 18 relative to the base hydrolysis (with a value of 1).

A column with polymer **16** containing Zn(II)Cyc complex (7.1×10^{-5} mol/g binding sites, with a contact volume of 0.1 ml) was eluted with BNPP (8.75×10^{-4} M in Tris/HCl buffer, pH 9.00) and the UV absorption increase followed generally for 100 ml of BNPP solution. After a brief adsorption of the phosphodiester onto the polymer a steady state was achieved (see Figure 3).

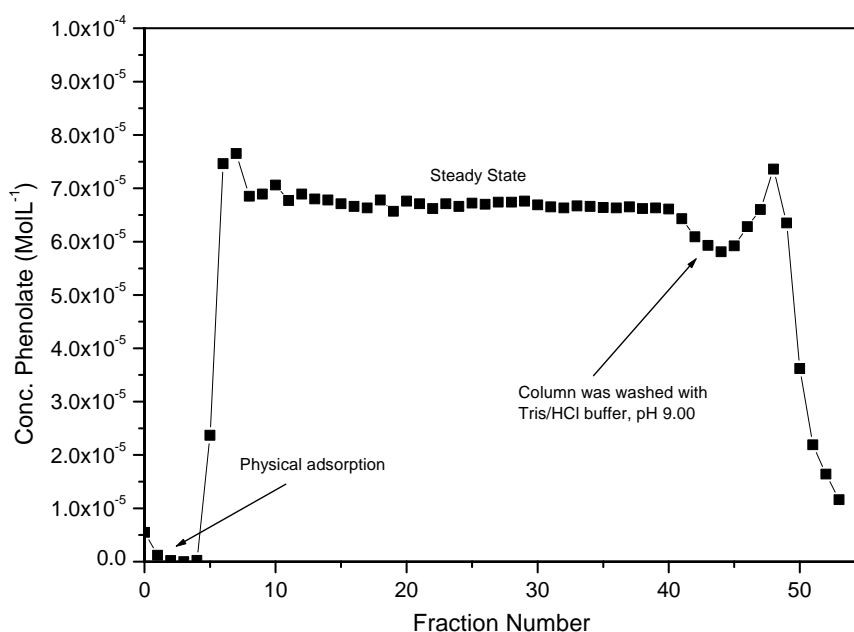


Figure 3. Concentration of 4-NP⁻ in each fraction after contact with polymer **16**.

During this steady state the entire reactor was an intense yellow. The pseudo-first-order rate constant (k_{cat}) of $(7.1 \pm 0.6) \times 10^{-3} \text{ LMol}^{-1}\text{s}^{-1}$ was calculated from Equation (14). Polymer **16** showed an average rate enhancement of $(4.3 \pm 0.3) \times 10^4$ relative to the base hydrolysis (with a value of 1).

Once all the BNPP had been eluted the column was washed with Tris/HCl buffer, pH 9.00 until 4-nitrophenolate could no longer be detected. Through this washing with buffer, the

reactor returned to its original colour, namely off white. The eluted samples were combined and allowed to pass over the same column again. This procedure was repeated 5 times. With each cycle the rate of reaction decreased (Table 5).

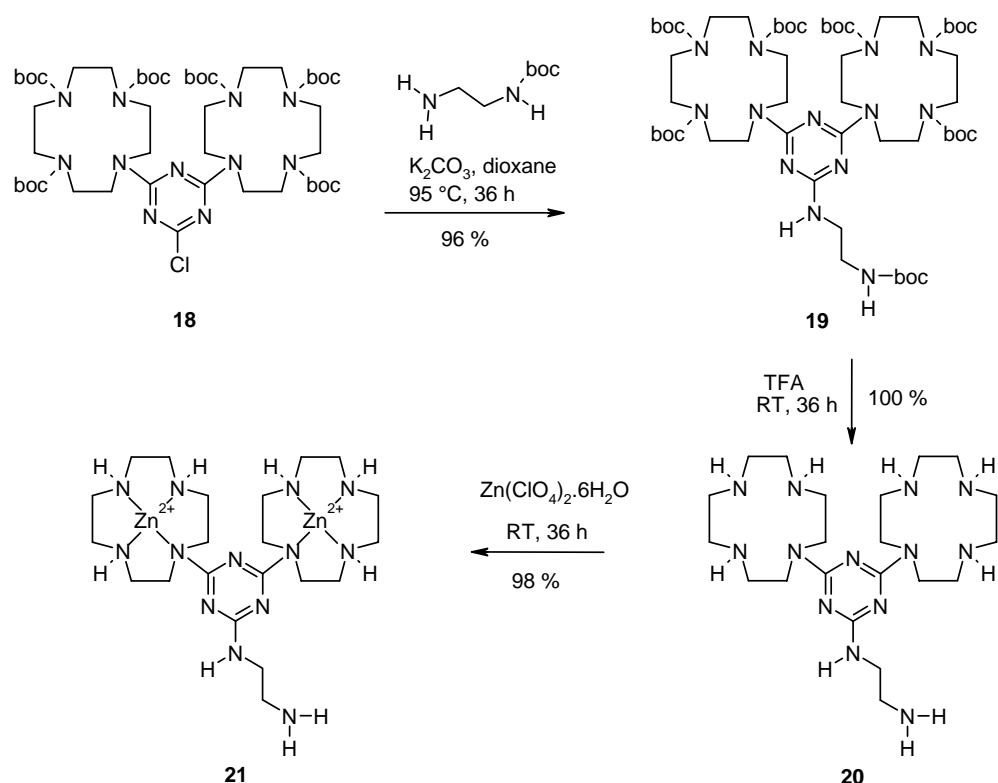
Table 5. Rate of reaction at steady state for the hydrolysis of BNPP by a PBR containing polymer **16** over 5 cycles.

Cycle No.	v_{cat} (MolL ⁻¹ s ⁻¹)
1	$2.27 \pm 0.02 \times 10^{-6}$
2	$1.03 \pm 0.02 \times 10^{-6}$
3	$0.72 \pm 0.03 \times 10^{-6}$
4	$0.31 \pm 0.02 \times 10^{-6}$
5	$0.27 \pm 0.02 \times 10^{-6}$

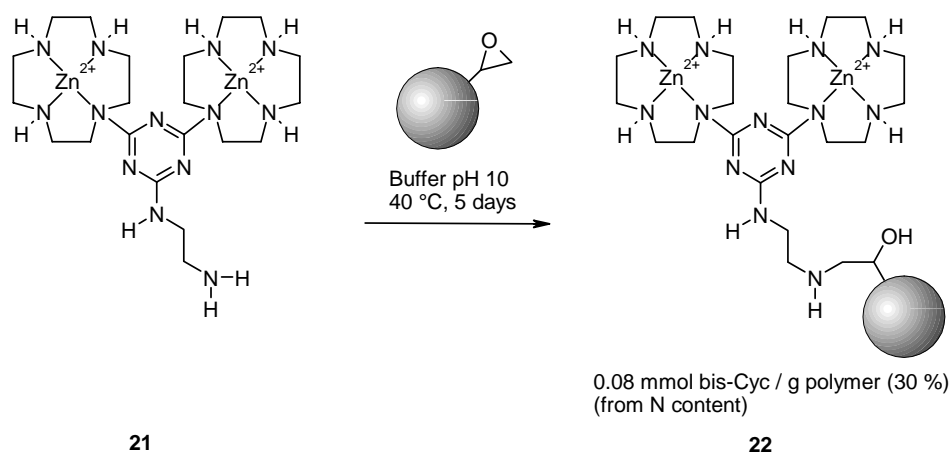
As the turnover rate for the 1st cycle was only 6% (5.5×10^{-6} mol NP were produced from 8.70×10^{-5} mol BNPP available), this decrease in v_{cat} cannot be attributed a limited amount of BNPP available. Rather, the decreasing v_{cat} values suggest catalyst inhibition through the phosphate monoester.

2.2.3 Synthesis of bis-Zn(II)Cyc Polymer

In order to obtain a bis-Zn(II)Cyc complex on a solid support, a suitable catalytic module which could be coupled to the epoxide polymer had to be synthesised. Compound **19**, was synthesised from the chloride **18** [49]. After removal of the boc-protecting groups with TFA and resulting complexation with aqueous zinc(II) perchlorate hexahydrate solution at pH 10, compound **21** was generated. Here the Zn(II) is already complexed before coupling to the polymer.

Scheme 7. Synthesis of bis-Zn(II)Cyc **21**

This amine could now be coupled with the epoxide polymer to yield the polymer bound bis-Zn(II)Cyc **22**. Only the primary amine in **21** is available as a nucleophile for the coupling reaction. The amines in the Cyc are deactivated due to the coordinated Zn(II) and the secondary amine in the linker is aniline like and thus has a low reactivity.

Scheme 8. Synthesis of the polymer bound bis-Zn(II)Cyc **22**

The loading of the bis-Zn(II)Cyc complex on the polymer is quite low. The data from ^{13}C NMR for compound **21** shows a differentiation between the two $\text{C}_{\text{aryl}}\text{-N}$ bonds (two signals at 170.8 and 171.3 ppm). This suggests that the primary amine can coordinate to one of the zinc atoms and thus not always be free to attack the epoxide. The fact that a high

resolution MS could also be obtained from this highly charged molecule further supports this assumption.

2.2.4 Kinetic measurements for the phosphodiester cleavage reaction with bis-Zn(II)Cyc complexes bound to a solid support

A column with polymer **22** containing bis-Zn(II)Cyc complex was eluted with BNPP. The flow rate however was so small (< 1 ml / hour) that the conditions for a PBR (back mixing and diffusion) could not be met. The reasons for the low flow rate lie most likely in the surface characteristics, such as high hydrophobicity of the polymer.

A stirred reactor (STR) in batch mode was set up in which the polymer is suspended in a defined amount of substrate over a membrane (in this case a glass frit) and stirred vigorously. This has the advantage that there is very little resistance to the flow of the substrate stream through the membrane.

The polymer **22** containing bis-Zn(II)Cyc complex (7.7×10^{-5} molg⁻¹ binding sites) was placed into a vessel with frit and eluted with aliquots of BNPP (8.75×10^{-4} M in Tris/HCl buffer, pH 9.00). Initial samples were allowed to drop through the frit where physical absorption of the phosphodiester onto the polymer occurred and until a steady state was achieved. 10 ml aliquots were now added to the polymer and mechanically stirred. After a defined time the BNPP solution was separated from the polymer and fresh BNPP was added.

In addition to the hydrophobic nature of the polymer, the physical handling of the STR was very difficult and factors such as substrate evaporation and membrane seepage generated large errors. Unfortunately no reliable rate constant could be generated. The observed reaction rates (v_{obs}) varied between 3×10^{-10} and 8×10^{-9} MolL⁻¹s⁻¹.

2.3 Conclusion

Artificial hydrolases as alternatives for non-enzymatic hydrolysis were prepared by attaching Zn(II) cyclen complexes with an alcohol pendant to a polymeric support. These modified polymers showed a 10^4 fold enhanced intrinsic reactivity for the hydrolysis of bis-*p*-nitrophenylphosphate over the non-catalysed reaction in solution (pH 9.0, 25 °C) when a packed bed reactor (PBR) was used. A batch process showed lower intrinsic reactivities.

2.4 Experimental

2.4.1 General

2.4.1.1 Spectroscopy

UV-VIS Spectra

Varian Cary BIO 50 UV/VIS/NIR Spectrometer. Use of a 1 cm quartz cell (Hellma) and Uvasol solvents (Merck). Reported as: λ_{max} in nm (ϵ).

NMR-Spectra

- Bruker AC-250 (^1H : 250.1 MHz, ^{13}C : 62.9 MHz), Measurement temperature: 24 °C.
- Bruker Avance 300 (^1H : 300.1 MHz, ^{13}C : 75.5 MHz), Measurement temperature: 27 °C.
- Bruker ARX-400 (^1H : 400.1 MHz, ^{13}C : 100.6 MHz), Measurement temperature: 21 °C.
- Bruker Avance 400 (^1H : 400.1 MHz, ^{13}C : 100.6 MHz), Measurement temperature: 27 °C.
- Bruker Avance 600 (^1H : 600.1 MHz, ^{13}C : 150.1 MHz), Measurement temperature: 27 °C.

The chemical shifts are in δ -values (ppm) relative to the internal (or external) standard TMS. Reported as: Chemical shift (multiplicity, coupling constant, number of protons, assignment). Reported assignments were determined with the help of COSY, HMQC, HSQC, and NOESY 2D-Spectra. Abbreviations: s = singlet, bs = broad singlet, d = doublet, bd = broad doublet, dd = doublet of doublets, t = triplet, q = quartet, m = multiplet, bm = broad multiplet, sept = septet. Error of reported values: chemical shift: 0.01 ppm for ^1H -NMR, 0.1 ppm for ^{13}C -NMR; Coupling constants: 0.1 Hz. The used solvent is reported for each spectrum.

Mass spectra

- Varian CH-5 (EI)
- Finnigan MAT 95 (CI; FAB and FD)
- Finnigan MAT TSQ 7000 (ESI)

Xenon serves as the ionisation gas for FAB.

2.4.1.2 Analysis

Melting Points

Melting points are uncorrected and were determined according to Tottoli using instrumentation from Büchi.

Elemental Analysis

Elemental analyses were carried out by the central analytical department of Merck KGaA, Darmstadt.

2.4.1.3 Synthesis

Column Chromatography

Silica gel Merck Geduran SI 60.

Thin Layer Chromatography

Aluminium sheets Merck 60 F²⁵⁴ Silica gel, thickness 0.2 mm.

Detection via UV light at 254 nm or through discolouration with ninhydrin in ethanol.

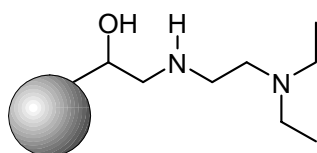
Solvents

Purification and drying according to accepted general procedures.^[50,51]

If not otherwise stated, commercially available solvent of the highest purity were used.

2.4.2 Synthesis of New Compounds

Fractogel-diethylaminoethylamine (9)



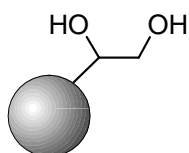
2-diethylaminoethylamine (700 mg, 6.02 mmol) and Fractogel[®] EMD Epoxy (M) (1.50 g) were added to carbonate buffer (60 ml, pH 10.0) and allowed to stir (KPG stirrer) at 40 °C for five days. The polymer was filtered and washed with 3 x 50 ml dichloromethane,

2 x 50 ml THF and 1 x 50 ml dichloromethane. After drying under high vacuum, a white polymer was obtained (1.60 g).

Elemental Analysis: C: 50.73, H: 6.94, N: 0.73

This corresponds to an approximate polymer loading of 0.26 mmol diamine / g polymer.

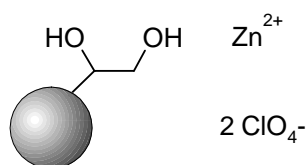
Fractogel (epoxy opening with H₂SO₄) (10)



Fractogel[®] EMD Epoxy (M) (1.20 g), with an epoxide loading of 394 mmol/g polymer,^[52] was suspended in H₂SO₄ (40 ml, 0.5 M) and allowed to stir (KPG stirrer) at 40 °C for 2 h. The polymer was filtered and washed with 5 x 50 ml water, 2 x 50 ml methanol and 1 x 50 ml dichloromethane. After drying under high vacuum, a white polymer was obtained (1.22 g).

Elemental Analysis: C: 52.3, H: 7.1, N: 0.0

Fractogel-zinc(II) diperchlorate (epoxy opening with H₂SO₄) (11)

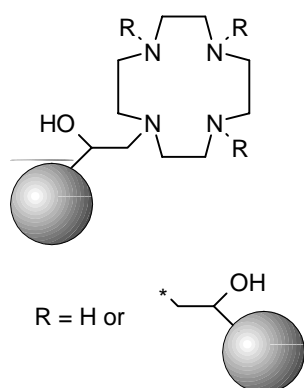


Polymer **10** (1.00 g) was suspended in carbonate buffer (20 ml, pH 10.0) to which zinc(II) perchlorate (1.12 g, 7.50 mmol) was added and allowed to stir (KPG stirrer) at 85 °C for 18 h. The polymer was filtered and washed with 3 x 50 ml water, 2 x 50 ml methanol and 1 x 50 ml dichloromethane. After drying under high vacuum, a white polymer was obtained (960 mg).

ICP-OES: Zn: 1.6 %

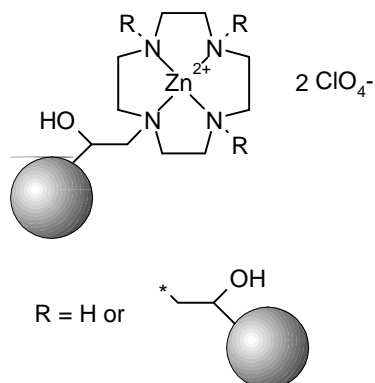
Elemental Analysis: C: 51.40, H: 6.86, N: 0.0

This corresponds to an approximate polymer loading of 0.366 mmol diol / g polymer.

Fractogel-1,4,7,10-tetraazacyclododecane (cross-linked) (12)

1,4,7,10-tetraazacyclododecane (0.413 g, 2.40 mmol) and Fractogel[®] EMD Epoxy (M) (3.00 g) were added to carbonate buffer (80 ml, pH 10) and allowed to stir (KPG stirrer) at 40 °C for five days. The polymer was filtered and washed with 3 x 50 ml dichloromethane, 2 x 50 ml THF and 1 x 50 ml dichloromethane. The polymer was resuspended in H₂SO₄ (60 ml, 0.5 M) and allowed to stir (KPG stirrer) at 40 °C for 2 h. The polymer was filtered and washed with 3 x 50 ml water, 2 x 50 ml THF and 1 x 50 ml dichloromethane. After drying under high vacuum, a white polymer was obtained (3.05 g).

Elemental Analysis: C: 50.2, H: 7.4, N: 1.7

Fractogel-1,4,7,10-tetraazacyclododecane-zinc(II) diperchlorate (cross-linked) (13)

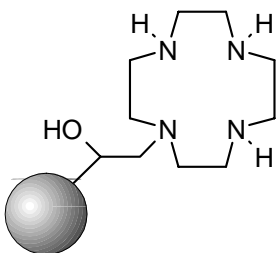
Polymer **12** (1.73 g) was suspended in carbonate buffer (35 ml, pH 10) to which zinc(II) perchlorate (1.86 g, 5.0 mmol) was added and allowed to stir (KPG stirrer) at 85 °C for 18 h. The polymer was filtered and washed with 3 x 50 ml water and then resuspended in 100 ml water and allowed to stir (KPG stirrer) at 40 °C for a further 3 hours. The polymer was filtered and washed with 3 x 100 ml water, 2 x 50 ml methanol and 1 x 50 ml dichloromethane. After drying under high vacuum, a white polymer was obtained (1.83 g).

ICP-OES: Zn: 8.9%

Elemental Analysis: C: 45.8, H: 6.8, N: 1.4

This corresponds to an approximate polymer loading of 0.25 mmol Zn-Cyc / g polymer, which is a yield of 96 % assuming the loading of diethylaminoethylamine is the maximum loading possible

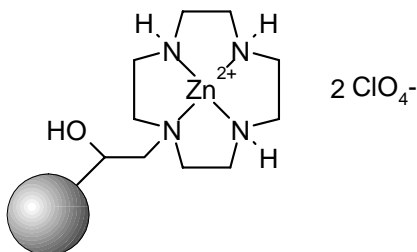
Fractogel-1,4,7,10-tetraazacyclododecane (15)



1,4,7-Tris-*tert*-butoxycarbonyl-1,4,7,10-tetraazacyclododecane **14** ^[44] (1.134 g, 2.40 mmol) and 3.00 g Fractogel[®] EMD Epoxy (M) were added to carbonate buffer (80 ml, pH 10) and allowed to stir (KPG stirrer) at 40 °C for five days. The polymer was filtered and washed with 3 x 50 ml dichloromethane, 2 x 50 ml THF and 1 x 50 ml dichloromethane. The polymer was resuspended in H₂SO₄ (60 ml, 0.5 M) and allowed to stir at 40 °C for 2 h. The polymer was filtered and washed with 3 x 50 ml water, 2 x 50 ml THF and 1 x 50 ml dichloromethane. The polymer was resuspended in TFA (20 ml) and allowed to stir at RT for 10 min. The polymer was filtered and then washed 2 x 50 ml with NaOH (2 M), 2 x 50 ml water, 2 x 50 ml THF and 1 x 50 ml dichloromethane. After drying under high vacuum, a white polymer was obtained (3.10 g).

Elemental Analysis: C: 51.8, H: 7.3, N: 0.6

Fractogel-1,4,7,10-tetraazacyclododecane-zinc(II) diperchlorate (16)



Polymer **15** (1.72 g) was suspended in carbonate buffer (35 ml, pH 10.0) to which zinc(II) perchlorate (1.86 g, 5.0 mmol) was added and allowed to stir (KPG stirrer) at 85 °C for 18 h. The polymer was filtered and washed with 3 x 50 ml water and then resuspended in

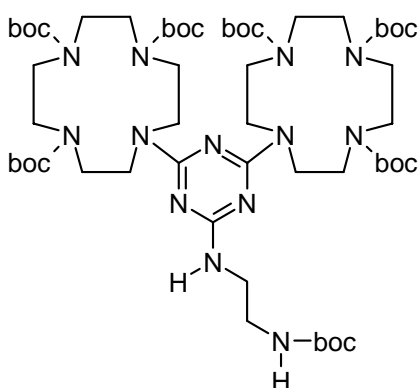
100 ml water and allowed to stir (KPG stirrer) at 40 °C for a further 3 hours. The polymer was filtered and washed with 3 x 100 ml water, 2 x 50 ml methanol and 1 x 50 ml dichloromethane. After drying under high vacuum, a white polymer was obtained (1.86 g).

ICP-OES: Zn: 11.7%

Elemental Analysis: C: 44.2, H: 6.6, N: 0.4

This corresponds to an approximate polymer loading of 0.07 mmol Zn-Cyc / g polymer, which is a yield of 27 % assuming the loading of diethylaminoethylamine is the maximum loading possible.

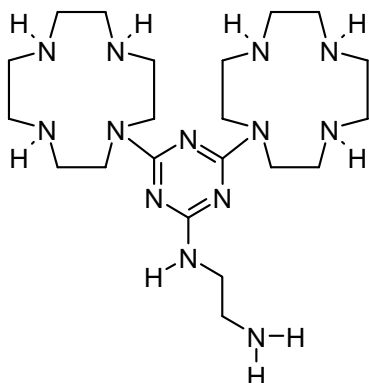
N*1*-[4,6-Bis-(4,7,10-triboc-1,4,7,10tetraaza-cyclododec-1-yl)-[1,3,5]triazin-2-yl]-ethane-1,2-diamine (19)



1-*N*-boc-2-aminoethane (180 mg, 1.12 mmol) was dissolved in dioxane (15 ml). Compound **18** (300 mg, 0.28 mmol) and potassium carbonate (310 mg, 2.24 mmol) were then added allowed to stir under nitrogen at 95 °C for 36 hours. The potassium carbonate was filtered off and the solution evaporated to dryness. The crude product was chromatographed on silica gel with 1:1 petroleum ether:ethyl acetate as eluent yielding product **9** (325 mg, 0.27 mmol, 96 %) as a white solid.

MP: 131 °C; **IR** (KBr): $\tilde{\nu}$ (cm⁻¹) = 2976, 2930, 1678, 1569, 1365, 1167; **¹H-NMR** (300 MHz, CDCl₃): δ [ppm] = 1.41 (s, 9 H, boc-CH₃), 1.42 (s, 18 H, boc-CH₃), 1.44 (s, 36 H, boc-CH₃), 1.97-2.05 (m, 2 H, CH₂), 3.00-3.90 (m, 34 H, Cyc-CH₂, CH₂), 4.89 (s, 1 H, N-H), 6.13 (bs, 1 H, N-H); **¹³C-NMR** (75 MHz, CDCl₃): δ [ppm] = 28.5 (+, boc-CH₃), 41.0 (–, CH₂), 50.2 (–, Cyc-CH₂), 78.8 (C_{quat}, boc-C), 79.8 (C_{quat}, boc-C), 80.2 (C_{quat}, boc-C), 156.5 (C_{quat}, boc-CO), 166.0 (C_{quat}, C_{aryl}-N); **MS** (ESI-MS, CH₂Cl₂/MeOH + 10 mmol/l NH₄OAc) *m/z* (%): 1181 (100) [MH]⁺; C₅₆H₁₀₁N₁₃O₁₄ + C₄H₈O₂ (1268.60) Found: C 57.14, H 8.11, N 14.57; Calculated: C 56.81, H 8.66, N 14.35.

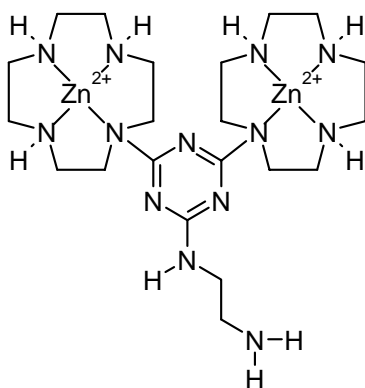
N*1*-[4,6-Bis-(1,4,7,10tetraaza-cyclododec-1-yl)-[1,3,5]triazin-2-yl]-ethane-1,2-diamine (20)



Compound **19** (1.18 g, 1.0 mmol) was dissolved in dichloromethane (40 ml), added to TFA (6.5 ml) and allowed to stir at RT for 36 h. The crude product was evaporated to dryness, passed over a strong basic ionic exchange column and washed with water. The solution was freeze dried yielding a white solid (479 mg, 1.0 mmol, 100 %).

MP: 155 °C ; **IR** (KBr): $\tilde{\nu}$ (cm⁻¹) = 3412, 3245, 2936, 1567, 1355, 1103, 635; **¹H-NMR** (300 MHz, CD₃OD): δ [ppm] 2.61 - 2.81 (m, 18 H, 16 H CH₂-Cyc, 2 H CH₂), 2.92 (bs, 8 H, 4 CH₂-Cyc), 3.41 (t, ³J = 6.3 Hz, 2 H, CH₂), 3.69 - 3.80 (m, 8 H, CH₂-Cyc); **¹³C-NMR** (75 MHz, CD₃OD): δ [ppm] = 42.7 (–, CH₂), 44.2 (–, CH₂), 46.8 (–, Cyc-CH₂), 49.4 (–, Cyc-CH₂), 49.7 (–, Cyc-CH₂), 167.4 (C_{quat}, C_{aryl}-N), 168.2 (C_{quat}, C_{aryl}-N); **MS** (ESI-MS, CH₃CN/MeOH) m/z (%): 241 (100) [M+2H]⁺, 480 (53) [MH]⁺; **HRMS** (PI-LSI-MS, NBA) calculated for C₂₁H₄₆N₁₃: 480.3999, found: 480.3998 ± 0.56 ppm);

Bis-Zn(II)Cyc amine (21)

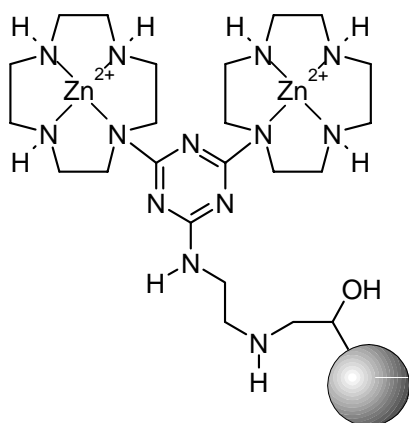


Compound **20** (247 mg, 0.52 mmol) was dissolved in methanol to which zinc(II) perchlorate (384 mg, 1.03 mmol) was added and allowed to stir under nitrogen at RT for 36 hours. The reaction was then allowed to reflux for 2 hours. The product was evaporated

to dryness, recrystallised from water/methanol and dried yielding the Zn(II) complex **21** (520 mg, 0.52 mmol, 100 %) as a white solid.

MP: 245 °C; **IR** (KBr): $\tilde{\nu}$ (cm⁻¹) = 3407, 3265, 2939, 1563, 1346, 1089, 627; **UV/Vis** (CH₃CN): λ_{max} (log ϵ) = 222 nm (4.561); **¹H-NMR** (400 MHz, CD₃CN): δ [ppm] 2.67 - 2.97 (m, 12 H, CH₂-Cyc), 2.98 - 3.27 (m, 14 H, CH₂-Cyc), 3.31 - 3.64 (m, 9 H, 2 CH₂-Cyc, 5 N-H), 3.65 - 3.80 (m, 1 H, N-H), 3.71 (dt, ³J = 6.0 Hz, 2 H, CH₂), 4.15 - 4.50 (m, 4 H, CH₂-Cyc), 6.10 - 6.80 (m, 3 H, N-H); **¹³C-NMR** (100 MHz, CD₃CN): δ [ppm] = 38.8 (–, CH₂), 41.5 (–, CH₂), 44.5 (–, Cyc-CH₂), 46.2 (–, Cyc-CH₂), 46.2 (–, Cyc-CH₂), 46.8 (–, Cyc-CH₂), 47.6 (–, Cyc-CH₂), 47.8 (–, Cyc-CH₂), 49.1 (–, Cyc-CH₂), 167.5 (C_{quat}, C_{aryl}-N), 170.8 (C_{quat}, C_{aryl}-N), 171.3 (C_{quat}, C_{aryl}-N); **MS** (ESI) m/z (%): 236 (100) [(L+2Zn²⁺+ClO₄⁻)]³⁺; **HRMS** (LSI-MS, CH₂Cl₂/NBA) calculated for C₂₁H₄₅N₁₃O₁₂Zn₂ [(L+2Zn²⁺)+3(ClO₄⁻)]⁺: 904.0959, found: 904.0960 ± 0.96 ppm);

Fractogel- bis-Zn(II)Cyclen (glycine ring opening) (**22**)



The Zn(II) complex **21** (438 g, 0.43 mmol) and Fractogel[®] EMD Epoxy (M) (700 mg) were added to carbonate buffer (30 ml, pH 10) and allowed to stir (KPG stirrer) at 40 °C for five days. The polymer was filtered and washed with 3 x 50 ml water, 2 x 50 ml methanol and 1 x 50 ml dichloromethane. After drying under high vacuum, a white polymer was obtained (722 mg).

Elemental Analysis: C: 51.31, H: 7.06, N: 1.41

This corresponds to an approximate polymer loading of 0.08 mmol bis-Zn-Cyc / g polymer, which is a yield of 30 % assuming the loading of diethylaminoethylamine is the maximum loading possible.

The polymer (700 mg) was resuspended in tris-HCl buffer (25 ml, pH 8.00) containing glycine (0.2 M) and allowed to stir at 40 °C overnight. The polymer was filtered and washed with 3 x 50 ml water, 2 x 50 ml methanol and 1 x 50 ml dichloromethane. After drying under high vacuum a white polymer was obtained (655 mg).

Elemental Analysis: C: 52.25, H: 6.70, N: 1.41

2.5 References

- [1] J. J. R. Fraústo da Silva, R. J. P. Williams, *The biological chemistry of elements*, Clarendon Press, Oxford, **1991**, Chapter 11
- [2] For recent review: S. Aoki, E. Kimura, *Rev. Mol. Biol.*, **2002**, *90*, 129-155
- [3] M. J. Jedrzejewski, P. Setlow, *Chem. Rev.*, **2001**, *101*, 608-618; J. A. Cowan, *Chem. Rev.*, **1998**, *98*, 1067-1087; D. E. Wilcox, *Chem. Rev.*, **1996**, *96*, 2435-2458; N. Sträter, W. N. Lipscomb, T. Klabunde, B. Krebs, *Angew. Chem., Int. Ed. Engl.*, **1996**, *35*, 2024-2055; E. H. Serpersu, D. Shortle, A. S. Mildvan, *Biochemistry*, **1987**, *26*, 1289-1300
- [4] N. H. Williams, B. Takasaki, M. Wall, J. Chin, *Acc. Chem. Res.*, **1999**, *32*, 485
- [5] G. Parkin, *Chem. Rev.*, **2004**, *104*, 699-767; W. N. Lipscomb, N. Sträter, *Chem. Rev.*, **1996**, *96*, 2375-2433; S. Aoki, E. Kimura, *Chem. Rev.*, **2004**, *104*, 769-787
- [6] For a recent review on Zinc Hydrolases see: S. Aoki, E. Kimura, *Comprehensive Coordination Chemistry II*, **2004**, *8*, 601-640
- [7] S. J. Lippard, J. M. Berg, *Principles of Bioinorganic Chemistry*, University Science Books, Mill Valley, CA, **1994**; A. J. Barrett, N. D. Rawlings, J. F. Woessner, Eds., *Handbook of Proteolytic Enzymes*, Academic Press, London, **2000**; J. F. Chlebowski, J. E. Coleman in *Meta Ions in Biological Systems (Ed H. Sigel)*, Marcel Dekker, New York, **1976**, Vol. 6, 1-140; B. L. Vallee, D. S. Auld, *Biochemistry*, **1990**, *29*, 5647-5657; B. L. Vallee, K. H. Falchuk, *Physiol. Rev.*, **1993**, *73*, 79-118; B. L. Vallee, D. S. Auld, *Acc. Chem. Res.*, **1993**, *26*, 543-551; J. E. Coleman, *Curr. Opin. Chem. Biol.*, **1998**, *2*, 222-234
- [8] B. L. Vallee, D. S. Auld, *Proc. Natl. Acad. Sci., USA*, **1990**, *87*, 220-224
- [9] D. S. Auld, *BioMetals*, **2001**, *14*, 271-313
- [10] P. A. Sutton, D. A. Buckingham, *Acc. Chem. Res.*, **1987**, *20*, 357-364
- [11] J. Chin, *Acc. Chem. Res.*, **1991**, *24*, 145-152
- [12] J. Suh, *Acc. Chem. Res.*, **1992**, *25*, 273-279
- [13] J. Suh in *Perspectives on Bioinorganic Chemistry (Eds. R. W. Hay, J. R. Dilworth, K. B. Nolan)*, JAI Press, London, **1996**, Vol. 3, 115-149
- [14] J. Suh, T. H. Park, B. K. Hwang, *J. Am. Chem. Soc.*, **1992**, *114*, 5141-5146; R. Breslow, *Acc. Chem. Res.*, **1995**, *28*, 146-153; E. Kimura, T. Koike in *Comprehensive Supramolecular Chemistry (Ed. D. N. Reinhoudt)*, Pergamon, Tokyo, **1996**, Vol. 10, 429-444; E. Kimura, T. Koike in *Bioinorganic Catalysis (Eds. J.*

- Reedijk, E. Bouwman), Marcel Dekker, New York, **1999**, 33-54; H. Vahrenkamp, *Acc. Chem. Res.*, **1999**, 32, 589-596; J. K. Bashkin, *Curr. Opin. Chem. Biol.*, **1999**, 3, 752-758; G. Parkin, *Chem. Commun.*, **2000**, 20, 1971-1985; G. Parkin in *Metal Ions in Biological Systems*, Marcel Dekker, New York, **2001**, Vol. 38, 411-460
- [15] E. Kimura, T. Koike, *Chem. Commun.*, **1998**, 15, 1495-1500
- [16] R. Krämer, *Coord. Chem. Rev.*, **1999**, 182, 243-261
- [17] E. Kimura, T. Shiota, T. Koike, M. Shiro, M. Kodama, *J. Am. Chem. Soc.*, **1990**, 112, 5805-5811
- [18] X. Zhang, R. van Eldik, T. Koike, E. Kimura, *Inorg. Chem.*, **1993**, 32, 5749-5755; E. Kimura, T. Koike, *Comments Inorg. Chem.*, **1991**, 11, 285-301; E. Kimura, *Yakugaku-Zasshi*, **1996**, 116, 587-605; E. Kimura, *Yakugaku-Zasshi*, **2002**, 122, 219-236; C. Bazzicalupi, A. Bencini, A. Bianchi, V. Fusi, C. Giorni, P. Paletti, B. Valtancoli, D. Zanchi, *Inorg. Chem.*, **1997**, 36, 2784-2790
- [19] T. Koike, E. Kimura, *J. Am. Chem. Soc.*, **1991**, 113, 8935-8941
- [20] E. Kimura, T. Koike, M. Shionoya in *Structure and Bonding: Metal Sites in Proteins and Models* (Eds. J. P. Sadler), Springer, Berlin, **1997**, 89, 1-28
- [21] P. Molenveld, J. F. J. Engbersen, D. N. Reinhoudt, *Chem. Soc. Rev.*, **2000**, 29, 75-86; E. L. Hegg, J. N. Burstyn, *Coordin. Chem. Rev.*, **1998**, 173, 133-165; J. R. Morrow, *Met. Ions Biol. Syst.*, **1997**, 33, 561-592; P. Hendry, A. M. Sargeson, *Prog. Inorg. Chem.*, **1990**, 38, 201-258
- [22] T. Koike, S. Kajitani, I. Nakamura, E. Kimura, M. Shiro, *J. Am. Chem. Soc.*, **1995**, 117, 1210-1219; T. Koike, E. Kimura, I. Nakamura, Y. Hashimoto, M. Shiro, *J. Am. Chem. Soc.*, **1992**, 114, 7338-7345
- [23] E. Kimura, Y. Kodama, T. Koike, M. Shiro, *J. Am. Chem. Soc.*, **1995**, 117, 8304-8311
- [24] S. Aoki, E. Kimura, *Rev. Mol. Biol.*, **2002**, 90, 129-155
- [25] H. Fujioka, T. Koike, N. Yamada, E. Kimura, *Heterocycles*, **1996**, 42, 775-787; T. Koike, E. Kimura, H. Fujioka, M. Shiro, *Chem. Eur. J.*, **1996**, 2, 617-623; S. Aoki, E. Kimura, *J. Am. Chem. Soc.*, **2000**, 122, 4542-4548; S. Aoki, C. Sigimuru, E. Kimura, *J. Am. Chem. Soc.*, **1998**, 122, 10094-10102
- [26] E. Kimura, S. Aoki, T. Koike, M. Shiro, *J. Am. Chem. Soc.*, **1997**, 119, 3068-3076
- [27] R. B. Silverman, *The Organic Chemistry of Drug Design and Drug Action*, Academic Press, San Diego, **1992**, 98-145
- [28] H. Dugas, *Bioorganic Chemistry*, Springer-Verlag, New York, **1996**, 3rd Edition, 3

-
- [29] J. Suh, *Acc. Chem. Res.*, **2003**, *36*, 562-570
- [30] J. Suh, Y. Cho, K. J. Lee, *J. Am. Chem. Soc.*, **1991**, *113*, 4198-4202; J. Suh, S. H. Hong, *J. Am. Chem. Soc.*, **1998**, *120*, 12545-12552; S. -J. Moon, J. W. Jeon, H. Kim, M. P. Suh, J. Suh, *J. Am. Chem. Soc.*, **2000**, *122*, 7742-7749; J. Suh, S. -J. Moon, *Inorg. Chem*, **2001**, *40*, 4890-4895; J. Jeon, S. J. Son, C. E. Yoo, I. S. Hong, J. B. Song, J. Suh, *J. Org. Lett.*, **2002**, *4*, 4155-4158
- [31] B.-B. Jang, K. P. Lee, D. H. Min, J. Suh, *J. Am. Chem. Soc.*, **1998**, *120*, 12008-12016
- [32] C. S. Jeung, J. B. Song, C. H. Kim, J. Suh, *Bioorg. Chem. Lett.*, **2001**, *11*, 3061-3064
- [33] G. Wulff, *Angew. Chem. Int. Ed. Engl.*, **1995**, *34*, 1812
- [34] M. Subat, A. S. Borovik, B. Koenig, *J. Am. Chem. Soc.*, **2004**, *126*, 3185-3190
- [35] R. Hettich, J.-J. Schneider, *J. Am. Chem. Soc.*, **1997**, *119* (9), 5638-5647
- [36] C. S. Jeung, C. H. Kim, K. Min, S. W. Suh, J. Suh, *Bioorg. Chem. Lett.*, **2001**, *11*, 2401-2404
- [37] C. E. Yoo, P. S. Chae, J. E. Kim, E. J. Jeong, J. Suh, *J. Am. Chem. Soc.*, **2003**, *125*, 14580-14589
- [38] R. M. Izatt, K. Pawlak, J. S. Bradshaw, R. I. Bruening, *Chem. Rev.*, **1991**, *91*, 1721-2085
- [39] Merck, Fractogel[®] EMD Epoxy (M), Art. No. 1.16961
- [40] H.-C. Gallmeier, PhD Thesis, University of Regensburg, **2002**
- [41] S. H. Gellman, R. Petter, R. Breslow, *J. Am. Chem. Soc.*, **1986**, *108*, 2388-2394
- [42] M. Mirnezami, L. Restrepo, J. A. Finch, *J. Colloid Interface Sci.*, **2003**, *259*, 36-42
- [43] T. W. Healy, V. R. Jellett, *J. Colloid Interface Sci.*, **1967**, *24*, 41-46
- [44] The 3-boc-Cyc was synthesised by a known method:
S. Brandes, C. Gros, F. Denat, P. Pullumbi, R. Guillard, *Bull. Soc. Chim. Fr.*, **1996**, *133*, 65-73
- [45] J. A. Dean, Lange's Handbook of Chemistry, McGraw-Hill, New York, **1973**, Vol. *11*, Chapter 5.; R. A. Robinson, A. I. Biggs, *Trans. Faraday Soc.*, **1955**, *51*, 901-903 (pK_a = 7.149 at 25 °C)
- [46] S. R. Logan, *Grundlagen der Chemischen Kinetik*, Wiley-VCH, Weinheim, **1997**, Chapters 1-3; H.-H. Perkampus, R. Kaufmann, *Kinetische Analyse mit Hilfe der UV-VIS-Spektrometrie*, Wiley-VCH, Weinheim, **1991**
- [47] Assuming the pK_a value of the catalytic module on the complex is the same as **5**, namely 7.51 at 25 °C

- [48] E. Kimura, Y. Kodama, T. Koike, M. Shiro, *J. Am. Chem. Soc.*, **1995**, *117*, 8304-8311 (Values are calculated from the k_{BNPP} values for **5** at 35 °C)
- [49] M. Subat, PhD Thesis, University of Regensburg, **2005**
- [50] Hünig, S.; Märkl, G.; Sauer, J. *Einführung in die apparativen Methoden in der Organischen Chemie*, 2nd Edition, Würzburg, Regensburg, **1994**
- [51] Author Collective, *Organikum*, 17th Edition, VEB Deutscher Verlag der Wissenschaften, Berlin, **1988**
- [52] Fractogel was reacted with thiosulfate and then titrated with 0.05 M HCl.

3. Synthesis of mono-dispersed spherical silica particles containing covalently bonded chromophores³

Abstract:

Organic-inorganic UV active hybrid materials have been prepared by a sol-gel process from benzophenone derivatives and tetraethylorthosilicate. The silica particles are spherical in shape and have a narrow size distribution which remains unchanged up to organic chromophore concentrations of 0.2 mmol/g. At higher concentrations the spheres become less regular and fuse. A dependence of the materials absorption properties on the particle size (at the same organic chromophore concentration) and on the concentration of surface grafted chromophores was noted. The most effective UV filter materials were found in a combination of silica incorporated chromophores and surface grafted chromophores at low overall chromophore concentration. A comparison of the chromophores photostability at standardised UV irradiation revealed an increase in stability for silica incorporated and surface immobilised benzophenone compared to benzophenone in homogeneous solution.

³ The results of this chapter have been patented :

Walencyk, T.; Carola, C.; Buchholz, H.; Synthesis of colloidal silica containing covalently bonded chromophores. *Eur. Pat. Appl.* **2004**, EP 04013515.4

The results of this chapter have been published:

Walencyk, T.; Carola, C.; Buchholz, H.; Koenig, B. *Int. J. Cos. Sci.* **2005**, 27, 1-14

3.1 Introduction

3.1.1 Background

The evolution of modern ultraviolet (UV) filters or sunscreen chemicals have come along way from the first reported emulsions containing benzyl salicylate and benzyl cinnamate in 1928.^[1,2] In 1943, with the patent of *p*-aminobenzoic acid (PABA) as a sunscreen chemical, the stage was set for a whole family of *p*-aminobenzoate derivatives to be incorporated into sunscreen formulations.^[3] PABA was a popular sunscreen in the 1950s and 1960s however its worldwide decline was due to reports questioning its dermatological safety and stability.^[4] During the next 50 years various classes of organic compounds including *p*-aminobenzoates, salicylates, cinnamates, benzophenones, anthranilates, dibenzoylmethanes and camphor derivatives were approved in Europe and the United States as UV filters.^[5,6] The majority of these filters protect against wavelengths in the UVB range (290-320 nm) which are known to cause erythema (sunburn),^[7] immunosuppression^[8] as well as skin cancer.^[9] The benzophenones, dibenzoylmethanes and terephthalylidenedicamphor sulfonic acid^[10,11] also absorb in the UVA range (315-380 nm) which promotes skin ageing, chronic photopathy and denaturation of cellular protein structures.^[12,13] Today's UV filters are expected to protect not only against sun burn but also against the long term damaging effects^[14,15] such as actinic aging or cutaneous cancer^[16] which UV radiation can inflict on the skin.^[17,18,19] UV filters are added to sunscreen products up to 10% for skin protection and more recently they are also present in many different cosmetic preparations for product stability.^[20] With such large amounts of UV filters being applied to the skin, the percutaneous absorption and consequent systemic distribution and effects of these chemicals must be considered.^[21,22]

3.1.2 Bioaccumulation and degradation of UV filters in humans

Evidence of bioaccumulation of UV filters in humans was shown in a study where 5 from 6 samples of human milk contained benzophenone-3 and/or octylmethoxycinnamate.^[23] In another study Hayden found that in humans up to 2% of an applied dose of benzophenone-3 and its metabolites were excreted in urine following topical application.^[24] The possible adverse effects of bioaccumulation was demonstrated by two

studies in which six frequently used UVA and UVB filters (benzophenone-3, butyl-methoxydibenzoylmethane, homosalate, 4-methylbenzylidene camphor, octyldimethyl-*p*-aminobenzoic acid and octylmethoxycinnamate) were analysed for their endocrine activities *in vitro* using MCF-7 breast cancer cells^[25] and *in vivo* in immature rats with the uterotrophic assay.^[26] Estrogenic activity was demonstrated for five compounds *in vitro* and for three *in vivo*, with EC₅₀ and ED₅₀ values in the range of other known xenogens.

3.1.3 Non-penetrating inorganic UV filters

Recently, micropigments such as microfine titanium dioxide (TiO₂) and zinc oxide (ZnO) have become a well known physical UV filter used in sunscreen formulations.^[27,28,29] These inorganic particles cover the skin and block the UV radiation from reaching the skin through reflection, light scattering and absorption (TiO₂ and ZnO are semiconductors).^[30] TiO₂ designed to optimally attenuate UV radiation has a mean particle size below 20 nm.^[31,32] In contrast to formulations containing macropigmented TiO₂ particles, formulations containing microfine TiO₂ are transparent on the skin and show a high cosmetic acceptance.^[33] Due to their high surface activity, such particles have the tendency to form agglomerates which cause them to lose their efficiency in the UV and increasing interaction in the visible range of the electromagnetic spectrum, hence appearing white when applied onto the skin.^[30,34] Various technologies such as coatings, dispersion techniques and formulation methods are employed to reduce this problem.^[30] Due to the large number of various techniques employed and contributing factors such as vehicle and analysis method, the dermal uptake properties of microfine TiO₂ has been controversially discussed in recent years.^[35] Two different studies confirmed that TiO₂ with a mean diameter of 20 nm does not penetrate the outer layer of the skin.^[36,37]

By combining the advantages of sunscreen chemicals, namely specific UV absorbance ranges, and those of physical UV blockers, namely non-skin penetrating, a new generation of sunscreen agents can be created. In the design of UV filters a good UV absorption in the range of 290–400 nm, photostability and dermatological compatibility are very important.^[38]

3.1.4 New advances in non-penetrating UV filters

In the year 2000 the first organic microparticles of diameter of less than 200 nm combining the absorption properties of organic UV filters with the scattering and reflection properties of inorganic UV filters such as TiO_2 , were approved as cosmetic filters by EU authorities.^[14,39] UV filters based on organic chromophores which were grafted on organosiloxane polymers or encapsulated in silica capsules soon followed.^[40,41,42] The amount of organic UV filter incorporated in such silica capsules is between 0.5 and 20 % by weight and the size of the particles varies between 10 nm and 10 μm . SiO_2 is used today in the cosmetic industry as a formulation filler.^[43,44] The SiO_2 is in the form of nanometre sized spheres of equal size, called Microspheres (MS).^[45] These MS do not penetrate the skin and are like tiny ball bearings, giving the skin a silky smooth feeling.

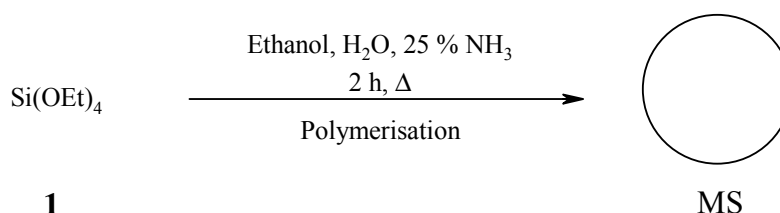
The following project aims to improve the properties of the functionalised silica particles. Instead of just encapsulating organic UV filters within silica capsules or post-functionalising silica with UV filters, a spherical polymer containing UV filters in its core and surface was synthesised. The dependence of the particle shape on the concentration and distribution of the organic chromophore and the photostability of the chromophore was examined.

3.2 Results and Discussion

3.2.1 Synthesis of Microspheres

Microspheres (MS) are synthesised from tetraethylorthosilicate (TEOS) **1** in a solution of ethanol, water and ammonia (Scheme 1). The size of the MS is influenced by the concentration of ammonia in solution and the temperature at which the polycondensation reaction takes place, and range from 25 to 500 nm in diameter. The general synthesis of equal sized spherical silica particles is outlined in Scheme 1.

Scheme 1. General synthesis of neat microspheres (MSN)

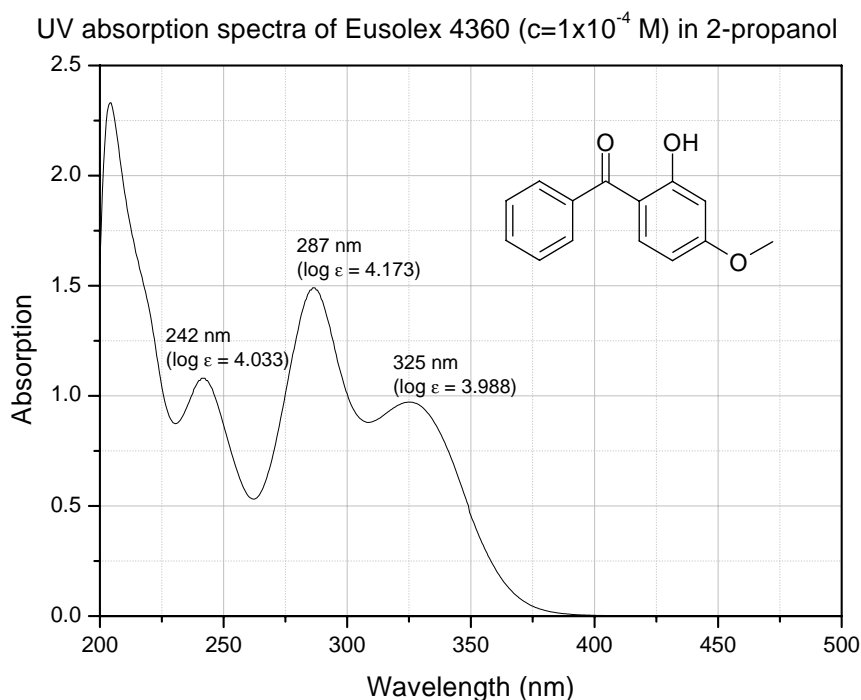


By introducing small amounts of a chromophore linked to triethoxysilyl functionality into the polymerisation, it is still possible to generate spherical hybrid silica particles even though the symmetry of the polymerisation is reduced.

3.2.2 Choice of UV filter

The class of UV filter used in the synthesis of the various microspheres were benzophenones, in particular (2-hydroxy-4-methoxyphenyl)-phenyl-methanone (benzophenone-3).

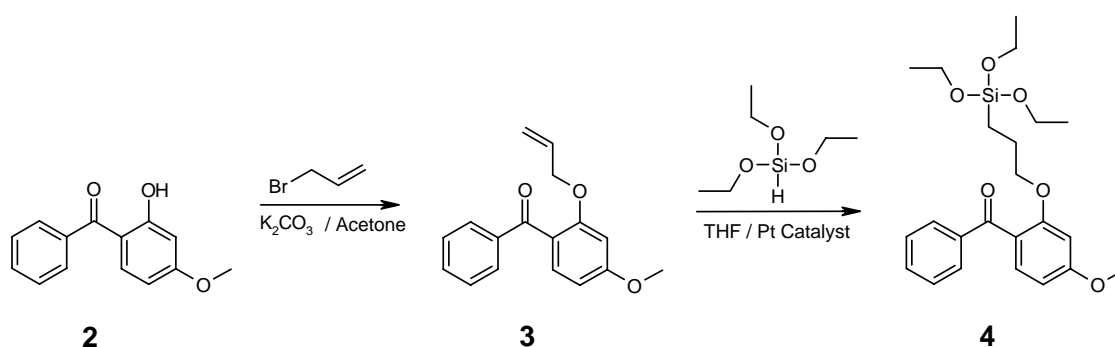
Figure 1. UV absorption spectra of (2-hydroxy-4-methoxy-phenyl)-phenyl-methanone in 2-propanol



Benzophenone-3 has a strong absorption in both the UVA (320 - 400 nm) and UVB (290 - 320 nm) region of the electromagnetic spectrum (Figure 1). In 2-propanol, benzophenone-3 has 3 peaks, at 242 nm ($\log \epsilon = 4.033$), 287 nm ($\log \epsilon = 4.173$) and 325 nm ($\log \epsilon = 3.988$). The UV characteristics were analysed at different concentrations in 2-propanol and it was found that the Beer-Lambert Law is obeyed up to a chromophore concentration of $2 \times 10^{-4} \text{ molL}^{-1}$.

3.2.3 Synthesis of monomer

In order to incorporate the UV filter with covalent bonds into the inorganic matrix, a triethoxysilyl functionality was added *via* a spacer to benzophenone-3.

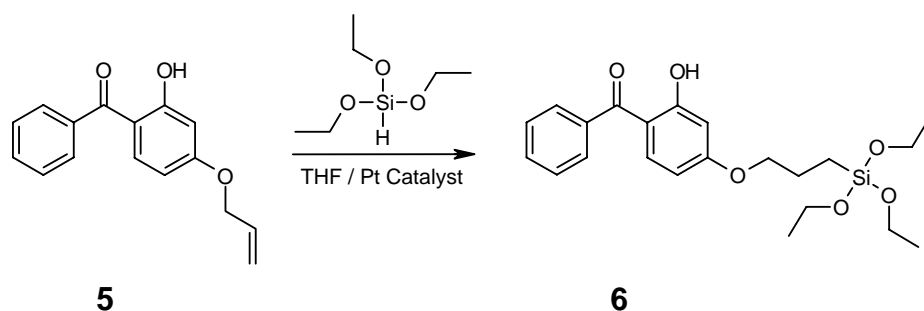
Scheme 2. Synthesis of a silyloxy monomer

Benzophenone-3, **2** was reacted with allyl bromide (potassium carbonate acted as the base) in acetone to yield the allyl ether in quantitative yields. The addition reaction of triethoxysilane and the allyl ether **3** in the presence of a Pt (0) catalyst yielded the desired silylated product **4** (Scheme 2). The silyl ether **4** would then be added as the UV active monomer to the polycondensation reaction. Destruction of the hydrogen bond in **3** was however responsible for loss of the UVA (325 nm) absorption peak (Figure 2) and an alternative site for allylation needed to be found.

Figure 2. Comparison of (2-hydroxy-4-methoxyphenyl)-phenyl-methanone and (2-allyloxy-4-methoxyphenyl)-phenyl-methanone

<p>2</p> <p>UV (CH₃CN) λ_{max} (log ε) 287 nm (4.172) UV (CH₃CN) λ_{max} (log ε) 325 nm (3.983)</p>	<p>3</p> <p>UV (CH₃CN) λ_{max} (log ε) 281 nm (3.869)</p>
--	---

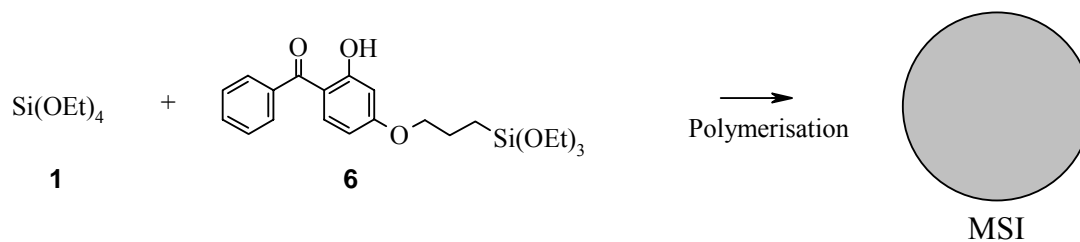
Commercially available 2-hydroxy-(4-allyloxyphenyl)-methanone, **5** allowed the further functionalisation to the silyl ether, whilst still retaining the phenol. Silylation was first attempted using hexachloroplatinic (IV) acid hexahydrate as the catalyst.^[46] Although the product was recovered, poor yields and purification difficulties due to instability of the product and high boiling point required that a new catalyst be sought. When platinum(0)-1,3-divinyl-1,1,3,3-tetramethyldisiloxane complex was used as the catalyst^[47] the reaction was much cleaner, however purification was still an issue (Scheme 3).

Scheme 3. Synthesis of 2-hydroxy-4-(3-triethoxysilylpropoxy)diphenylketone

Purification of 2-hydroxy-4-(3-triethoxysilylpropoxy)diphenylketone, **6** was attempted with high vacuum distillation (230 °C at 0.5 mbar). The harsh conditions caused decomposition of the product and only small amounts (< 30 %) of **6** could be recovered. Before trying to improve the purification of the reaction, the product **6** was purchased directly. It was decided to only use commercially available **6** for the synthesis of the monospheres, thus reducing the time taken to synthesise the various MS and all MS were synthesised with the same purity of **6**. The reaction model can however be used for other molecules bearing a hydroxyl group which may be of interest in the future.

3.2.4 Microspheres containing a chromophore (MSI)

Commercially available 2-hydroxy-4-(3-triethoxysilylpropoxy)diphenylketone **6** was added in various proportions to tetraethylorthosilicate (TEOS) **1** in the presence of ethanol, water and ammonia solution (Scheme 4). By varying the ammonia concentration and temperature, three sizes (100 nm, 250 nm and 500 nm diameter) of MS were prepared each with the maximum chromophore loading whilst still remaining spherical. (MSI = MicroSpheres with chromophores Inside) MS with a comparable diameter were functionalised with the same chromophore on the surface and taken as a reference.

Scheme 4. General synthesis of Microspheres containing a chromophore (MSI)

Once the polymerisation was complete, the ammonia was removed *via* evaporation, and the MS were washed to remove any unreacted chromophore starting material. The washing

method varied according to the size of the particles. MS sized 250 nm and 500 nm sedimented well and were washed using centrifugation (Washing Method B). The smaller 100 nm monospheres did not sediment fully in the centrifuge vial, and an alternative method in washing the MS was found in soxhlet extraction with dichloromethane (Washing Method A). All MS were washed until all physically bonded starting material was removed from the MS. Once the MS were washed, the mass of the residual oil containing only **6** (verified by GC-MS) was then subtracted from the initially added amount of the starting material **6**, from which the chromophore loading could be calculated. No residual **1** was found in the oil suggesting that it was completely incorporated into the MS. On average 75 % of the added chromophore took part in the polymerisation, regardless of the size of the MS.

A linear increase in carbon content was noted with increased loading of chromophore in the MS (Table 1). In MS containing only Si and O (MSN = Neat MicroSpheres), the small amount of carbon found can be attributed to ethoxy groups of the TEOS which did not react in the polymerisation.^[48]

Table 1. Carbon content of 100 nm, 250 nm and 500 nm MS with various chromophore loadings

MS loading (mmol/g)	%C	MS loading (mmol/g)	%C	MS loading (mmol/g)	%C
MSI-100		MSI-250		MSI-500	
0	1.3	0	3.2	0	4.3
0.118	3.2	0.208	6.9	0.106	5.5
0.216	5.3	0.313	8.1	0.213	7.2
0.316	6.8	0.428	10.5	0.306	7.9
0.409	8.4	0.524	11.9	0.391	9.6
0.511	10.5	0.897	17.2	0.506	11.0

The concentration of chromophore added during the polymerisation determines whether the resulting MS retain their spherical shape and size distribution when compared to the pure SiO₂ reference MS. The chromophore **6** is not symmetrical and introduces an impurity into the ordered polymerisation of a monosphere. When this impurity reaches a certain concentration it interferes so much with the polymerisation that equal sized spherical

particles can no longer form. The size of the MS did not affect the chromophore loading capacity.

Figure 3. SEM images of 100 nm MS containing various amounts of chromophore

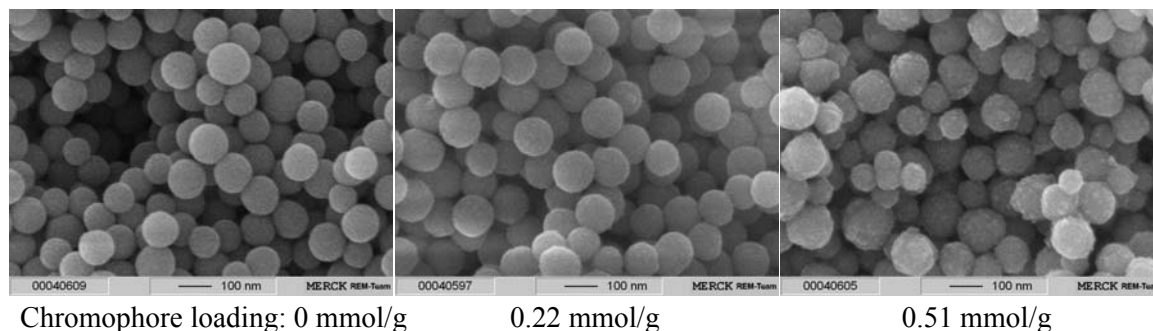


Figure 4. SEM images of 250 nm MS containing various amounts of chromophore

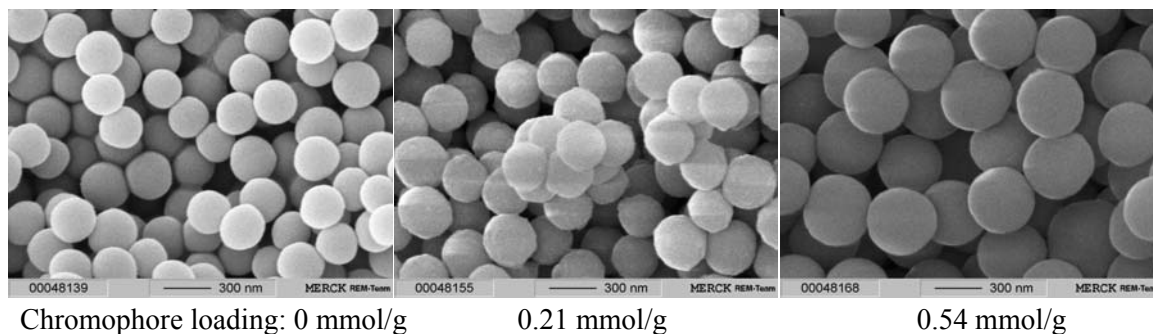


Figure 5. SEM images of 500 nm MS containing various amounts of chromophore



Figures 3, 4 and 5 show the effect of chromophore concentration on the shape for MS of diameter 100 nm, 250 nm and 500 nm respectively. When the loading is low (≤ 0.2 mmol/g) the MS are of equal size and spherical. As good as no aggregation occurs and the chromophores are evenly distributed throughout the suspension. As the chromophore loading increases more and more aggregation occurs, the MS become less spherical and have a larger size distribution, resulting in that the chromophores are no

longer evenly distributed in the suspension. Although the size of the MS does not affect the loading of the chromophore, it does affect the UV properties of the MS. Table 2 summarises the UV properties of MS containing the maximum loading of chromophore whilst still remaining spherical and with a narrow size distribution. The extinction coefficient κ describes the UV properties of the entire polymer. The molar extinction coefficient ϵ describes the UV properties with respect to the amount of chromophore in the MS. The fact that both κ and ϵ decrease with increasing diameter suggests that the chromophores located within the core of the larger MS cannot absorb UV light.

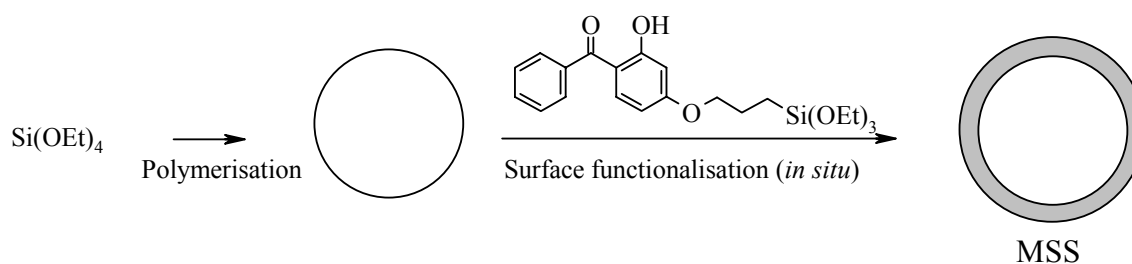
Table 2. UV data for MS containing the maximum loading of chromophores

MS diameter (nm)	MS loading (maximum) (mmol/g)	Extinction Coefficient, κ (Lg ⁻¹ cm ⁻¹)	Molar Extinction Coefficient, ϵ (Lmol ⁻¹ cm ⁻¹)
100	0.22	2.221	10269
250	0.21	2.003	9628
500	0.21	1.864	8751

3.2.5 Microspheres with chromophores on the surface (MSS)

Microspheres with a functionalised surface (MSS = MicroSpheres with chromophore on the Surface) have previously been reported.^[45] Their synthesis is a two step process in which first MSN are synthesised and transferred into ethanol, where they are stored as a suspension. In the second step a chromophore similar to **6** is slowly added to the ethanol suspension. The final washing step is replaced by a high vacuum distillation to remove any unreacted chromophore. This tedious procedure was simplified to a one pot reaction with milder washing method using a centrifuge.

Firstly, TEOS was added to a mixture of ammonia, ethanol and water and MSN of a set size (250 and 500 nm diameter) were synthesised. Once the polymerisation was complete, the chromophore **6** (up to a maximum to 10 mol%) dissolved in ethanol was added directly and the reaction allowed to stir for 2 hours at the set temperature (see Scheme 5). The functionalised microspheres were then separated from the remaining reactants in the same way as for MSI (Washing Method B).

Scheme 5. General synthesis of Microspheres with a functionalised surface (MSS)

Figures 6 and 7 show MS of fixed diameter 250 nm and 500 nm respectively, with various amounts of chromophore on the surface (**MSS-250** and **MSS-500** respectively). When the chromophore loading is low, only parts of the surface have been functionalised. As the loading increases the entire surface becomes covered with chromophore and individual spheres adhere together. A linear increase in carbon content was noted with increased loading of chromophore in the MS.

Figure 6. SEM images of 250 nm MS with various amounts of chromophore on the surface

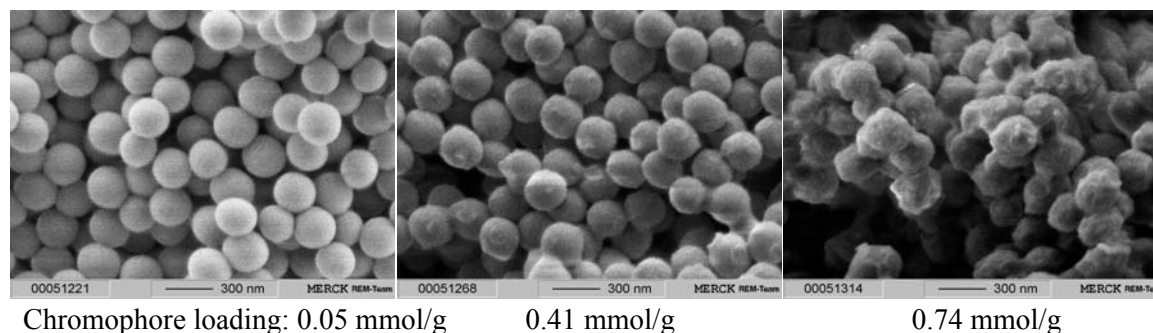


Figure 7. SEM images of 500 nm MS with various amounts of chromophore on the surface

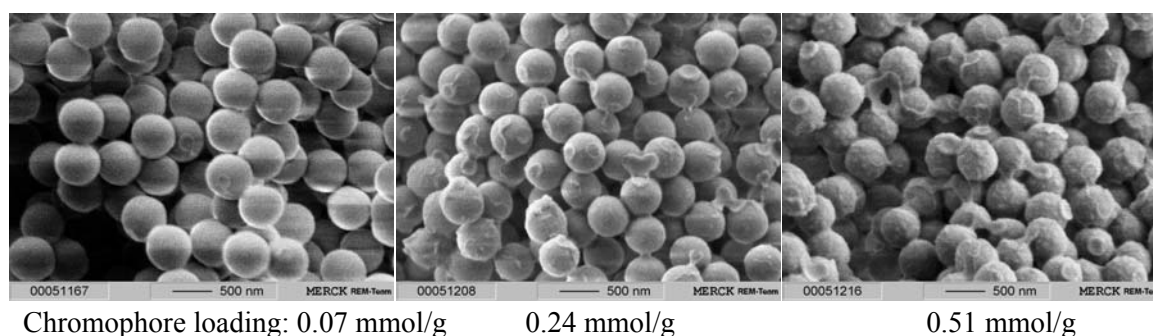


Table 3 summarises the UV properties of MSS (of diameter 250 and 500 nm) with the minimum and maximum loading of chromophore on the surface whilst still remaining spherical. The extinction coefficient, κ describes the UV properties of the entire polymer. The molar extinction coefficient, ϵ describes the UV properties with respect to the amount of chromophore in the MS.

Table 3. UV data for MSI with the minimum and maximum loading chromophore on the surface

MS diameter (nm)	MS loading (mmol/g)	Extinction Coefficient, κ (Lg ⁻¹ cm ⁻¹)	Molar Extinction Coefficient, ϵ (Lmol ⁻¹ cm ⁻¹)
250	0.05 ^[a]	0.610	13224
250	0.41 ^[b]	1.725	4240
500	0.07 ^[a]	0.602	8538
500	0.24 ^[b]	1.429	6020

^[a] The loading at which the highest ϵ values was observed.

^[b] The maximum loading whilst still forming spherical MS of narrow size distribution.

MSS exhibit the highest ϵ values when only the minimal amount of chromophore is on the surface. This suggests that with an increase in the chromophore concentration on the surface, the molecules interact causing a decrease in UV absorption ability. MS with a smaller diameter have a larger surface area and thus with the same polymer and chromophore amount, the distribution on the surface is more homogeneous for small MS. This is supported by the fact that MS with a smaller surface area show a sharper decline in ϵ (with increasing chromophore loading) than MS with a larger diameter.

For MSI, the chromophores are evenly spaced throughout the matrix. The interactions between chromophore molecules are not as frequent, as the chromophore molecules are much further apart within the matrix, than the chromophore molecules of MSS. For MSI, increasing the chromophore concentration simply increases the UV absorption properties.

3.2.6 Microspheres containing chromophores in the core and on the surface (MSIG)

In an attempt to further improve the UV activity, MS containing chromophores in the core as well as on the surface were synthesised. This was achieved by post-functionalising the surface of MSI *in situ* with either the unreacted chromophore **6** (MSIG = MicroSpheres with chromophores Inside and Grafted on surface) or additional chromophore **6** (MSIGC = MicroSpheres with chromophores Inside and Grafted on surface with additional Chromophore). The top synthesis route in Scheme 6 describes the MSIG while the bottom route describes MSIGC.

Scheme 6. General synthesis of chromophore containing MS and with a functionalised surface

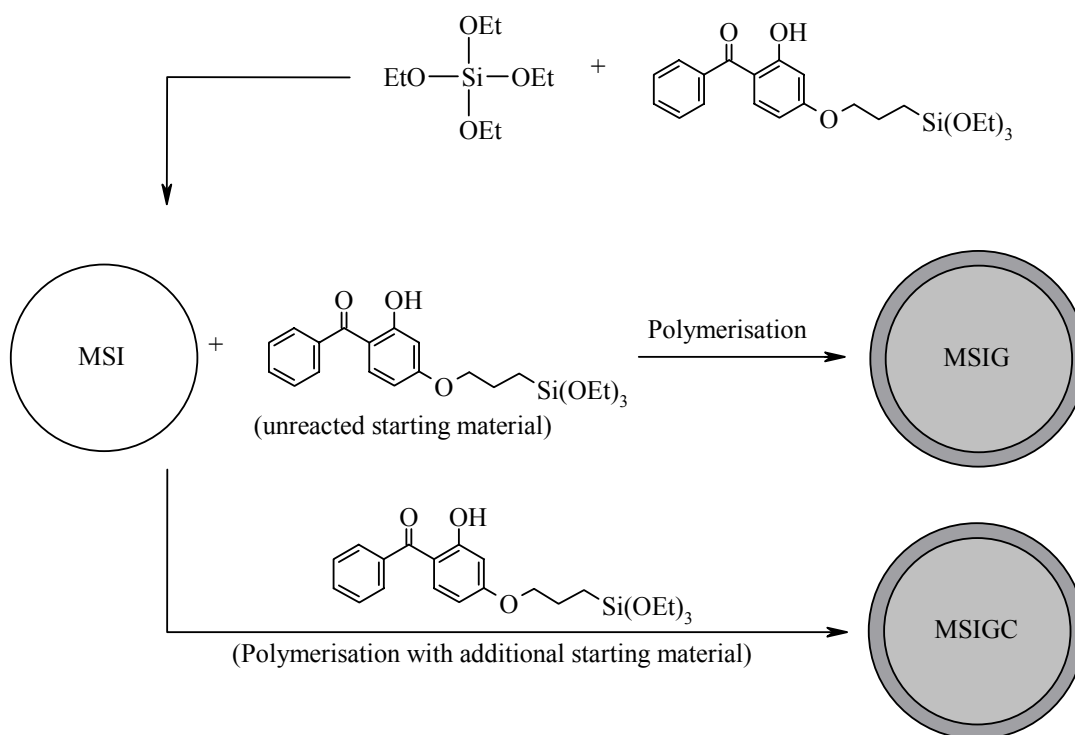
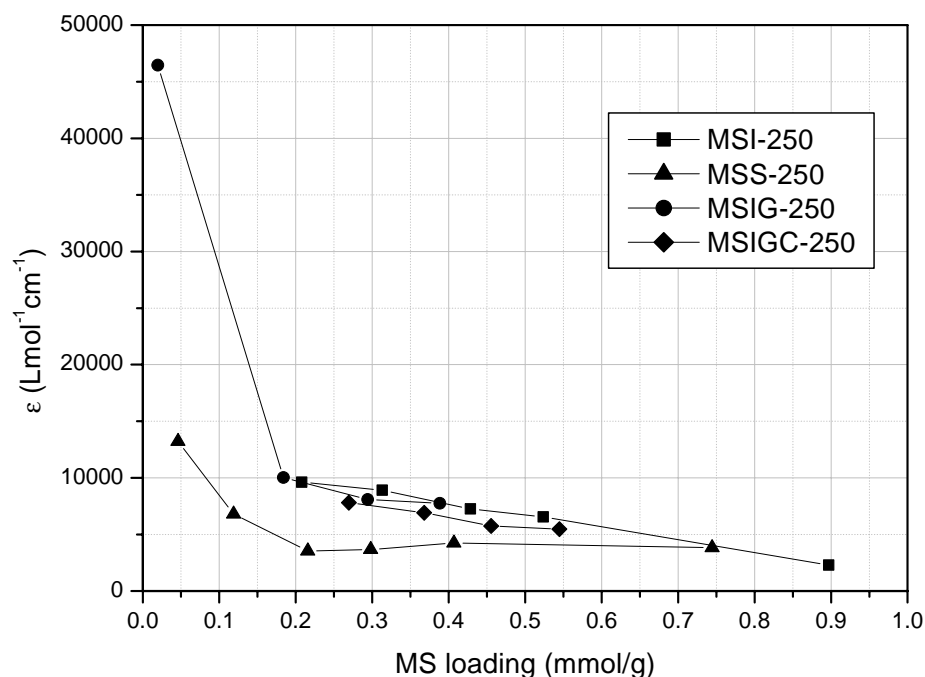


Figure 8 compares the ϵ values of chromophore containing MS (MSI, square), MS with chromophore on the surface (MSS, triangle), chromophore containing MS and with a grafted surface (MSIG, circle) and MS containing chromophore and with a grafted surface with additional chromophores (MSIGC, diamond).

Figure 8. UV data for **MSI-250**, **MSS-250**, **MSIG-250** and **MSIGC-250**

Of all the MS of 250 nm diameter the best ϵ value was generated by **MSIG-250-1**. Here the MS contains chromophore and the minimal amount of chromophore was functionalised on the surface. This polymer thus combines the advantages of utilising the volume of the sphere as well as optimising the concentration of chromophores on the surface.

3.2.7 Photostability

The reduction of UV-induced decomposition of UV filters is an active field of research in the cosmetic industry.^[6] In order to test if incorporation of a chromophore into a matrix increases its photostability, studies were carried out on two polymers with similar chromophore loadings. The photo-degradation of **MSI-250-2** (0.31 mmol/g) and **MSS-250-4** (0.30 mmol/g) were compared to that of benzophenone-3 (**2**) and **6**.

The Minimal Erythral Dose (MED) is used to describe the erythral potential of UV radiation and 1 MED is defined as the effective UV dose that causes a perceptible reddening of previously unexposed human skin. An MED of 1 for an individual with skin type II (light to medium hair, eyes and skin) is 20 minutes in the midday sun in midsummer. An exposure of 5 MED produces a painful sunburn, whilst 10 MED can cause

oedema, vesiculation and bullae formation.^[49,50] The method for measuring photostability is based on an established method.^[51] Samples were irradiated for 130.5 min at 89.6 W/m² (corresponds to 5 MED) using a Suntest CPS with xenon radiator (radiation filter limited to ≥ 290 nm). The UV spectrum after irradiation was compared to samples which were not irradiated. Table 4 summarises the percentage of UV absorption activity remaining after irradiation at 5 MED.

Table 4. Photostability (%) of selected **MSI-250-2** and **MSS-250-4** at 5 MED

Integrated region	Benzophenone-3	6	MSI-250-2	MSS-250-4
UV (290-400 nm)	79 \pm 3	80 \pm 3	93 \pm 1	89 \pm 1
UVA (320-400 nm)	80 \pm 3	78 \pm 3	95 \pm 1	88 \pm 1
UVB (290-320 nm)	77 \pm 2	86 \pm 2	89 \pm 1	89 \pm 2

Samples with benzophenone-3 and its silyloxy derivative **6** retain 79 and 80 % of their UV absorption ability after irradiation over the entire UV spectrum respectively. When **6** is immobilised onto the surface of a MS as in **MSS-250-4**, its photostability increases to 89 %. A further improvement in photostability is noted when the chromophore is incorporated into the matrix as in **MSI-250-2**, where 93 % of the UV absorption ability retains after irradiation.

The increased photostability of a chromophore embedded in a matrix over a chromophore in solution might be explained by a higher degree of caging of the silylated chromophore^[52] and a more facile energy dissipation onto the silica bulk around it.^[53,54]

3.3 Conclusion

Spherical, sub-micron sized organic-inorganic hybrid polymers with a narrow size distribution were synthesised. A loading of up to approximately 0.2 mmol organic chromophore per gram of material gave a regular spherical particle shape for different particle sizes. Increasing amounts of organic chromophore incorporation lead to non-regular shape and particle fusion. The UV absorption properties of the material depend on chromophore concentration and particle size. At the same incorporated chromophore concentration, the extinction coefficient of regular shaped particles decreases with increasing size, due to the poorer accessibility of inner chromophores. The UV absorption ability of material with surface grafted chromophores strongly depends on concentration. At higher loadings a decrease in UV absorption ability is noted, which corresponds to a non linear Beer Lambert behaviour at high concentrations. The highest effective UV absorption of functionalised silica particles was found in a combination of incorporated and grafted organic chromophores at low concentration. Incorporation of the benzophenone chromophore into a silica matrix or the immobilisation on a silica surface increased the photostability of the compounds as compared with its properties in solution.

The study leads to the conclusion that organic-inorganic hybrid materials from silica and benzophenone chromophores have interesting UV filter properties. To gain the optimal performance from the complementing properties of the inorganic and the organic component, the dependence of particle shape and UV absorption properties on the chromophore concentration and the mode of immobilisation must be considered.

3.4 Experimental

3.4.1 General

3.4.1.1 Spectroscopy

UV-VIS Spectra

Varian Cary BIO 50 UV/VIS/NIR Spectrometer. Use of a 1 cm quartz cell (Hellma) and Uvasol solvents (Merck). Reported as: λ_{max} in nm (ϵ).

The colloidal silica (50 mg) was placed into a 100 ml volumetric flask containing 50 ml 2-propanol. The flask was placed into an ultrasound bath until a homogenous suspension was achieved. The volumetric flask was then made up to the mark and homogenised again. A sample was directly taken and measured using an Integrating (Ulbricht) Sphere (taking absorption, transmission and scattering into account).

Photostability

The colloidal silica (500 mg) was placed into a 50 ml volumetric flask containing a 70:30 ethanol:isopropylmyristate solvent mixture. 20 μl of the suspension was spread over a glass slide with a surface area of 10 cm^2 . For each sample four glass slides were irradiated at 5 MED with a Suntest CPS with xenon radiator (radiation filter limited to ≥ 290 nm) equipped with a Solar-Standard filter 310-400 nm, whilst a further four glass slides were kept in the dark. After irradiation, the colloidal silica particles were washed from the glass slides into a 10 ml volumetric flask containing methanol. UV absorptions were measured using a Varian Cary 300 Bio with Integrating (Ulbricht) Sphere.

3.4.1.2 Analysis

Elemental Analysis

Elemental analyses were carried out by the central analytical department of Merck KGaA, Darmstadt.

Scanning Electron Microscopy (SEM)

SEM analyses were carried out by the central analytical department of Merck KGaA, Darmstadt.

The colloidal silica was submitted as a fine powder for analysis. No difference was noted in aggregation of particles whether the samples were submitted as a dry solid or in an ethanol suspension. When the MS were suspended in ethanol, they could simply be evaporated to dryness without them losing their spherical properties. This was not the case when ammonia or water was present in the suspension.

3.4.1.3 Synthesis

Solvents

Purification and drying according to accepted general procedures.^[55,56]

If not otherwise stated, commercially available solvent of the highest purity were used.

Washing Method A – Soxhlet solid extraction

The reaction mixture was evaporated under reduced pressure to 50% of its volume. An azeotropic distillation was carried out leaving the product in ethanol. The suspension was evaporated slowly under reduced pressure yielding a fine solid. The crude MS were placed in a 100 ml soxhlet and extracted with 30 ml of DCM for 24 hours. The soxhlet sleeve was washed with DCM to remove any remaining educt. Filtration of the DCM using a pressure filter with a 0.45 μm filter, recovered residual MS which had seeped through the soxhlet sleeve. The filtrate was washed three times with DCM and then added to the bulk washed MS. The clear mother liquor was evaporated to dryness leaving a yellow-brown oil.

Washing Method B – Centrifuge

The reaction mixture was evaporated under reduced pressure to 50% of its volume and then centrifuged using PC cone centrifuge vials at 3500 rpm for 20 minutes. The clear mother liquor was decanted and the sedimented colloidal silica resuspended using an ultrasound bath and a spatula in fresh ethanol. This procedure was repeated a further four times. The mother liquor was concentrated and centrifuged again (two ethanol washes) to remove any colloidal silica which may have been decanted into the mother liquor. The clear mother liquor was evaporated to dryness leaving a yellow-brown oil.

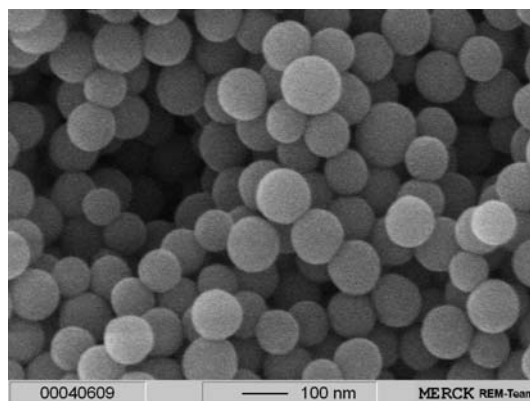
3.4.2 Synthesis of New Compounds

MS100

Ethanol (160 ml, 2.7 mol) and deionised water (82 ml, 4.6 mol) were placed into a 500 ml 4 neck round and stirred using a mechanical stirrer (Teflon stirrer, 160 rpm) and heated to 58 °C in a water bath. Tetraethylorthosilicate (TEOS) (21.15 g, 101.5 mmol) **1**, was also heated to 58 °C (no stirring) in the same water bath (water bath temperature of 60 °C). Once the temperature of the ethanol-water azeotrope had reached a stable 58 °C, 25% ammonia solution (9.4 ml, 0.13 mol) was injected into the azeotrope (at the edge of the vessel) via a syringe. The stirring was increased (470 rpm) to ensure good mixing. Once the temperature of the mixture had reached 58 °C again, **1** was poured positively via a funnel into the azeotrope and allowed to stir for exactly 15 seconds. After 15 seconds the stirring was stopped and the reaction was allowed to stand at 58 °C (the reaction was slightly exothermic but the water bath temperature was kept at 60 °C) for 2 hours. The product was washed using Washing Method A, yielding a white solid of 6.80 g. No starting material was recovered.

Elemental Analysis of solid found: C 1.3, H 1.4, Si 42.3.

SEM image of **MS-100**



MSI-100-1 to MSI-100-5

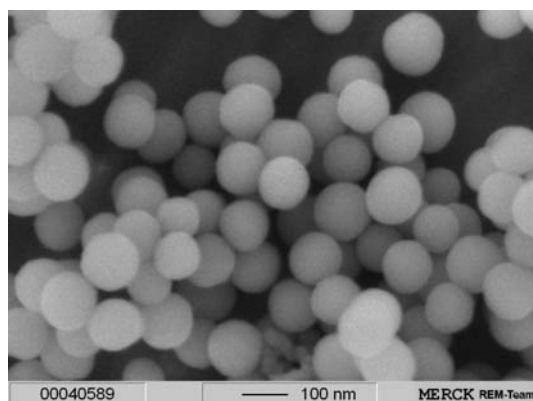
The procedure is identical to the synthesis of **MS100**, except that varying reactant proportions of **1** and 2-hydroxy-4-(3-triethoxysilylpropoxy) diphenylketone **6** were added instead of just **1** alone: **MSI-100-1** (100.5 mmol **1** and 1.0 mmol **6**), **MSI-100-2** (99.5 mmol **1** and 2.0 mmol **6**), **MSI-100-3** (98.4 mmol **1** and 3.1 mmol **6**), **MSI-100-4**

(97.4 mmol **1** and 4.1 mmol **6**) and **MSI-100-5** (91.4 mmol **1** and 10.2 mmol **6**). The products were washed using Washing Method A. The yields of the reactions are tabulated below:

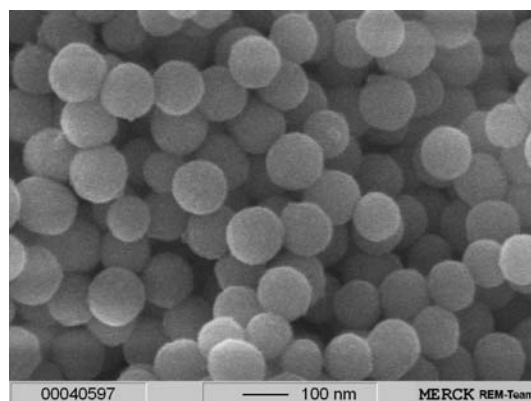
Reaction Number	MS recovered (g)	MS loading (mmol/g)	Extinction coefficient κ ($\text{Lg}^{-1}\text{cm}^{-1}$)	Molar extinction coefficient ϵ ($\text{Lmol}^{-1}\text{cm}^{-1}$)	C ^[a] (%)	H (%)	Si (%)
MSI-100-1	6.08	0.118	1.128	9588	3.2	1.6	40.5
MSI-100-2	7.31	0.216	2.221	10269	5.3	1.9	38.4
MSI-100-3	7.36	0.316	2.872	9086	6.8	2.0	37.7
MSI-100-4	7.49	0.409	3.651	8933	8.4	1.9	37.1
MSI-100-5	7.60	0.511	2.788	5452	10.5	2.3	36.3

[a] Nitrogen content was not detectable. Oxygen content could not be reported due to SiO_2 formation.

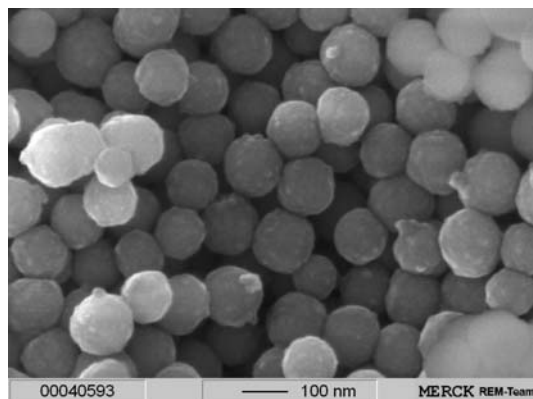
SEM image of **MS-100-1**



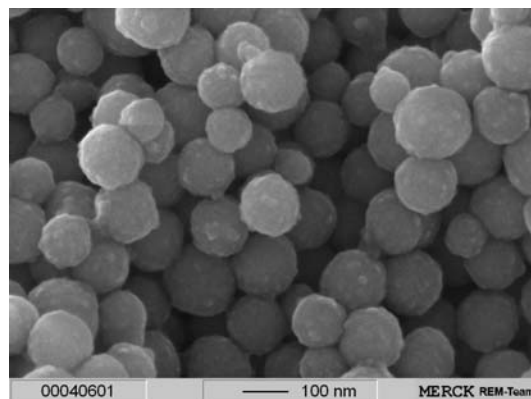
SEM image of **MS-100-2**

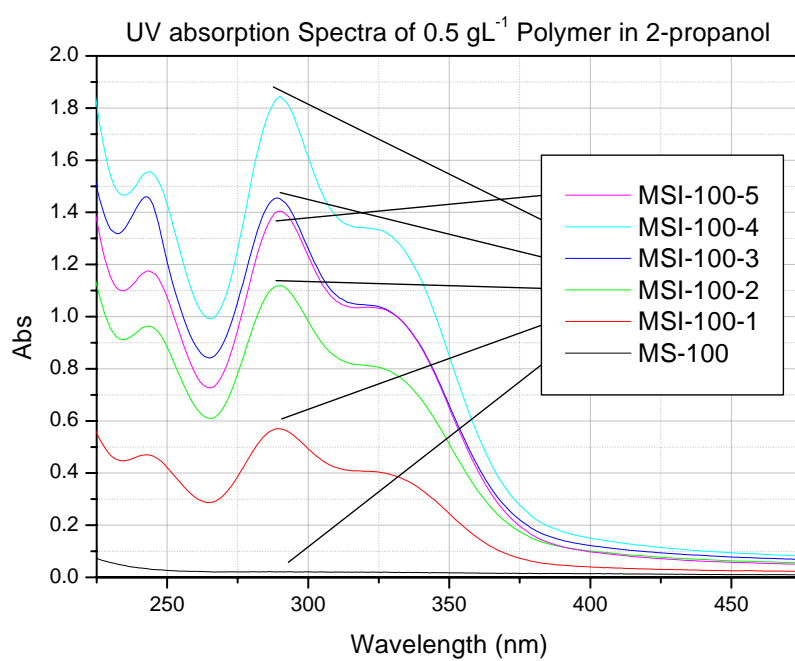
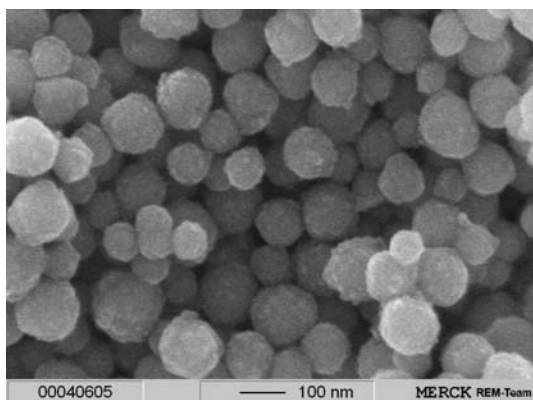


SEM image of **MS-100-3**



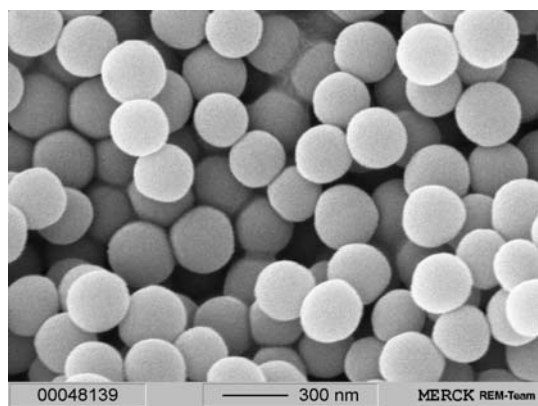
SEM image of **MS-100-4**



SEM image of **MS-100-5**

MS250

Ethanol (150 ml, 2.6 mol) and deionised water (56 ml, 3.1 mol) were placed into a 500 ml 4 neck round and stirred using a mechanical stirrer (Teflon stirrer, 160 rpm) and heated to 60 °C in a water bath. Compound **1** (21.15 g, 101.5 mmol) was also heated to 60 °C (no stirring) in the same water bath (water bath temperature of 62 °C). Once the temperature of the ethanol-water azeotrope had reached a stable 60 °C, 25% ammonia solution (35 ml, 0.47 mol) was injected into the azeotrope (at the edge of the vessel) via a syringe. The stirring was increased (470 rpm) to ensure good mixing. Once the temperature of the mixture had reached 60 °C again, **1** was poured positively via a funnel into the azeotrope and allowed to stir for exactly 15 seconds. After 15 seconds the stirring was stopped and the reaction was allowed to stand at 60 °C (the reaction was slightly exothermic but the water bath temperature was kept at 62 °C) for 2 hours. The product was washed using Washing Method B, yielding a white solid of 6.8 g. No starting material was recovered. Elemental Analysis of solid found: C 3.2, H 1.9, Si 40.0.

SEM image of MS-250**MSI-250-1 to MSI-250-5**

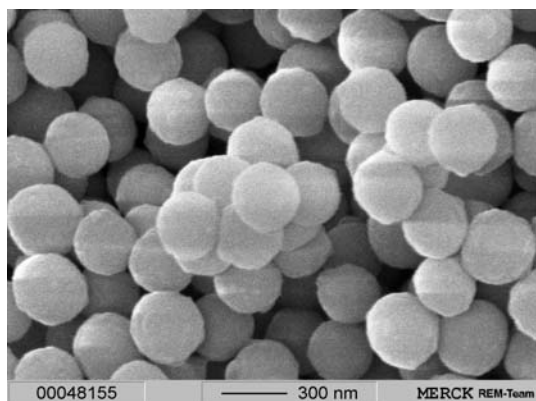
The procedure is identical to the synthesis of **MS250**, except that varying reactant proportions of **1** and 2-hydroxy-4-(3-triethoxysilylpropoxy) diphenylketone **6** were added instead of just **1** alone: **MSI-250-1** (100.5 mmol **1** and 1.0 mmol **6**), **MSI-250-2** (99.5 mmol **1** and 2.0 mmol **6**), **MSI-250-3** (98.4 mmol **1** and 3.1 mmol **6**), **MSI-250-4** (97.4 mmol **1** and 4.1 mmol **6**) and **MSI-250-5** (91.4 mmol **1** and 10.2 mmol **6**). The

products were washed using Washing Method B. The yields of the reactions are tabulated below:

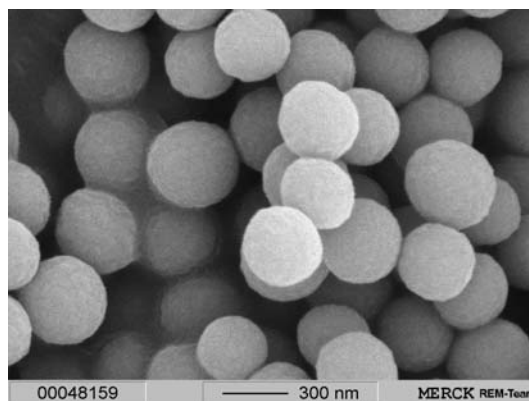
Reaction Number	MS recovered (g)	MS loading (mmol/g)	Extinction coefficient κ ($\text{Lg}^{-1}\text{cm}^{-1}$)	Molar extinction coefficient ϵ ($\text{Lmol}^{-1}\text{cm}^{-1}$)	C ^[a] (%)	H (%)	Si (%)
MSI-250-1	7.09	0.208	2.003	9628	6.9	2.1	34.0
MSI-250-2	7.42	0.313	2.789	8907	8.1	2.2	37.4
MSI-250-3	7.58	0.428	3.108	7255	10.5	2.3	36.4
MSI-250-4	7.77	0.524	3.430	6551	11.9	2.4	35.4
MSI-250-5	8.37	0.897	2.062	2299	17.2	2.7	32.6

^[a] Nitrogen content was not detectable. Oxygen content could not be reported due to SiO_2 formation.

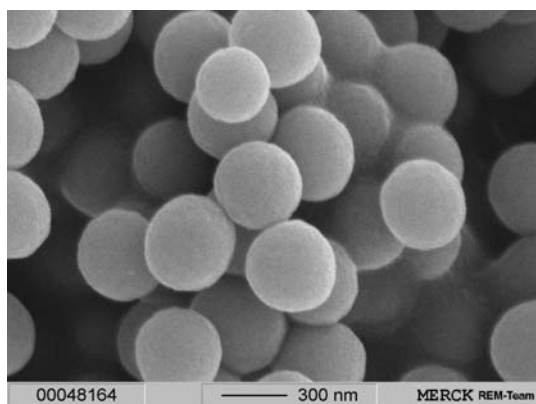
SEM image of **MS-250-1**



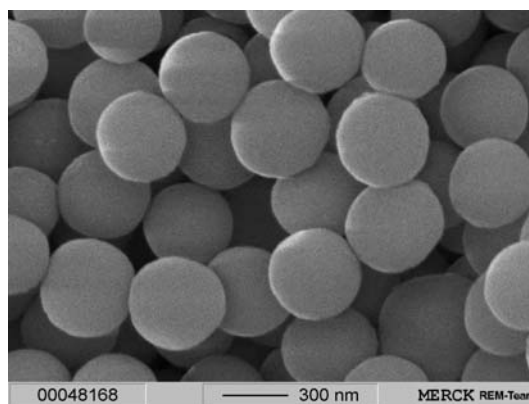
SEM image of **MS-250-2**

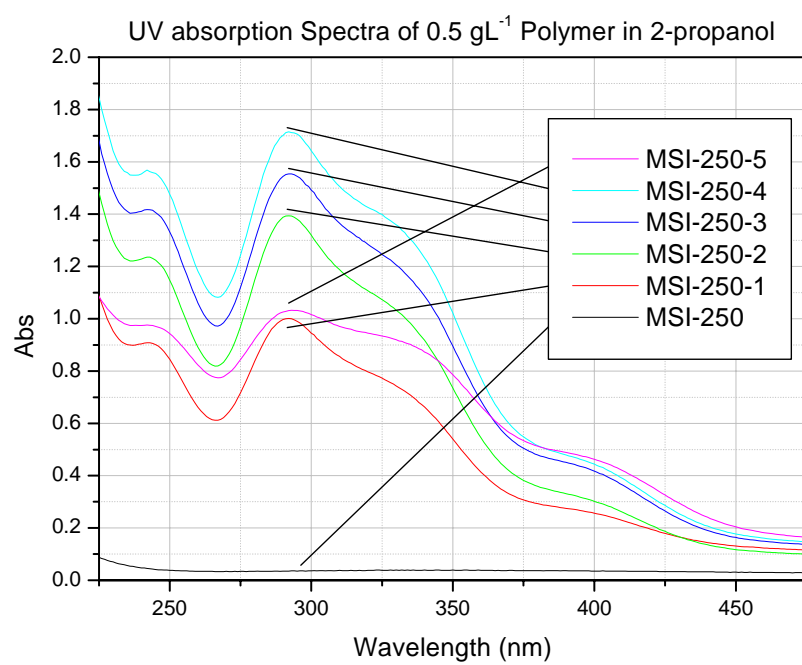
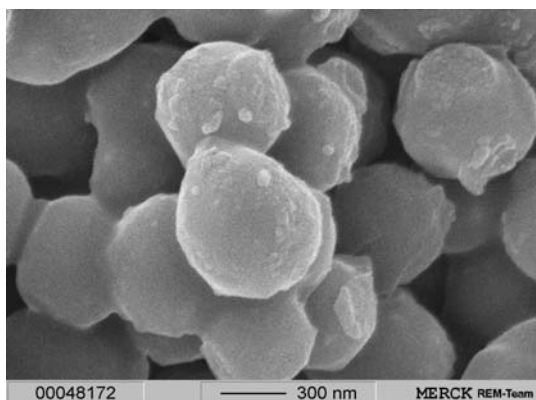


SEM image of **MS-250-3**



SEM image of **MS-250-4**

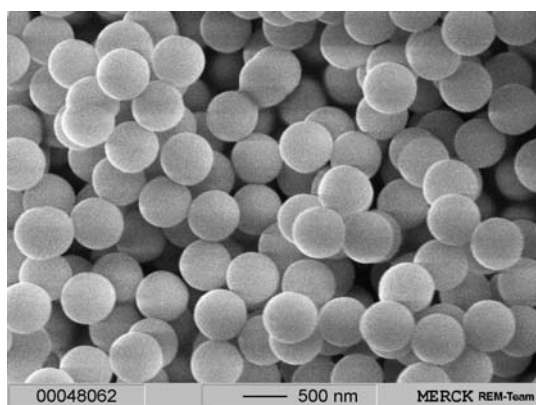


SEM image of **MS-250-5**

MS500

The procedure is identical to the synthesis of **MS250**, except that the reaction is heated to 30 °C instead of 60 °C. The product was washed using Washing Method B, yielding a white solid of 7.4 g. No starting material was recovered.

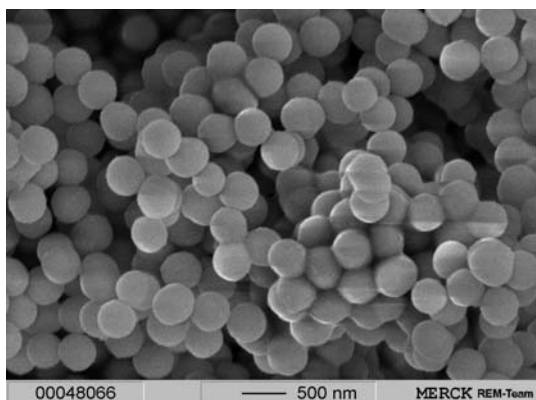
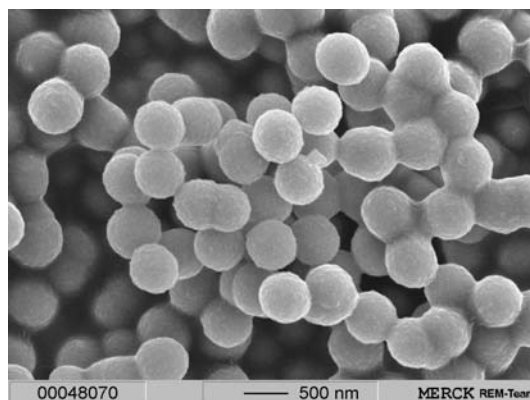
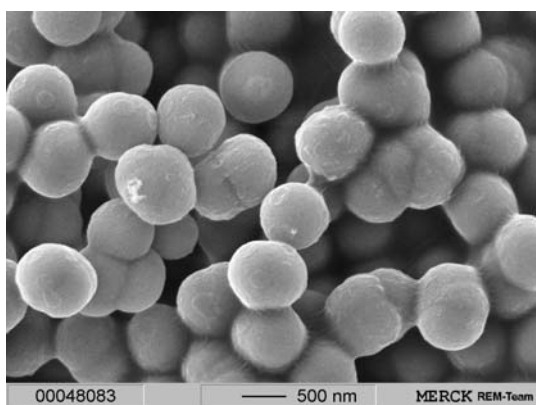
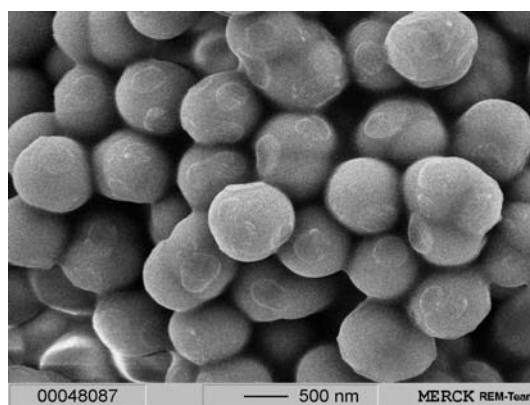
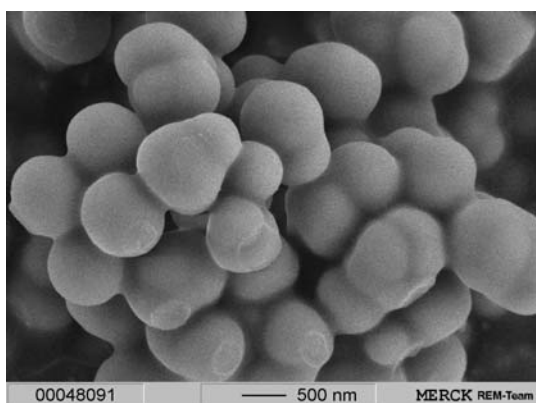
Elemental Analysis of solid found: C 4.3, H 2.2, Si 32.2.

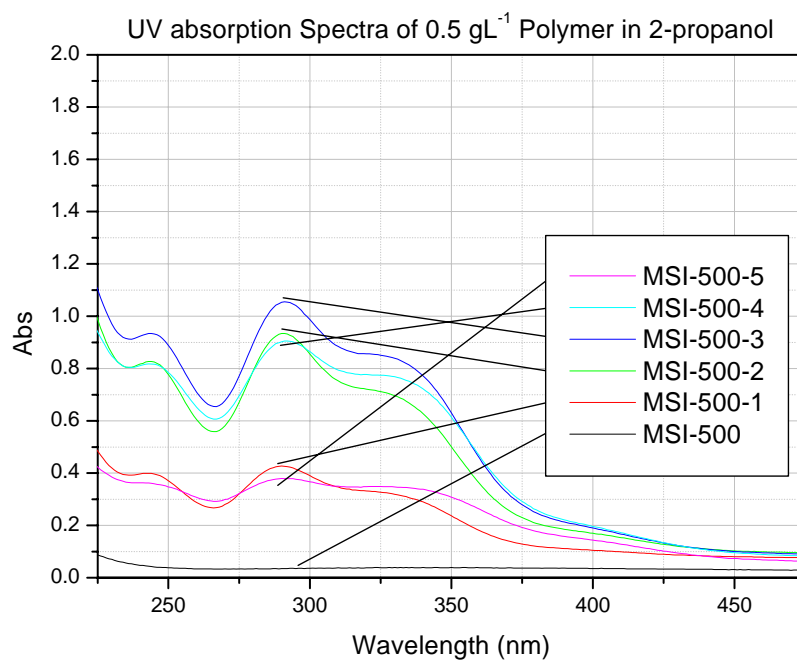
SEM image of MS-500**MSI-500-1 to MSI-500-5**

The procedure is identical to the synthesis of **MSI-250-1 to MSI-250-5**, except that the reactions are heated to 30 °C instead of 60 °C. The products were washed using Washing Method B. The yields of the reactions are tabulated below:

Reaction Number	MS recovered (g)	MS loading (mmol/g)	Extinction coefficient κ (Lg ⁻¹ cm ⁻¹)	Molar extinction coefficient ϵ (Lmol ⁻¹ cm ⁻¹)	C ^[a] (%)	H (%)	Si (%)
MSI-500-1	7.18	0.104	0.850	7989	5.5	2.2	38.6
MSI-500-2	7.35	0.213	1.864	8751	7.2	2.3	37.1
MSI-500-3	7.37	0.306	2.109	6881	7.9	2.3	37.0
MSI-500-4	7.56	0.391	1.810	4628	9.6	2.4	35.7
MSI-500-5	7.60	0.506	0.758	1499	11.0	2.5	35.6

^[a] Nitrogen content was not detectable. Oxygen content could not be reported due to SiO₂ formation.

SEM image of **MS-500-1**SEM image of **MS-500-2**SEM image of **MS-500-3**SEM image of **MS-500-4**SEM image of **MS-500-5**

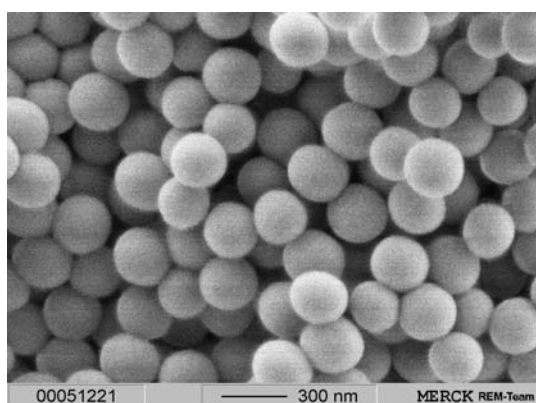
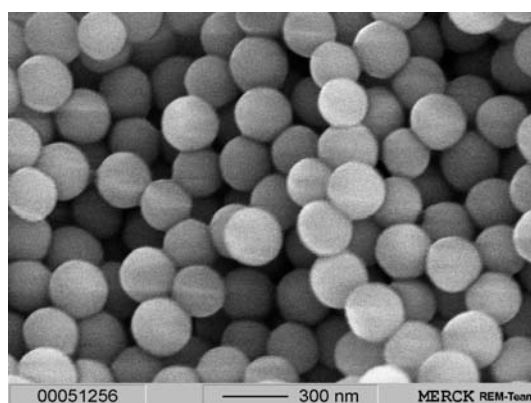
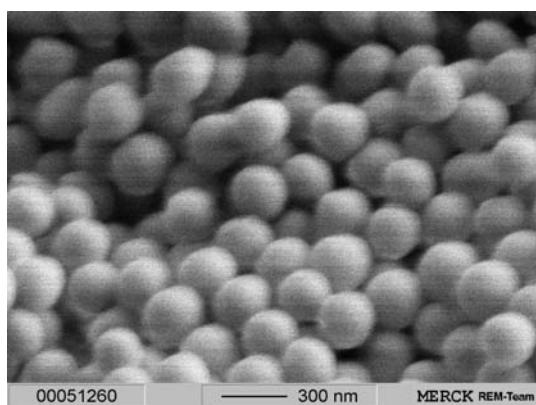
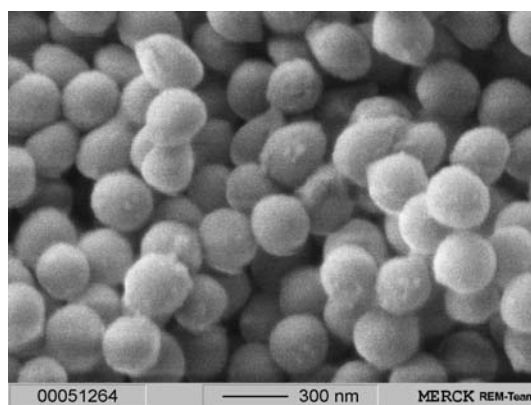
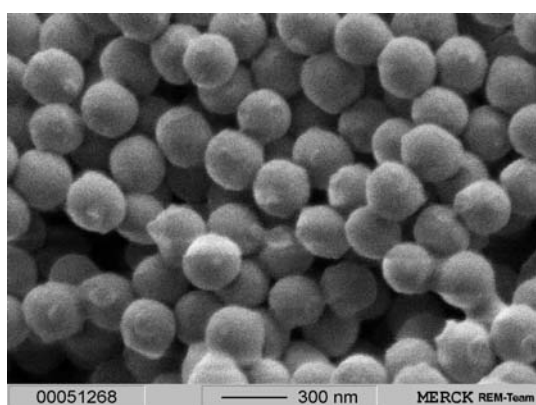
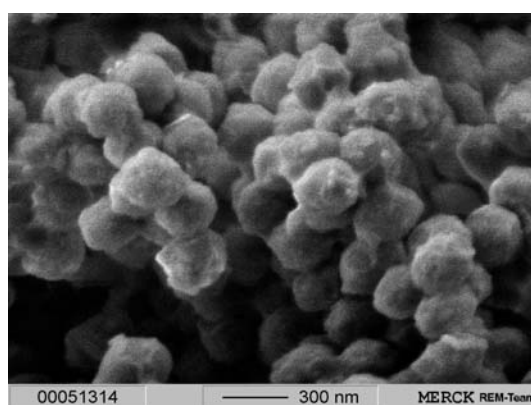


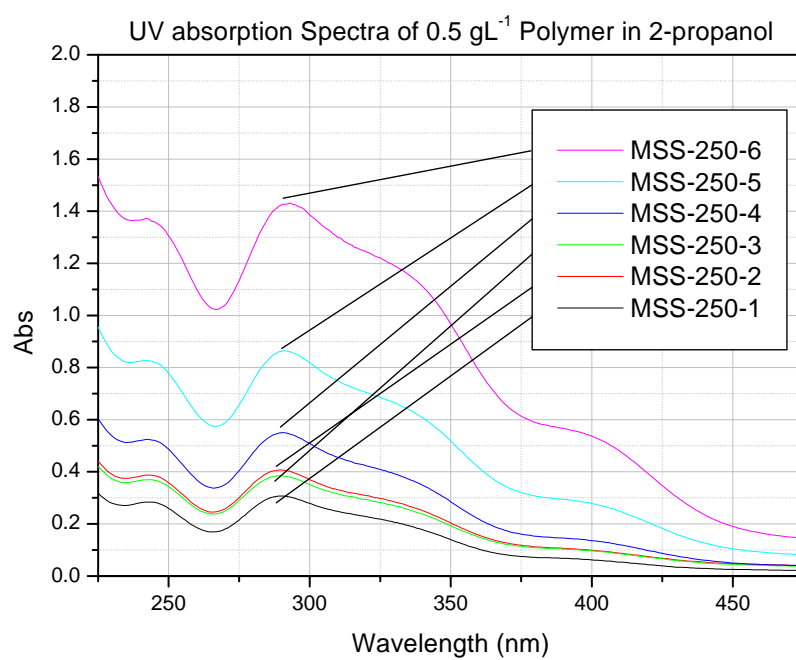
MSS-250-1 to MSS-250-6

Ethanol (150 ml, 2.6 mol) and deionised water (56 ml, 3.1 mol) were placed into a 500 ml 4 neck round and stirred using a mechanical stirrer (Teflon stirrer, 160 rpm) and heated to 60 °C in a water bath. Compound **1** (21.15 g, 101.5 mmol) was also heated to 60 °C (no stirring) in the same water bath (water bath temperature of 62 °C). Once the temperature of the ethanol-water azeotrope had reached a stable 60 °C, 25% ammonia solution (35 ml, 0.47 mol) was injected into the azeotrope (at the edge of the vessel) via a syringe. The stirring was increased (470 rpm) to ensure good mixing. Once the temperature of the mixture had reached 60 °C again, **1** was poured positively via a funnel into the azeotrope and allowed to stir for exactly 15 seconds. After 15 seconds the stirring was stopped and the reaction was allowed to stand at 60 °C (the reaction was slightly exothermic but the water bath temperature was kept at 62 °C) for 2 hours. After 2 hours the stirring (470 rpm) was restarted and the suspension was allowed to stir for 30 minutes. 2-hydroxy-4-(3-triethoxysilylpropoxy) diphenylketone **6** [0.425 g (1.0 mmol), 0.850 g (2.0 mmol), 1.275 g (3.1 mmol), 1.700 g (4.1 mmol), 2.125 g (5.1 mmol) and 4.249 g (10.2 mmol) for **MSS-250-1**, **MSS-250-2**, **MSS-250-3**, **MSS-250-4**, **MSS-250-5** and **MSS-250-6** respectively] was dissolved in 100 ml ethanol in a 100 ml pressure equalising funnel. The solution was added drop-wise into the stirring suspension over one hour. The suspension was allowed to stir for a further two hours at 60 °C. The product was washed using Washing Method B. A yield of 7.05 g of a fine solid was obtained for **MSS-250-1**. The yields of the remaining reactions are tabulated below:

Reaction Number	MS recovered (g)	MS loading (mmol/g)	Extinction coefficient κ (Lg ⁻¹ cm ⁻¹)	Molar extinction coefficient ϵ (Lmol ⁻¹ cm ⁻¹)	C ^[a] (%)	H (%)	Si (%)
MSS-250-1	7.05	0.046	0.610	13224	5.2	2.1	40.7
MSS-250-2	7.19	0.119	0.808	6795	6.6	2.2	40.3
MSS-250-3	7.33	0.216	0.764	3541	6.6	2.2	39.5
MSS-250-4	7.54	0.298	1.095	3676	8.1	2.3	39.4
MSS-250-5	7.70	0.407	1.725	4240	9.6	2.4	38.0
MSS-250-6	8.88	0.744	2.855	3835	13.7	2.7	35.9

^[a] Nitrogen content was not detectable. Oxygen content could not be reported due to SiO₂ formation.

SEM image of **MSS-250-1**SEM image of **MSS-250-2**SEM image of **MSS-250-3**SEM image of **MSS-250-4**SEM image of **MSS-250-5**SEM image of **MSS-250-6**

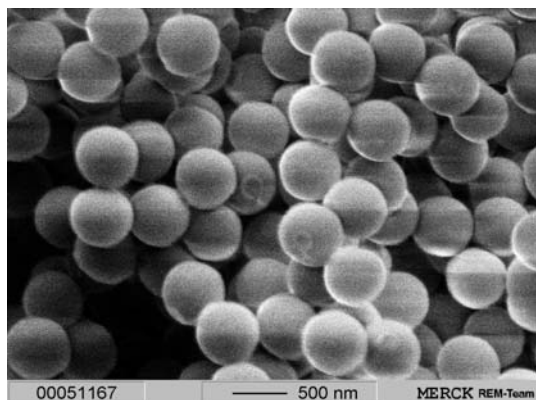
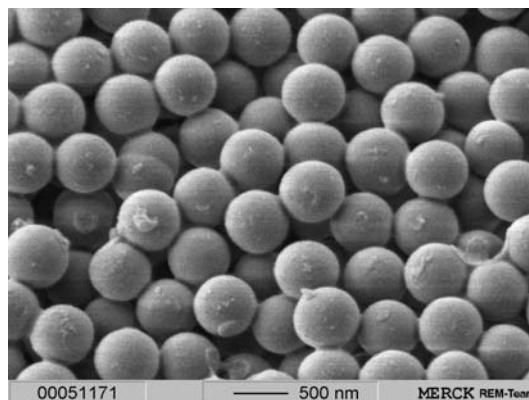


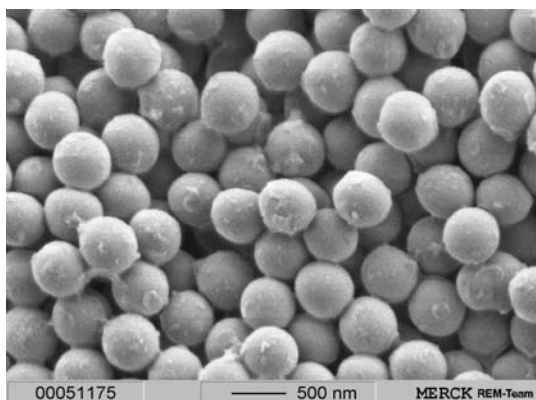
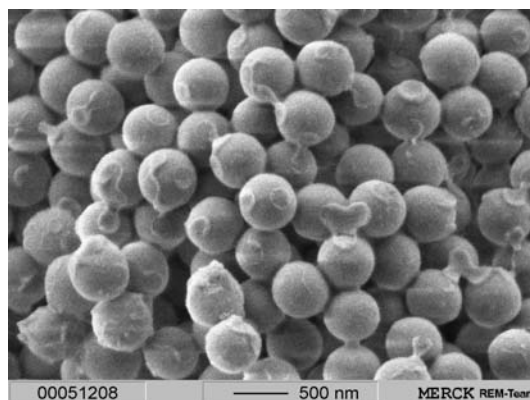
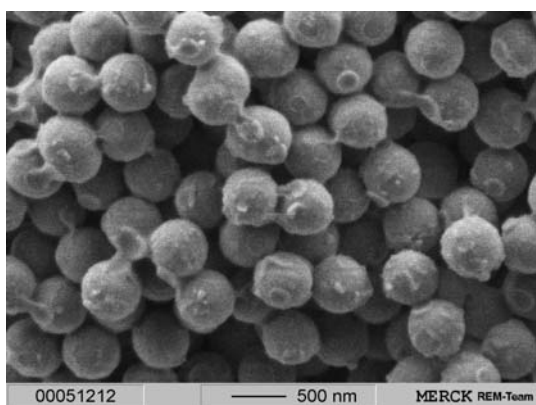
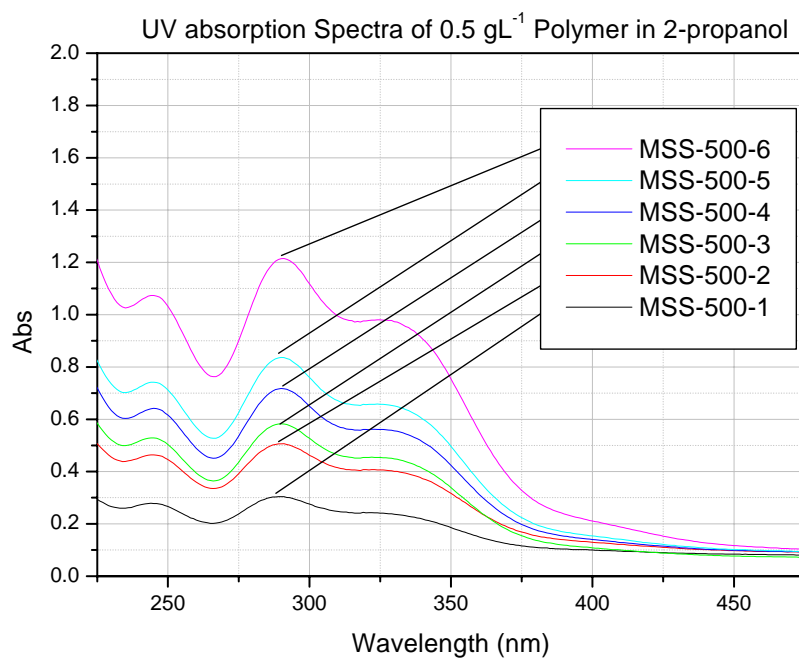
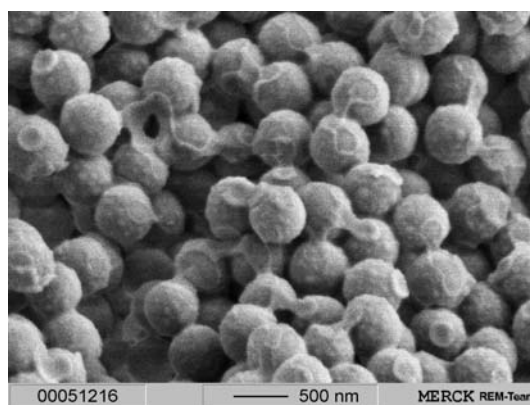
MSS-500-1 to MSS-500-6

The procedure is identical to the synthesis of **MSS-250-1** to **MSS-250-6**, except that the reactions are heated to 30 °C instead of 60 °C. The product was washed using Washing Method B. A yield of 7.35 g of a fine solid was obtained. The yields of the remaining reactions are tabulated below:

Reaction Number	MS recovered (g)	MS loading (mmol/g)	Extinction coefficient κ (Lg ⁻¹ cm ⁻¹)	Molar extinction coefficient ϵ (Lmol ⁻¹ cm ⁻¹)	C ^[a] (%)	H (%)	Si (%)
MSS-500-1	7.35	0.071	0.602	8538	6.0	2.4	39.3
MSS-500-2	7.45	0.141	1.009	7163	6.9	2.4	39.2
MSS-500-3	7.52	0.183	1.160	6349	7.3	2.4	38.9
MSS-500-4	7.68	0.237	1.429	6020	8.1	2.5	38.9
MSS-500-5	7.76	0.275	1.665	6062	9.1	2.6	38.3
MSS-500-6	8.38	0.512	2.425	4740	12.3	2.8	37.2

^[a] Nitrogen content was not detectable. Oxygen content could not be reported due to SiO₂ formation.

SEM image of **MSS-500-1**SEM image of **MSS-500-2**

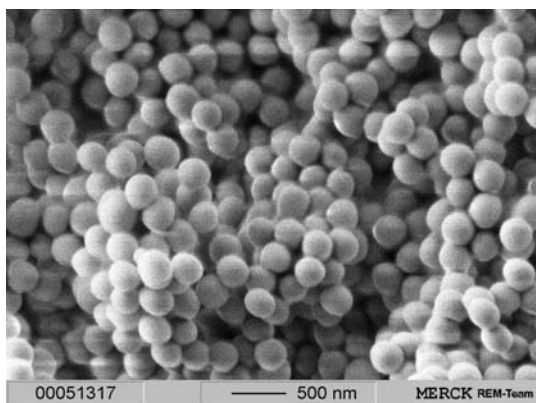
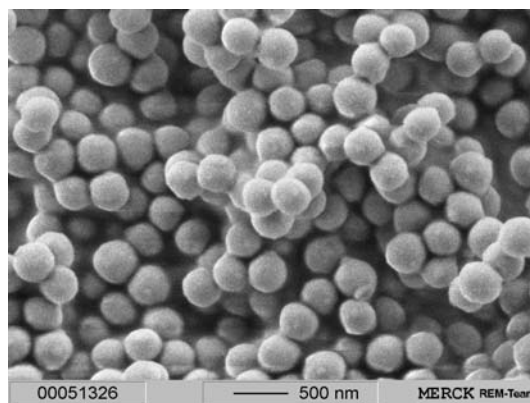
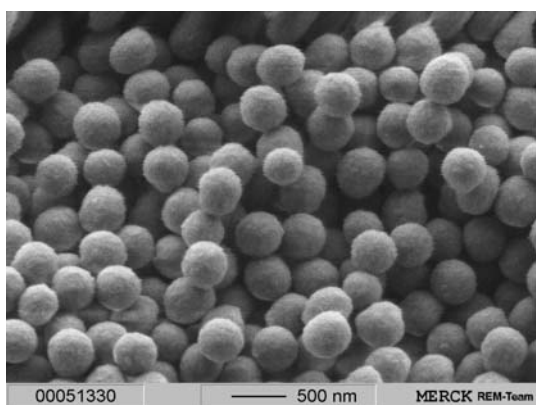
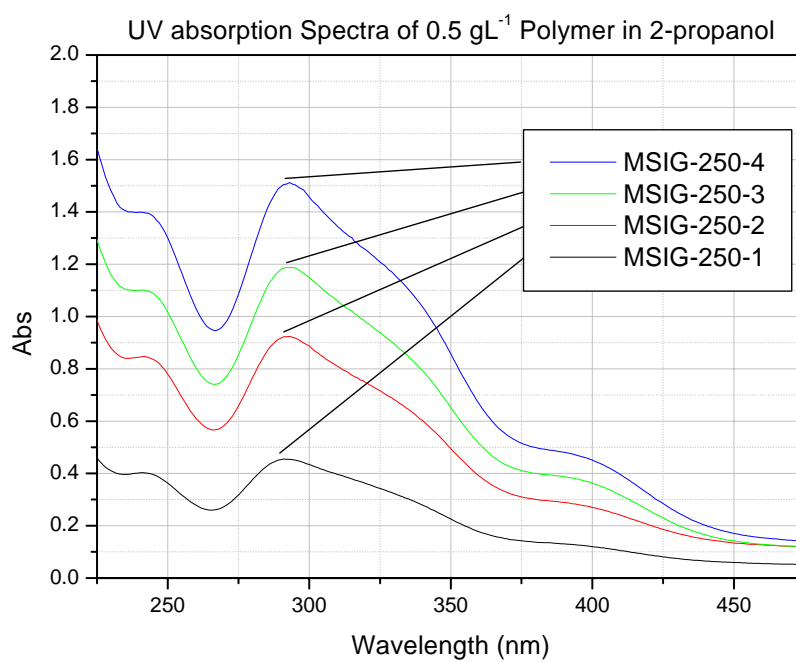
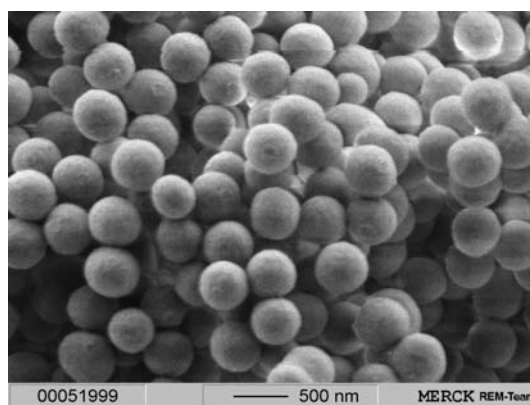
SEM image of **MSS-500-3**SEM image of **MSS-500-4**SEM image of **MSS-500-5**SEM image of **MSS-500-6**

MSIG-250-1 to MSIG-250-4

Ethanol (150 ml, 2.6 mol) and deionised water (56 ml, 3.1 mol) were placed into a 500 ml 4 neck round and stirred using a mechanical stirrer (Teflon stirrer, 160 rpm) and heated to 60 °C in a water bath. A mixture of **1** and **6** [for **MSIG-250-1** (100.5 mmol **1** and 1.0 mmol **6**), **MSIG-250-2** (99.5 mmol **1** and 2.0 mmol **6**), **MSIG-250-3** (98.4 mmol **1** and 3.1 mmol **6**) and **MSIG-250-4** (97.4 mmol **1** and 4.1 mmol **6**) respectively] was also heated to 60 °C (no stirring) in the same water bath (water bath temperature of 62 °C). Once the temperature of the ethanol-water azeotrope had reached a 60 °C, 25 % ammonia solution (35 ml, 0.47 mol) was injected into the azeotrope (at the edge of the vessel) via a syringe. The stirring was increased (470 rpm) to ensure good mixing. Once the temperature of the mixture had reached 60 °C again the mixture of **1** and **6** was poured positively via a funnel into the azeotrope and allowed to stir for exactly 15 seconds. After 15 seconds the stirring was stopped and the reaction was allowed to stand at 60 °C (the reaction was slightly exothermic but the water bath temperature was kept at 62 °C) for 2 hours. After 2 hours the stirring (470 rpm) was restarted. The suspension was allowed to stir for 2.5 hours at 60 °C. The product was washed using Washing Method B. A yield of 7.08 g of a fine solid was obtained for **MSIG-250-1**. The yields of the remaining reactions a tabulated below:

Reaction Number	MS recovered (g)	MS loading (mmol/g)	Extinction coefficient κ (Lg ⁻¹ cm ⁻¹)	Molar extinction coefficient ϵ (Lmol ⁻¹ cm ⁻¹)	C ^[a] (%)	H (%)	Si (%)
MSIG-250-1	7.08	0.020	0.909	46456	5.1	2.1	40.0
MSIG-250-2	7.23	0.184	1.847	10037	6.7	2.2	38.7
MSIG-250-3	7.47	0.294	2.376	8081	8.5	2.4	37.6
MSIG-250-4	7.63	0.389	3.014	7758	9.8	2.5	36.8

^[a] Nitrogen content was not detectable. Oxygen content could not be reported due to SiO₂ formation.

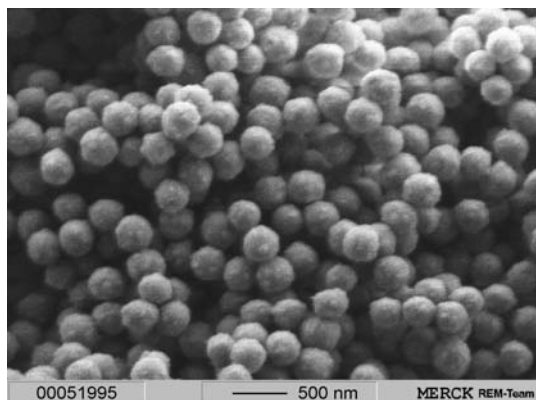
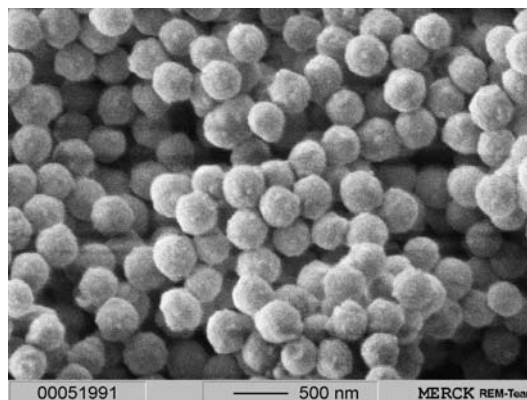
SEM image of **MSIG-250-1**SEM image of **MSIG-250-2**SEM image of **MSIG-250-3**SEM image of **MSIG-250-4**

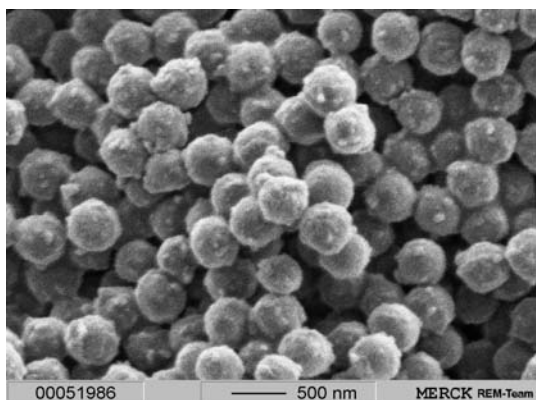
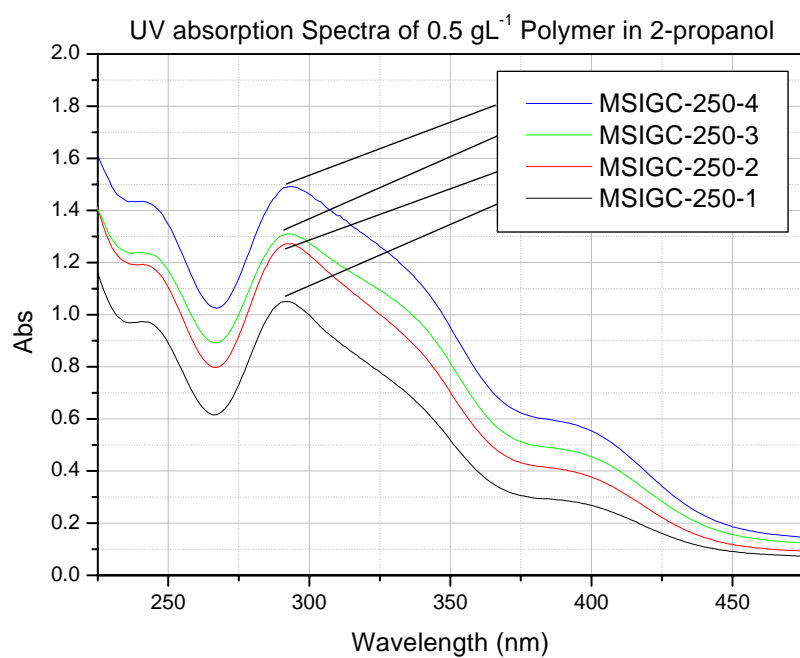
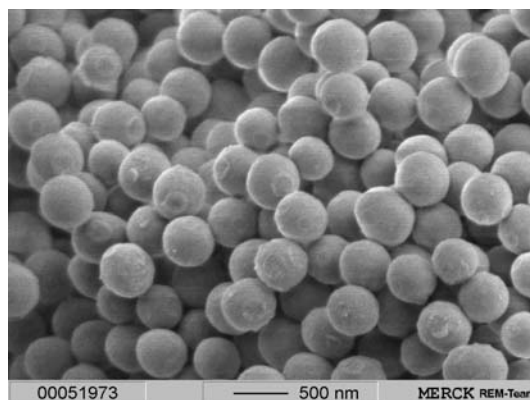
MSIGC-250-1 to MSIGC-250-4

The procedure is identical to the synthesis of **MSIG-250-1** to **MSIG-250-4**, except that on restarting the stirring for the second time, additional **6** (850 mg, 2 mmol) dissolved in 100 ml ethanol was added drop-wise into the stirring suspension over one hour. The suspension was allowed to stir for a further two hours at 60 °C. The product was washed using Washing Method B. A yield of 7.43 g of a fine solid was obtained for **MSIGC-250-1**. The yields of the remaining reactions are tabulated below:

Reaction Number	MS recovered (g)	MS loading (mmol/g)	Extinction coefficient κ (Lg ⁻¹ cm ⁻¹)	Molar extinction coefficient ϵ (Lmol ⁻¹ cm ⁻¹)	C ^[a] (%)	H (%)	Si (%)
MSIGC-250-1	7.43	0.269	2.102	7804	7.8	2.3	38.4
MSIGC-250-2	7.60	0.368	2.543	6912	8.5	2.4	37.2
MSIGC-250-3	7.82	0.456	2.619	5748	10.5	2.5	36.2
MSIGC-250-4	8.01	0.545	2.978	5469	11.0	2.6	35.6

^[a] Nitrogen content was not detectable. Oxygen content could not be reported due to SiO₂ formation.

SEM image of **MSIGC-250-1**SEM image of **MSIGC-250-2**

SEM image of **MSIGC-250-3**SEM image of **MSIGC-250-4**

3.5 References

- [1] Patini, G. *Drug Cosmet. Ind.* **1988**, 143, 43
- [2] Tavenrath, S. So wundervoll sonnengebräunt – Kleine Kulturgesichte des Sonnenbadens, Jonas, Marburg, **2000**, 77
- [3] Safer and more successful sun tanning, *Consumers Guide*, Wallaby Pocketbooks, New York, **1979**, 31
- [4] Kligman, A. M. *J. Invest. Dermatol.* **1966**, 47, 393
- [5] Groves, G. The Sunscreen Industry in Australia: Past, Present and Future. In *Sunscreens - Development, evaluation and regulatory aspects* (Lowe, N. J.; Shaath, N. A.; Pathak, M. A., ed.), Marcel Dekker, New York, **1997**, Chapter 13
- [6] Shaath, N. A. Evolution of Modern Sunscreen Chemicals. In *Sunscreens - Development, evaluation and regulatory aspects* (Lowe, N. J.; Shaath, N. A.; Pathak, M. A.; ed.), Marcel Dekker, New York, **1997**, Chapter 1
- [7] Lischka, G. *Therapiewoche* **1986**, 36, 2239
- [8] Chapman, R. S. *Photochem. Photobiol.* **1995**, 61, 223
- [9] Setlow, R. B. *Proc. Natl. Acad. Sci. USA*, **1993**, 90, 6666
- [10] Seite, S.; Moyal, D.; Richard, S.; de Rigal, J.; Leveque, J. L.; Hourseau, C.; Fourtanier, A. *J. Photochem. Photobiol.; B: Biol.* **1998**, 44, 69
- [11] Fourtanier, A.; Labat-Robert, J.; Kern, P.; Berrebi, C.; Gracia, A. M.; Boyer, B. *Photochem. Photobiol.* **1992**, 55, 549
- [12] Wlaschek, M. *J. Invest. Dermatol.* **1993**, 101, 164
- [13] Aghazarian, V.; Tchiakpe, L.; Reynier, J. P.; Gayte-Sorbier, A. *Drug Dev. Ind. Pharm.* **1999**, 25, 1277
- [14] Schrader, K. *Parf. Kosm.* **1995**, 7, 411
- [15] Osterwalder, U.; Luther, H.; Herzog, B. *SÖFW Journal* **2001**, 127(7), 45
- [16] Taylor, C. R.; Stern, R. S.; Leyden, J. J.; Gilchrest, B. A. *J. Am. Acad. Dermatol.* **1990**, 22, 1
- [17] Scharfetter-Kochanek, K.; Wenk, J.; Brenneisen, B.; Blaudschrun, R.; Wlaschek M. Molecular role of reactive oxygen species in photoaging and tumour progression. In *Skin cancer and radiation* (Altmeyer, P. et al. ed.), Springer, Heidelberg, **1997**, 115
- [18] Ziegler, A.; Jonason, A. S.; Leffeli, D. J. *Nature* **1994**, 372, 773
- [19] Ananthaswamy, H. N.; Laughlin, S. M.; Cox, P.; Evans, R. L.; Ullrich, S. E.; Kripke, M. L. *Nat. Med.* **1997**, 3, 510

-
- [20] Schlumpf, M.; Berger, L.; Cotton, B.; Conscience-Egli, M.; Durrer, S.; Fleischmann, I.; Haller, V.; Maerker, K.; Lichtensteiger, W. *SÖFW Journal* **2001**, 127(7), 10
- [21] Watkinson, A. C.; Brian, K. R.; Walters, K. A.; Hadgraft, J. *Int. J. Cos. Sci.* **1992**, 14, 265
- [22] When a UV filter molecule such as for example a cinnamate derivative is excited the UV radiation is converted into photochemical energy which allows for an equilibrium between the *cis* and *trans* isomers which absorb at more or less the same wavelength.[Schrader, A.; Jakupovic, J.; Baltes, W. *J. Soc. Cosm. Chem.* **1994**, 1, 43] Schrader also showed that with time, the UV filter undergoes UV-induced decomposition into smaller molecular products which can penetrate the skin.[Schrader, A. *SÖFW Journal* **1997**, 123(8), 503] In order to reduce such effects, the maximum sun protection factor (SPF) is required from the minimum amount of UV filter. This can be achieved by varying the formulation of sunscreens. It has been widely demonstrated that transdermal penetration into the skin,[Marginean Lazar G.; Braillet, A.; Fructus, A. E.; Arnaud-Battandier, J.; Ferrier, D.; Marty, J. P. *Drug Cosmet. Ind.* **1996**, 158, 50; Walters, K. A.; Brian, K. R.; Howes, D.; James, V. J.; Kraus, A. L.; Teetsel, N. M.; Toulon, M.; Watkinson, A. C.; Gettings, S. D. *Food Chem. Toxicol.* **1997**, 35, 1219] permeation through the skin[Jiang, R.; Roberts, M. S.; Collins, D. M.; Benson, H. A. E. *Br. J. Clin. Pharmacol.* **1999**, 48, 635] and retention of UV filters in the skin [Treffel, P.; Gabard, B. *Pharm. Res.* **1996**, 13(5), 770] from topical sunscreen products can differ significantly between formulations used.[Chatelain, E.; Gabard, B.; Surber, C. *Skin Pharmacol. Appl. Skin Physiol.* **2003**, 16, 28]
- [23] Hany, J.; Nagel, R. *Deutsche Lebensmittel-Rundschau* **1997**, 91, 341
- [24] Hayden, C. G.; Roberts, M. S.; Benson, H. A. *Lancet* **1997**, 350, 863
- [25] Schlumpf, M.; Berger, L.; Cotton, B.; Conscience, M.; Haller, V.; Steinmann, B.; Lichtensteiger, W. *Environ. Health Perspect.* **2001**, 109, 293
- [26] Schlumpf, M.; Berger, L.; Cotton, B.; Conscience-Egli, M.; Durrer, S.; Fleischmann, I.; Haller, V.; Maerker, K.; Lichtensteiger, W. *SÖFW Journal*, **2001**, 127(7), 10
- [27] Mitchnik, M. *Drug & Cosmetic Industry* **1993**, 153(2), 38
- [28] Raab, W. *Apotheker J.* **1994**, 1, 14
- [29] Robb, J. L. *Drug & Cosmetic Industry* **1994**, 154(3), 32

-
- [30] Anderson, M. W.; Hewitt, J. P.; Spruce, S. R. Broad-Spectrum Physical Sunscreens. In *Sunscreens - Development, evaluation and regulatory aspects* (Lowe, N. J.; Shaath, N. A. and Pathak, M. A, ed.), Marcel Dekker, New York, **1997**, Chapter 18
- [31] Judin, V. P. S. *Chem. Brit.* **1993**, 6, 503
- [32] Kerker, M. *The Scattering of Light and Other Electromagnetic Radiation*, Academic Press, New York, **1969**
- [33] Tichy, S. *SÖFW Journal* **1992**, 188, 612
- [34] Judin, V. P. S.; Salonen, V. T. *SÖFW Journal*, **1993**, 199, 491
- [35] Müller-Goymann, C. C.; Bennat, C.; Grünefeld, J. *Parfümerie und Kosmetik* **1998**, 5, 24
- [36] Bennat, C.; Müller-Goymann, C. C. *Int. J. Cos. Sci.* **2000**, 22, 271
- [37] Pfluecker, F.; Hohenberg, H.; Hölzle, E.; Will, T.; Pfeiffer, S.; Wepf, R.; Diembeck, W.; Wenck, H.; Gers-Barlag, H. *Int. J. Cos. Sci.* **1999**, 21, 399
- [38] Scholz, V.; Neunhoeffler, H.; Driller, H.; Witte, G.; Pfluecker, F. *SÖFW Journal* **2001**, 127(4), 3
- [39] Osterwalder, U.; Luther, H.; Herzog, B. 47 SEPAWA Congress **2000**, Proceedings 153; Luther H.; *PCT Int. Appl.* **2000**, WO 2000078277
- [40] Fujioka, K. *Fragrance Journal* **2002**, 30(7), 51
- [41] Frater, G.; Schwarzenbach, R.; Van Oycke, S. F. M. *PCT Int. Appl.* **1992**, WO 9220690
- [42] Pfluecker, F.; Driller, H.; Vouzellaud, L.; Marchio, F.; Guinard, H.; Chaudhuri, R. K. *PCT Int. Appl.* **2003**, WO 2003011239. In this invention it is claimed that all known organic UV filters can be encapsulated by silica capsules obtained from the sol-gel process as is described in the patents WO 00/09652, WO 00/72806 and WO 00/71084
- [43] Pfluecker, F.; Anselmann, R.; Kirschbaum, M.; Buchholz, H.; Driller, H. *Eur. Pat. Appl.* **2002**, EP 1205177
- [44] Buchholz, H.; Poetsch, E.; Pfluecker, F.; Anselmann, A.; Roskopf, R.; Kirschbaum, M. *Eur. Pat. App.* **2002**, EP 1205178
- [45] MS with chromophores on their surface have been patented by Merck KGaA. [Pfluecker, F.; Anselmann, R.; Kirschbaum, M.; Buchholz, H.; Driller, H. *Eur. Pat. Appl.* **2002**, EP 1205177; Buchholz, H.; Poetsch, E.; Pfluecker, F.; Anselmann, A.; Roskopf, R.; Kirschbaum, M. *Eur. Pat. App.* **2002**, EP 1205178]

-
- [46] Chernyshev, E. A, Belyakova, Z. V.; Knyazeva, L. K.; Pomerantseva, M. G. and Efimova, L. A.; *Russian Chem. Bull.* **1998** 47, 1374
- [47] Ashby et al. *US Patent*, **1981**, 4,278,804
- [48] Gellermann, C.; Storch, W.; Wolter, H. *J. Sol-Gel Sci. & Tech.* **1997**, 8, 173
- [49] Lowe, N. J.; Friedlander J. Sunscreens: Rationale for Use to Reduce Photodamage. In *Sunscreens - Development, evaluation and regulatory aspects* (Lowe, N. J.; Shaath, N. A.; Pathak, M. A, ed.), Marcel Dekker, New York, **1997**, Chapter 2
- [50] Roberts J. *Management of Wilderness and Environmental Emergencies* (Auerbach, P. ed.), Mosby, St. Louis, **1989**
- [51] Berset, G.; Gonzenbach, H.; Christ, R.; Martin, R.; Deflandre, A.; Mascotto, R. E.; Jolley, J. D. R.; Lowell, W.; Pelzer, R.; Stiehm, T. *Int. J. Cos. Sci.* **1996**, 18, 167
- [52] Suratwala, T.; Gardlund, Z.; Davidson, K.; Uhlmann, D. R.; Bonilla, S.; Peyghambarian, N. *J. Sol-Gel. Sci. Tech.* **1997**, 8, 973
- [53] Fairhurst, D.; Mitchnick M. Particulate Sun Blocks: General Principles. In *Sunscreens - Development, evaluation and regulatory aspects* (Lowe, N. J.; Shaath, N. A.; Pathak, M. A, ed.), Marcel Dekker, New York, **1997**, Chapter 17
- [54] Matsumoto, N.; Takeda, K.; Teramae, H.; Fujino M. In *Silicon-Based Polymer Science* (Zeigler, J. M.; Fearon, F. W. G. ed.), ACS, Washington, **1990**, 515
- [55] Hünig, S.; Märkl, G.; Sauer, J. *Einführung in die apparativen Methoden in der Organischen Chemie*, 2nd Edition, Würzburg, Regensburg, **1994**
- [56] Author Collective, *Organikum*, 17th Edition, VEB Deutscher Verlag der Wissenschaften, Berlin, **1988**

4. Chromone derivatives which bind to human hair⁴

Abstract:

Chromone derivatives bearing a quaternary ammonium functionality which bind to human hair were synthesised. The radical scavenging activity, according to the DPPH assay, of the chromone derivatives is considerably lower compared with flavonoids. The compounds show interesting UV absorption properties that depend on the position of a methoxy substituent. A bathochromic shift of 29 nm was observed when the methoxy group on the ammonium salts were shifted from position 7 to position 6.

⁴ The results of this chapter have been patented :

Walencyk, T.; Carola, C.; Rosskopf, R.; Buchholz, H. Chromone derivatives which bind to hair. *Germ. Pat. Appl.* **2005**, DE 102005011534.9

The results of this chapter are submitted for publication :

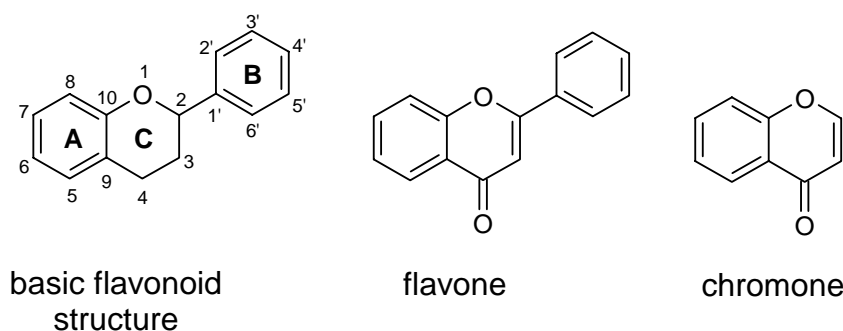
Walencyk, T.; Carola, C.; Buchholz, B.; Koenig, B. *Tetrahedron* **2005**, submitted

4.1 Introduction

4.1.1 Chromones

Chromones are a group of naturally occurring compounds that are ubiquitous in nature especially in plants.^[1] They are oxygen-containing heterocyclic compounds with a benzoannulated γ -pyrone ring, with the parent compound being chromone (4*H*-chromen-4-one, 4*H*-1-benzopyran-4-one).^[2,3] Molecules containing the chromone structure (for example chromones and flavonoids) have a wide range of biological activities including tyrosine and protein kinase C inhibitors, antifungal, antiallergenic, antiviral, antitubulin, antihypertensive and anticancer agents, as well being active at benzoazepine receptors, lipoxygenase, cyclooxygenase and modulating P-glycoprotein-mediated multidrug resistance (MDR).^[2-6] Due to their abundance in plants and their low mammalian toxicity, chromone derivatives are present in large amounts in the diet of humans.^[7,8]

Figure 1. Basic structure of flavonoids, flavones and chromones



4.1.2 Biological Activity of Flavonoids

Many of these biological actions are attributed to the ability of flavonoids to transfer electrons, chelate metal catalysts,^[9] activate antioxidant enzymes,^[10] reduce α -tocopherol radicals,^[11] inhibit oxidases^[12] as well as through their possible influences on the intracellular redox status, however the precise mechanisms remain unclear.^[13] Recent studies have speculated that the classical hydrogen-donating antioxidant activity of flavonoids^[14-16] is unlikely to be the sole explanation for cellular effects.^[17-19] The bioactive forms of flavonoids *in vivo* are not those found in plants but rather conjugates and metabolites arising from these on intestinal absorption.^[20-24]

4.1.3 Structure Activity Relationships

The relationship between the radical scavenging activity of flavonoid derivatives and their structure has been studied in depth.^[5,25-28] In general, the radical scavenging activity depends on the number and location of hydroxyl groups. This determines the availability of phenolic hydrogens and the possibility of stabilisation of the resulting phenoxyl radicals *via* electron delocalisation or hydrogen bonding.^[15,28,29]

4.1.4 Reactive Oxygen Species

By definition a free radical is any atom with at least one unpaired electron in the outermost shell.^[30] Oxygen acts as the terminal electron acceptor within the electron transport system that produces energy in the form of adenosine triphosphate (ATP).^[31] Oxygen-centred free radicals or reactive oxygen species (ROS) are formed when the electron flow becomes uncoupled (transfer of unpaired single electrons).^[26] ROS are capable of oxidising cellular proteins, nucleic acids and lipids, and contribute to cellular aging,^[32] mutagenesis,^[33] carcinogenesis,^[34] coronary heart disease,^[35] inflammation^[36] and brain dysfunction.^[37] Such oxidations can be terminated by enzymatic means or by free radical scavenging of antioxidants.^[38]

4.1.5 Multifunctional Chromones

The antioxidant characteristics of flavonoids in combination with their favourable UV absorption properties are also exploited by plants to protect them from the sun's UV radiation and scavenge UV-generated ROS.^[39] For example, there is evidence that flavonoids in leaves, deposited in either the epidermal cells or in the waxy upper leaf surface provide protection from the potential damage of UVB radiation.^[40] This use could also be utilised in the protection of human hair from UV-radiation. It is well known that exposure to UV-radiation can damage hair fibres. UVB radiation is the principal radiation responsible for hair protein loss (causing dryness, reduced strength, rough surface texture, decreased luster, stiffness and brittleness). UVA radiation is responsible for colour changes regardless of hair type.^[41] Hair melanins provide some photochemical protection to hair proteins, especially at lower wavelengths where both the hair pigments and proteins absorb radiation.^[42] These melanins also immobilise many of the free radicals generated by

UV-radiation, however in the process they are often degraded or bleached.^[43] The aim of this project is to synthesise a chromone derivative, bearing a cationic functionality which binds to human hair.

4.2 Results and discussion

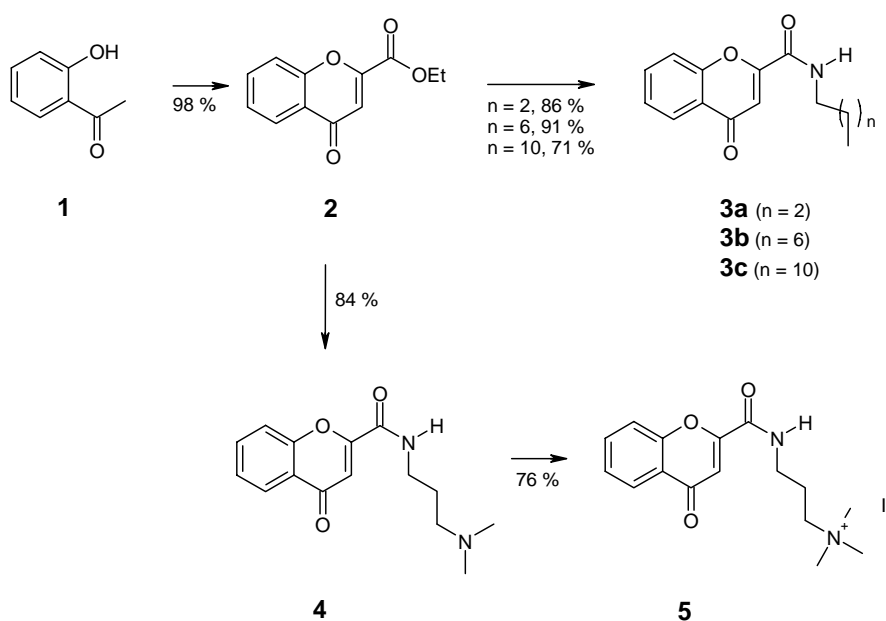
4.2.1 Background

As the structural features of chromones largely influence their biological activity, the position of further functionalisation is critical. The B-ring of flavanone is not present in chromone and thus is an ideal position to further functionalise without influencing the structural effects of the other groups the chromone skeleton.

Quaternary ammonium compounds (cationic surfactants, cationic polyelectrolytes and cationic quaternary derivatives of hydrolyzed proteins) have been widely used as hair conditioning agents.^[44] The deposition (substantivity) of such compounds can effect the hair fibre friction, stiffness, gloss, anti-static qualities and strength of hair.^[42] By synthesising a chromone derivative with a quaternary ammonium functionality it was hoped that this compound would show not only biological activity but also hair substantivity.

4.2.2 Synthesis of Chromone Derivatives with Hair Substantivity

The synthetic strategy chosen for the preparation of the 2-amido-chromone required the preparation of 2-ethylester-chromone **2**. Condensation of **1** with diethyl oxalate in the presence of sodium ethanoxide in ethanol and followed by acidic cyclisation afforded the ester **2**.^[6,45] By reacting different amines with **2**, a variety of chromone amides were synthesised (Scheme 1).

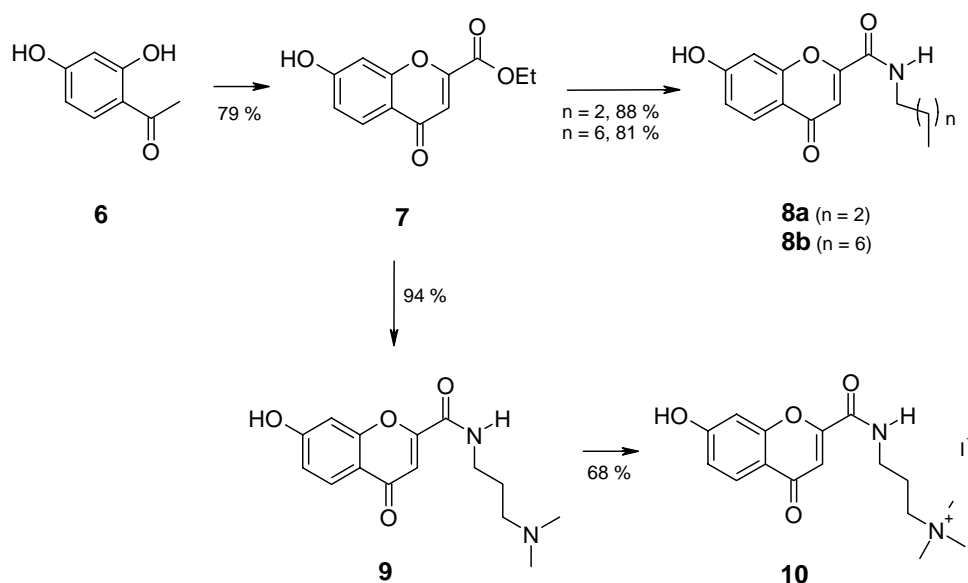
Scheme 1. General synthesis of unsubstituted 2-amido chromones

Reacting the ester **2** with either an n-alkyl amine (butylamine, octylamine, dodecylamine) or 3-dimethylaminopropylamine gave the amides **3** and **4**, respectively. Treatment of the latter with methyl iodide gave the trimethyl ammonium salt **5**.

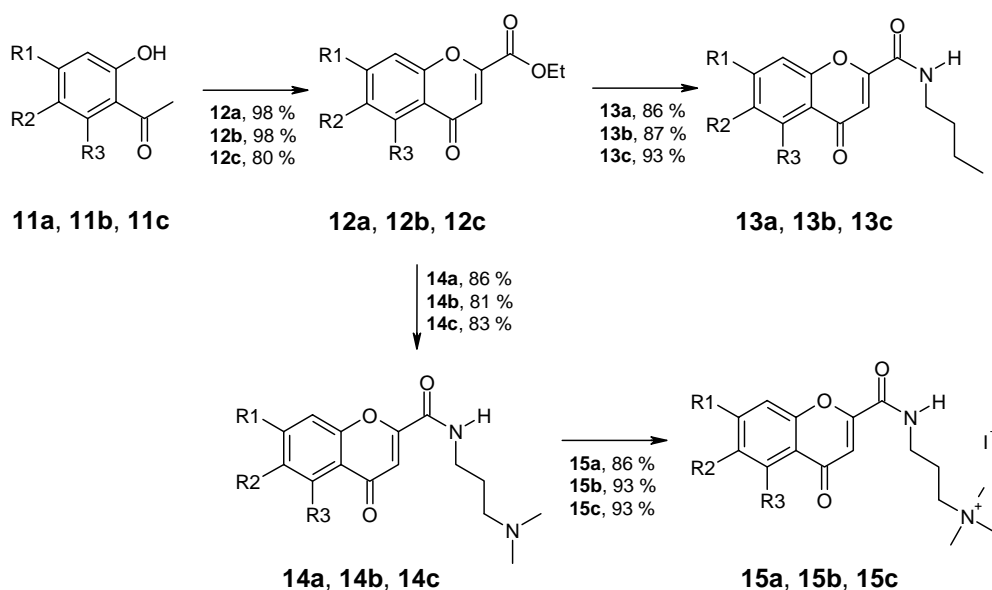
Although numerous other methods exist for introducing a new functionality at the C-2 position of chromone,^[4,5,46-49] the chosen synthetic route is short, has two possibilities for introducing diversity needed to generate a small library and utilises cheap reagents which is an important factor for industrial applications.

4.2.3 Synthesis of substituted chromone derivatives

In order to increase the biological activity of **3** and **5**, the 7-hydroxy-4-oxo-4H-chromene-2-carboxylic acid ethyl ester was synthesised. Due to the formation of a zwitterion in compound **9** this synthetic route was not expanded for other hydroxy-4-oxo-4H-chromene-2-carboxylic acid ethyl esters with other substitution patterns. The zwitterion was stable over a wide pH range and could not be extracted from aqueous media. By protecting the phenol with a suitable protecting group, the amine could then be extracted in acid media. The protecting group chosen was methoxy as methoxy acetophenones are cheap and commercially available.

Scheme 2. General synthesis of hydroxyl substituted 2-amido chromones

Thus, the methoxy derivatives **12** were synthesised (Scheme 3). Although in general hydroxyl groups give a better radical scavenging activity,^[26] there are some examples where a hydroxyl group is deleterious and methoxy group beneficial to biological activity.^[5,50] Compound **12** was prepared from the commercially available **11**. The methoxy derivatives **14** could now be easily synthesised and purified without fear of zwitterion formation.

Scheme 3. General synthesis of methoxy substituted 2-amido chromones

for **11a** - **15a** ($R1 = \text{OCH}_3$, $R2 = \text{H}$, $R3 = \text{H}$)

for **11b** - **15b** ($R1 = \text{H}$, $R2 = \text{OCH}_3$, $R3 = \text{H}$)

for **11c** - **15c** ($R1 = \text{H}$, $R2 = \text{H}$, $R3 = \text{OCH}_3$)

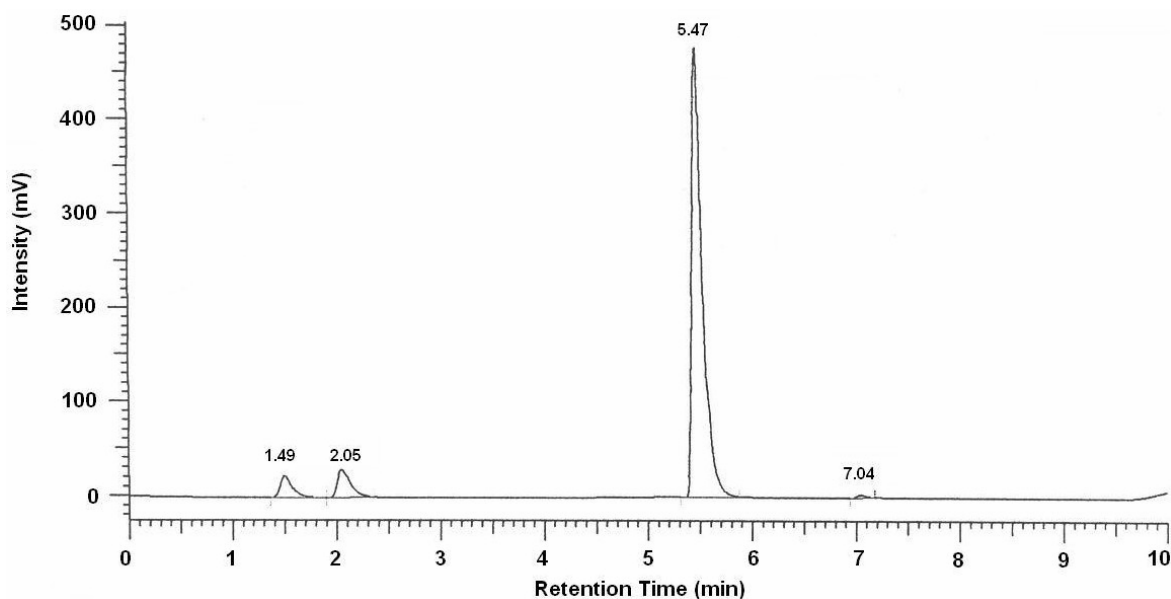
Numerous attempts with various conditions at O-demethylating **14a-c** failed.^[51,52,53,54] Alternative protecting groups that can withstand the reaction conditions and are industrially feasible need to be examined in order to readily synthesise hydroxyl derivatives.

4.2.4 Hair Substantivity

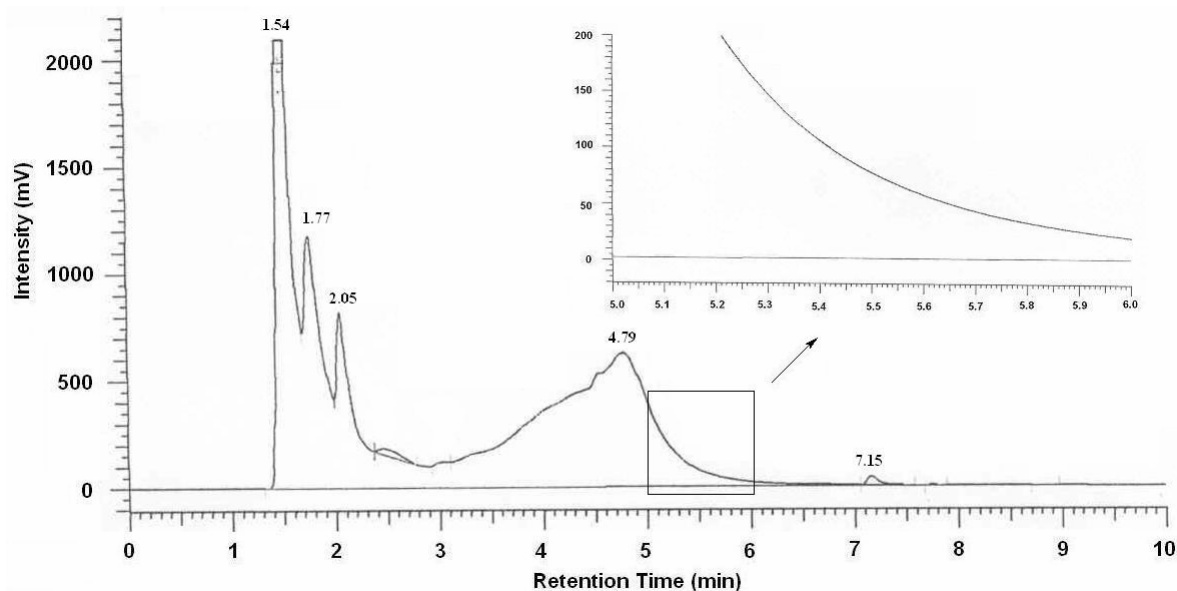
Compounds **2**, **3**, and **5** served as models for hair binding assay. Although there are various methods to measure the substantivity of cationic species to hair,^[44,55] many are complicated, require specialised instrumentation and are time-consuming. As many compounds contained in cosmetic products including cationic surfactants^[56] and dyes^[57] can penetrate into hair fibres, it is important to choose an analytical method which can quantitatively recover the analyte.

Although a number of methods for hair substantivity were tested,^[58] only two (MALDI-MS^[59] and hair digestion followed by HPLC analysis) could confirm the presence of compound bound to hair. The practicality of HPLC analysis and the large number of samples made the HPLC method very feasible. The compound was dissolved in a 70:30 ethanol:water mixture, to which then sterile, washed hair was added and allowed to stir for one hour. The hair was then thoroughly washed with water and air dried. A sample of this 'treated' hair was dissolved in sodium hydroxide solution at 60 °C and then analysed via HPLC. This method^[60] which was adapted from an analytical procedure used for the detection of anabolic steroids in livestock has the advantage that even small amounts of compounds can be quantitatively recovered.

Figure 2 shows the chromatogram of **2** after having been subjected to the same conditions used in the hair substantivity test but without coming in contact with any hair. The main peak at 5.47 min corresponds to the carboxylic acid, 4-Oxo-4H-chromene-2-carboxylic acid which is generated under the strong basic conditions. In the absence of such harsh conditions **2** has a retention time of 2.04 min (a residual peak is still visible).

Figure 2. Chromatogram of **2** after being subjected to strong basic conditions (digestion)

Digested blonde human hair was taken as a reference showing characteristic peaks at 1.54 min, 1.77 min, 2.05 min and 4.79 min (see Figure 3). The reference does not contain, nor is contaminated with, any 4-Oxo-4H-chromene-2-carboxylic acid (no peak is visible between 5 min and 6 min).

Figure 3. Chromatogram of digested blonde hair

Digested hair which had previously been stirred with **2** and then washed thoroughly, showed a peak at 5.47 min in addition to the characteristic peaks of digested hair (Figure 4). On spiking this sample with a small amount of the digested product of **2**, the

peak at 5.47 min increased in intensity (and no new peaks are visible) confirming that **2** binds to human hair (Figure 5).

Figure 4. Chromatogram of digested blonde hair after being treated with **2**

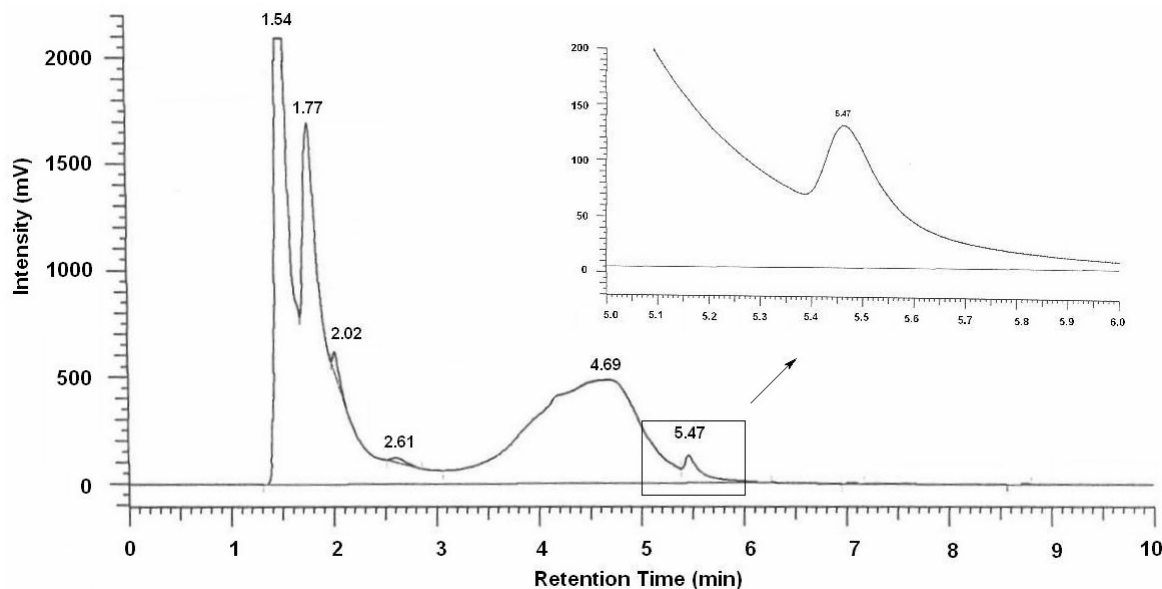
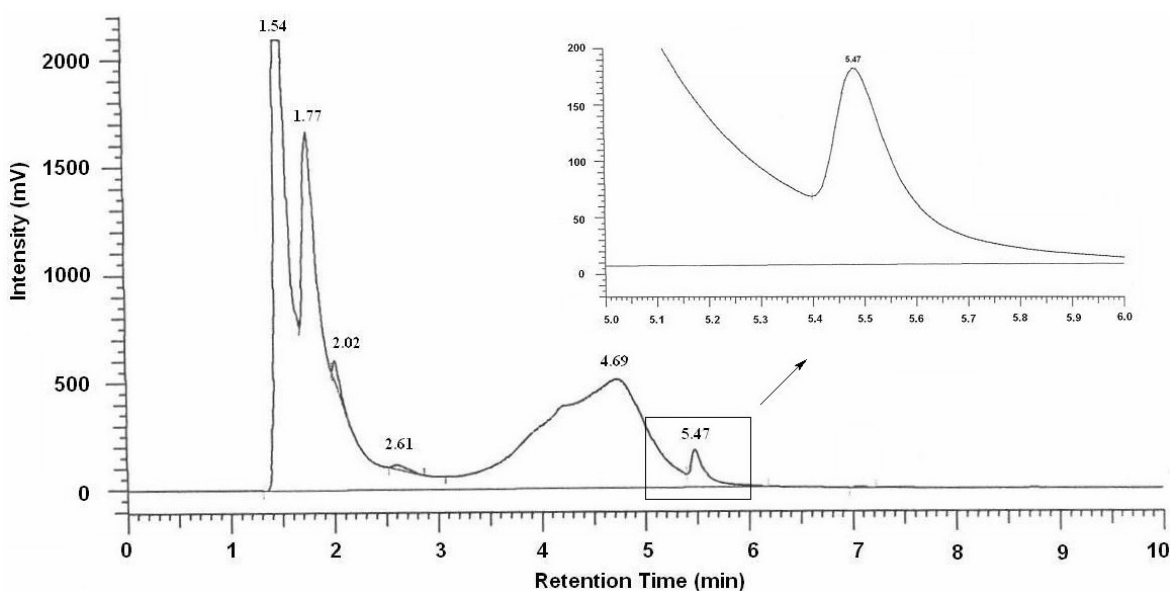


Figure 5. Chromatogram of digested blonde hair after being treated with **2** (spiked with digested **2**)



In addition to **2**, a number of other compounds were tested for their hair substantivity (Table 1). Tests were carried out on both bleached human hair and on brown human hair. The hair substantivity effect of all tested compounds was independent of hair type.

Table 1. Hair substantivity of chromones

Compound	Hair Substantivity
2	None
3a	None
3b	Possible
3c	- ^a
8b	Possible
5	Yes
15a	Yes
15b	Yes
15c	Yes

a) could not be tested to due solubility problems

The results show that compounds bearing a quaternary ammonium salt bind well to hair. An ester or butyl amide failed to show any binding. There is some evidence to show that an octyl amide functionality may bind to hair, however due to their poor solubility in ethanol/water mixtures, definite binding could not be confirmed. However the use of long alkyl chains in hair care products suggests that some interactions must take place.

4.2.4.1 SEM Images of treated and untreated hair

Scanning electron microscopy (SEM) images of treated and untreated hair were compared to assess if the treatment of hair with such compounds causes a visible change in the hair surface. Figure 6 and 7 shows SEM images of untreated hair and hair treated with **2** respectively. As to be expected no differences could be seen.

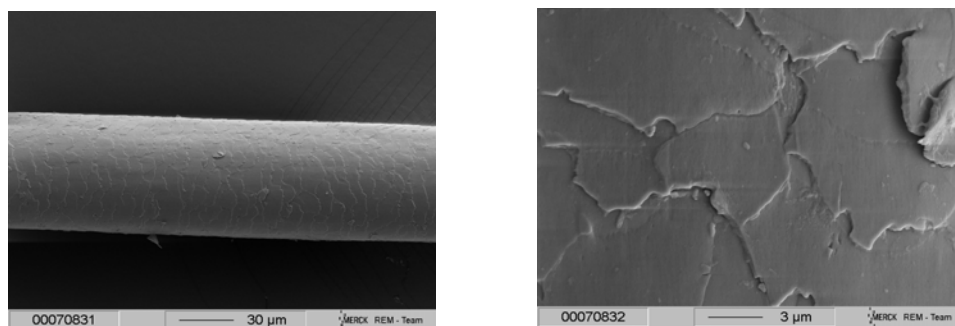
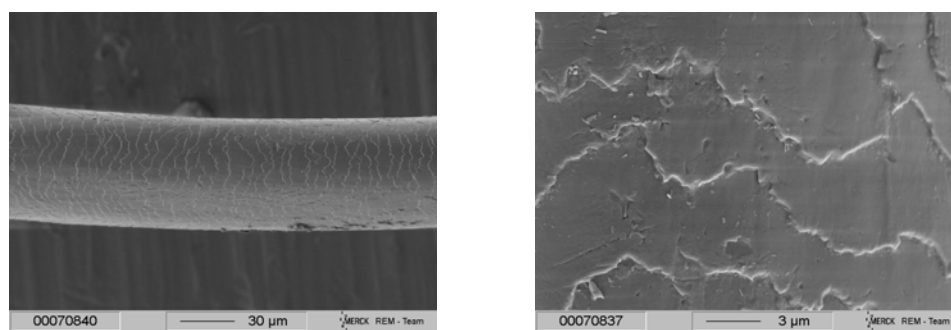
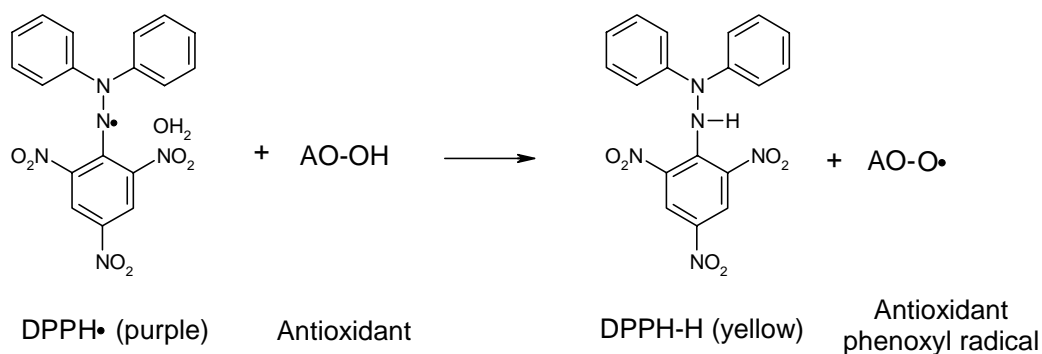
Figure 6. SEM images of brown European hair

Figure 7. SEM images of brown European hair treated with **2**

4.2.5 Antioxidant activities

The DPPH (2,2-diphenyl-1-picrylhydrazyl) assay was used to screen the radical scavenging potential of the compounds. The DPPH radical, DPPH[•] is a relatively stable paramagnetic free radical which accepts a hydrogen radical to become a stable diamagnetic molecule. The DPPH[•] hydrate is violet in colour, and in the presence of a free radical quencher forms 2,2-diphenyl-1-picrylhydrazine, which is yellow (Figure 8). By monitoring the decrease in intensity of DPPH[•] at 515 nm, the radical scavenger abilities of the antioxidant molecule can be determined. This is commonly expressed as the amount of antioxidant required to decrease the initial DPPH[•] concentration to 50 % (EC₅₀).

Figure 8. DPPH[•] hydrate and its reduced form, DPPH-H

As chromones lack the B-ring of flavonoids, which is responsible for much of their antioxidant power, the radical scavenging ability of chromones remain modest. However, as the objective of this project is not to generate a powerful antioxidant, but rather to synthesise a molecule which could bind to hair and protect it from UV-radiation and its effects, such as being able to scavenge UV-generated ROS, the observed activities suffice. Table 2 shows the EC₅₀ values of selected chromone derivatives.

Table 2. Radical Scavenging Activity

Compound	EC ₅₀
2	>200
7	40
Acid of 7 ^a	>80
8a	7.7
8b	7.8
10	16 ^b
15a	19.3
15b	- ^c
15c	- ^c

a) The acid of **7** is has previously been synthesised.^[61]

b) Estimate as sample was contaminated through inorganic salts. Measured value (24.1).

c) Samples polymerised during assay.

Although no clear relationship is shown, it is evident that hydroxyl or methoxy substitution on the A ring and an amide (instead of an acid or ester) functionality improve the radical scavenging abilities of the compounds.

4.2.6 Cyclic Voltammetry

In flavonoids the reduction potential is strongly dependant on the electron donating properties of the B-ring as this is generally more electron rich as the A-ring.^[62] As chromones do not possess the B-ring, the A-ring should influence the electronic chemical properties of the chromone. The electrochemical properties of compounds **15a**, **15b** and **15c** were measured by cyclic voltammetry^[63,64] in acetonitrile. All three samples showed an electrochemical irreversible behaviour. Relative to the half wave reduction potential of Fc/Fc^+ , a shift of +30 mV, +60 mV and +50 mV was observed for **15a**, **15b** and **15c** respectively. Although these shifts are small and close to the experimental error (± 20 mV) the general trend of increased reduction potential with increased electron donating properties of the substituent is indicated.

4.2.7 UV absorption of substituted chromones

The UV absorption properties of three different chromone derivatives (ester, alkyl amide and ammonium salt) with varying substitution patterns (methoxy substitution at position 7-, 6- or 5-) were measured. Tables 3, 4 and 5 summarise the results.

Table 3. Molar extinction coefficients for ethyl ester derivatives

Compound	R1	R2	R3	Wavelength, λ_{\max} [nm], Molar extinction coefficient (ϵ) ^{a)}			
12a	OCH ₃	H	H	212 (4.44)	238 (4.29)		310 (4.01)
12b	H	OCH ₃	H	206 (4.45)	238 (4.22)	253 (4.31)	343 (3.77)
12c	H	H	OCH ₃		238 (4.22)	271 (4.00)	327 (3.64)

a) Methanol was used as solvent

Table 4. Molar extinction coefficients for alkyl amide derivatives

Compound	R1	R2	R3	Wavelength, λ_{\max} [nm], Molar extinction coefficient (ϵ) ^{a)}			
13a	OCH ₃	H	H	212 (4.42)	236 (4.35)	255 (4.10) ^{b)}	304 (4.04)
13b	H	OCH ₃	H	205 (4.43)	230 (4.25)	252 (4.36)	338 (3.75)
13c	H	H	OCH ₃		238 (4.29)	260 (4.16)	323 (3.71)

a) Methanol was used as solvent

b) Present as a shoulder

Table 5. Molar extinction coefficients for quaternary ammonium derivatives

Compound	R1	R2	R3	Wavelength, λ_{\max} [nm], Molar extinction coefficient (ϵ) ^{a)}			
5	H	H	H	204 (4.62)	246 (4.43)		304 (3.83)
15a	OCH ₃	H	H	210 (4.47)	242 (4.32)		304 (3.80)
15b	H	OCH ₃	H	205 (4.42)	248 (4.34)		333 (3.54)
15c	H	H	OCH ₃		242 (4.25)		319 (3.53)

a) CH₃CN was used as solvent

A bathochromic shift was observed for the chromone -esters, -alkyl amides and -ammonium salts upon substitution of a methoxy group at either position 5, 6 or 7. As expected the alkyl chain length has no effect on the UV absorption. When compared to **5**, a red shift of 29 nm and 15 nm was observed for the **15b** and **15c** respectively, whilst **15a** had the same λ_{max} . Thus, by altering the chromone substitution pattern, the UV absorption properties can be tailored to individual needs. For example **15a** would protect better against UVB radiation and thus hair protein loss, whilst **15b** would protect better against UVA radiation and hair colour changes.

4.3 Conclusion

Chromone derivatives containing a quaternary ammonium functionality which bound to human hair were synthesised. The substitution pattern of the methoxy group was systematically changed to probe its effect on the redox potential and the UV absorption properties. The general radical scavenger activity of all derivatives is lower if compared to flavonoids. The UV absorption of the derivatives depends on the position of the methoxy groups. If the substituent is shifted from the 7 to 6 position, a bathochromic shift of the UV absorption of 29 nm results.

4.4 Experimental

4.4.1 General

4.4.1.1 Spectroscopy

IR-Spectra

Bio-Rad FT-IR-Spectrometer FTS 155.

UV-VIS Spectra

Varian Cary BIO 50 UV/VIS/NIR Spectrometer. Use of a 1 cm quartz cell (Hellma) and Uvasol solvents (Merck). Reported as: λ_{max} in nm (ϵ).

NMR-Spectra

- Bruker AC-250 (^1H : 250.1 MHz, ^{13}C : 62.9 MHz), Measurement temperature: 24 °C.
- Bruker Avance 300 (^1H : 300.1 MHz, ^{13}C : 75.5 MHz), Measurement temperature: 27 °C.
- Bruker ARX-400 (^1H : 400.1 MHz, ^{13}C : 100.6 MHz), Measurement temperature: 21 °C.
- Bruker Avance 400 (^1H : 400.1 MHz, ^{13}C : 100.6 MHz), Measurement temperature: 27 °C.
- Bruker Avance 600 (^1H : 600.1 MHz, ^{13}C : 150.1 MHz), Measurement temperature: 27 °C.

The chemical shifts are in δ -values (ppm) relative to the internal (or external) standard TMS. Reported as: Chemical shift (multiplicity, coupling constant, number of protons, assignment). Reported assignments were determined with the help of COSY, HMQC, HSQC, and NOESY 2D-Spectra. Abbreviations: s = singlet, bs = broad singlet, d = doublet, bd = broad doublet, dd = doublet of doublets, t = triplet, q = quartet, m = multiplet, bm = broad multiplet, sept = septet. Error of reported values: chemical shift: 0.01 ppm for ^1H -NMR, 0.1 ppm for ^{13}C -NMR; Coupling constants: 0.1 Hz. The used solvent is reported for each spectrum.

Mass spectra

- Varian CH-5 (EI)
- Finnigan MAT 95 (CI; FAB and FD)
- Finnigan MAT TSQ 7000 (ESI)

Xenon serves as the ionisation gas for FAB.

4.4.1.2 Analysis

Melting Point

Melting points are uncorrected and were determined according to Tottoli using instrumentation from Büchi.

Elemental Analysis

Elemental analyses were carried out by the microanalytical laboratory of the School of Chemistry and Pharmacy, University of Regensburg.

Scanning Electron Microscopy (SEM)

SEM analyses were carried out by the central analytical department of Merck KGaA, Darmstadt.

HPLC

HPLC analyses were carried out by Ralf Roskopf, Pigments R&D Cosmetic, Merck KGaA in Darmstadt:

A Merck Hitachi LaChrom (Interface L-7000, UV detector L-7400, Column Oven L-7350, Autosampler L-7200, Pump L-7100) with a Chromolith RP-18e 100-4.6 column was used. Wavelength 220 - 400 nm; Column temperature 30 °C; Injection Volume 50 µl; Solvent A: acetonitrile, Solvent B: water buffered at pH 2.6.

Pump Method: 0.0 min, 20 % A, 80 % B, 0.75 ml/min
 7.5 min, 80 % A, 20 % B, 1.00 ml/min
 9.0 min, 20 % A, 80 % B, 1.00 ml/min
 10.0 min, 20 % A, 80 % B, 0.75 ml/min

Cyclic Voltammetry

The cyclic voltammetry measurements were conducted in dry acetonitrile with 0.1 molL⁻¹ NBu₄⁺ BF₄⁻ as electrolyte and under argon. The working electrode was a graphite electrode, the counter electrode a platinum wire and the reference electrode Ag/AgCl in LiCl saturated ethanol. The PGSTAT 20 is from the company Eco Chemie and is controlled by the program GPES V 3.0.

4.4.1.3 Synthesis

Column Chromatography

Silica gel Merck Geduran SI 60.

Thin layer chromatography

Aluminium sheets Merck 60 F²⁵⁴ Silica gel, thickness 0.2 mm.

Detection via UV light at 254 nm or through discolouration with ninhydrin in ethanol.

Solvents

Purification and drying according to accepted general procedures.^[65,66]

If not otherwise stated, commercially available solvent of the highest purity were used.

4.4.1.4 Hair Substantivity

The substance to be tested (1 mg) was dissolved in ethanol:water (70:30, 50 ml) and allowed to stir at room temperature using a magnetic stirrer. Commercially available,^[67] washed, sterile human hair (1.00 g, 0.4 - 0.7 cm pieces) was added to the solution and allowed to stir vigorously for one hour. The hair was filtered and washed three times with fresh solvent. The hair sample was dried overnight at 40 °C and 200 mbar, yielding 1.00 g of treated hair.

The treated hair (0.5 g) was added to a solution of NaOH (1 M, 4 ml) and allowed to stir at 65 °C for 2 hours, forming a brown suspension. The reaction mixture was neutralised with HCl (2M, 2 ml) after which methanol (3 ml) and THF (1 ml) were added and the mixture allowed to stir for a further hour.

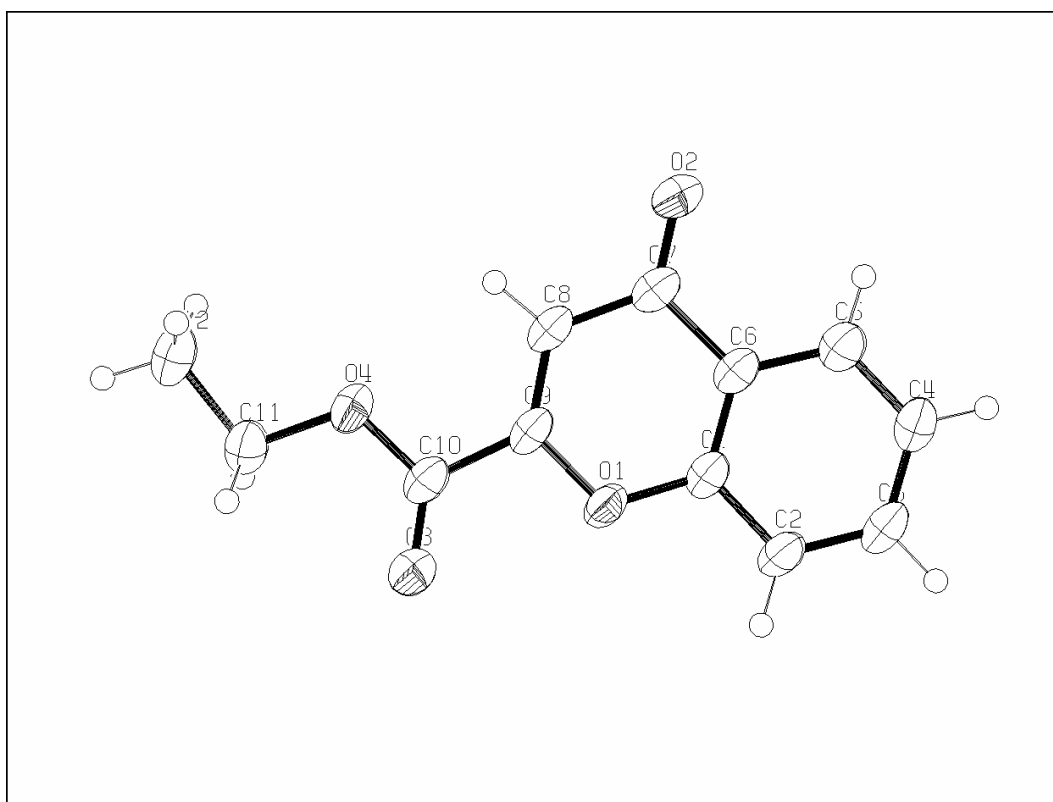
A sample (5 mg) of only the substance to be tested (no hair) was subjected to the same conditions to control the stability of the substance. The suspension was centrifuged (4000 rpm, 10 min) and the mother liquor decanted. The mother liquor was then filtered (0.2 µm polypropylene filter) to yield a clear light brown solution. A sample of only hair (no substance) was subjected to the same conditions and used as a reference. The hair substantivity test was carried out using both bleached European and natural light-middle brown European hair. No difference was noted in hair substantivity due to hair type.

4.4.1.5 X-ray Crystallography

4-Oxo-4H-chromene-2-carboxylic acid ethyl ester (2)

Crystal Data: $C_{12}H_{10}O_4$, $M_r = 218.20$, monoclinic, space group P 21/c, $a = 4.7382$ (6) Å, $b = 9.7230$ (9) Å, $c = 22.457$ (2) Å, $\alpha = 90^\circ$, $\beta = 97.190$ (14)°, $\gamma = 90^\circ$, $V = 1026.45$ (19) Å³, $Z = 4$, $D_x = 1.412$ Mg/m³, λ (Mo- K_α) = 0.71073 Å, $\mu = 0.107$ mm⁻¹, $F(000) = 456$, $T = 173$ (1) K, graphite monochromator. A translucent, colourless needle with dimensions of 0.560 x 0.080 x 0.060 mm was used to measure 8075 reflections (1960 unique reflections, $R_{int} = 0.0910$) from 2.78° to 25.80° on a STOE-IPDS diffractometer with the rotation method.

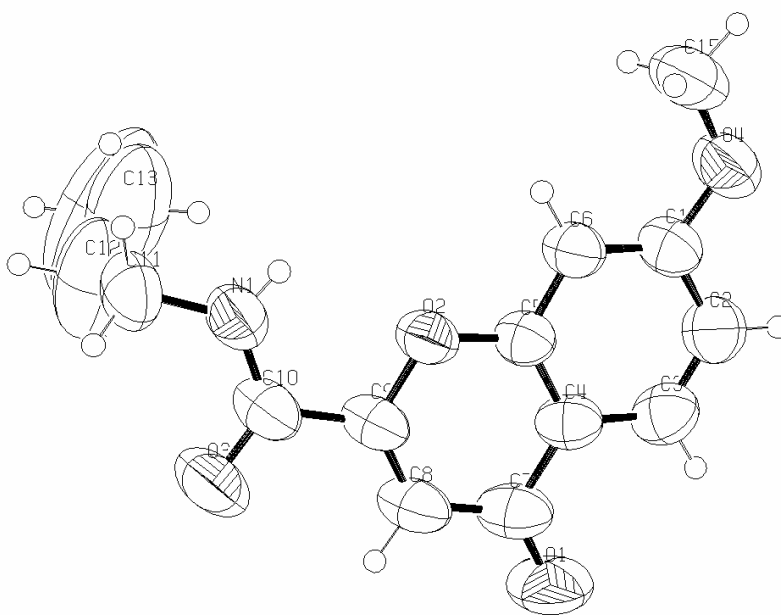
Structure refinement: The F^2 value was refined using the full-matrix least-squares refinement method, with a goodness-of-fit of 0.704 for all reflections and 145 parameters. The final R-Index R 0.0410 ($wR^2 = 0.1012$). $\Delta\rho_{min} = -0.212$ e Å⁻³, $\Delta\rho_{max} = 0.210$ e Å⁻³.



7-Methoxy-4-oxo-4H-chromene-2-carboxylic acid butylamide (13a)

Crystal Data: $C_{15}H_{17}NO_4$, $M_r = 275.30$, monoclinic, space group P 21/c, $a = 7.7733$ (8) Å, $b = 18.000$ (9) Å, $c = 10.5369$ (9) Å, $\alpha = 90^\circ$, $\beta = 98.003$ (11)°, $\gamma = 90^\circ$, $V = 1460.0$ (3) Å³, $Z = 4$, $D_x = 1.253$ Mg/m³, λ (Mo- K_α) = 0.71073 Å, $\mu = 0.091$ mm⁻¹, $F(000) = 584$, $T = 297$ (1) K, graphite monochromator. A translucent, colourless prism with dimensions of 0.300 x 0.260 x 0.060 mm was used to measure 9603 reflections (2573 unique reflections, $R_{int} = 0.0438$) from 2.26° to 25.30° on a STOE-IPDS diffractometer with the rotation method.

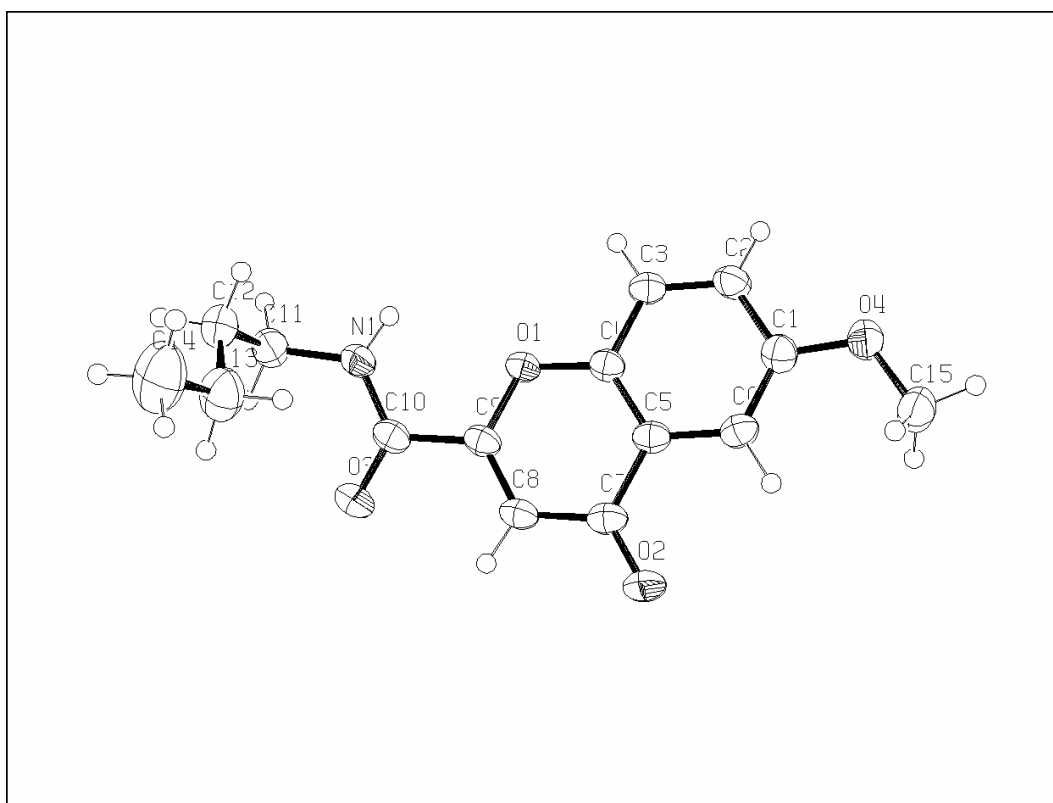
Structure refinement: The F^2 value was refined using the full-matrix least-squares refinement method, with a goodness-of-fit of 0.800 for all reflections and 184 parameters. The final R-Index R 0.0497 ($wR^2 = 0.1153$). $\Delta\rho_{min} = -0.142$ e Å⁻³, $\Delta\rho_{max} = 0.255$ e Å⁻³.



6-Methoxy-4-oxo-4H-chromene-2-carboxylic acid butylamide (13b)

Crystal Data: $C_{15}H_{17}NO_4$, $M_r = 275.30$, monoclinic, space group $P 2_1/c$, $a = 4.7091 (5) \text{ \AA}$, $b = 26.573 (2) \text{ \AA}$, $c = 11.3445 (11) \text{ \AA}$, $\alpha = 90^\circ$, $\beta = 97.612 (12)^\circ$, $\gamma = 90^\circ$, $V = 1407.1 (2) \text{ \AA}^3$, $Z = 4$, $D_x = 1.299 \text{ Mg/m}^3$, $\lambda (\text{Mo-}K_\alpha) = 0.71073 \text{ \AA}$, $\mu = 0.095 \text{ mm}^{-1}$, $F(000) = 584$, $T = 173 (1) \text{ K}$, graphite monochromator. A translucent, colourless stick with dimensions of $0.360 \times 0.120 \times 0.060 \text{ mm}$ was used to measure 11598 reflections (2718 unique reflections, $R_{\text{int}} = 0.0524$) from 1.97° to 25.93° on a STOE-IPDS diffractometer with the rotation method.

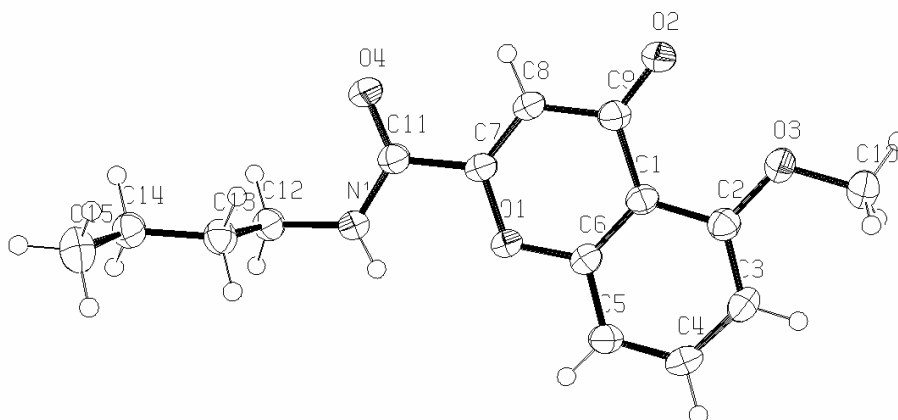
Structure refinement: The F^2 value was refined using the full-matrix least-squares refinement method, with a goodness-of-fit of 0.879 for all reflections and 211 parameters. The final R-Index $R 0.0386$ ($wR^2 = 0.0989$). $\Delta\rho_{\text{min}} = -0.133 \text{ e \AA}^{-3}$, $\Delta\rho_{\text{max}} = 0.349 \text{ e \AA}^{-3}$.



5-Methoxy-4-oxo-4H-chromene-2-carboxylic acid butylamide (13c)

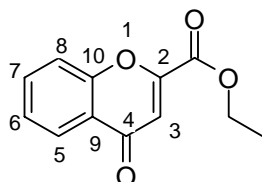
Crystal Data: $C_{15}H_{17}NO_4$, $M_r = 275.30$, monoclinic, space group P 2₁/c, $a = 4.7288$ (5) Å, $b = 23.526$ (2) Å, $c = 12.5669$ (11) Å, $\alpha = 90^\circ$, $\beta = 94.998$ (11) $^\circ$, $\gamma = 90^\circ$, $V = 1392.8$ (2) Å³, $Z = 4$, $D_x = 1.313$ Mg/m³, λ (Mo- K_α) = 0.71073 Å, $\mu = 0.096$ mm⁻¹, $F(000) = 584$, $T = 173$ (1) K, graphite monochromator. A translucent, colourless stick with dimensions of 0.320 x 0.080 x 0.080 mm was used to measure 12888 reflections (2680 unique reflections, $R_{int} = 0.0362$) from 2.38 $^\circ$ to 25.90 $^\circ$ on a STOE-IPDS diffractometer with the rotation method.

Structure refinement: The F^2 value was refined using the full-matrix least-squares refinement method, with a goodness-of-fit of 0.857 for all reflections and 184 parameters. The final R-Index R 0.0356 ($wR^2 = 0.0762$). $\Delta\rho_{min} = -0.132$ e Å⁻³, $\Delta\rho_{max} = 0.201$ e Å⁻³.



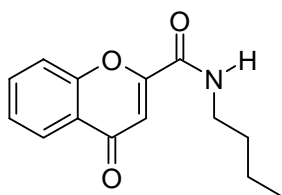
4.4.2 Synthesis of New Compounds

4-Oxo-4H-chromene-2-carboxylic acid ethyl ester (2)^[68]



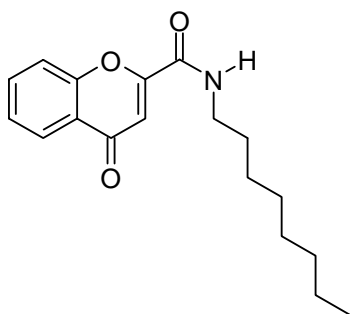
Sodium (1.49 g, 65 mmol) was dissolved in absolute ethanol (100 ml). Diethyloxalate (5.12 g, 35 mmol) and 2-hydroxyacetophenone (2.04 g, 15 mmol) were dissolved in absolute ethanol (10 ml) and added to the sodium ethanolate solution. The solution was allowed to reflux for 1 hour. Concentrated HCl was added dropwise until the reaction was acidic and a white precipitate formed. The white precipitate was filtered and the yellow solution concentrated to a slurry. The slurry was extracted with ethyl acetate, dried over Na_2SO_4 and evaporated to give a light yellow solid. The solid was recrystallised from methanol/diisopropylether (4:1) to yield white needles (3.20 g, 14.6 mmol, 98 %).

MP: 63 °C; **IR** (KBr): $\tilde{\nu}$ (cm^{-1}) = 3447, 3067, 2985, 2938, 1734, 1647, 1466, 758; **$^1\text{H-NMR}$** (600 MHz, CDCl_3): δ [ppm] = 1.43 (t, J = 7.1 Hz, 3 H, CH_3), 4.46 (q, J = 7.1 Hz, 2 H, CH_2), 7.11 (s, 1 H, H-3), 7.44 (ddd, J = 1.2 Hz, 7.1 Hz, 8.0 Hz, 1 H, H-6), 7.61 (ddd, J = 0.4 Hz, 1.2 Hz, 8.5 Hz, 1 H, H-8), 7.74 (ddd, J = 1.7 Hz, 7.1 Hz, 8.5 Hz, 1 H, H-7), 8.20 (ddd, J = 0.4 Hz, 1.7 Hz, 8.0 Hz, 1 H, H-5); **$^{13}\text{C-NMR}$** (150 MHz, CDCl_3): δ [ppm] = 14.1 (+, CH_3), 63.0 (-, CH_2), 114.8 (+, C-3), 118.8 (+, C-8), 124.4 (C_{quat} , C-9), 125.7 (+, C-5), 125.9 (+, C-6), 134.7 (+, C-7), 152.2 (C_{quat} , C-2), 156.0 (C_{quat} , C-10), 160.6 (C_{quat} , C=O), 178.4 (C_{quat} , C-4); **MS** (ESI-MS, EtOH/MeOH + 10 mmol/l NH_4OAc) m/z (%): 219 (100) $[\text{MH}]^+$; **Elemental Analysis:** $\text{C}_{12}\text{H}_{10}\text{O}_4$ Calc: C 66.05; H 4.62; Found: C 66.07; H 4.72

4-Oxo-4H-chromene-2-carboxylic acid butylamide (3a)

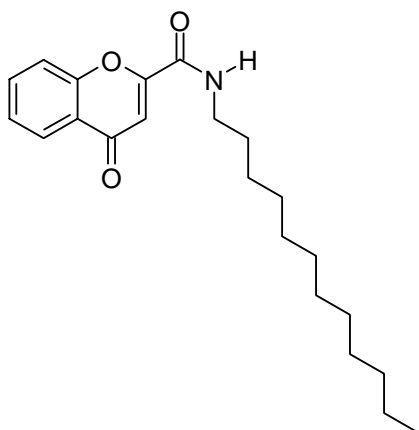
Ethyl-4-oxo-4H-chromene-2-carboxylate (655 mg, 3 mmol) was dissolved in the butylamine (658 mg, 9 mmol) allowed to stir at 50 °C for 10 minutes. The solvent was evaporated leaving a yellow solid. Glacial acetic acid (5 ml) was added and allowed to stir at 70 °C for 10 minutes. The mixture was added to ice water and a white precipitate formed which was filtered, washed with water and dried. The white solid was recrystallised from ethyl acetate to yield white needles (630 mg, 2.6 mmol, 86 %).

MP: 130 °C; **IR** (KBr): $\tilde{\nu}$ (cm⁻¹) = 3319, 3079, 2954, 2868, 1685, 1642, 1387, 755; **UV/VIS** (MeOH): λ_{max} [nm] (log ϵ) = 202 (4.37), 236 (4.29), 305 (3.85); **¹H-NMR** (300 MHz, DMSO): δ [ppm] = 0.91 (t, J = 7.2 Hz, 3 H, CH₃), 1.34 (qd, J = 7.2 Hz, 14.1 Hz, 2 H, CH₂), 1.54 (XX, J = 7.2 Hz, 2 H, CH₂), 3.30 (q, J = 7.2 Hz, 2 H, CH₂), 6.82 (s, 1 H, H-3), 7.53 (ddd, J = 1.0 Hz, 7.1 Hz, 8.0 Hz, 1 H, H-6), 7.73 (dd, J = 1.0 Hz, 8.5 Hz, 1 H, H-8), 7.89 (ddd, J = 1.7 Hz, 7.1 Hz, 8.5 Hz, 1 H, H-7), 8.05 (dd, 1.7 Hz, 8.0 Hz, 1 H, H-5), 9.10 (t, J = 5.6 Hz, 1 H, N-H); **¹³C-NMR** (75 MHz, DMSO): δ [ppm] = 13.6 (+, CH₃), 19.5 (-, CH₂), 30.8 (-, CH₂), 38.8 (-, CH₂), 110.2 (-, C-3), 118.7 (+, C-8), 123.5 (C_{quat}, C-9), 124.8 (+, C-5), 125.9 (+, C-6), 134.9 (+, C-7), 155.0 (C_{quat}, C-2), 155.7 (C_{quat}, C-10), 158.7 (C_{quat}, C=O), 177.2 (C_{quat}, C-4); **MS** (CI-MS, NH₃) m/z (%): 263.1 (100) [M+NH₃]⁺, 246.1 (26) [MH]⁺; **Elemental Analysis:** C₁₄H₁₅NO₃ Calc: C 68.56; H 6.16; N 5.71; Found: C 68.58; H 6.04; N 5.61

4-Oxo-4H-chromene-2-carboxylic acid octylamide (3b)

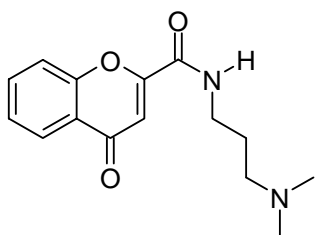
Ethyl-4-oxo-4H-chromene-2-carboxylate (655 mg, 3 mmol) and octylamine (1163 mg, 9 mmol) were dissolved in dichloromethane (5 ml) and allowed to reflux for 10 minutes. The solvent was evaporated leaving a light yellow solid. Glacial acetic acid (5 ml) was added and allowed to stir at 70 °C for 10 minutes. The mixture was added to ice water and extracted with ethyl acetate. The organic layer was dried over Na₂SO₄ and evaporated to give a white solid. The solid was recrystallised from ethyl acetate to yield white needles (826 mg, 2.7 mmol, 91 %).

MP: 131 °C; **IR** (KBr): $\tilde{\nu}$ (cm⁻¹) = 3314, 2927, 2849, 1684, 1646, 1529, 1392, 751; **UV/VIS** (MeOH): λ_{max} [nm] (log ϵ) = 202 (4.36), 236 (4.29), 305 (3.84); **¹H-NMR** (300 MHz, CDCl₃): δ [ppm] = 0.85 - 0.91 (m, 3 H, CH₃), 1.24 - 1.46 (m, 10 H, 5 x CH₂), 1.61 - 1.72 (m, 2 H, CH₂), 3.49 (tq, J = 6.2 Hz, 7.2 Hz, 2 H, CH₂), 6.91 (s, 1H, N-H), 7.16 (s, 1 H, H-3), 7.45 (ddd, J = 1.0 Hz, 7.2 Hz, 8.1 Hz, 1 H, H-6), 7.52 (dd, J = 0.5 Hz, 8.5 Hz, 1 H, H-8), 7.73 (ddd, J = 1.7 Hz, 7.2 Hz, 8.5 Hz, 1 H, H-7), 8.22 (dd, J = 1.7 Hz, 8.0 Hz, 1 H, H-5); **¹³C-NMR** (75 MHz, CDCl₃): δ [ppm] = 14.1 (+, CH₃), 22.6 (-, CH₂), 26.7 (-, CH₂), 27.0 (-, CH₂), 29.1 (-, CH₂), 29.2 (-, CH₂), 29.5 (-, CH₂), 31.8 (-, CH₂), 40.1 (-, CH₂), 112.1 (+, C-3), 118.0 (+, C-8), 124.4 (C_{quat}, C-9), 126.0 (+, C-5), 126.2 (+, C-6), 134.5 (+, C-7), 154.8 (C_{quat}, C-2), 155.3 (C_{quat}, C-10), 159.2 (C_{quat}, C=O), 178.2 (C_{quat}, C-4); **MS** (CI-MS, NH₃) m/z (%): 319.1 (100) [M+NH₃]⁺, 302.1 (40) [MH]⁺; **Elemental Analysis:** C₁₈H₂₃NO₃ Calc: C 71.73; H 7.69, N 4.65; Found: C 71.62; H 7.58, N 4.43

4-Oxo-4H-chromene-2-carboxylic acid dodecylamide (3c)

Ethyl-4-oxo-4H-chromene-2-carboxylate (1.96 g, 9 mmol) and dodecylamine (5.0 g, 27 mmol) were dissolved in dichloromethane (10 ml) and allowed to reflux for 10 minutes. The solvent was evaporated giving a light yellow solid. Glacial acetic acid (10 ml) was added and allowed to stir at 70 °C for 10 minutes. The mixture was added to ice water and extracted with ethyl acetate. The organic layer was dried over Na₂SO₄ and evaporated to give a yellow solid. The solid was recrystallised from ethyl acetate to yield white needles (2.30 g, 6.4 mmol, 71 %).

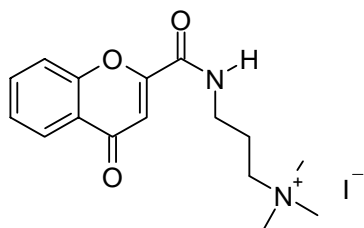
MP: 108 °C; **IR** (KBr): $\tilde{\nu}$ (cm⁻¹) = 3319, 2959, 2932, 2850, 1982, 1642, 1522, 1387, 753; **UV/VIS** (MeOH): λ_{max} [nm] (log ϵ) = 203 (4.37), 236 (4.29), 305 (3.83); **¹H-NMR** (300 MHz, DMSO): δ [ppm] = 0.83 (t, J = 6.7 Hz, 3 H, CH₃), 1.16 - 1.33 (m, 18 H, 9 x CH₂), 1.48 - 1.60 (m, 2 H, CH₂), 3.28 (m, 2 H, CH₂), 6.81 (s, 1H, H-3), 7.53 (ddd, J = 1.0 Hz, 7.2 Hz, 8.0 Hz, 1 H, H-6), 7.73 (dd, J = 0.6 Hz, 8.5 Hz, 1 H, H-8), 7.89 (ddd, J = 1.7 Hz, 7.2 Hz, 8.5 Hz, 1 H, H-7), 8.05 (dd, J = 1.7 Hz, 8.0 Hz, 1 H, H-5), 9.12 (t, J = 5.8 Hz, 1 H, N-H); **¹³C-NMR** (75 MHz, DMSO): δ [ppm] = 13.8 (+, CH₃), 22.0 (-, CH₂), 26.3 (-, CH₂), 28.6 (-, CH₂), 28.7 (-, CH₂), 28.8 (-, CH₂), 28.9 (-, CH₂), 28.9 (-, CH₂), 28.9 (-, CH₂), 31.2 (-, CH₂), 39.2 (-, CH₂), 39.4 (-, CH₂), 110.2 (+, C-3), 118.7 (+, C-8), 123.5 (C_{quat}, C-9), 124.8 (+, C-5), 125.9 (+, C-6), 134.9 (+, C-7), 155.0 (C_{quat}, C-2), 155.7 (C_{quat}, C-10), 158.7 (C_{quat}, C=O), 177.2 (C_{quat}, C-4); **MS** (CI-MS, NH₃) m/z (%): 375.2 (100) [M+NH₃]⁺, 358.2 (56) [MH]⁺; **Elemental Analysis:** C₂₂H₃₁NO₃ Calc: C 73.92; H 8.74; N 3.92; Found: C 73.75; H 8.75; N 3.74

4-Oxo-4H-chromene-2-carboxylic acid (3-dimethylamino-propyl)-amide (4)

Ethyl-4-oxo-4H-chromene-2-carboxylate (655 mg, 3 mmol) and 3-dimethylamino-propylamine (920 mg, 9 mmol) were dissolved in dichloromethane (5 ml) and allowed to reflux for 20 minutes. The solvent was evaporated, glacial acetic acid (5 ml) was added and the solution allowed to stir at 70 °C for 10 minutes. The mixture was added to ice water and extracted with ethyl acetate. The organic layer was dried over Na₂SO₄ and evaporated to give a yellow solid. The solid was recrystallised from ethyl acetate to yield white needles (691 mg, 2.5 mmol, 84 %).

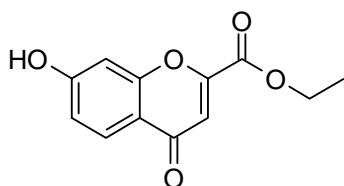
MP: 125 °C; **IR** (KBr): $\tilde{\nu}$ (cm⁻¹) = 3289, 2976, 2946, 2805, 1686, 1640, 1534, 1460, 1392, 759; **UV/VIS** (MeOH): λ_{max} [nm] (log ϵ) = 203 (4.37), 236 (4.29), 305 (3.84); **¹H-NMR** (300 MHz, DMSO): δ [ppm] = 1.69 (p, J = 6.9 Hz, 2 H, CH₂), 2.15 (s, 6 H, 2 x CH₃), 2.28 (t, J = 6.9 Hz, 2 H, CH₂), 3.33 (dd, J = 7.2 Hz, 12.7 Hz, 2 H, CH₂), 6.82 (s, 1 H, H-3), 7.53 (ddd, J = 1.0 Hz, 7.2 Hz, 8.0 Hz, 1 H, H-6), 7.71 (dd, J = 0.7 Hz, 8.5 Hz, 1 H, H-8), 7.89 (ddd, J = 1.7 Hz, 7.2 Hz, 8.5 Hz, 1 H, H-7), 8.05 (dd, J = 1.7 Hz, 8.0 Hz, 1 H, H-5), 9.25 (t, J = 5.5 Hz, 1 H, N-H) ; **¹³C-NMR** (75 MHz, DMSO): δ [ppm] = 26.4 (-, CH₂), 38.0 (-, CH₂), 45.1 (+, 2 x CH₃), 56.9 (-, CH₂), 110.2 (+, C-3), 118.6 (+, C-8), 123.5 (C_{quat}, C-9), 124.9 (+, C-5), 125.9 (+, C-6), 134.9 (+, C-7), 155.0 (C_{quat}, C-2), 155.6 (C_{quat}, C-10), 158.7 (C_{quat}, C=O), 177.2 (C_{quat}, C-4); **MS** (PI-EIMS) m/z (%): 58.1 (100) [Me₂N=CH₂]⁺, 274.1 (11) [M]⁺⁺; **Elemental Analysis:** C₁₅H₁₈N₂O₃ Calc: C 65.68; H 6.61; N 10.21; Found: C 65.63; H 6.41; N 10.08

Trimethyl-{3-[(4-oxo-4H-chromene-2-carbonyl)-amino]-propyl}-ammonium iodide (5)



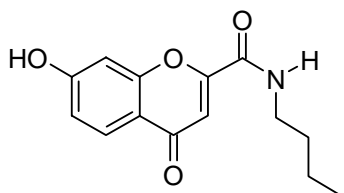
Iodomethane (260 mg, 1.83 mmol) was dissolved in chloroform (5 ml) and added to a solution of 4-Oxo-4H-chromene-2-carboxylic acid (3-dimethylamino-propyl)-amide (500 mg, 1.82 mmol) in chloroform (5 ml). The solution was allowed to stir at RT for 30 min and then at reflux for 15 min upon which a precipitate formed. The yellow precipitate was filtered and washed with chloroform yielding a light yellow solid (578 mg, 1.39 mmol, 76 %).

MP: 240 °C+; **IR** (KBr): $\tilde{\nu}$ (cm⁻¹) = 3404, 3022, 2956, 1673, 1643, 1458, 740; **UV/VIS** (CH₃CN): λ_{max} [nm] (log ϵ) = 204 (4.62), 246 (4.43), 304 (3.83); **¹H-NMR** (300 MHz, DMSO): δ [ppm] = 1.95 - 2.06 (m, 2 H, CH₂), 3.07 (s, 9 H, 3 x CH₃), 3.34 - 3.44 (m, 6 H, 2 x CH₂), 6.86 (s, 1 H, H-3), 7.55 (ddd, J = 1.0 Hz, 7.2 Hz, 8.0 Hz, 1 H, H-6), 7.75 (d, J = 8.5 Hz, 1 H, H-8), 7.92 (ddd, J = 1.7 Hz, 7.2 Hz, 8.5 Hz, 1 H, H-7), 8.06 (dd, J = 1.7 Hz, 8.0 Hz, 1 H, H-5), 9.25 (t, J = 5.9 Hz, 1 H, N-H); **¹³C-NMR** (75 MHz, DMSO): δ [ppm] = 22.6 (-, CH₂), 36.3 (-, CH₂), 52.1 (+, CH₃), 52.2 (+, CH₃), 52.2 (+, CH₃), 63.2 (-, CH₂), 110.5 (+, C-3), 118.6 (+, C-8), 123.5 (C_{quat}, C-9), 124.9 (+, C-5), 126.0 (+, C-6), 135.0 (+, C-7), 155.0 (C_{quat}, C-2), 155.4 (C_{quat}, C-10), 159.2 (C_{quat}, C=O), 177.2 (C_{quat}, C-4); **MS** (ESI, H₂O/AcN) m/z (%): 289.0 (100) [K]⁺; **Elemental Analysis:** C₁₆H₂₁N₂O₃I Calc: C 46.17; H 5.08; N 6.73; Found: C 45.79; H 4.70; N 6.51

7-Hydroxy-4-oxo-4H-chromene-2-carboxylic acid ethyl ester (7)^[69]

Sodium (1.84 g, 80 mmol) was dissolved in absolute ethanol (100 ml). Diethyloxalate (7.31 g, 50 mmol) and 2,4-dihydroxyacetophenone (2.28 g, 15 mmol) were dissolved in absolute ethanol (10 ml) and added to the sodium ethanolate solution. The solution was allowed to reflux for 1 hour. Concentrated HCl was added dropwise until the reaction was acidic and a white precipitate formed. The white precipitate was filtered off and the yellow/brown filtrate concentrated to a slurry. The slurry was extracted with ethyl acetate, dried over Na₂SO₄ and evaporated to give a light orange solid. The solid was recrystallised from methanol/diisopropylether (3:1) to yield white needles (2.78 g, 12 mmol, 79 %).

MP: 210 - 211 °C; **IR** (KBr): $\tilde{\nu}$ (cm⁻¹) = 3521, 3109, 1742, 1640, 1601, 1570, 1456, 1253, 829; **UV/VIS** (MeOH): λ_{max} [nm] (log ϵ) = 211 (4.44), 239 (4.24), 313 (3.96); **¹H-NMR** (600 MHz, DMSO): δ [ppm] = 1.34 (t, J = 7.1 Hz, 3 H, CH₃), 4.37 (q, J = 7.1 Hz, 2 H, CH₂), 6.82 (s, 1 H, H-3), 6.90 (d, J = 2.2 Hz, 1 H, H-8), 6.96 (dd, J = 2.2 Hz, 8.7 Hz, 1 H, H-6), 7.89 (d, J = 8.7 Hz, 1 H, H-5), 11.02 (s, 1 H, OH); **¹³C-NMR** (150 MHz, DMSO): δ [ppm] = 13.8 (+, CH₃), 62.5 (-, CH₂), 102.4 (+, C-8), 113.6 (+, C-3), 115.8 (+, C-6), 116.6 (C_{quat}, C-9), 126.7 (+, C-5), 151.5 (C_{quat}, C-2), 157.1 (C_{quat}, C-10), 159.9 (C_{quat}, C=O), 163.5 (C_{quat}, C-7), 176.1 (C_{quat}, C-4); **MS** (EI-MS, 70 eV) m/z (%): 234.1 (100) [M]⁺; **HRMS** (C₁₂H₁₀O₅)⁺ Calc: 234.0528; Found: 234.0528 ± 0.76 ppm; **Elemental Analysis:** C₁₂H₁₀O₅ Calc: C 61.54; H 4.30; Found: C 60.97; H 4.21

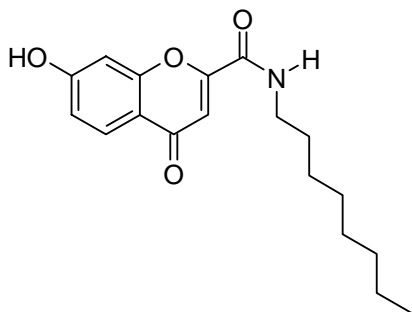
7-Hydroxy-4-oxo-4H-chromene-2-carboxylic acid butylamide (8a)

Ethyl-7-hydroxy-4-oxo-4H-chromene-2-carboxylate (585 mg, 2.5 mmol) and butylamine (512 mg, 7 mmol) were dissolved in dichloromethane (10 ml) and allowed to reflux for 10 minutes. The solvent was evaporated upon which a light yellow solid formed. Glacial

acetic acid (10 ml) was added and allowed to stir at 70 °C for 10 minutes. The mixture was added to ice water. The precipitate was filtered off, washed with water and dried. The solid was recrystallised from ethyl acetate/diisopropylether (4:1) to yield a light brown solid (573 mg, 2.2 mmol, 88 %).

MP: 240 °C+; **IR** (KBr): $\tilde{\nu}$ (cm⁻¹) = 3340, 3195, 3081, 2960, 2875, 1639, 1618, 1394, 829; **UV/VIS** (MeOH): λ_{max} [nm] (log ϵ) = 211 (4.41), 238 (4.31), 307 (3.98); **¹H-NMR** (300 MHz, DMSO): δ [ppm] = 0.90 (t, J = 7.2 Hz, 3 h, CH₃), 1.32 (qd, J = 7.2 Hz, 14.2 Hz, 2 H, CH₂), 1.47 - 1.58 (m, 2 H, CH₂), 3.28 (dd, J = 6.9 Hz, 13.2 Hz, 2 H, CH₂), 6.69 (s, 1 H, H-3), 6.94 (dd, J = 2.3 Hz, 8.7 Hz, 1 H, H-6), 6.99 (d, J = 2.2, 1 H, H-8), 7.88 (d, J = 8.7 Hz, 1 H, H-5), 9.06 (t, J = 5.8 Hz, N-H), 10.98 (s, 1 H, OH); **¹³C-NMR** (75 MHz, DMSO): δ [ppm] = 13.6 (+, CH₃), 19.5 (-, CH₂), 30.9 (-, CH₂), 38.8 (-, CH₂), 102.6 (+, C-8), 110.1 (+, C-3), 115.6 (+, C-6), 116.4 (C_{quat}, C-9), 126.6 (+, C-5), 155.1 (C_{quat}, C-2), 156.9 (C_{quat}, C-10), 158.8 (C_{quat}, C=O), 163.1 (C_{quat}, C-7), 176.3 (C_{quat}, C-4); **MS** (CI-MS, NH₃) m/z (%): 262.2 (100) [MH]⁺; **Elemental Analysis:** C₁₄H₁₅NO₄ Calc: C 64.36; H 5.79; N 5.36; Found: C 64.12; H 5.48; N 5.11

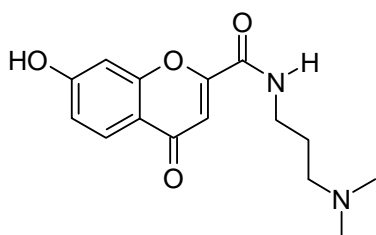
7-Hydroxy-4-oxo-4H-chromene-2-carboxylic acid octylamide (8b)



Ethyl-7-hydroxy-4-oxo-4H-chromene-2-carboxylate (585 mg, 2.5 mmol) and octylamine (905 mg, 7 mmol) were dissolved in dichloromethane (10 ml) and allowed to reflux for 10 minutes. The solvent was evaporated upon which a brown solid formed. Glacial acetic acid (10 ml) was added and allowed to stir at 70 °C for 10 minutes. The mixture was added to ice water yielding a precipitate, which was filtered off, washed with water and dried. The solid was recrystallised from ethyl acetate to yield a white solid (642 mg, 2.0 mmol, 81 %).

MP: 215 °C; **IR** (KBr): $\tilde{\nu}$ (cm⁻¹) = 3256, 3155, 2947, 2919, 2853, 1634, 1598, 1530, 1388, 1242, 838; **UV/VIS** (MeOH): λ_{max} [nm] (log ϵ) = 210 (4.44), 238 (4.33), 308 (3.99); **¹H-NMR** (600 MHz, DMSO): δ [ppm] = 0.84 (t, J = 6.7 Hz, 3 H, CH₃), 1.20 - 1.31 (m, 10 H, 5 x CH₂), 1.50 - 1.56 (m, 2 H, CH₂), 3.27 (dd, J = 6.7 Hz, 13.4 Hz, 2 H, CH₂), 6.69 (s, 1 H, H-3), 6.94 (dd, J = 1.9 Hz, J = 8.7 Hz, 1 H, H-6), 6.99 (d, J = 1.9 Hz, 1 H, H-8), 7.88 (d, J = 8.7 Hz, 1 H, H-5), 9.03 (t, J = 5.5 Hz, 1 H, N-H), 10.96 (s, 1 H, OH); **¹³C-NMR** (150 MHz, DMSO): δ [ppm] = 13.8 (+, CH₃), 22.0 (-, CH₂), 26.3 (-, CH₂), 28.5 (-, CH₂), 28.6 (-, CH₂), 28.7 (-, CH₂), 31.1 (-, CH₂), 39.1 (-, CH₂), 102.6 (+, C-8), 110.1 (+, C-3), 115.6 (+, C-6), 116.4 (C_{quat}, C-9), 126.6 (+, C-5), 155.1 (C_{quat}, C-2), 156.9 (C_{quat}, C-10), 158.8 (C_{quat}, C=O), 163.1 (C_{quat}, C-7), 176.2 (C_{quat}, C-4); **MS** (ESI, DCM/MeOH + 10 mmol/l NH₄Ac) m/z (%): 318.1 (100) [MH]⁺; **Elemental Analysis:** C₁₈H₂₃NO₄ Calc: C 68.12; H 7.30; N 4.41; Found: C 67.85; H 7.30; N 4.24

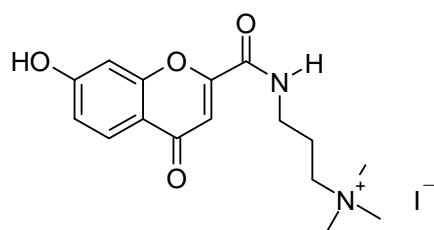
7-Hydroxy-4-oxo-4H-chromene-2-carboxylic acid (3-dimethylamino-propyl)-amide (9)



Ethyl-7-hydroxy-4-oxo-4H-chromene-2-carboxylate (1.17 g, 5 mmol) and 3-dimethylaminopropylamine (1.53 g, 15 mmol) were dissolved in dichloromethane (10 ml) and allowed to reflux for 1 hour. The solvent was evaporated, glacial acetic acid (10 ml) was added and allowed to stir at 70 °C for 10 minutes. The mixture was added to ice water and extracted with ethyl acetate. The aqueous layer was neutralised with sodium hydrogen carbonate and extracted with ethyl acetate. The aqueous layer was made basic with sodium carbonate and extracted with ethyl acetate. The aqueous layer was made acidic with concentrated HCl and then evaporated to dryness giving a yellow solid. The yellow solid was added to methanol and a white solid crystallised out, which was filtered off. The yellow filtrate was evaporated to dryness and repeatedly dissolved in methanol until no further white solid crystallised. The yellow mother liquor was evaporated to dryness yielding a yellow solid, which was dissolved in boiling ethanol, filtered and evaporated to dryness yielding a yellow solid (1.37 g, 4.7 mmol, 94 %).

MP: 240 °C+; **IR** (KBr): $\tilde{\nu}$ (cm⁻¹) = 3455, 3273, 3064, 2999, 1683, 1650, 1619, 1548, 1468, 1272, 786; **UV/VIS** (MeOH): λ_{\max} [nm] (log ϵ) = 210 (3.92), 237 (3.80), 307 (3.46); **¹H-NMR** (300 MHz, DMSO): δ [ppm] = 2.00 (t, J = 7.2 Hz, 2 H, CH₂), 2.72 (s, 6 H, 2 x CH₃), 2.89 (t, J = 7.2 Hz, 2 H, CH₂), 3.02 - 3.18 (m, 2 H, CH₂), 6.72 (s, 1 H, H-3), 7.00 (dd, J = 2.2 Hz, 8.8 Hz, 1 H, H-6), 7.16 (d, J = 2.2 Hz, 1 H, H-5), 7.86 (d, J = 8.8 Hz, 1 H, H-8), 9.40 (t, J = 5.9 Hz, 1 H, N-H), 11.36 (s, 1 H, OH); **¹³C-NMR** (75 MHz, DMSO): δ [ppm] = 21.8 (-, CH₂), 36.0 (-, CH₂), 41.8 (+, 2 x N-CH₃), 53.3 (-, CH₂), 102.7 (+, C-8), 110.2 (+, C-3), 115.8 (+, C-6), 116.3 (C_{quat}, C-9), 126.5 (+, C-5), 154.8 (C_{quat}, C-2), 156.9 (C_{quat}, C-10), 159.2 (C_{quat}, C=O), 163.4 (C_{quat}, C-7), 176.3 (C_{quat}, C-4); **MS** (ESI, DCM/MeOH + 10 mmol/l NH₄Ac) m/z (%): 291.1 (100) [MH]⁺; **HRMS** (C₁₅H₁₈N₂O₄)⁺ Calc: 290.1266; Found: 290.1266 ± 0.7 ppm

{3-[(7-Hydroxy-4-oxo-4H-chromene-2-carbonyl)-amino]-propyl}-trimethyl-ammonium iodide (10)

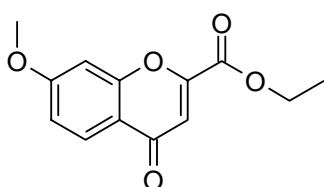


7-Hydroxy-4-oxo-4H-chromene-2-carboxylic acid (3-dimethylamino-propyl)-amide (436 mg, 1.5 mmol) was added to acetonitrile (30 ml) containing sodium carbonate (415 mg, 5 mmol). Iodomethane (227 mg, 1.6 mmol) was added to the suspension and allowed to stir at RT overnight. The reaction mixture was evaporated to dryness and resuspended in methanol. A white precipitate was filtered off and the resulting yellow mother liquor evaporated to dryness yielding a light yellow solid (439 mg, 1 mmol, 68 %).

MP: 240 °C+; **IR** (KBr): $\tilde{\nu}$ (cm⁻¹) = 3445, 3266, 3064, 2979, 1681, 1645, 1252, 832; **¹H-NMR** (300 MHz, DMSO): δ [ppm] = 1.90 - 2.02 (m, 2 H, CH₂), 3.07 (s, 9 H, 3 x CH₃), 3.27 - 3.40 (m, 4 H, 2 x CH₂), 6.66 (s, 1 H, H-3), 6.80 (d, J = 2.2 Hz, 1 H, H-8), 6.83 (dd, J = 2.2 Hz, 8.6 Hz, 1 H, H-6), 7.79 (d, J = 8.6 Hz, 1 H, H-5), 9.15 (t, J = 5.9 Hz, 1 H, N-H); **¹³C-NMR** (75 MHz, DMSO): δ [ppm] = 22.7 (-, CH₂), 36.2 (-, CH₂), 52.1 (+, 3 x N-CH₃), 63.2 (-, CH₂), 102.3 (+, C-8), 110.2 (+, C-3), 114.5 (C_{quat}, C-9), 117.2 (+, C-6), 126.2 (+,

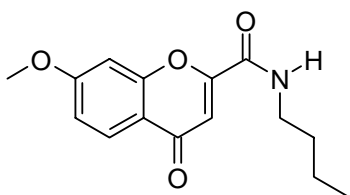
C-5), 154.3 (C_{quat} , C-2), 157.4 (C_{quat} , C-10), 159.4 (C_{quat} , C=O), 167.1 (C_{quat} , C-7), 175.9 (C_{quat} , C-4); **MS** (ESI, $\text{H}_2\text{O}/\text{AcN}$) m/z (%): 305.0 (100) $[\text{M}]^+$; **HRMS** ($\text{C}_{16}\text{H}_{21}\text{N}_2\text{O}_4$) $^+$ Calc: 305.1501; Found: 305.1500 \pm 1.23 ppm

7-Methoxy-4-oxo-4H-chromene-2-carboxylic acid ethyl ester (12a)^[68]



Sodium (1.49 g, 65 mmol) was dissolved in absolute ethanol (100 ml). Diethyloxalate (5.12 g, 35 mmol) and 2-hydroxy-4-methoxyacetophenone (2.49 g, 15 mmol) were dissolved in absolute ethanol (10 ml) and added to the sodium ethanolate solution. The solution was allowed to reflux for 1 hour. Concentrated HCl was added dropwise until the reaction was acidic and a white precipitate formed. The white precipitate was filtered and the yellow solution concentrated to a slurry. The slurry was extracted with ethyl acetate, dried over Na_2SO_4 and evaporated to give a light yellow solid. The solid was recrystallised from methanol/diisopropylether (4:1) to yield a yellow solid (3.65 g, 14.7 mmol, 98 %).

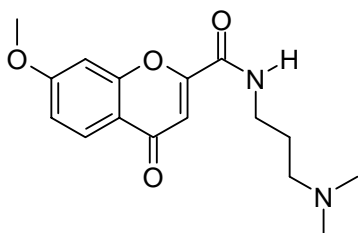
MP: 109 °C; **IR** (KBr): $\tilde{\nu}$ (cm^{-1}) = 3459, 3110, 2997, 2856, 1742, 1664, 1628, 1442, 1258, 838; **UV/VIS** (MeOH): λ_{max} [nm] ($\log \epsilon$) = 212 (4.44), 238 (4.29), 310 (4.01); **$^1\text{H-NMR}$** (300 MHz, DMSO): δ [ppm] = 1.34 (t, J = 7.1 Hz, 3 H, CH_3), 3.91 (s, 3 H, O- CH_3), 4.38 (q, J = 7.1 Hz, 2 H, CH_2), 6.85 (s, 1 H, H-3), 7.07 (dd, J = 2.4 Hz, 8.9 Hz, 1 H, H-6), 7.19 (d, J = 2.4 Hz, 1 H, H-8), 7.91 (d, J = 8.9 Hz, 1 H, H-5); **$^{13}\text{C-NMR}$** (75 MHz, DMSO): δ [ppm] = 13.8 (+, CH_3), 56.2 (+, O- CH_3), 62.5 (-, CH_2), 100.8 (+, C-8), 113.8 (+, C-3), 115.6 (+, C-6), 117.5 (C_{quat} , C-9), 126.7 (+, C-5), 151.5 (C_{quat} , C-2), 157.1 (C_{quat} , C-10), 159.9 (C_{quat} , C=O), 163.5 (C_{quat} , C-7), 176.1 (C_{quat} , C-4); **MS** (EI-MS, 70 eV) m/z (%): 248.1 (100) $[\text{M}]^{+}$; **Elemental Analysis**: $\text{C}_{13}\text{H}_{12}\text{O}_5$ Calc: C 62.9; H 4.87; Found: C 62.67; H 4.67

7-Methoxy-4-oxo-4H-chromene-2-carboxylic acid butylamide (13a)

Ethyl-7-methoxy-4-oxo-4H-chromene-2-carboxylate (590 mg, 2.4 mmol) and butylamine (512 mg, 7 mmol) were dissolved in dichloromethane (10 ml) and allowed to reflux for 10 minutes. The solvent was evaporated yielding a light yellow solid. Glacial acetic acid (10 ml) was added and allowed to stir at 70 °C for 10 minutes. The mixture was poured into ice water, the precipitate was filtered off, washed with water and dried. The solid was recrystallised from dichloromethane/diisopropylether (1:1) to yield white needles (562 mg, 2.0 mmol, 86 %).

MP: 130 °C; **IR** (KBr): $\tilde{\nu}$ (cm⁻¹) = 3349, 2959, 2869, 1655, 1610, 1357, 843; **UV/VIS** (MeOH): λ_{max} [nm] (log ϵ) = 212 (4.42), 236 (4.35), 255 (sh 4.10), 304 (4.04); **¹H-NMR** (300 MHz, CDCl₃): δ [ppm] = 0.97 (t, J = 7.3 Hz, 3 H, CH₃), 1.43 (qd, J = 7.3 Hz, 14.4 Hz, 2 H, CH₂), 1.64 (td, J = 7.3 Hz, 14.9 Hz, 2 H, CH₂), 3.48 (dd, J = 6.9 Hz, 13.4 Hz, 2 H, CH₂), 3.91 (s, 3 H, O-CH₃), 6.89 (d, J = 2.3 Hz, 1 H, H-8), 6.99 (dd, J = 1.9 Hz, 8.9 Hz, 1 H, H-6), 7.09 (s, 1 H, H-3), 8.10 (d, J = 8.9 Hz, 1 H, H-5); **¹³C-NMR** (75 MHz, CDCl₃): δ [ppm] = 13.8 (+, CH₃), 20.1 (-, CH₂), 31.5 (-, CH₂), 39.8 (-, CH₂), 56.0 (+, O-CH₃), 100.4 (+, C-8), 112.2 (+, C-3), 115.0 (+, C-6), 118.2 (C_{quat}, C-9), 127.4 (+, C-5), 154.6 (C_{quat}, C-2), 157.0 (C_{quat}, C-10), 159.3 (C_{quat}, C=O), 164.7 (C_{quat}, C-7), 177.5 (C_{quat}, C-4); **MS** (CI-MS, NH₃) m/z (%): 276.2 (100) [MH]⁺; **Elemental Analysis:** C₁₅H₁₇NO₄ Calc: C 65.44; H 6.22; N 5.09; Found: C 65.43; H 5.82; N 4.91

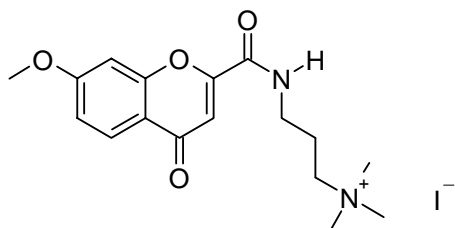
7-Methoxy-4-oxo-4H-chromene-2-carboxylic acid (3-dimethylamino-propyl)-amide (14a)



Ethyl-7-methoxy-4-oxo-4H-chromene-2-carboxylate (620 mg, 2.5 mmol) and 3-dimethylaminopropylamine (766 mg, 7.5 mmol) were dissolved in dichloromethane (10 ml) and the reaction mixture was refluxed for 1 hour. The solvent was evaporated, glacial acetic acid (10 ml) was added and the solution allowed to stir at 70 °C for 10 minutes. The mixture was added to ice water and extracted with ethyl acetate. The aqueous layer was neutralised with sodium hydrogen carbonate and extracted with ethyl acetate. The aqueous layer was made basic with sodium carbonate and extracted with ethyl acetate. The organic layer was dried over Na₂SO₄ and evaporated to give a yellow solid (654 mg, 2.1 mmol, 86 %).

MP: 127 - 128 °C; **IR** (KBr): $\tilde{\nu}$ (cm⁻¹) = 3440, 3257, 3032, 2950, 1667, 1630, 1442, 845; **¹H-NMR** (300 MHz, CDCl₃): δ [ppm] = 1.79 (td, J = 5.9 Hz, 11.8 Hz, 2 H, CH₂), 2.36 (s, 6 H, 2 x CH₃), 2.51 - 2.58 (m, 2 H, CH₂), 3.58 (td, J = 5.2 Hz, 5.9 Hz, 2 H, CH₂), 3.91 (s, 3 H, O-CH₃), 6.80 (d, J = 2.3 Hz, 1 H, H-5), 6.99 (dd, J = 2.3 Hz, 8.9 Hz, H-6), 7.05 (s, 1 H, H-3), 8.11 (d, J = 8.9 Hz, 1 H, H-8), 9.28 (s, 1 H, N-H); **¹³C-NMR** (75 MHz, CDCl₃): δ [ppm] = 24.8 (-, CH₂), 40.6 (-, CH₂), 45.6 (+, 2 x N-CH₃), 55.8 (+, O-CH₃), 59.2 (-, CH₂), 100.5 (+, C-8), 111.8 (+, C-3), 114.5 (+, C-6), 118.3 (C_{quat}, C-9), 127.5 (+, C-5), 155.1 (C_{quat}, C-2), 157.1 (C_{quat}, C-10), 159.2 (C_{quat}, C=O), 164.6 (C_{quat}, C-7), 177.7 (C_{quat}, C-4); **MS** (ESI, H₂O/AcN) m/z (%): 305.0 (100) [MH]⁺; **HRMS** (C₁₆H₂₀N₂O₄)⁺⁺ Calc: 304.1423; Found: 304.1421 ± 0.44 ppm

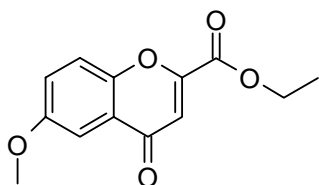
{3-[(7-Methoxy-4-oxo-4H-chromene-2-carbonyl)-amino]-propyl}-trimethyl-ammonium iodide (15a)



7-Methoxy-4-oxo-4H-chromene-2-carboxylic acid (3-dimethylamino-propyl)-amide (456 mg, 1.5 mmol) was dissolved in chloroform (10 ml), iodomethane (284 mg, 2 mmol) added and the reaction mixture was allowed to stir at RT for 1 hour. The solution was heated to reflux for 10 min, the formed precipitate filtered off and washed with chloroform. The precipitate was dried yielding a white solid (575 mg, 1.3 mmol, 86 %).

MP: 208 °C (decomposition); **IR** (KBr): $\tilde{\nu}$ (cm⁻¹) = 3490, 3411, 3257, 3012, 2954, 1676, 1633, 1604, 1442, 848; **UV/VIS** (CH₃CN): λ_{max} [nm] (log ϵ) = 210 (4.47), 242 (4.32), 304 (3.80); **¹H-NMR** (600 MHz, DMSO): δ [ppm] = 1.97 - 2.03 (m, 2 H, CH₂), 3.07 (s, 9 H, 3 x CH₃), 3.35 - 3.39 (m, 2 H, CH₂), 3.36 - 3.41 (m, 2 H, CH₂), 3.93 (s, 3 H, O-CH₃), 6.78 (s, 1 H, H-3), 7.13 (dd, J = 2.4 Hz, 8.9 Hz, H-6), 7.18 (d, J = 2.4 Hz, 1 H, H-8), 7.97 (d, J = 8.9 Hz, 1 H, H-5), 9.19 (s, 1 H, N-H); **¹³C-NMR** (150 MHz, DMSO): δ [ppm] = 22.7 (-, CH₂), 36.3 (-, CH₂), 52.2 (+, 3 x N-CH₃), 56.1 (+, O-CH₃), 63.3 (-, CH₂), 100.8 (+, C-8), 110.6 (+, C-3), 115.3 (+, C-6), 117.5 (C_{quat}, C-9), 126.5 (+, C-5), 155.1 (C_{quat}, C-2), 156.9 (C_{quat}, C-10), 159.3 (C_{quat}, C=O), 164.3 (C_{quat}, C-7), 176.4 (C_{quat}, C-4); **MS** (ESI, H₂O/AcN) m/z (%): 319.0 (100) [M]⁺; **HRMS** (C₁₇H₂₃N₂O₄)⁺ Calc: 319.1657; Found: 319.1661 \pm 1.16 ppm

6-Methoxy-4-oxo-4H-chromene-2-carboxylic acid ethyl ester (12b)

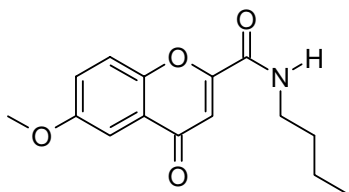


Sodium (1.49 g, 65 mmol) was dissolved in absolute ethanol (100 ml). Diethyloxalate (5.12 g, 35 mmol) and 2-hydroxy-5-methoxyacetophenone (2.49 g, 15 mmol) were dissolved in absolute ethanol (10 ml) and added to the sodium ethanolate solution. The solution was allowed to reflux for 1 hour. Concentrated HCl was added dropwise until the

reaction was acidic and a white precipitate formed. The white precipitate was filtered off and the yellow solution was concentrated to a slurry. The slurry was extracted with ethyl acetate, dried over Na₂SO₄ and evaporated to give a light yellow solid. The solid was recrystallised from methanol/diisopropylether (3:1) to yield a yellow solid (3.66 g, 14.8 mmol, 98 %).

MP: 98 °C; **IR** (KBr): $\tilde{\nu}$ (cm⁻¹) = 3455, 3114, 3078, 2984, 2844, 1740, 1657, 1610, 1488, 1288, 839; **UV/VIS** (MeOH): λ_{max} [nm] (log ϵ) = 206 (4.45), 238 (4.22), 253 (4.31), 343 (3.77); **¹H-NMR** (600 MHz, CDCl₃): δ [ppm] = 1.42 (t, J = 7.1 Hz, 3 H, CH₃), 3.89 (s, 3 H, O-CH₃), 4.45 (q, J = 7.1 Hz, 2 H, CH₂), 7.10 (s, 1 H, H-3), 7.32 (dd, J = 3.2 Hz, 9.2 Hz, 1 H, H-7), 7.53 (dd, J = 0.4 Hz, 3.2 Hz, 1 H, H-5), 7.54 (dd, J = 0.4 Hz, 9.2 Hz, 1 H, H-8); **¹³C-NMR** (150 MHz, CDCl₃): δ [ppm] = 14.1 (+, CH₃), 56.0 (+, O-CH₃), 62.9 (-, CH₂), 104.6 (+, C-5), 113.8 (+, C-3), 120.2 (+, C-8), 125.0 (+, C-7), 125.2 (C_{quat}, C-9), 150.8 (C_{quat}, C-10), 152.0 (C_{quat}, C-2), 157.5 (C_{quat}, C-6), 160.6 (C_{quat}, C=O), 178.3 (C_{quat}, C-4); **MS** (PI-EIMS, 70 eV) m/z (%): 248.0 (100) [M]⁺⁺; **Elemental Analysis:** C₁₃H₁₂O₅ Calc: C 62.90; H 4.87; Found: C 62.67; H 4.66

6-Methoxy-4-oxo-4H-chromene-2-carboxylic acid butylamide (13b)

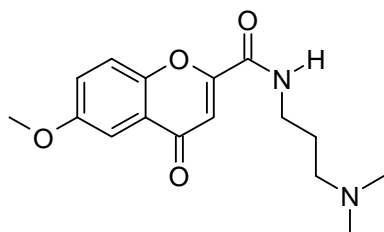


Ethyl-6-methoxy-4-oxo-4H-chromene-2-carboxylate (590 mg, 2.4 mmol) and butylamine (512 mg, 7 mmol) were dissolved in dichloromethane (10 ml) and the reaction mixture was refluxed for 10 minutes. The solvent was evaporated upon which a light yellow solid formed. Glacial acetic acid (10 ml) was added and allowed to stir at 70 °C for 10 minutes. The mixture was added to ice water, the precipitate was filtered off, washed with water and dried. The solid was recrystallised from dichloromethane/diisopropylether (1:3) to yield white needles (572 mg, 2.1 mmol, 87 %).

MP: 146 °C; **IR** (KBr): $\tilde{\nu}$ (cm⁻¹) = 3305, 3091, 2956, 2869, 1639, 1610, 1359, 833; **UV/VIS** (MeOH): λ_{max} [nm] (log ϵ) = 205 (4.43), 230 (4.25), 252 (4.36), 338 (3.75); **¹H-NMR** (300 MHz, CDCl₃): δ [ppm] = 0.98 (t, J = 7.3 Hz, 3 H, CH₃), 1.43 (qd, J = 7.3

Hz, 14.3 Hz, 2 H, CH₂), 1.65 (td, J = 7.3 Hz, 14.9 Hz, 2 H, CH₂), 3.49 (dd, J = 7.1 Hz, 13.3 Hz, 2 H, CH₂), 3.90 (s, 3 H, O-CH₃), 7.15 (s, 1 H, H-3), 7.31 (dd, J = 3.1 Hz, 9.2 Hz, 1 H, H-7), 7.45 (d, J = 9.2 Hz, 1 H, H-8), 7.56 (d, J = 3.0 Hz, 1 H, H-5); ¹³C-NMR (75 MHz, CDCl₃): δ [ppm] = 13.8 (+, CH₃), 20.1 (-, CH₂), 31.5 (-, CH₂), 39.8 (-, CH₂), 56.0 (+, O-CH₃), 105.1 (+, C-5), 111.2 (+, C-3), 119.4 (+, C-8), 124.6 (+, C-7), 125.1 (C_{quat}, C-9), 150.0 (C_{quat}, C-10), 154.6 (C_{quat}, C-2), 157.5 (C_{quat}, C-6), 159.3 (C_{quat}, C=O), 178.1 (C_{quat}, C-4); **MS** (CI-MS, NH₃) m/z (%): 276.2 (100) [MH]⁺; **Elemental Analysis**: C₁₅H₁₇NO₄ Calc: C 65.44; H 6.22; N 5.09; Found: C 65.33; H 5.92; N 4.80

6-Methoxy-4-oxo-4H-chromene-2-carboxylic acid (3-dimethylamino-propyl)-amide (14b)

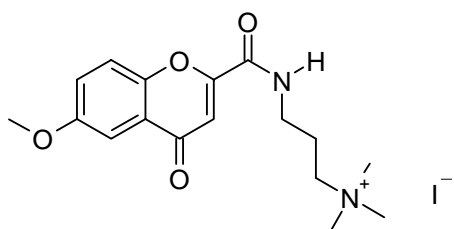


Ethyl-6-methoxy-4-oxo-4H-chromene-2-carboxylate (620 mg, 2.5 mmol) and 3-dimethylaminopropylamine (766 mg, 7.5 mmol) were dissolved in dichloromethane (10 ml) and the reaction mixture was refluxed for 1 hour. The solvent was evaporated, glacial acetic acid (10 ml) was added and the solution allowed to stir at 70 °C for 10 minutes. The mixture was added to ice water and extracted with ethyl acetate. The aqueous layer was neutralised with sodium hydrogen carbonate and extracted with ethyl acetate. The aqueous layer was made basic with sodium carbonate and extracted with ethyl acetate. The organic layer was dried over Na₂SO₄ and evaporated to give a yellow solid (615 mg, 2.1 mmol, 81 %).

MP: 108-109 °C; **IR** (KBr): $\tilde{\nu}$ (cm⁻¹) = 3434, 3305, 3041, 2945, 1680, 1641, 1385, 830; ¹H-NMR (300 MHz, DMSO): δ [ppm] = 1.68 (p, J = 6.9 Hz, 2 H, CH₂), 2.15 (s, 6 H, 2 x CH₃), 2.28 (t, J = 6.9 Hz, 2 H, CH₂), 3.32 (dd, J = 6.9 Hz, 13.3 Hz, 2 H, CH₂), 3.86 (s, 3 H, O-CH₃), 6.79 (s, 1 H, H-3), 7.40 (d, J = 3.1 Hz, 1 H, H-5), 7.48 (dd, J = 3.1 Hz, 9.1 Hz, 1 H, H-7), 7.66 (d, J = 9.1 Hz, 1 H, H-8), 9.23 (t, J = 5.6 Hz, 1 H, N-H); ¹³C-NMR (75 MHz, DMSO): δ [ppm] = 26.4 (-, CH₂), 37.9 (-, CH₂), 45.0 (+, 2 x CH₃), 55.7 (+, O-CH₃), 56.8 (-, CH₂), 104.5 (+, C-5), 109.3 (+, C-3), 120.2 (+, C-8), 124.1 (+, C-7), 124.3 (C_{quat}, C-9),

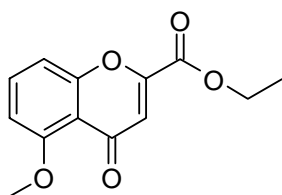
149.6 (C_{quat} , C-10), 155.4 (C_{quat} , C-2), 156.8 (C_{quat} , C-6), 158.7 (C_{quat} , C=O), 176.9 (C_{quat} , C-4); **MS** (CI-MS, NH_3) m/z (%): 305.2 (100) $[\text{MH}]^+$; **HRMS** ($\text{C}_{16}\text{H}_{20}\text{N}_2\text{O}_4$) $^{+}$ Calc: 304.1423; Found: 304.1425 \pm 0.71 ppm

{3-[(6-Methoxy-4-oxo-4H-chromene-2-carbonyl)-amino]-propyl}-trimethyl-ammonium iodide (15b)



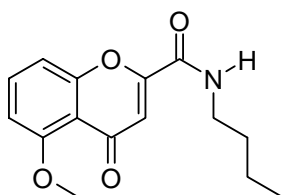
6-Methoxy-4-oxo-4H-chromene-2-carboxylic acid (3-dimethylamino-propyl)-amide (456 mg, 1.5 mmol) was dissolved in chloroform (10 ml), iodomethane (284 mg, 2 mmol) was added and the reaction mixture was allowed to stir at RT for 1 hour. The solution was heated to reflux for 10 min, the formed precipitate filtered off and washed with chloroform. The precipitate was dried yielding a white solid (620 mg, 1.4 mmol, 93 %).

MP: 240 °C +; **IR** (KBr): $\tilde{\nu}$ (cm^{-1}) = 3422, 3298, 3031, 3013, 2945, 1680, 1651, 1615, 1485, 828; **UV/VIS** (CH_3CN): λ_{max} [nm] (log ϵ) = 205 (4.42), 248 (4.34), 333 (3.54); **$^1\text{H-NMR}$** (300 MHz, DMSO): δ [ppm] = 1.93 - 2.06 (m, 2 H, CH_2), 3.07 (s, 9 H, 3 x CH_3), 3.30 - 3.41 (m, 4 H, 2 x CH_2), 3.87 (s, 3 H, O- CH_3), 6.83 (s, 1 H, H-3), 7.42 (d, J = 3.1 Hz, 1 H, H-5), 7.51 (dd, J = 3.1 Hz, 9.2 Hz, 1 H, H-7), 7.70 (d, J = 9.2 Hz, 1 H, H-8), 9.24 (t, J = 5.9 Hz, 1 H, N-H); **$^{13}\text{C-NMR}$** (75 MHz, DMSO): δ [ppm] = 22.6 (-, CH_2), 36.2 (-, CH_2), 52.1 (+, 3 x CH_3), 55.7 (+, O- CH_3), 63.2 (-, CH_2), 104.5 (+, C-5), 109.5 (+, C-3), 120.3 (+, C-8), 124.2 (+, C-7), 124.3 (C_{quat} , C-9), 149.6 (C_{quat} , C-10), 155.1 (C_{quat} , C-2), 156.8 (C_{quat} , C-6), 159.2 (C_{quat} , C=O), 176.9 (C_{quat} , C-4); **MS** (ESI, $\text{H}_2\text{O}/\text{AcN}$) m/z (%): 319.0 (100) $[\text{M}]^+$; **Elemental Analysis**: $\text{C}_{17}\text{H}_{23}\text{N}_2\text{O}_4\text{I}$ Calc: C 45.75; H 5.19; N 6.28; Found: C 45.40; H 5.14; N 6.51; **HRMS** ($\text{C}_{17}\text{H}_{23}\text{N}_2\text{O}_4$) $^{+}$ Calc: 319.1658; Found: 319.1660 \pm 0.76 ppm

5-Methoxy-4-oxo-4H-chromene-2-carboxylic acid ethyl ester (12c)^[68]


Sodium (1.49 g, 65 mmol) was dissolved in absolute ethanol (100 ml). Diethyloxalate (5.12 g, 35 mmol) and 2-hydroxy-6-methoxyacetophenone (2.49 g, 15 mmol) were dissolved in absolute ethanol (10 ml) and added to the sodium ethanolate solution. The solution was allowed to reflux for 1 hour. Concentrated HCl was added dropwise until the reaction was acidic and a white precipitate formed. The white precipitate was filtered off and the yellow solution concentrated to a slurry. The slurry was extracted with ethyl acetate, dried over Na₂SO₄ and evaporated to give a light yellow solid. The solid was recrystallised from methanol/diisopropylether (2:1) to yield a yellow solid (2.99 g, 12.1 mmol, 80 %).

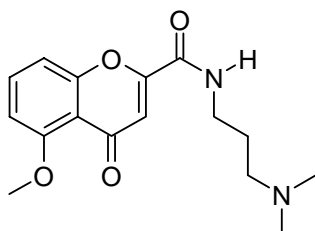
MP: 124 °C; **IR** (KBr): $\tilde{\nu}$ (cm⁻¹) = 3433, 3084, 2988, 2844, 1728, 1659, 1507, 1478, 1269, 800; **UV/VIS** (MeOH): λ_{max} [nm] (log ϵ) = 238 (4.22), 271 (4.00), 327 (3.64); **¹H-NMR** (300 MHz, CDCl₃): δ [ppm] = 1.40 (t, J = 7.1 Hz, 3 H, CH₃), 3.97 (s, 3 H, O-CH₃), 4.42 (q, J = 7.1 Hz, 2 H, CH₂), 6.83 (d, J = 8.5 Hz, 1 H, H-6), 6.99 (s, 1 H, H-3), 7.14 (dd, J = 0.9 Hz, 8.5 Hz, 1 H, H-8), 7.59 (t, J = 8.5 Hz, 1 H, H-7); **¹³C-NMR** (75 MHz, CDCl₃): δ [ppm] = 14.1 (+, CH₃), 56.5 (+, O-CH₃), 62.8 (-, CH₂), 106.9 (+, C-6), 110.6 (+, C-8), 115.3 (C_{quat}, C-9), 116.5 (+, C-3), 134.7 (+, C-7), 150.3 (C_{quat}, C-2), 158.0 (C_{quat}, C-10), 159.8 (C_{quat}, C-5), 160.6 (C_{quat}, C=O), 178.0 (C_{quat}, C-4); **MS** (PI-EIMS, 70 eV) m/z (%): 248.0 (100) [M]⁺; **Elemental Analysis:** C₁₃H₁₂O₅ Calc: C 62.90; H 4.87; Found: C 62.84; H 4.75

5-Methoxy-4-oxo-4H-chromene-2-carboxylic acid butylamide (13c)

Ethyl-5-methoxy-4-oxo-4H-chromene-2-carboxylate (590 mg, 2.4 mmol) and butylamine (512 mg, 7 mmol) were dissolved in dichloromethane (10 ml) and the reaction mixture was allowed to reflux for 10 minutes. The solvent was evaporated giving a light yellow solid. Glacial acetic acid (10 ml) was added, the solution was allowed to stir at 70 °C for 10 min, added to ice water, the precipitate filtered off, washed with water and dried. The solid was recrystallised from dichloromethane/diisopropylether (2/1) to yield white needles (607 mg, 2.2 mmol, 93 %).

MP: 128 °C; **IR** (KBr): $\tilde{\nu}$ (cm⁻¹) = 3314, 3090, 2961, 1650, 1605, 1387, 794; **UV/VIS** (MeOH): λ_{max} [nm] (log ϵ) = 238 (4.29), 260 (4.16), 323 (3.71); **¹H-NMR** (300 MHz, CDCl₃): δ [ppm] = 0.96 (t, J = 7.3 Hz, 3 H, CH₃), 1.35 - 1.47 (m, 2 H, CH₂), 1.63 (td, J = 7.3 Hz, 15.0 Hz, 2 H, CH₂), 3.47 (dd, J = 6.8 Hz, 13.6 Hz, 2 H, CH₂), 3.97 (s, 3 H, O-CH₃), 6.84 (d, J = 8.4 Hz, 1 H, H-6), 7.03 (s, 1 H, H-3), 7.05 (d, J = 8.4 Hz, 1 H, H-8), 7.60 (t, J = 8.4 Hz, 1 H, H-7); **¹³C-NMR** (75 MHz, CDCl₃): δ [ppm] = 13.8 (+, CH₃), 20.1 (-, CH₂), 31.5 (-, CH₂), 39.7 (-, CH₂), 56.6 (+, O-CH₃), 107.0 (+, C-6), 109.8 (+, C-8), 113.7 (+, C-3), 115.0 (C_{quat}, C-9), 134.5 (+, C-7), 152.8 (C_{quat}, C-2), 157.3 (C_{quat}, C-10), 159.2 (C_{quat}, C-5), 160.1 (C_{quat}, C=O), 177.9 (C_{quat}, C-4); **MS** (CI-MS, NH₃) m/z (%): 276.1 (100) [MH]⁺; **Elemental Analysis:** C₁₅H₁₇NO₄ Calc: C 65.44; H 6.22; N 5.09; Found: C 65.40; H 6.00; N 4.96

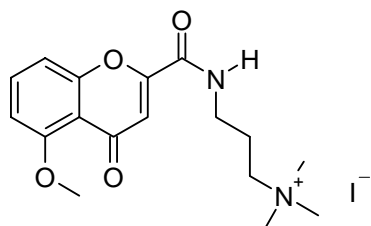
5-Methoxy-4-oxo-4H-chromene-2-carboxylic acid (3-dimethylamino-propyl)-amide (14c)



Ethyl-5-methoxy-4-oxo-4H-chromene-2-carboxylate (620 mg, 2.5 mmol) and 3-dimethylaminopropylamine (766 mg, 7.5 mmol) were dissolved in dichloromethane (10 ml) and the reaction mixture was refluxed for 1 hour. The solvent was evaporated, glacial acetic acid (10 ml) was added and the solution allowed to stir at 70 °C for 10 minutes. The mixture was added to ice water and extracted with ethyl acetate. The aqueous layer was neutralised with sodium hydrogen carbonate and extracted with ethyl acetate. The aqueous layer was made basic with sodium carbonate and extracted with ethyl acetate. The organic layer was dried over Na₂SO₄ and evaporated to give a yellow solid (627 mg, 2.1 mmol, 83 %).

MP: 87 - 88 °C; **IR** (KBr): $\tilde{\nu}$ (cm⁻¹) = 3420, 3312, 3080, 2955, 1650, 1603, 798; **¹H-NMR** (300 MHz, DMSO): δ [ppm] = 1.67 (p, J = 6.9 Hz, 2 H, CH₂), 2.15 (s, 6 H, 2 x CH₃), 2.27 (t, J = 6.9 Hz, 2 H, CH₂), 3.31 (dd, J = 6.9 Hz, 13.3 Hz, 2 H, CH₂), 3.86 (s, 3 H, O-CH₃), 6.61 (s, 1 H, H-3), 7.02 (d, J = 8.4 Hz, 1 H, H-6), 7.20 (dd, J = 0.7 Hz, 8.4 Hz, 1 H, H-8), 7.75 (t, J = 8.4 Hz, 1 H, H-7), 9.17 (t, J = 5.6 Hz, 1 H, N-H); **¹³C-NMR** (75 MHz, DMSO): δ [ppm] = 26.4 (-, CH₂), 37.9 (-, CH₂), 45.0 (+, 2 x CH₃), 56.0 (+, O-CH₃), 56.8 (-, CH₂), 107.4 (+, C-6), 109.9 (+, C-8), 111.8 (+, C-3), 114.0 (C_{quat}, C-9), 134.9 (+, C-7), 153.3 (C_{quat}, C-2), 156.9 (C_{quat}, C-10), 158.7 (C_{quat}, C-5), 159.1 (C_{quat}, C=O), 176.4 (C_{quat}, C-4); **MS** (CI-MS, NH₃) m/z (%): 305.2 (100) [MH]⁺; **HRMS** (C₁₆H₂₀N₂O₄)⁺ Calc: 304.1424; Found: 304.1425 ± 1.1 ppm

{3-[(5-Methoxy-4-oxo-4H-chromene-2-carbonyl)-amino]-propyl}-trimethyl-ammonium iodide (15c)



5-Methoxy-4-oxo-4H-chromene-2-carboxylic acid (3-dimethylamino-propyl)-amide (456 mg, 1.5 mmol) was dissolved in chloroform (10 ml), iodomethane (284 mg, 2 mmol) was added and the reaction mixture was allowed to stir at RT for 1 hour. The solution was heated to reflux for 10 min, the formed precipitate filtered off and washed with chloroform. The precipitate was dried yielding a white solid (625 mg, 1.4 mmol, 93 %).

MP: 240 °C +; **IR** (KBr): $\tilde{\nu}$ (cm⁻¹) = 3433, 3244, 3018, 2940, 1683, 1650, 1602, 1475, 802; **UV/VIS** (CH₃CN): λ_{max} [nm] (log ϵ) = 242 (4.25), 319 (3.53); **¹H-NMR** (300 MHz, DMSO): δ [ppm] = 1.92 - 2.04 (m, 2 H, CH₂), 3.06 (s, 9 H, 3 x CH₃), 3.30 - 3.41 (m, 4 H, 2 x CH₂), 3.87 (s, 3 H, O-CH₃), 6.65 (s, 1 H, H-3), 7.04 (d, J = 8.4 Hz, 1 H, H-6), 7.23 (dd, J = 0.7 Hz, 8.4 Hz, 1 H, H-8), 7.77 (t, J = 8.4 Hz, 1 H, H-7), 9.17 (t, J = 5.9 Hz, 1 H, N-H); **¹³C-NMR** (75 MHz, DMSO): δ [ppm] = 22.6 (-, CH₂), 36.2 (-, CH₂), 52.1 (+, 3 x CH₃), 56.1 (+, O-CH₃), 63.2 (-, CH₂), 107.5 (+, C-6), 109.9 (+, C-8), 112.0 (+, C-3), 114.0 (C_{quat}, C-9), 135.0 (+, C-7), 153.1 (C_{quat}, C-2), 156.9 (C_{quat}, C-10), 159.1 (C_{quat}, C-5), 159.2 (C_{quat}, C=O), 176.3 (C_{quat}, C-4); **MS** ESI, H₂O/AcN) m/z (%): 319.0 (100) [M]⁺; **HRMS** (C₁₇H₂₃N₂O₄)⁺ Calc: 319.1658; Found: 319.1660 ± 1.02 ppm

4.5 References

- [1] Barton, D.; Ollis, W. D. *Comprehensive Organic Chemistry*, Vol. 4, Pergamon Press, Oxford, **1979**
- [2] Ya Sosnovskikh, V. *Russian. Chem. Rev.* **2003**, 72, 489
- [3] Ellis, G. P. in *The Chemistry of Heterocyclic Compounds*, Vol. 31, Wiley, New York, **1977**, 749
- [4] For a review of the biological activities and synthesis of chromone derivatives see Horton, D. A.; Bourne, G. T.; Smythe, M. L. *Chem. Rev.* **2003**, 103, 893
- [5] Hadjeri, M.; Barbier, M.; Ronot, X.; Mariotte, A.-M.; Boumendjel, A.; Boutonnat, J. *J. Med. Chem.* **2003**, 46, 2125
- [6] Ellis, G. P.; Barker, G. *Progr. Med. Chem.* **1972**, 9, 65
- [7] Beecher, G. R.; *J. Nutri.* **2003**, 133, 3248S
- [8] Hoult, J. R. S.; Moroney, M. A.; Paya, M. *Methods Enzymol.* **1994**, 234, 443
- [9] Ferrali, M.; Signorini, C.; Caciotti, B.; Sugherini, L.; Ciccoli, L.; Giachetti, D.; Comporti, M. *FEBS Lett.* **1997**, 416, 123
- [10] Elliott, A. J.; Scheiber, S. A.; Thomas, C.; Pardini, R. S. *Biochem. Pharmacol.* **1992**, 44, 1603
- [11] Hirano, R.; Sasamoto, W.; Matsumoto, A.; Itakura, H.; Igarashi, O.; Kondo, K. *J. Nutri. Sci. Vitaminol.* **2001**, 47, 357
- [12] Cos, P.; Ying, L.; Calomme, M.; Hu, J. P.; Cimanga, K.; Van Poel, B.; Pieters, L.; Vlietnck, A. J.; Vanden Berghe, D. *J. Nat. Prod.* **1998**, 61, 71
- [13] Williams, R. J.; Spencer, J. P. E.; Rice-Evans, C. *Free Radic. Biol. Med.* **2004**, 36, 838
- [14] Rice-Evans, C. *Curr. Med. Chem.* **2001**, 8, 797
- [15] Rice-Evans, C.; Miller, N. J.; Paganga, G. *Free Radic. Biol. Med.* **1996**, 20, 933
- [16] Rice-Evans, C. *Biochem. Soc. Symp.* **1995**, 61, 103
- [17] Spencer, J. P. E.; Schroeter, H.; Crossthwaithe, A. J.; Kuhnle, G.; Williams, R. J.; Rice-Evans, C. *Free Radic. Biol. Med.* **2001**, 31, 1139
- [18] Spencer, J. P. E.; Schroeter, H.; Kuhnle, G.; Srai, S. K.; Tyrrell, R. M.; Hahn, U.; Rice-Evans, C. *Biochem. J.* **2001**, 354, 493
- [19] Schroeter, H.; Spencer, J. P.; Rice-Evans, C.; Williams, R. J. *Biochem. J.* **2001**, 358, 547

-
- [20] Spencer, J. P. E.; Schroeter, H.; Rechner, A. R.; Rice-Evans, C. *Antioxid. Redox Signal.* **2001**, *3*, 1023
- [21] Spencer, J. P. E.; Srai, S. K.; Rice-Evans, C. Metabolism in the small intestine and gastrointestinal tract. In: Rice-Evans, C.; Packer, L., eds. *Flavonoids in health and disease*. Marcel Dekker, New York; **2003**, 363
- [22] Walle, T.; Walgren, R. A.; Walle, U. K.; Galijatovic, A.; Vaidyanathan, J. B. Understanding the bioavailability of flavonoids through studies in Caco-2 cells. In: Rice-Evans, C.; Packer, L., eds. *Flavonoids in health and disease*. Marcel Dekker, New York; **2003**, 349
- [23] Day, A. J.; Williamson, G. Absorption of quercetin glycosides. In: Rice-Evans, C.; Packer, L., eds. *Flavonoids in health and disease*. Marcel Dekker, New York; **2003**, 31
- [24] Donovan, J. L.; Waterhouse, A. L. Bioavailability of flavanol monomers. In: Rice-Evans, C.; Packer, L., eds. *Flavonoids in health and disease*. Marcel Dekker, New York; **2003**, 413
- [25] Pietta, P.-G. *J. Nat. Prod.* **2000**, *63*, 1035
- [26] Amić, D.; Davidović-Amić, D.; Bešlo, D.; Trinajstić, N. *Croatica. Chemica Acta* **2003**, *76*, 55
- [27] Heim, K. E.; Tagiaferro, A. R.; Bobilya, D. J. *J. Nutri. Biochem.* **2002**, *13*, 572
- [28] Bors, W.; Heller, W.; Michel, C.; Saran, M. *Methods Enzymol.* **1990**, *186*, 343
- [29] van Acker, S. A. B. E.; van den Berg, D. J.; Tromp, M. N. J. L.; Griffioen, D. H.; van der Vijgh, W. J. F.; Bast, A. *Free Radic. Biol. Med.* **1996**, *20*, 331
- [30] Karlsson, J. Introduction to Nutraology and Radical Formation. In: Antioxidants and Exercise. Illinois, Human Kinetics Press, 1997, p 1-143
- [31] Davies, K. J. *Biochem. Soc. Symp.* **1995**, *61*, 1
- [32] Sastre, J.; Pallardo, F. V.; Vina, J. *IUBMB Life* **2000**, *49*, 427
- [33] Takabe, W.; Niki, E.; Uchida, K.; Yamada, S.; Satoh, K.; Noguchi, N. *Carcinogenesis* **2001**, *21*, 935
- [34] Kawanishi, S.; Hiraku, Y.; Oikawa, S. *Mutat. Res.* **2001**, *488*, 65
- [35] Khan, M. A.; Baseer, A. *J. Pak. Med. Assoc.* **2000**, *50*, 261
- [36] Middleton, E.; Kandaswami, C. *Biochem. Pharmacol.* **1992**, *43*, 1167
- [37] Kuresh, A.; Shukitt-Hale, B.; Joseph, J. A. *Free Radic. Biol. Med.* **2004**, *37*, 1683
- [38] Korkina, L. G.; Afans'ev, I. B. *Adv. Pharmacol.* **1997**, *38*, 151
- [39] Shirley, B. W. *Trends Plant Sci.* **1996**, *31*, 377

-
- [40] Kootstra, A. *Plant Mol. Biol.* **1994**, 26, 771
- [41] Nogueira, A. C. S.; Joeke, I. J. *Photochem. Photobiol. B: Biol.* **2004**, 74, 109
- [42] Robbins, C. R. *Chemical and Physical Behaviour of Human Hair*. 4th Ed., New York, Springer, 2002
- [43] Tolgyesi, E. *Cosmet. Toiletr.* **1983**, 98, 29
- [44] Nguyen, N. V.; Cannell, D. W.; Mathews, R. A.; Oei, H. H. Y. *J. Soc. Cosmet. Chem.* **1992**, 43, 259
- [45] Bantick, J. R.; Cairns, H.; Chambers, A.; Hazard, R.; King, J.; Lee, T. B.; Minshall, R. *J. Med. Chem.* **1976**, 19, 817
- [46] Leahy, J. J. J.; Golding, B. T.; Griffin, R. J.; Hardcastle, I. R.; Richardson, C.; Rigoreau, L.; Smith, G. C. M. *Bioorg. Med. Chem. Lett.* **2004**, 14, 6083
- [47] Harikrishnan, L. S.; Showalter, H. D. H. *Tetrahedron* **2000**, 56, 515
- [48] Miao, H.; Yang, Z. *Org. Lett.* **2000**, 2, 1765
- [49] Nakatani, K.; Okamoto, A.; Yamanuki, M.; Saito, I. *J. Org. Chem.* **1994**, 59, 4360
- [50] Wiese, M.; Pajeva, I. K. *Curr. Med. Chem.* **2001**, 8, 685
- [51] Ahmad, R.; Saá, J. M.; Cava, M. P. *J. Or. Chem.* **1977**, 42, 1228
- [52] Gray, C. A.; Kaye, P. T.; Nchinda, A. T. *J. Nat. Prod.* **2003**, 66, 1144
- [53] Kitagawa, M.; Yamamoto, K.; Katakura, S.; Kanno, H.; Yamada, K.; Nagahara, T.; Tanaka, M. *Chem. Pharm. Bull.* **1991**, 39, 2681
- [54] Horie, T.; Kobayashi, T.; Kawamura, Y.; Yoshida, I.; Tominaga, H.; Yamashita, K. *Bull. Chem. Soc. Jpn.* **1995**, 68, 2033; Kawamura, Y.; Takatsuki, H.; Torii, F.; Horie, T. *Bull. Chem. Soc. Jpn.* **1994**, 67, 511
- [55] Monteiro, V. F.; Natal, A. M. D.; Soledade, L. E. B.; Longo, E. *Mater. Res.* **2003**, 6, 501
- [56] Wortmann, F.-J.; Gotsche, M.; Schmidt-Lewerkühne, H. *Int. J. Cos. Sci.* **2004**, 26, 61
- [57] Kelch, A.; Wessel, S.; Will, T.; Hintze, U.; Wepf, R.; Wiesendanger, R. *J. Microscopy*, **2000**, 200, 179
- [58] The compound was dissolved in ethanol:water (70:30), commercially available, washed, sterile human hair was added and allowed to stir at room temperature for one hour. Samples (100 µl) were taken at 0 min (before the addition of the hair), 5 min, 15 min and 60 min and UV absorption was measured. Parallel to this, samples were taken from a solution containing only hair (and no active substance) and used

as a reference. No changes in UV absorption within experimental error were noted, regardless of substance tested or hair type (brown or bleached hair).

After 60 min the hair was filtered and washed three times with fresh solvent. The hair sample was dried overnight at 40 °C and 200 mbar, placed into a crucible containing liquid nitrogen and ground to a fine powder. Due to the small quantities of substance on the hair, IR analysis of the ground sample could not confirm the presence of the substance when compared to the reference (for neither brown nor bleached hair).

- [59] A sample of the treated hair (bleached) and the corresponding reference sample were analysed using MALDI-MS. Here a definite peak at M^+ can be seen, when compared to the reference sample.
- [60] Hubbard, D. L.; Wilkins, D. G.; Rollins, D. E. *Drug Metab. Dispos.* **2000**, 28, 1464; Haasnoot, W.; Stouten, P.; Schilt, R.; Hooijerink, D. *Analyst* **1998**, 123, 2707; Nielen, M. W. F.; Hooijerink, H.; Essers, M. L.; Lasaroms, J. J. P.; van Bennekom, E. O.; Brouwer, L. *Anal. Chim. Acta* **2003**, 483, 11
- [61] Hosseinimehr, S. J.; Shafiee, A.; Mozdarani, H.; Akhlagpour, S.; Froughizadeh, M. *J. Radiat. Res.* **2002**, 43, 293
- [62] Jovanovic, S. V.; Steenken, S.; Tomic, M.; Marjanovic, B.; Simic, M. G. *J. Am. Chem. Soc.* **1994**, 116, 4846
- [63] Speiser, B. *Chemie in unsere Zeit* **1981**, 15, 62
- [64] Heinze, J. *Angew. Chem.* **1984**, 96, 823
- [65] Hünig, S.; Märkl, G.; Sauer, J. *Einführung in die apparativen Methoden in der Organischen Chemie*, 2nd Edition, Würzburg, Regensburg, **1994**
- [66] Author Collective, *Organikum*, 17th Edition, VEB Deutscher Verlag der Wissenschaften, Berlin, **1988**
- [67] Hair was purchased from Kerling International Haarfabrik GmbH - bleached European hair (washed) and natural light-middle brown European hair (washed). The hair was cut into 0.4 to 0.7 cm pieces prior to use.
- [68] Has been previously synthesised: Ellis, G. P.; Shaw, D. *J. Med. Chem.* **1972**, 15, 865
- [69] Has been previously synthesised: Fiton, A. O; Hatton, B. T. *J. Chem. Soc. C: Org.* **1970**, 18, 2609

5. Appendix

Patents and Publications

Walencyk, T.; Koenig, B. Immobilised zinc (II) cyclen complexes as catalytic reagents for phosphodiester hydrolysis. *Chim. Inorg. Acta.* **2005**, 358, 2269

Walencyk, T.; Carola, C.; Buchholz, H. Synthesis of colloidal silica containing covalently bonded chromophores. *Eur. Pat. Appl.* **2004**, EP 04013515.4

Walencyk, T.; Buchholz, H.; Carola, C.; Koenig, B. Synthesis of mono-dispersed spherical silica particles containing covalently bonded chromophores. *Int. J. Cos. Sci.* **2005**, 27, 1-14

Walencyk, T.; Carola, C.; Roskopf, R.; Buchholz, H. Chromone derivatives which bind to hair. *Germ. Pat. Appl.* **2005**, DE 102005011534.9

Walencyk, T.; Buchholz, H.; Carola, C.; Koenig, B. Chromone derivative which bind to hair. *Tetrahedron* **2005**, submitted

Klein, M.; Walencyk, T.; Koenig, B. Electronic effects of the Bergman Cyclisation of enediynes. A Review. *Collect. Czech. Chem. Commun.* **2003**, 69, 945

Conferences and Presentations

- 10.2001 DECHEMA “Chemical Nanotechnology Talks II”
Frankfurt a.M., Germany
- 10.2002 International Quality Network 1st Summer School “Medicinal Chemistry”
Regensburg, Germany
- 06.2003 Symposium “Molecular Recognition”
Prag, Czech Republic
- 06.2004 DECHEMA “Nano 2004”
Wiesbaden, Germany (Poster Presentation)
- 10.2004 International Quality Network 2nd Summer School “Medicinal Chemistry”
Regensburg, Germany (Poster Presentation)
- 12.2004 Institute for Organic Chemistry “Christmas Colloquium”
Regensburg, Germany (Oral Presentation)

Curriculum Vitae

Personal Details

Name: Thomas Walenzyk
Date of Birth: 02.08.1977
Place of Birth: Rüsselsheim
Status: single

Primary and Secondary Education

1983 - 1986 Yale Primary School, Thornlie, Western Australia
1987 - 1989 Sacred Heart Primary School, Thornlie, Western Australia
1990 - 1994 St. Norbert College, Queens Park, Western Australia

Tertiary Education

03.1995 - 09.1998 Bachelor of Science (chemistry and environmental science)
Murdoch University, Western Australia
10.1998 - 05.1999 Honours in Chemistry (II-A)
Murdoch University, Western Australia
Honours Thesis entitled "Towards the asymmetric synthesis of benzoisochromans: A progressive investigation into the C-4 bromination of 2,3-dihydroxybenzaldehyde and its derivatives" under Prof. Dr. R. G. F. Giles.
10.2001 - 03.2005 PhD in Chemistry under Prof. Dr. B. König
University of Regensburg, Germany

Professional Experience

11.1997 - 03.1998 Research Scientist, ALCOA Pty. Ltd., Kwinana, Western Australia
09.1999 - 06.2001 Clinical Research Associate, IMFORM GmbH, Darmstadt, Germany
05.2000 - 09.2000 Clinical Trial Manager, Sankyo Europe GmbH, Düsseldorf, Germany
07.2001 - 12.2004 Research Scientist, Merck KGaA, Darmstadt, Germany